PONTIFICIA
UNIVERSIDAD
CATÓLICA DE
VALPARAÍSO

UNIVERSIDAD TECNICA
FEDERICO SANTA MARIA

PONTIFICIA UNIVERSIDAD CATÓLICA DE VALPARAÍSO

UNIVERSIDAD TECNICA FEDERICO SANTA MARIA

PROGRAMA CONJUNTO DE DOCTORADO EN BIOTECNOLOGIA

Understanding the role of the cell fate determinant Numb during human neurodevelopment

Thesis submitted in fulfillment of the requirements for the degree of

PhD in Biotechnology

Rene Gonzalez Vargas

Director: Sergio Marshall, PhD

Sponsor DBT: Danny Reinberg, PhD

Abril 2026

CONSTANCIA DE VALIDACIÓN Y CONFIDENCIALIDAD DE MONOGRAFÍA A REPOSITORIO ACADÉMICO

1.- IDENTIFICACIÓN DEL TRABAJO ACADÉMICO

Tipo de monografía (marcar una opción): ☐ Memoria o trabajo de título ☒ Tesis de Postgrado

Título del trabajo: Understanding the role of the cell fate determinant Numb during human neurodevelopment

Nombre del candidato(a): Rene Patricio Gonzalez Vargas_____

Carrera / Grado: Doctorado en Biotecnología_____

Campus: PUCV/NYU/University of Miami_____ **Departamento:** Instituto de Biología_____

2.- VALIDACIÓN DEL PROFESOR GUÍA/DIRECTOR DE TESIS

Yo, Sergio Marshall_____, en mi calidad de profesor(a) guía/director(a) del trabajo académico mencionado anteriormente **DEJO CONSTANCIA** que:

- He revisado esta versión del documento y corresponde a la versión final aprobada del trabajo.
- El trabajo cumple con los requisitos académicos y de formato establecidos por la institución.

3.- EVALUACIÓN DE CONFIDENCIALIDAD POR PROPIEDAD INDUSTRIAL (marcar una opción)

☒ El trabajo **NO contiene** información que amerite confidencialidad y puede ser publicado de inmediato en repositorio con acceso abierto.

☐ El trabajo **CONTIENE** información con potenciales implicancias de propiedad industrial o intelectual y requiere un periodo de confidencialidad (**embargo**) por **(marcar una opción)**:

☐ 6 meses ☐ 12 meses ☐ 2 años ☐ 3 años ☐ 5 años ☐ 10 años

Fundamentación de la necesidad de confidencialidad (obligatorio si se solicita embargo):

_____

_____

_____

4.- FIRMAS

Profesor(a) guía o director(a) de memoria o tesis:

Fecha: _____10 de Julio 2026_____ **Firma:** _____  _____

Estudiante o Candidato(a):

Fecha: _____10 de Julio 2026_____ **Firma:** _____  _____

Este formulario debe ser insertado como página 2 de la memoria o tesis, completado y firmado por estudiante y profesor(a) antes de la entrega en portal PRISMA de Biblioteca USM.

Dedicated to

This chapter of my life is dedicated to my wife, Rossana, and to our dog, Bali. Without your love, companionship, and unwavering support, this journey would not have been possible.

Thank you for walking beside me through every step of it.

Our family it’s my greatest pride.

I love you with all my heart and soul.

“ I am because we are ”

Abstract

Cortical neurogenesis in mammals relies on the precise balance between neural progenitor self-renewal and differentiation, orchestrated by evolutionarily conserved cell fate determinants. Among these, Numb a cytoplasmic adaptor protein first identified in *Drosophila* for its role in asymmetric cell division has emerged as a critical regulator of neural development through antagonism of Notch signaling and modulation of endocytic trafficking. However, the specific contributions of human Numb isoforms during cortical neuron differentiation remain poorly understood.

This thesis investigates the expression dynamics, subcellular localization, and functional requirements of Numb isoforms throughout human embryonic stem cell (hESC)-derived cortical neurogenesis. Using CRISPR-mediated genome editing, we generated dTAG-inducible degradation systems targeting endogenous Numb at exon 1, enabling isoform-inclusive depletion.

Unexpectedly, acute Numb degradation induced rapid and irreversible cell death in hESCs at concentrations as low as 0.05 nM, demonstrating an absolute requirement for Numb that could not be rescued by exogenous isoform expression or compensated by the endogenous paralog Numblike (Numbl). Chromatin immunoprecipitation sequencing (ChIP-seq) revealed that Numb transcriptional regulation diverges from classical Polycomb repression paradigms: the Numb promoter remained in an open chromatin state throughout differentiation, enriched for active histone marks (H3K27ac, H3K4me3) and devoid of repressive PRC2 components (EZH2, H3K27me3), suggesting post-transcriptional mechanisms govern Numb protein abundance. Analysis of published RNA-seq datasets from hESCs and iPSC-derived cortical differentiation protocols revealed a striking developmental switch in Numb isoform expression: exon 9-containing isoforms (p72, p71) predominated in undifferentiated stem cells and early neural progenitors, whereas exon 9-skipping isoforms (p66, p65) became progressively enriched during neuronal commitment and maturation. This isoform transition was highly conserved across independent datasets, correlating temporally with neural progenitor cell

specification and neuronal differentiation. Immunofluorescence analyses using a validated monoclonal antibody revealed context-dependent subcellular localization of Numb, shifting between cytoplasmic and nuclear compartments in a cell density-dependent manner, consistent with distinct functional roles for PTB-long (membrane-associated) and PTB-short (nuclear) isoforms.

Despite systematic optimization of rescue strategies including varied timing, dosage, and oscillatory treatment protocols designed to mimic Notch pathway dynamics exogenous Numb expression failed to prevent dTAG-induced lethality, highlighting the exquisite sensitivity of hESCs to endogenous Numb levels and suggesting non-redundant functions that cannot be recapitulated by ectopic expression.

Collectively, these findings position Numb as a non-redundant, essential regulator of early human neural development, operating at the intersection of chromatin accessibility, alternative splicing, post-translational control, and membrane trafficking. The developmental transition from proliferation-associated (exon 9-containing) to differentiation-promoting (exon 9-skipping) isoforms represents a conserved mechanism fine-tuning the balance between progenitor maintenance and neuronal commitment during human corticogenesis, with profound implications for understanding neurodevelopmental disorders and potential therapeutic interventions.

Acknowledgments

To Danny Reinberg and Sergio Marshall**,** my mentors. Thank you for trusting in me and offering not only the opportunity to pursue a PhD abroad, but also a life-changing experience that reshaped my view of science and of life. Thank you for giving me the tools to nurture and expand my scientific curiosity, and for showing me through your example, the value of hard work and perseverance in achieving my goals. Beyond being remarkable professionals, you are both even greater human beings, and I am deeply grateful for the guidance and inspiration you have given me.

To Reuven, thank you for your guidance throughout this process. Your advice, your ability to find the right words when science felt overwhelming, and your constant encouragement were crucial for helping me move forward.

To the Reinberg Lab**,** including former and current members from both New York University (NYU) and the University of Miami, your feedback, support, and shared learning experiences made me not only a better PhD candidate, but also a better person. You encouraged me to grow, to challenge myself, and to strive toward becoming the best version of who I can be.

To the DBT program from PUCV-UTFSM, thank you for inspiring your students to pursue their dreams. A special thanks to Sandra Zelada, your kindness and support made all the difference in this journey.

To my loved ones, my parents and my friends, your love knows no borders or time. Thank you for your endless support, patience, and affection.

TABLE OF CONTENTS

LIST OF TABLES.

LIST OF FIGURES.

CHAPTER 1

I.- INTRODUCTION.

1.1 - Mammalian neurodevelopment and cell fate decision.

Cell fate specification during mammalian neurogenesis is a fundamental process that occurs within neurogenic niches of the brain, governing how neural stem and progenitor cells generate the diverse neuronal and glial populations that constitute the central nervous system (CNS). This process relies on the precise coordination of intrinsic genetic programs and extrinsic signaling cues to ensure the correct balance between self-renewal and differentiation. Neural progenitor cells IPCs must decide at each division whether to remain as progenitors or to commit to a neuronal or glial lineage, a decision that is tightly regulated both spatially and temporally to maintain tissue homeostasis and proper brain architecture [1-5].

Neurogenic niches are complex, multicellular environments composed of Neural stem cells (NSCs), progenitors, neuroblasts, and a network of supporting cells, including astrocytes, microglia, endothelial cells, and extracellular matrix components [6-18]. Astrocytes regulate neurogenesis through both direct contact and the secretion of trophic factors such as FGF-2, IGF-1, VEGF, Wnt, and TGF-β [7,19,20]. Microglia modulate neurogenesis by releasing soluble factors and through cell–cell interactions, while endothelial cells and the surrounding vasculature provide oxygen, nutrients, and angiogenic signals for stem cell maintenance. Together, these elements create a dynamic microenvironment that coordinates proliferation, differentiation, and integration of newborn neurons [8,10-13,17,21-24]. During early embryonic development, neuroepithelial cells (NECs) constitute the earliest neural stem cells of the neural tube. NECs undergo symmetric proliferative divisions that expand the progenitor pool and establish the foundation of the neuroepithelium [23,25-27].

As development progresses, NECs progressively transform into radial glial progenitors (RGPs), which retain apical–basal polarity and serve as the principal neural stem cells of the developing cortex. RGPs are capable of both symmetric and asymmetric divisions: symmetric divisions maintain or expand the progenitor population, while asymmetric divisions produce one progenitor and one differentiated daughter cell. These asymmetric divisions are critical for generating cellular diversity while preserving the progenitor reservoir [9,23,26,28-31]. RGPs give rise to intermediate progenitor cells (IPCs), also known as basal progenitors, which are typically located in the subventricular zone. IPCs divide symmetrically to produce pairs of postmitotic neurons or, less frequently, additional progenitors, thereby amplifying neuron production during corticogenesis [22,25,32-36]. The successive generation of neurons from NECs, then to RGPs, into IPCs establishes the layered structure of the mammalian cortex, where early-born neurons populate the deep layers and late-born neurons migrate past them to form the superficial layers in an inside-out pattern (FIG 1) [13,15,22,25,29,32,35,37,38].

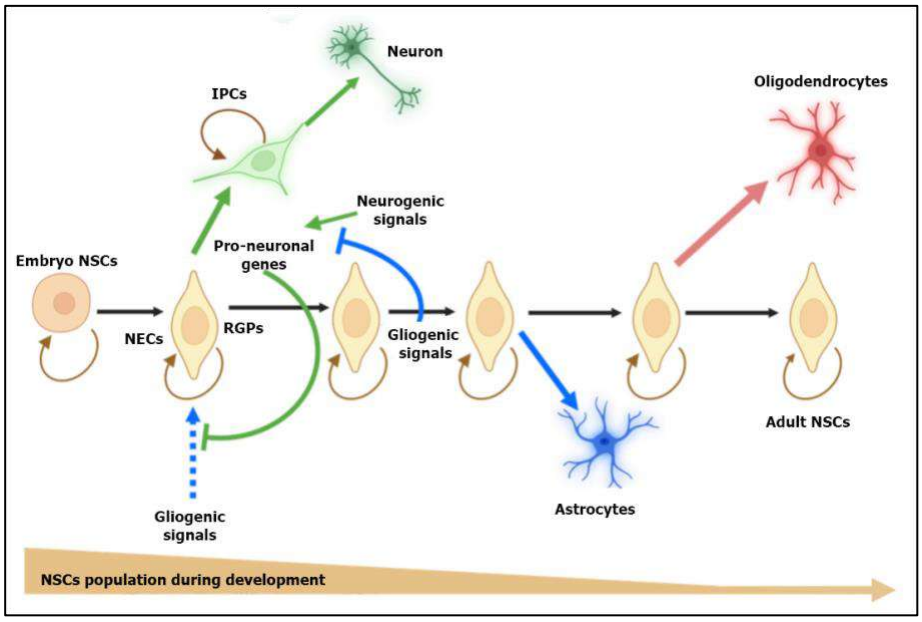

Figure 1: Scheme of the cellular phenotype generated during development from a population of NSCs.

NSCs proliferate symmetrically (brown arrow) to increase their pool or asymmetrically (black) to give rise, directly or indirectly, in a time-dependent manner, to neurons (green arrows), astrocytes (blue arrows), and oligodendrocytes (red arrow). Neuroepithelial Stem cells (NECs), Neural Stem Cells (NSCs); Radial Glial Progenitor Cells (RGPs), Intermediate progenitor cells (IPCs) radial glial progenitor cells. Blue doted arrow: repressed gliogenic signals, green arrow: pro-neuronal genes repressing gliogenic signals, Blunt blue arrow: gliogenic signals repressing neuronal genes [39].

1.2 - Cortical neurogenesis and progenitor diversity.

The mammalian neocortex represents the most evolutionarily recent and complex region of the central nervous system, responsible for sensory integration, motor control, and higher-order cognitive functions. Excitatory neocortical neurons are generated from neural progenitor cells located along the embryonic ventricles between embryonic day (E)10.5 and E17.5 in mice, and approximately gestational weeks (GW) 7 to 27 in humans [40,41]. The precise temporal and spatial regulation of progenitor proliferation and differentiation during this developmental window is essential for establishing functional cortical circuits. Perturbations in these processes lead to severe structural and functional abnormalities, including microcephaly, autism spectrum disorder, epilepsy, and schizophrenia [1,2,4,5].

1.3 - Temporal progression of neurogenesis.

Human brain development follows highly conserved spatiotemporal principles across mammals. It begins with neurulation, during which the neural plate, specified from the embryonic ectoderm folds and fuses to form the neural tube, the precursor of the central nervous system. As development proceeds, the neural tube segregates into lineage-restricted vesicles that give rise to the forebrain, midbrain, and hindbrain (FIG 2A). The inner wall of the neural tube contains neuroepithelial stem cells (NECs), which expand the proliferative ventricular zone (VZ) [14,35,42]. NECs then transform into radial glial cells (RGCs) that produce postmitotic excitatory and inhibitory neurons and subsequently glia (FIG 2 A-B). NECs subsequently transition into radial glial cells (RGCs), the primary neural stem cells that generate postmitotic excitatory and inhibitory neurons, followed later by glial lineages. In mammals, neurogenesis is amplified through intermediate progenitor cells (IPCs) the immediate progeny of RGCs that divide in the subventricular zone (SVZ) (FIG 2B) [43,44].

In the developing cortex, excitatory neuron precursors migrate radially along the RGC scaffold to populate the cortical plate in the classic “inside-out” pattern: late-born upper-

layer neurons migrate past early-born deep-layer neurons [45]. Inhibitory interneurons, by contrast, arise mainly from the ganglionic eminences and reach the cortex via tangential migration (FIG 2, A-B) [46-49].

Neuronal differentiation, migration, and maturation occur in overlapping waves, driving progressive radial and regional diversification of cell types across the dorsal forebrain. As neurons approach their destinations, they extend axons and dendrites through highly motile growth cones, integrating local environmental cues to establish connectivity [50]. The formation of dendritic spines and synapses marks the assembly of neuronal networks, followed by prolonged periods of activity-dependent synaptic and dendritic pruning, which continue into young adulthood (FIG 2B) [43,51,52]. Non-neuronal populations arise later: astrocytes and oligodendrocytes are produced by RGCs after neurogenesis ends and continue their maturation postnatally, supporting neuronal function through synaptic regulation and axonal myelination [43,52,53] (FIG 2 A-B). Meanwhile, microglia, derived from hematopoietic progenitors, and endothelial cells, which form the developing vasculature, migrate into the neuroectoderm and play essential roles in shaping embryonic brain development [54].

Because of the remarkable complexity of the mammalian brain, the pace and trajectory of neurodevelopment vary substantially across species. In particular, human radial glia-mediated neurogenesis proceeds far more slowly extending over approximately three months compared with about one week in mice and 1-2 months in macaques [2,52,55-57]. This prolonged neurogenic period, driven in part by distinct genetic programs, is thought to contribute to the disproportionate enlargement and expanded computational capacity of the human forebrain [58]. Extended timelines are also a hallmark of human neuronal differentiation and maturation, observed not only in the cortex [52,59] but also in multiple other brain regions [48,60-62], leading to an increase in the volume of neurons with more elaborate neurites and synapses [51,56,57,63]. These prolonged periods of growth and refinement likely underlie the increased size, complexity, and plasticity of the human brain. However, they may also render human neurodevelopment more vulnerable to genetic perturbations or environmental stressors, which have a longer window of opportunity to disrupt normal developmental trajectories [43,64].

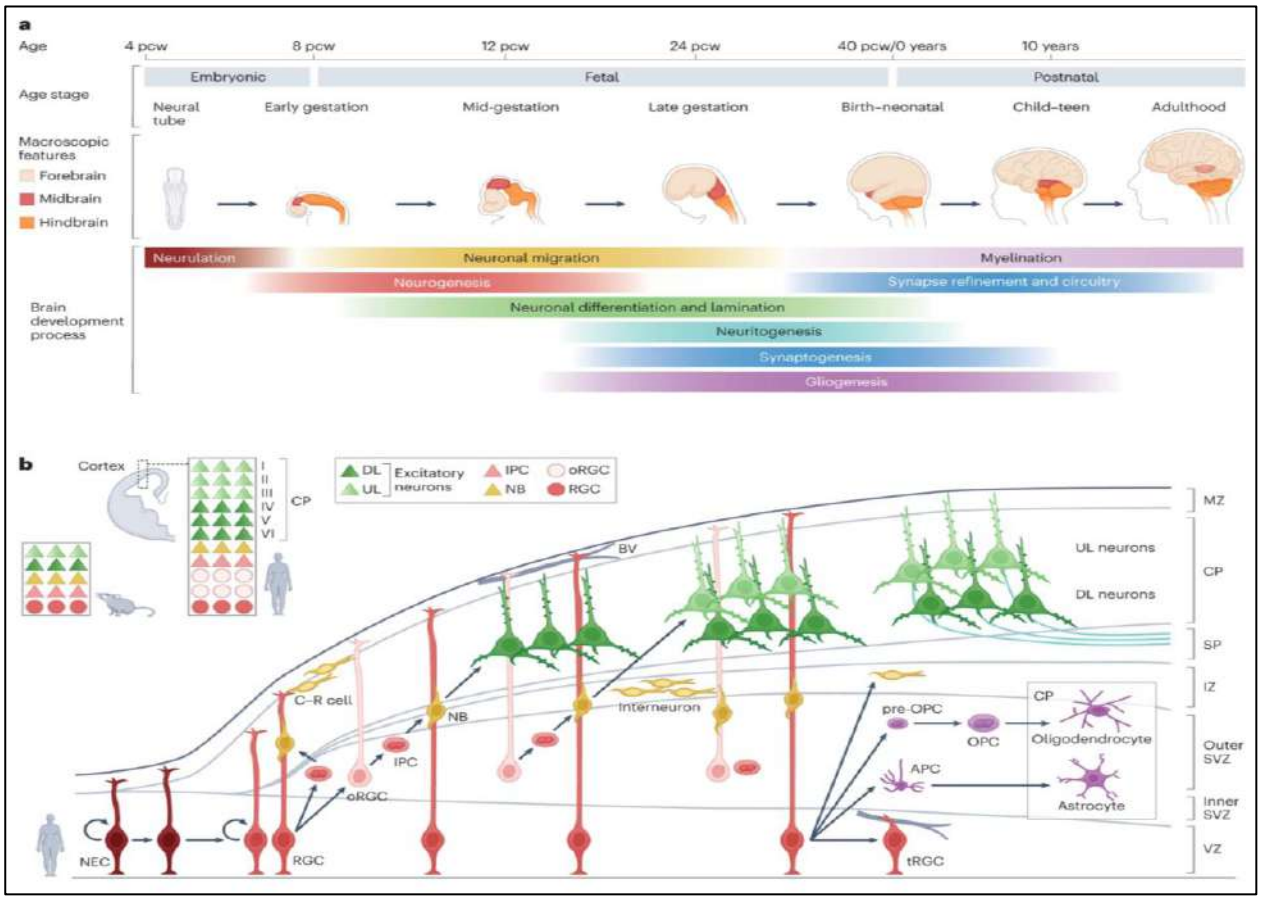

Figure 2: Key processes on human brain development **[65].**

Summary of the major developmental processes and their temporal sequence during human brain development. (A) The schematic illustrates key stages including neurulation and neuroepithelial cell proliferation, neural stem cell-mediated neurogenesis, radial and tangential migration of neural precursor cells to their target regions, followed by neuronal differentiation and maturation to establish cortical lamination and identity. Subsequent stages include the growth of neurites, synapse formation, and gliogenesis. (B) Main steps on human neurogenesis. Radial glia in the ventricular zone begin to produce projection neurons, at the same time, RG generate intermediate progenitors and outer RG, which establish the subventricular zone (SVZ) and act as transit-amplifying cells to increase neuronal production. After neurogenesis is complete, neural progenitors transition to a gliogenic mode, generating astrocytes and oligodendrocytes. Cajal-Retzius cells primarily migrate into neocortical layer I from non-cortical locations, whereas other projection neurons are born in the neocortical VZ and/or SVZ and migrate along radial glial processes to reach their final laminar destination. Outer radial glial cells (oRGCs), subventricular zone (SVZ), subplate (SP), cortical plate (CP), pre-oligodendrocyte precursor cells (pre-OPCs), truncated RGCs (tRGCs), astrocyte precursor cell (APC), blood vessel (BV), blood vessel, Cajal-Retzius (C-R); deep layer (DL), intermediate progenitor cell (IPC),intermediate zone (IZ), marginal zone (MZ), neuroblast (NB), neuroepithelial cell (NEC); Post-conception week (pcw), upper layer (UL), ventricular zone (VZ).

1.4 - Molecular determinants of neuronal fate.

The identity and connectivity of each cortical neuron are dictated by both the timing of its birth and the transcriptional program it activates. Layer-specific transcription factors such as TBR1, CTIP2 (BCL11B), SATB2, and CUX1 orchestrate projection patterns and synaptic specificity, ensuring accurate circuit assembly across cortical layers [66,67].

Molecules that regulate cell polarity, cell adhesion, and endocytic trafficking, including Numb play essential roles in controlling asymmetric divisions, neuronal positioning, and axon guidance [17,22,23,27,68]. Through these mechanisms, Numb functions as a critical determinant of the balance between progenitor self-renewal and neuronal commitment [9,37,69-75].

Intrinsic regulators include transcription factors such as NeuroD1 and Sox2 also control NSC maintenance, proliferation, and differentiation. Epigenetic modifications, notably histone methylation by enhancer of zeste homolog 2 (EZH2), regulate gene expression during neurogenesis, with EZH2 levels decreasing as neurogenesis progresses [76,77]. MicroRNAs, including miR-9 and miR-124, modulate neuronal differentiation and maturation [35,39,78,79]. In addition to intrinsic programs, extrinsic cues dynamically influence neurogenic outcomes. Classical neurotransmitters including glutamate, GABA, serotonin, acetylcholine, and dopamine modulate neural stem cell proliferation, differentiation, and survival even before synapse formation. Neurotrophic factors such as brain-derived neurotrophic factor (BDNF), insulin-like growth factor 1 (IGF-1), and vascular endothelial growth factor (VEGF) further promote progenitor proliferation, neuronal differentiation, and maturation [80-82].

Cortical neurogenesis thus exemplifies the highly coordinated interplay of cell cycle dynamics, transcriptional and epigenetic regulation, polarity cues, and extracellular signaling. Together, these mechanisms ensure the precise specification, migration, and integration of neurons that underlie the architectural and functional sophistication of the mammalian brain [13,15,18,25,32,52].

1.5 - Brief of regulatory pathways balancing symmetric and asymmetric division during neurogenesis.

The equilibrium between symmetric and asymmetric division is central to determining whether neural progenitors maintain stemness or undergo lineage commitment [23,26,27,29,83,84]. In the early stages of cortical development, symmetric proliferative divisions expand the progenitor pool, whereas during the neurogenic phase, asymmetric divisions generate neuronal or glial progeny while preserving a subset of stem-like progenitors [25,40,47,52,59]. This balance is orchestrated through an interplay of intrinsic polarity cues and extrinsic signaling pathways that collectively ensure temporal precision and developmental robustness [23,41,65,85,86].

Among the major pathways involved, Notch signaling plays a pivotal role in maintaining progenitor identity [44,58,72,73,75,87,88]. High Notch activity sustains the expression of *Hes1* and *Hes5*, repressing proneural genes such as *Neurog2* and *Ascl1* to prevent premature differentiation [89-92]. Asymmetric inhibition of Notch, mediated by the asymmetric segregation cell fate determinants like Numb protein, regulates neuronal commitment in one of the daughter cells [69,75,93,94].

Numb, localize preferentially to one daughter cell during mitosis, dictating divergent fates after division. The precise orientation of the mitotic spindle relative to the ventricular surface ensures that one daughter inherits apical polarity components and retains progenitor identity, while the other loses apical contact and begins neuronal differentiation [28,33,72,84,95-99].

This balance is fundamental for proper cortical formation, as disruptions in these mechanisms can lead to abnormal progenitor depletion, cortical malformations, or uncontrolled proliferation associated with neurodevelopmental disorders and tumorigenesis [20,100-104].

1.6- The discovery of Numb in *Drosophila* neurodevelopment.

Numb it was first discovered in *Drosophila melanogaster* in the early 1990s during genetic screens aimed at identifying regulators of sensory organ development [6,105-108]. Numb owes its name to the fact that its loss of function in *Drosophila* mutants causes a dramatic loss of sensory neurons, causing flies to become “numb” [105,106]. Mutations in numb produced a striking phenotype in which certain sensory neurons were duplicated at the expense of other cell types, revealing its pivotal role in asymmetric cell division and cell fate determination. Subsequent studies showed that Numb protein localizes asymmetrically during mitosis in neuroblasts, being inherited by only one daughter cell, where it functions as a negative regulator of the Notch signaling pathway. This discovery provided one of the first mechanistic insights into how asymmetric segregation of cell fate determinants drives neural diversification principles later shown to be conserved in mammalian neurogenesis [105,107-112].

1.7- Numb structure in *Drosophila*.

In *Drosophila melanogaster*, the numb gene was originally identified as a single-copy locus on the X chromosome that encodes a cytoplasmic protein of approximately 48 kDa, essential for establishing cell fate asymmetry during neurogenesis and sensory organ development. Unlike its mammalian homologs, *Drosophila* numb does not generate multiple isoforms through alternative splicing, emphasizing the evolutionary expansion and specialization of this family in vertebrates [6,105-107,109].

The *Drosophila* Numb protein consists of two major functional domains connected by a short regulatory linker that integrates polarity cues during asymmetric division. At its N-terminus, the PTB domain mediates membrane association through binding to phosphoinositide and *NPXY* motifs present in specific target proteins such as Sanpodo and α-adaptin, enabling Numb’s recruitment to define cortical regions [111,113-116].

Following the PTB domain, a short linker segment contains several phosphorylation sites that serve as regulatory switches controlling Numb's subcellular distribution (FIG 3) [115-117].

During neuroblast division, phosphorylation of these residues by components of the Par3/Par6/aPKC [32,113,115,118-120] polarity complex and by Lethal giant larvae (Lgl) restricts Numb localization to the basal cortex, opposite the aPKC-enriched apical domain [121,122]. This polarized segregation ensures that only one daughter cell inherits Numb after cytokinesis. The C-terminal proline-rich region (PRR), which is intrinsically disordered and enriched in protein interaction motifs such as *PxxP*, NPF, and *PPXY*, functions as a versatile scaffold for endocytic adaptors and signaling regulators. Through these interactions, the PRR enables Numb to modulate the internalization and degradation of signaling receptors, including Notch, thereby linking cortical polarity to differential cell fate determination in the two daughter cells [17,70,118,121,123,124].

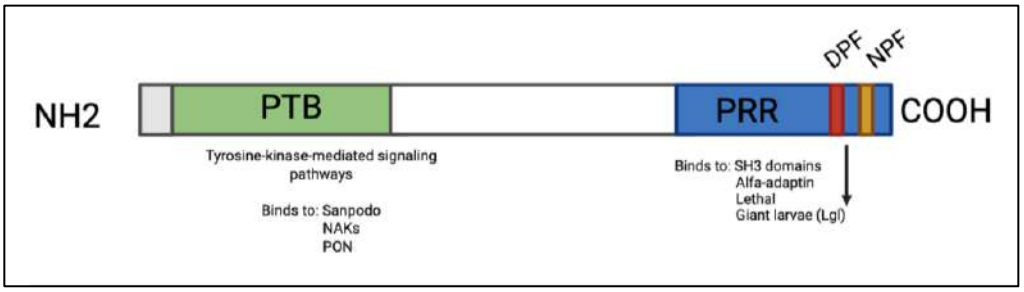

Figure 3: Drosophila Numb.

The N-terminal phosphotyrosine-binding (PTB) domain and a C-terminal proline-rich region (PRR). The PTB domain enables Numb to bind membrane-associated proteins such as Sanpodo and components of the endocytic machinery, anchoring it to the basal cortex during mitosis. The PRR, in turn, contains multiple *PxxP* motifs that serve as docking sites for adaptor proteins containing SH3 domains, such as α-Adaptin and Lethal (2) giant larvae (Lgl).

1.8- Numb's role in asymmetric cell division in *Drosophila.*

Numb entered the scientific landscape over two decades ago, when it was first identified as an intrinsic regulator of cell fate specification during asymmetric cell division (ACD) in *Drosophila* [105]. In sensory organ precursor (SOP) cells, Numb is uniformly distributed along the plasma membrane during interphase [125]. However, as the cell enters mitosis, Numb becomes selectively enriched at one of the two spindle poles. This asymmetric localization leads to its unequal partitioning during cytokinesis: the daughter cell that inherits Numb (pIIb) adopts a distinct developmental trajectory compared to its sibling cell (pIIa), establishing Numb as a key determinant of differential cell fate [106,107].

In the intricate choreography of neurodevelopment, *Drosophila's* SOP cells is one of the best-understood model systems to explain how asymmetric cell division orchestrate the cell fate decision specificity [105,110,115,119,126-128].

The neurodevelopment of *Drosophila melanogaster* is a highly regulated process that begins with the neuroectoderm, where neural stem cells, neuroblasts, delaminate and undergo asymmetric divisions to generate a diverse array of neurons and glial cells [123,129-131]. Each neuroblast divides asymmetrically, producing a larger self-renewing neuroblast and a smaller ganglion mother cell (GMC), which differentiates into neurons or glia [132].

Neurodevelopment in *Drosophila* relies on precise control of asymmetric cell division, a mechanism that generates cellular diversity by producing daughter cells with distinct fates [105,106,110,115,119,126-128]. *Drosophila* Numb (dNumb), it was initially discovered in a genetic screen for mutations affecting sensory organ development [105-107]. Specifically, numb encodes a membrane-associated protein that is asymmetrically distributed during the division of SOP cells [105,110,115,119,126-128]. It is segregated during mitosis into only one of the two daughter cells, where it functions to inhibit Notch signaling, thereby allowing the two daughter cells to adopt different fates. This discovery provided one of the first mechanistic links between asymmetric protein localization and differential cell fate determination [33,106,123,133].

The first division of the SOP, known as the pI cell, is asymmetric and produces two daughter cells with distinct fates: the pIIa cell, which is Notch-active and gives rise to support cells, and the pIIb cell, which inherits Numb and is Notch-inhibited, leading to neural fate determination. These two cells then undergo further divisions to generate the full sensory organ structure [16,105-108,111,119,134,135].

The pIIa cell divides to form a socket and the shaft cells, both of which contribute to the external bristle structure of the sensory organ of Drosophila [105-107]. Meanwhile, the pIIb cell divides asymmetrically, producing a glial cell (which typically undergoes apoptosis) and a pIIb cell [123,125]. The pIIb cell then divides once more, giving rise to a neuron responsible for sensory function and a sheath cell that ensheathes the neuron [6,105-107,126,131,136,137]. This precisely orchestrated sequence of asymmetric divisions ensures the proper development of the external sensory organ, with Numb playing a critical role in cell fate determination by antagonizing Notch signaling (FIG 4) [31,105,108,110,111,119,126,128,136-138].

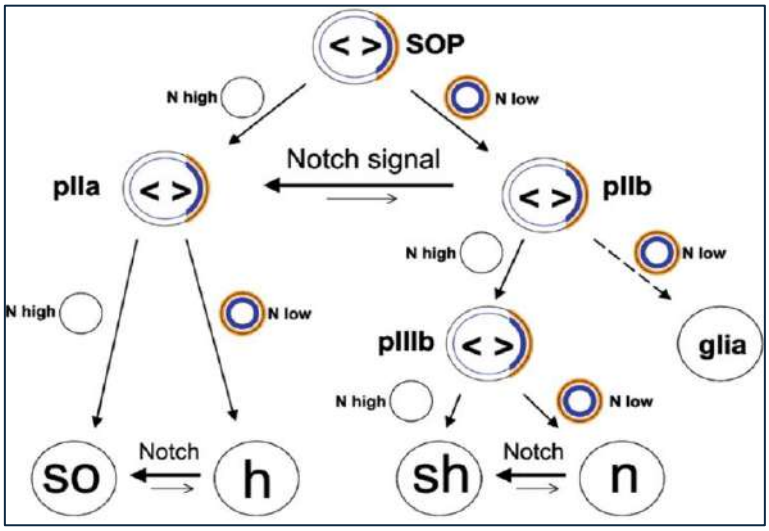

***Figure 4: During sensory organ precursor cells (SOP) division in Drosophila* [139].**

Numb (orange) becomes asymmetrically localized at the plasma membrane overlying one of the centrosomes prior to cytokinesis. At this site, Numb recruits α-Adaptin (blue), forming a cortical complex that segregates into only one of the two daughter cells, the pIIb. In this cell, the inherited Numb/α-Adaptin complex promotes endocytosis and downregulation of Notch receptor activity (N), thereby specifying a distinct cell fate. Through successive rounds of asymmetric division, this mechanism governs all binary fate decisions within the sensory organ lineage, ultimately generating five differentiated cell types: the socket (so), hair (h), sheath (sh), neuron (n), and glial cells.

1.9- How does Numb determine cell fate in *Drosophila?*

Numb serves as an adapter that links the AP-2 complex to the intracellular domain of Notch on one side of a dividing SOP cells [138,140]. This targets the receptor for endocytosis and reduces Notch signaling in the pIIb cell. After division, reciprocal signaling between the two daughter cells can lead to competition, and small differences could be amplified by negative-feedback loops [141]. Once inherited, Numb functions as an inhibitor of the Notch signaling pathway, a key regulator of cell fate decision to orchestrate cell fate decision [58,95,126]. A slight reduction of Notch levels in one of the two cells should be enough to bias this competition and to establish the pIIb cell fate in the cell that inherits Numb [95]. This inhibition allows the Numb-positive cell to adopt a neural fate, while the Numb-negative cell remains responsive to Notch signaling, leading to different developmental trajectories [28,95,105,106,108,111]. Through this mechanism, conserved trough evolution, including vertebrates, Numb is important for the proper formation of the nervous system, influencing neuronal differentiation and maintaining a balance between progenitor cells and differentiated neurons [6,105,106,138,142,143].

When Numb function is abolished, SOP cells fail to undergo proper asymmetric division and instead mis-differentiate entirely into pIIa cells, producing the generation of four outer support cells while completely lacking neurons or glia [106,111,114]. In *Drosophila*, SOP cells with Numb mutations exhibit a loss-of-function phenotype, characterized by a significant reduction in sensory neurons, effectively rendering them "numb" [111,114]. Conversely, ectopic expression of Numb during SOP division skews all progeny toward the pIIb fate, leading to the exclusive production of neurons and glial cells while completely eliminating outer support cells, showing that Numb is one of the major contributors to asymmetric cell fate establishment (FIG 5) [84,144].

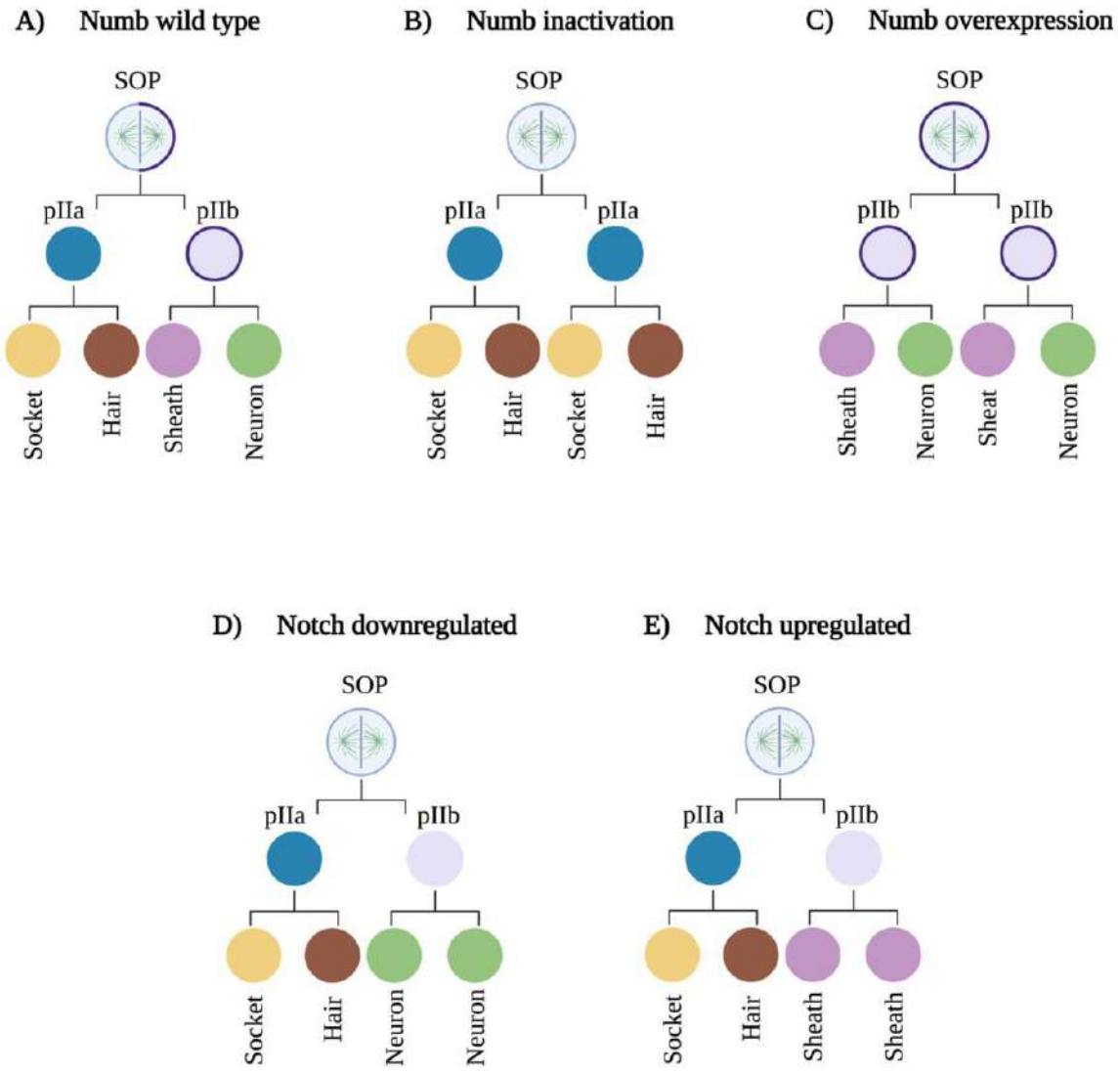

Figure 5: Embryonic phenotypes of the sensory organs precursor cells in Drosophila. Modified from [145].

Numb WT its capable of to produce the entire variety of support and neuronal types in *Drosophila*. Numb inactivation or overexpression shows changes in the formation of pIIa and pIIb ratio, decreasing cell diversity. Notch mutants show opposite phenotype that Numb, demonstrating their relation and opposite functions during Drosophila neurodevelopment.

In addition to the intrinsic Numb signal, extrinsic signals are also required to produce a normal SOP lineage[108,146]. Loss of either Delta (Notch ligand), Notch, or Suppressor of Hairless (Su(H)) function results in neuron and glial fate, in contrast to the Numb loss-of-function phenotype [108,126,147]. If the function of Notch is reduced in this manner, a transformation of sheath cells to neurons is observed in external sensory and chordotonal organs [111]. If the function of Notch is increased, by overexpressing an activated variant or even the wild-type protein, the opposite effect is observed, *i.e.,* transformation of neurons into sheath cells (FIG 5). These observations are compatible with the knowledge that Notch receptor protein is involved in cellular decisions made either by the IIa and IIb cells or by their progenies, which are required for these cells to take on the corresponding fates [98,137,148,149].

The phenotypic traits observed after modulation of Notch function are strikingly similar to the defects caused by perturbation of numb function, but of opposite polarity. That is to say, a reduction in numb function has the same effect as an increase in Notch function, and vice versa. This implies that in the neuronal and glial fates, Numb may give resistance to Notch-mediated signals [105,107,126]. The observation that Notch mutant phenotypes are opposite to Drosophila Numb mutant phenotypes suggests that Notch and Drosophila Numb engage in antagonistic roles during asymmetric divisions of brain progenitors (FIG 5) [95,108,113].

1.10- The discovery of Numb in mammalian neurodevelopment.

The discovery of Numb in *Drosophila melanogaster* laid the foundation for understanding its evolutionarily conserved role in regulating asymmetric cell division and cell fate decisions. In flies, Numb functions by antagonizing Notch signaling, ensuring that daughter cells adopt distinct identities during neurogenesis [6,20,88,109,124,126,128,129,150-152]. This fundamental mechanism has been preserved in mammals, where Numb continues to act as a critical determinant of neural progenitor behavior [6,16,99,106,108,109,123,143,144,151,153,154]. While the mammalian context is more complex, with multiple Numb isoforms and additional layers of regulation the core function of Numb in modulating signaling pathways like Notch remains central [27-29,33,35,37-39,44,45,50,75,97-101]. This conservation underscores the biological significance of Numb across species trough evolution and highlights its relevance in studying the molecular mechanisms that govern mammalian brain development [109,127,142-144,153,155-161].

1.11- Evolutionary origin of Numb.

Numb appears in evolution roughly with the emergence of bilaterally symmetrical animals, marking an important innovation in the coordination of cell polarity and fate determination [109,157,162]. Mammalian Numb homologs likely evolved from a single ancestral gene, which underwent duplication and subsequent divergence to give rise to two gene families: Numb and Numb-like (Numbl) [157,163].

Phylogenetic analyses show that mammalian Numb and Numbl form two distinct clusters, suggesting that the duplication event occurred prior to the diversification of major vertebrate lineages [157,164]. Supporting this, a single Numb-related gene exists in the basal chordate *Ciona intestinalis*, implying that one of the two duplicated vertebrate genes evolved into Numbl through the acquisition of Numbl-specific motifs, leading to functional diversification within the family (FIG 6) [157,165].

Two of the major cellular processes in which Numb participates in endocytosis and ubiquitination, have deep evolutionary roots. Endocytosis is considered one of the defining characteristics distinguishing eukaryotes from prokaryotes, with evidence suggesting that it was already present in the last eukaryotic common ancestor (LECA) [157,164,166,167].

Similarly, ubiquitination long thought to be unique to eukaryotic systems also exhibits evolutionary precursors in prokaryotes, including ubiquitin-like proteins and components of the enzymatic machinery responsible for post-translational modification [168-170]. Thus, by the time Numb emerged in phylogenesis, both endocytosis and ubiquitination were already well-established, conserved cellular systems, deeply integrated into eukaryotic physiology. It is therefore unlikely that Numb evolved directly alongside these processes. Instead, Numb may have been recruited into their regulation, exploiting these pre-existing molecular frameworks to mediate polarized trafficking and signaling [157,165,171,172].

Notably, the evolutionary appearance of Numb approximately coincides with the emergence of the PAR polarity complex, a central determinant of asymmetric cell division [157,173]. While basic polarity mechanisms likely trace back to the earliest cellular life forms, proteins of the PAR complex such as PAR-3, PAR-6, and aPKC can be clearly identified only in early metazoans, approximately 500 million years ago, during the rise of bilateral animals (e.g., nematodes, flies, and mammals) [109,122,157,173,174]. This temporal overlap suggests that Numb may have evolved (or co-evolved) with the PAR complex, functioning as a molecular bridge between polarity establishment and downstream fate determinants.

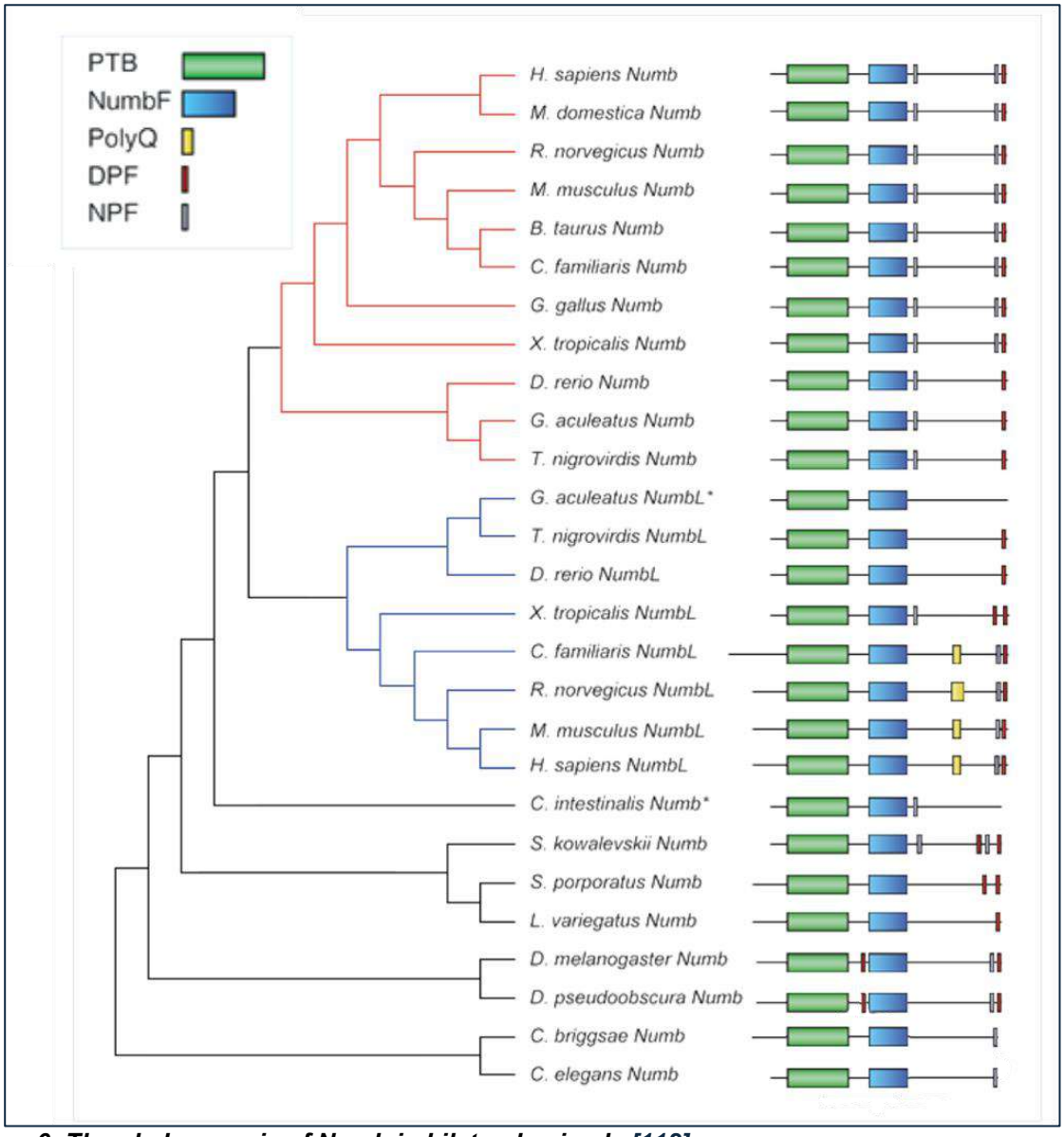

Figure 6: The phylogenesis of Numb in bilateral animals [112].

The PTB (Phospho-Tyrosine Binding) domain (green), polyglutamine domain (PolyQ) (yellow) the NumbF domain (blue) found in the Numb family of proteins adjacent to the PTB domain, DPF (red) responsible for binding to α-adaptin and NPF motif (gray) responsible for binding to the EH domain of endocytic proteins.

1.12- Role of Numb in mouse embryogenesis.

The mammalian homolog of *Drosophila* Numb was independently cloned and characterized by several groups, revealing it to be a highly conserved protein both structurally and functionally trough evolution [13,71,75,109,143,175-177]. Its characteristic PTB and PRR domains are preserved, allowing Numb to interact with endocytic and polarity regulators in a manner analogous to its *Drosophila* counterpart [99,109,124].

During mouse cortical neurogenesis, m-Numb is asymmetrically localized to the apical membrane of dividing ventricular cells [9,68,72,74,96,127,150,151,155,178]. Therefore, in an asymmetric horizontal division, m-Numb is segregated predominantly to the apical daughter cell that remains as a progenitor [85,151]. Numb can physically interact with the intracellular domain of the mammalian Notch homologue, Notch1, which is also present in cortical progenitors [85]. It has been shown that mechanisms for asymmetric divisions during neurogenesis are evolutionarily conserved and that the presence of Numb in apical daughter cells suppresses Notch activity in these cells, thereby allowing them to remain as progenitors [6,74,86,109]. Presumably, the higher Notch1 activity in the basal daughter cell allows it to take on a fate different from that of a neural progenitor [85,92]. Once it has migrated to the cortical plate, the basal daughter cell may require other factors to regulate Notch signaling before it can terminally differentiate into a neuron, since Notch signaling usually directs cells towards nonneuronal fates.

Remarkably, heterologous expression of mammalian Numb in *Drosophila* embryos not only mimics the activity of fly Numb but can also rescue numb mutant phenotypes, underscoring the deep evolutionary conservation of its structure and function in cell fate determination [9,10].

In the developing mouse embryo, Numb expression is both ubiquitous and dynamically regulated, with pronounced enrichment in neuroepithelial cells, somites, heart, and vasculature [150,151]. Genetic ablation studies have demonstrated that Numb is indispensable for early embryonic development. Homozygous $Numb^{-/-}$ embryos exhibit severe neural tube closure defects, abnormal neuroepithelial organization, and disrupted

somite patterning, typically resulting in embryonic lethality around E11.5-E12.5 [86,151,179]. These phenotypes reflect the fundamental requirement for Numb in establishing epithelial polarity and coordinating cell fate specification within multiple germ layers.

Beyond its canonical role as a Notch antagonist, Numb participates in diverse signaling and trafficking pathways crucial for embryogenesis. It regulates endocytosis of Notch and integrins, modulates cell adhesion through E-cadherin trafficking, and contributes to p53 stabilization and apoptotic control during morphogenesis. These pleiotropic activities position Numb as a central coordinator of developmental signaling, linking polarity cues with fate determination and tissue morphogenesis [6,24,68,75,83,108,111,124,139,145,151,180-185].

1.13- Nervous tissue-specific knockout of Numb in mice.

Genetic studies in mice have firmly established that Numb is indispensable for early embryonic development. Homozygous global knockouts (*Numb*$^{-/-}$) exhibit embryonic lethality around E11.5, accompanied by severe morphogenetic defects, including cranial neural tube closure failure, aberrant neuronal differentiation, and disorganization of the central nervous system (CNS)[11,12,151].

In addition to neural abnormalities, angiogenic remodeling and placental development are also impaired, leading to compromised embryonic viability [151,179]. At the molecular level, loss of Numb results in a reduction of differentiated motor and sensory neurons and decreased expression of key neuronal markers such as NeuroD, DLL3, and NF160, suggesting that neurogenesis is delayed or arrested rather than enhanced [93]. In the peripheral nervous system (PNS), dorsal root ganglia exhibit a loss of sensory neurons, whereas sympathetic ganglia develop normally, revealing a lineage-specific requirement for Numb in sensory neurogenesis [93].

To overcome early lethality and investigate tissue-specific functions, conditional knockout (cKO) strategies have been employed using Cre-loxP recombination under neural lineage-specific promoters such as Nestin-Cre (pan-neural progenitors), D6-Cre (cortical progenitors), Emx1-Cre (dorsal forebrain), and Wnt1-Cre (sensory ganglia) [13,15,18]. Surprisingly, these Numb cKO mice are viable and fertile without overt gross developmental abnormalities, indicating that the embryonic lethality observed in global knockouts cannot be solely attributed to neural defects [93,151]. Nonetheless, detailed analyses revealed enhanced Notch signaling, expansion of the progenitor pool, and delayed or defective neuronal differentiation, underscoring Numb's role as a critical antagonist of Notch signaling and a regulator of timely neurogenesis [75,85,150,151].

The functional complexity of Numb's role is further highlighted by differences among individual knockout lines. For example, forebrain-specific deletion leads to premature neuronal differentiation, consistent with a requirement for Numb in maintaining progenitor identity [11]. Conversely, other allelic combinations show impaired neurogenesis in the hindbrain, suggesting that Numb's influence on progenitor maintenance versus

differentiation is region-specific and context dependent [12]. These apparent discrepancies likely reflect the presence of partial redundancy with its vertebrate paralog, Numb-like (Numbl) [74,85,93,163,178].

Indeed, while single knockouts of either Numb or Numbl alone do not overtly disrupt neural development, combined loss of both genes, using Numb conditional deletion in Numbl$^{-/-}$ or Numbl $^{flox/flox}$ backgrounds produces severe neurodevelopmental defects [13-16,18]. These include loss of apico-basal polarity, premature cell-cycle exit, depletion of neural progenitor pools, and disrupted cortical lamination. Neural progenitors in these compound mutants fail to maintain proper polarity and asymmetric divisions, leading to aberrant cortical architecture and misregulation of Notch signaling [85,151,163,186].

These conditional knockout studies demonstrate that Numb plays a pivotal, dosage-sensitive role in maintaining the balance between progenitor self-renewal and neuronal differentiation during neurogenesis [93,179]. Although Numb-like provides partial compensation, Numb exerts non-redundant functions essential for establishing neural polarity, regulating asymmetric cell division, and ensuring the coordinated progression of neural development in the mammalian brain [6,86,179].

1.14- Numb gene.

The mammalian Numb gene represents the evolutionary counterpart of the *Drosophila* numb gene and encodes a cytoplasmic protein that functions as a key determinant of cell fate asymmetry.

The numb gene consists of 13 exons, 10 of which are protein-coding, Numb gene encodes a membrane-associated protein or scaffold protein involved in bringing together multiple proteins into a functional unit or pathway that is primarily found in the cell and peripheral membrane [127,153]. However, it is also to be present in the endosomal membrane, clathrin vesicles, the basolateral membrane, nuclei, and cytoplasm [73,83,96,166,187-192].

For clarity, Numb it is often referred to as containing 10 exons, and we will adopt the same convention here [109,124,127,166]. These coding exons can undergo alternative splicing, generating multiple Numb isoforms with distinct structural and functional properties. This splicing diversity allows Numb to modulate processes such as cell fate determination, polarity, and signaling in a context-dependent manner [124,127,144,153,156,157,166,193]. Both human and mouse Numb genes share a highly conserved domain architecture composed of an N-terminal PTB domain, a central linker region, and a C-terminal PRR domain. These structural modules mediate Numb's function as an adaptor protein that coordinates signal transduction, endocytosis, and cell polarity during development.

Eukaryotic Numb mRNA can undergo alternative splicing to produce at least 4 different isoforms Numb, with predicted molecular masses of p65, p66, p71, and p72 kDa at the protein level produced by the inclusion or exclusion of exon 3 and 9 (FIG 7) [124,127,144,153,156,157,166,193,194]. Human Numb gene is located on the 14q24.3 chromosomal region that encodes an endocytic protein of the same name [109,124]. Numb is expressed in different adult human tissues, with the highest levels being found in the blood, lung, and gallbladder and the lowest in the pancreas [124,194]. However, Numb expression fluctuates according to developmental stage, reaching its maximum at the two-cell embryo stage and progressively declining in subsequent stages prior to blastocyst formation [194].

Expression studies have shown that Numb is widely expressed during embryonic development and in adult tissues, with high levels detected in neuroepithelial cells, neural progenitors, and epithelial tissues [6,85,109,195]. During cortical neurogenesis, Numb becomes asymmetrically distributed to one pole of dividing progenitor cells, ensuring that its inheritance by only one daughter cell leads to Notch signaling inhibition and neuronal differentiation, while its absence in the other allows continued progenitor identity [16,106,108,109,124,153]. This asymmetric segregation of Numb thus provides a mechanistic basis for cell fate asymmetry and lineage diversification in mammalian neurodevelopment [6,28,84,109,151,178,196].

Overall, the mammalian Numb gene encodes a multifunctional adaptor protein whose structural complexity and splicing diversity enable it to integrate polarity cues, endocytic pathways, and signaling networks to regulate a broad range of developmental processes [83,109,124,139,143,197]. Its evolutionary conservation and isoform specialization underline its central role in coordinating asymmetric cell division, stem cell maintenance, and tissue morphogenesis across vertebrates [13,37,99,109,124,143,177,196].

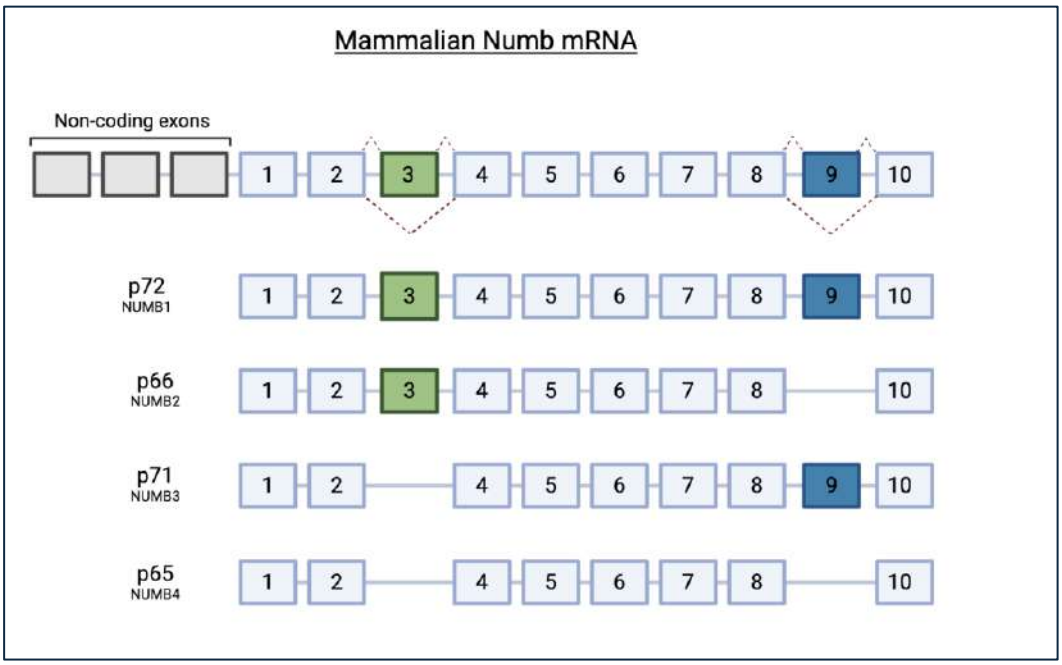

Figure 7: Mammalian Numb and splice variants.

Numb mRNA contains 13 exons. The first 3 it doesn't codify to protein. Splice variants are generated by alternative splicing, being the exon 3 (green) and exon 9 (blue) involved in this process. These splicing events help to produce 4 main variants, partially described in mammalian neurodevelopment, Numb1 (p72), Numb2 (p66), Numb3 (p71) and Numb4 (p65).

1.15- Numb protein.

Structurally, Numb exhibits a modular architecture: an N-terminal PTB domain [198,199] and a C-terminal PRR containing multiple Src homology 3 (SH3) domain-binding sites [109,124,156]. The PRR also harbors two DPF motifs, which serve as binding sites for the clathrin adaptor α-adaptin, and one NPF motif, which interacts with proteins containing Eps15 homology (EH) domains. These motifs are conserved across vertebrate Numb isoforms, Numb-like (Numbl), and dNumb [73,116,118,143,153].

The mammalian numb gene produces four protein isoforms via alternative splicing of two exons: 3 and 9, one in the PTB domain and one in the PRR, respectively [124,127]. Isoforms p72 (Numb1) and p66 (Numb2) contain an 11-amino acid insert in the PTB domain, PTB-long (PTB^{L}), whereas p71 (Numb3) and p65 (Numb4) have the shorter PTB domain (PTB^{S}). Similarly, p72 and p66 include a 48-amino acid insert in the PRR (PRR^{L}), which is absent in p71 and p65 (PRR^{S}) (TABLE 1) [124,127,166]. Functional studies in immortalized mouse neural crest lines and rat neural crest stem cells reveal that PRR^{S} isoforms promote neuronal differentiation, while PRR^{L} isoforms favor proliferation. The PTB domain also affects subcellular localization: PTB^{L}-containing isoforms localize to the plasma membrane, whereas PTB^{S} isoforms are primarily cytoplasmic [127]. These isoform-specific properties highlight how Numb functions are diversified through domain structure and protein interactions [124,127,156].

Common Name	Isoform	PTB Domain	PRR Domain	Exon 3 (PTB insert)	Exon 9 (PRR insert)
p72	**NUMB1**	**PTB^{L}** 11 aa insert.	**PRR^{L}** 48 aa insert	Included	Included
p66	**NUMB2**	**PTB^{L}** 11 aa insert.	**PRR^{S}** lacks 48 aa insert	Included	Excluded
p71	**NUMB3**	**PTB^{S}** lacks 11 aa insert	**PRR^{L}** 48 aa insert	Excluded	Included
p65	**NUMB4**	**PTB^{S}** lacks 11 aa insert	**PRR^{S}** lacks 48 aa insert	Excluded	Excluded

Table 1: Mammalian Numb protein diversity according their PTB and PRR domain.

1.16- Mammalian Numb Isoforms.

1.16.1- Numb isoforms diversification.

In the context of the intricate regulatory networks that govern mammalian development, a single protein often cannot fulfill all the necessary functional demands hence, molecular versatility is achieved through mechanisms such as alternative splicing. In this framework, the Numb gene exemplifies such regulatory adaptability by producing multiple protein isoforms, each with distinct structural features and context-specific functions [69,109,124,194].

These studies revealed that Numb undergoes alternative splicing at two critical regions. The first involves an 11-amino acid insert within the PTB domain, encoded by exon 3. This insertion markedly alters Numb's tertiary structure and binding specificity, enhancing its ability to associate with the plasma membrane, whereas isoforms lacking this insert are predominantly cytoplasmic [109,115,117,124,153,154,200]. The second splicing event occurs within the central PRR, where the inclusion or exclusion of exon 9 generates a 48 amino acid insert, further diversifying Numb isoform structure and function [109,124,127]. Together, these two splicing events at exons 3 and 9 define the four major Numb isoforms, each with distinct subcellular localizations and regulatory capacities [109,124,127].

Numb isoforms are commonly classified based on their PTB domain composition and molecular weight. Among the alternative splice variants, as it was mentioned before, only four are translated into proteins: p72 (Isoform 1), p66 (Isoform 2), p71 (Isoform 3), and p65 (Isoform 4) [109,124,127,153,166]. Isoform 1 (p72) is the longest transcript and includes all coding exons (FIG 8). Isoform 2 (p66) lacks exon 9, while Isoform 3 (p71) lacks exon 3. The shortest variant, Isoform 4 (p65), lacks both exons 3 and 9 (FIG 8) [109,124,127,153].

Early expression profiling, using Northern blotting and RT-PCR, showed that PRR-long isoforms (PRR^L or Ex9in) predominate in undifferentiated neural progenitors and decline during neuronal differentiation, whereas PRR-short isoforms (PRR^S or Ex9sk) become enriched in mature neurons [127,153]. Functional studies in both *Drosophila* and mammalian neural progenitor models demonstrated that PRR^S isoforms robustly drive cells toward a neuronal fate, while PRR^L isoforms fail to induce differentiation and instead sustain a progenitor-like, proliferative state [69,109,124,144].

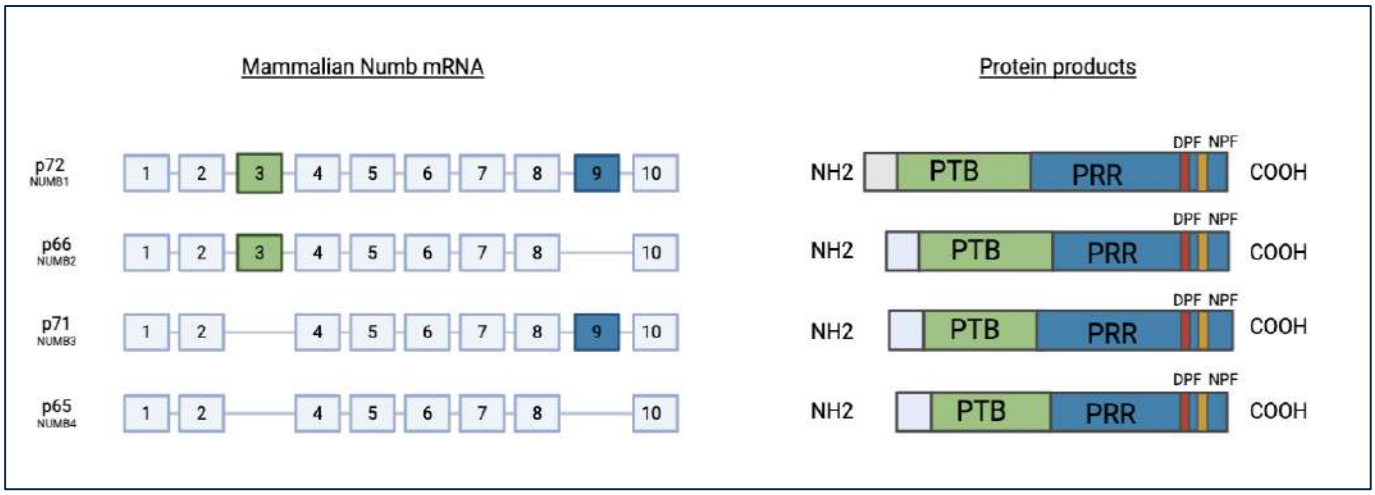

Figure 8: Mammalian Numb gene and protein diversification.

A) Mammalian Numb and splice variants. Numb mRNA contains 10 exons. The first 3 it doesn't codify to protein. Splice variants are generated by alternative splicing, being the exon 3 (green) and exon 9 (blue) involved in this process B) Mammalian Numb isoforms p72, p71, p66, p65 structure shows the main protein-protein interactor domains: PTB (green), PRR (blue), DPF (red) and NPF (yellow) motifs. DPF: aspartic acid-proline-phenylalanine motifs and NPF: asparagine proline-phenylalanine motif.

Mechanistically, these opposing outcomes are linked to isoform-specific modulation of Notch signaling [58] PRR^S isoforms attenuate Notch activity to facilitate differentiation, whereas PRR^L isoforms maintain Notch signaling to promote progenitor expansion [6,109,124]. Together, these early findings established an isoform-dependent regulatory axis in which alternative splicing of Numb fine-tunes the balance between self-renewal and differentiation through context-specific modulation of intracellular signaling pathways [94,109,124,127,144,153,156,166,187].

These foundational observations laid the groundwork for later studies connecting isoform balance to endocytic trafficking, cell fate determination, and cancer biology, however, the biological significance and process-specific roles of the PTB-domain isoforms remain unresolved [83,94,109,115,117,124,127,144,153,156,166,173,181,187,196,200-202].

1.17- Mammalian Numb isoforms function.

1.17.1- Tissue-specific patterns and functional implications.

Numb isoforms expression is highly tissue-dependent and tightly correlated with developmental stage and cellular identity [109,124,194]. In pluripotent stem cells, both exon 3 and 9 are widely included, favoring the expression of p72 (PTB^{L}-PRR^{L}) [194]. In contrast, differentiated tissues, particularly in the adult brain, immune system, and pituitary, express isoforms lacking both exons p65 (PTB^{S}-PRR^{S}), which supports a role in differentiation and reduced proliferative capacity [194].

Tissues with self-renewal capacity such as testis, gastrointestinal tract, and pancreas tend to express PTB^{S} isoforms (p71, p65), indicating a possible role for these isoforms in progenitor maintenance and tissue homeostasis [109,124,194]. Interestingly, certain tissues, like kidney cortex, prostate, and esophageal mucosa, display nearly equal levels of all four isoforms, suggesting a complex regulatory environment where fine-tuning of Numb splicing may modulate distinct signaling outputs [124,194].

1.17.1.1- Examples of Numb isoforms role in neurodevelopment.

Alternative splicing is an essential mechanism for post transcriptional regulation of gene expression and for the diversification of gene products [203-205]. Sequence-specific RNA-binding proteins govern mechanisms that activate and repress splice sites or modulate exon or intron definition [203-206].

During development, Numb isoform expression is highly stage-dependent, with PRR^{L} isoforms enriched in progenitors and PRR^{S} isoforms dominating in differentiated neurons [69,124,194]. Functional perturbation studies confirm that PRR^{L} isoforms sustain proliferation and antagonize differentiation, while PRR^{S} isoforms drive neuronal maturation, via stronger antagonism of Notch signaling through endocytic degradation [69,72,73,84,94,108,109,124,127,153,166,173,207].

Another example of how Numb isoforms regulate progenitor proliferation and differentiation comes from studies of splicing defects, which are increasingly implicated in neurodevelopmental disorders [166,194,203,205,206,208,209]. Polyglutamine-binding protein 1 (PQBP1), a nuclear factor involved in alternative splicing, is strongly expressed in the embryonic cerebral cortex, striatum, and hippocampus [208,210]. Conditional knockout of Pqbp1 in neural stem/progenitor cells prolongs the cell cycle and leads to a microcephaly phenotype, highlighting its essential role in brain growth.

In the striatum, the largest component of the basal ganglia, required for movement control and associated with addictive behaviors, PQBP1 regulates the balance of intermediate progenitor proliferation and differentiation by modulating Numb splicing [208]. Mechanistically, PQBP1 controls the inclusion of exon 9 in Numb transcripts, thereby regulating the ratio of PRR^{L} and PRR^{S} isoforms. During striatal development, isoforms that includes exon 9 (PRR^{L}) predominate at embryonic day 11.5 (E11.5) but are progressively replaced by isoforms without exon 9 (PRR^{S}) as development proceeds, a switch observed both at the RNA and protein level. Importantly, PRR^{L} isoforms are enriched in progenitor tissues and promote cell proliferation, whereas PRR^{S} isoforms are enriched in adult tissues and favor differentiation. Consistent with this developmental

transition, PQBP1 depletion reduces exon 9 inclusion and increases exon 9-skipped isoform expression, resulting in impaired progenitor proliferation, premature differentiation, and ultimately defective striatal neurogenesis [208,210]. Numb also has been implicated in synapse formation, neuronal function, and neurite growth [93], primarily through the regulation of Notch-dependent expression of the transient receptor potential channel TRPC6, a voltage-gated calcium channel (VGCC) [70,94,211]. Calcium signaling is well established as a key regulator of neural progenitor differentiation, axon outgrowth, and synaptic plasticity [211-214].

In neuronal differentiation, Numb expression increases in rat primary hippocampal and cortical neuronal cultures [70]. Functional studies show that the PTB^S domain of Numb promotes neurite outgrowth via activation of VGCCs, while the PRR^L domain contributes to neuronal branching and splice-site dependent regulation of VGCC activity. From day 1 to day 9 of in vitro culture, Numb expression remains consistently elevated in hippocampal neurons, suggesting a sustained role for Numb in postnatal neuronal development and in maintaining neuroepithelial architecture [70,71].
Neurite outgrowth depends on intracellular calcium signaling and Numb-mediated outgrowth specifically requires VGCC activation [70,71]. Indeed, the calcium chelator BAPTA-AM completely abolishes neurite extension in cells expressing either PTB^S/PRR^S or PTB^S/PRR^L isoforms, confirming that the PTB^S domain is the principal determinant of neurite outgrowth. Interestingly, cells expressing the PTB^S/PRR^L isoform display greater neurite length and increased dendritic branching compared to those with PTB^S/PRR^S, highlighting a unique contribution of the PRR^L domain to neuronal branching [70].

Together, these findings underscore that distinct Numb isoforms exert specialized functions in shaping neuronal architecture, with the PTB^S domain driving neurite extension and the PRR^L domain fine-tuning dendritic branching, thereby integrating Numb into the broader regulatory network of calcium-dependent neuronal development [70,94,211,213,214]. These isoform-specific functions highlight how Numb acts not only as a structural regulator of neuronal architecture but also as a molecular interpreter of

splicing decisions. In this context, upstream regulation by splicing factors such as RBM4 in neurodevelopment [203].
RBM5/6 and RBM10 splicing factors in cancer cell proliferation [203,215] becomes particularly important, as it dictates the balance of Numb isoforms that engage distinct signaling pathways to orchestrate neurite extension, dendritic branching, and ultimately neuronal fate [203,216-218].

By linking isoform diversity to calcium-dependent mechanisms of neuronal growth, RBM4 establishes Numb as a central effector at the intersection of splicing regulation, Notch signaling, and activity-dependent neuronal development [203,218,219].

Emerging evidence identifies RNA-binding motif 4 (RBM4) as a pivotal splicing regulator that shapes neuronal fate decisions through control of Numb isoform diversity [203,217,220]. By promoting Ex3in and suppressing Ex9in, RBM4 drives the production of Numb isoforms optimized for neuronal differentiation and neurite outgrowth [203,220]. This splicing switch is not merely a molecular detail but a developmental checkpoint [203].

Loss of RBM4 disrupts this balance, leading to aberrant Numb isoform ratios, impaired Mash1 expression, and defective neurite outgrowth. Importantly, re-expression of specific Numb isoforms such as p66 or p65 rescues these defects, confirming that RBM4 exerts its developmental role primarily through isoform-specific Numb functions. Thus, RBM4 and Numb together constitute a regulatory module that integrates splicing, Notch signaling, and cytoskeletal dynamics to control neural progenitor maintenance, neuronal differentiation, and cortical architecture [203,217-220]. Interestingly, the same Numb isoforms regulated by RBM4 during neurodevelopment also intersect with Tau biology, linking splicing-driven progenitor fate decisions to mechanisms of neuronal protection against Tau toxicity [155,221,222].

Tau is a microtubule-associated protein critical for neuronal polarity, axonal transport, and cytoskeletal stability, and its dysregulation underlies tauopathies and contributes to neurodegeneration [222-224]. Emerging evidence links Tau regulation to Numb [155,222]. Numb controls intracellular Tau homeostasis by limiting Tau accumulation and

preventing the formation of toxic oligomers. Mechanistically, Numb may influence Tau both directly, through regulating protein turnover and trafficking, and indirectly, by modulating signaling pathways that affect neuronal survival [155]. Isoform-specific roles are particularly relevant: the long isoform Numb-p72 has been shown to protect neurons in tauopathy models, rescuing dendritic morphology, synaptic responses, and overall neuronal viability [155,221,222,224]. Given that Numb isoforms are themselves developmentally regulated by alternative splicing, this points to a coordinated mechanism in which Numb shapes progenitor fate decisions during neurodevelopment while simultaneously providing a safeguard against Tau toxicity in post-mitotic neurons. Together, these findings suggest that Numb sits at the intersection of developmental programs and neurodegenerative processes, highlighting it as a potential therapeutic target in Tau-related disorders [155,222,224]. Numb functions as a versatile scaffold protein that integrates endocytosis, signaling, and cell fate decisions. Through its isoform-dependent regulation of receptor trafficking, Numb controls whether key molecules such as Notch, integrins, and growth factor receptors are recycled to sustain signaling or targeted for degradation to terminate it [225-227]. This balance is critical in neurodevelopment, where Numb isoforms coordinate the timing of progenitor maintenance versus differentiation, and it is frequently hijacked in cancer, where shifts in new Numb splicing events sustaining proliferative and invasive programs [100,156,158,221,228].

By linking membrane trafficking with polarity cues and adhesion dynamics, Numb positions itself at the crossroads of neurogenesis, endocytic control, and tumorigenesis, making it a unifying regulator across diverse biological systems [112,142,166,173,196,229].

1.17.1.2- Examples of Numb isoforms role in endocytic trafficking.

Endocytic trafficking is a fundamental process to regulates the abundance and signaling potential of surface receptors such as Notch, integrins, and Eph receptors. By controlling whether these receptors are recycled back to the plasma membrane (PM) or targeted for degradation, endocytosis fine-tunes the signaling thresholds that drive neural progenitors toward self-renewal, differentiation, or lineage commitment. Numb plays a central role in this process by acting as a splicing-dependent factor [73,83,93,96,188,196,207,226,229].

Through its conserved NPF motif, Numb interacts with the endocytic adaptors EPS15 and EPS15L1, scaffold proteins recruited early in clathrin-coated vesicle formation [189,230]. These interactions, particularly enriched in the PRR^{L} Numb isoforms, facilitate internalization of specific receptors such as Ephrin type-B receptor 2 (EPHB2), implicated in tumorigenesis as well as pathological forms of angio-genesis, via Numb p72–EPS15/EPS15L1 complexes thereby act as hubs that link cargo selection to downstream endocytic trafficking and receptor fate [173,207,231,232]. Numb also binds integrins like integrin beta-5 (ITGB5) through its PTB domain [166]. Depletion of either Numb or EPS15/EPS15L1 reduces ITGB5 clustering in the PM [233,234]. This relation Numb-ITGB5 act as bidirectional signaling units that anchor the actin cytoskeleton to the extracellular matrix, mediate cell ECM adhesion during mitosis, providing structural platforms in skeletal muscle, and enhance growth factor receptor signaling [207,231-234].

The Anaplastic Lymphoma Kinase (ALK), a receptor tyrosine kinase, also undergoes ligand-induced internalization and sorting through endocytic pathways to regulate its signaling output, normally expressed only transiently during nervous system development, with minimal levels in adult tissues [235]. While knockout studies suggest ALK is non-essential for normal development [236], aberrant ALK activation through mutations, amplifications, or translocations drives several cancers, including anaplastic large-cell lymphoma and non-small-cell lung cancer (NSCLC) [237]. Oncogenic ALK sustains tumorigenesis by hyperactivating MAPK proliferation and PI3K/Akt survival pathways [235-237].

Endocytosis is a key regulatory mechanism of ALK activity [238]. Normally, ligand-induced ALK activation triggers internalization and sorting through endocytic compartments, where receptors are either recycled back to the plasma membrane or targeted for lysosomal degradation [238]. This trafficking decision is mediated by Numb, which couple ALK and other receptors to clathrin-mediated internalization and post-endocytic fate. Numb can act as a tumor suppressor by promoting receptor downregulation, thereby dampening oncogenic signaling. However, in cancers where Numb function is lost or isoform expression is altered, ALK may escape degradation, remain stabilized at the cell surface, and prolong oncogenic signaling cascades [238,239].

Beyond kinase inhibition, ALK regulation is intimately linked to endocytic control [238,240]. Together, EPS15, Numb, and ALK form a regulatory triad: EPS15/15L1 supply the structural scaffold for clathrin-coated pit formation, Numb functions as the cargo adaptor that directs receptor fate, and ALK represents the signaling receptor whose oncogenic output is governed by the efficiency of this machinery [238-240]. Loss of Numb can also disrupt autophagy, an alternative degradative route used by receptors such as Notch [241]. Compared the effects of Numb isoforms p66 (PTB^{L}-PRR^{S}) and p72 (PTB^{L}-PRR^{L}) over expression on the endosomal trafficking of the ALK receptor tyrosine kinase suggested that p72 and p66 have different effects on ALK trafficking: whereas p66 promotes degradation, p72 promotes recycling of ALK to the membrane. In addition, Numb p72, but not p66, enhanced accumulation of ALK within fast-recycling vesicles [238,239].

Disruption of this axis through Numb loss, isoform imbalance, or EPS15 dysfunction may stabilize ALK at the plasma membrane, prolonging MAPK and PI3K/Akt signaling and driving tumorigenesis [189,238,239] . Thus, therapeutic strategies aimed at restoring Numb/EPS15 function or leveraging ALK's reliance on endocytosis represent promising avenues to complement existing ALK inhibitors (e.g., crizotinib, ceritinib, alectinib are already FDA-approved) and overcome resistance [242].

On this way, alternative splicing of Numb acts as a molecular switch that determines whether receptors are degraded to terminate signaling or recycled to reinforce it, ultimately guiding progenitor cells through critical neurodevelopmental decisions. Together, EPS15, Numb, and ALK form a regulatory triad, where EPS15/15L1 provide the structural platform for clathrin-coated pit formation, Numb serves as the cargo adaptor, and ALK is the signaling receptor whose oncogenic potential is dictated by the efficiency of this endocytic machinery [189,196,238,239]. Targeting this axis, either by restoring Numb/EPS15 function or exploiting ALK's dependence on endocytic trafficking offers new therapeutic opportunities beyond kinase inhibition [83,96,238,239].

1.17.1.3- Examples of Numb isoforms role in cancer.

To date, it remains controversial whether Numb functions primarily as a tumor suppressor or as an oncogene. On one hand, Numb downregulation has been reported in multiple tumor types, including breast, colorectal, oral, endometrial, and lung cancers. In these contexts, its tumor suppressor activity is associated with inhibition of the Notch signaling pathway, stabilization of p53, stimulation of Wnt signaling, and regulation of epithelial–mesenchymal transition [158,166,183]. In particular, PTB^{L} isoforms (p66, p72) directly bind MDM2, preventing p53 degradation and preserving its tumor suppressive activity [183]. Loss of these isoforms compromises p53 stability, highlighting how alternative splicing of Numb mRNA serves as a critical determinant of tumor initiation and progression across multiple cancer types [158,159,181].

Moreover, several microRNAs, such as miR-31, miR-146, miR-543, miR-335, and miR-9, enhance oncogenicity by antagonizing Numb [78,243-245]. On the other hand, experimental evidence indicates that Numb can act as an oncogenic modulator in hepatocellular carcinoma, lung adenocarcinoma, and squamous cell carcinoma, where it promotes cell proliferation, migration, and invasion [246,247]. Thus, a systematic understanding of the context-dependent roles and clinical significance of Numb in diverse cancers is still lacking.

In ovarian cancer (OC), aberrant regulation of Numb splicing is driven by the serine/arginine-rich splicing factor 9 (SRSF9), which is upregulated and correlates with

poor prognosis [234,248]. Mechanistically, SRSF9 recognizes non N6-methyladenosine (m6A) modified Numb mRNA and promotes retention of exon 9 generating oncogenic isoforms that sustain Notch signaling and tumor growth [248,249] .

Importantly, m6A modification acts as a safeguard against this process: an m6A motif at the 5′ terminal of Numb exon 10 recruits the m6A reader HNRNPA2B1, which competitively binds Numb mRNA and prevents SRSF9-mediated splicing. Experimental depletion of SRSF9 or antisense oligonucleotide-mediated correction of Numb splicing effectively suppresses OC progression in vitro and in vivo, highlighting a critical m6A-SRSF9-Numb axis that contributes to tumorigenesis and represents a potential therapeutic target [234,248,249].

In breast cancer (BC), Numb's tumor suppressor role is tied to its PTB^{L}-isoforms [159,250]. Their loss leads to reduced p53 stability, increased chemoresistance, and poor outcomes in p53- tumors, making Numb splicing a potential biomarker and therapeutic target in BC [250]. A similar mechanism operates in hepatocellular carcinoma (HCC), where the splicing factor polypyrimidine tract binding protein 1 (PTBP1) drives the inclusion of isoforms with exon 9 [251]. In mice, Numb mRNA has shown the predominate isoforms, PTB^{L} at E11.5 and the PRR^{S} variants becomes dominant gradually during striatal development, showing this differential function [179,208,251]. PTBP1 overexpression promotes invasion and migration, whereas its knockdown restores the tumor-suppressive PRR^{S} isoforms and reduces malignancy, underscoring how splicing factors directly reprogram Numb function [208,251].

Isoform balance also shapes tumor biology in medulloblastoma, where stem-like cancer cells predominantly express p72 isoform while the tumor-suppressive p66 isoform is diminished. Forced expression of p66 reduces stemness, whereas p72 maintains it, showing how Numb isoform ratios directly influence cancer cell identity [252].

Another example occurs with the RNA-binding protein Quaking-5 (QKI-5), characterized several cancer-associated QKI mutations that cause dysregulation of the splicing of its downstream targets like Numb [209,253]. QKI is frequently downregulated and exhibits anti-tumor activity in lung cancer [253,254]. Has been shown that QKI-5 inhibits cell

proliferation in part by regulating the splicing of Numb exon 9 to prevent the inappropriate activation of Notch signaling [253,254]. Mechanistically, QKI-5 competes with a core splicing factor SF1 for binding to the branchpoint to inhibit exon 9 splicing of Numb, promoting PRR^S isoforms and support tumor suppression [254]. Onto the other hand, loss of QKI, often in synergy with factors such as NONO that promote skipping of exon 9, disrupts this balance, driving uncontrolled proliferation [203,255].

Evidence supports the existence of at least two novel human Numb isoforms, p55 (Numb5) and p54 (Numb6), which arise from alternative splicing that excludes exon 7 of the human Numb gene, thereby reducing their ability to antagonize Notch signaling [156,252]. These isoforms are transient and rarely expressed but are detected in cell types with strong polarity and migratory behavior, such as human amniotic fluid cells, glioblastoma, and metastatic tumor cell [156,197,252]. Structurally, compared to the canonical isoforms, p55 and p54 both lack exon 7 resulting in a shortened C-terminal tail and a truncated PRR domain, with p55 and p54 carrying a PTB^L and PTB^S variant respectively [156,197].

Functional studies show that Numb p55 and p54 promote cytoskeletal remodeling and migratory behaviors, with Numb p55 inducing lamellipodia and Numb p54 driving filopodia. Both dynamic formation are essential for processes such as tissue morphogenesis, wound healing, and cancer cell invasion through interactions with proteins such as cell division control protein 42 homolog **(**CDC42), vimentin, and IQ motif-containing GTPase-activating protein 1 (IQGAP1) [156].

Their overexpression in mouse models is sufficient to trigger tumorigenesis, and in breast cancer cells Numb p54 enhances epithelial-to-mesenchymal transition (EMT) via upregulation of Slug, loss of E-cadherin, and activation of Akt signaling, resulting in increased invasion and migration [197].

Unlike the well-characterized Numb isoforms (p72–p65), which inhibit Notch and repress JAG1 expression, Numb p55 and p54 fail to downregulate JAG1 in glioblastoma [156]. Notably, the high JAG1 levels observed in high-grade gliomas and glioblastoma cells can be significantly reduced by Numb p66 and p65, but not by Numb p55 or p54. Their enrichment in aggressive breast and brain tumors suggests that Numb p55 and p54 function as dominant-negative isoforms, positioning them as potential biomarkers and therapeutic targets in cancer [156,197]. Clinically, elevated Numb p55 or p54 expression correlates with higher tumor grade, underscoring their contribution to tumor progression, although the regulatory mechanisms driving their splicing and their precise roles across cancer types remain to be fully elucidated [156,197].

The emergence of oncogenic isoforms such as Numb p55 and p54 further underscores the plasticity of Numb's role in cancer, highlighting isoform regulation as both a biomarker of prognosis and a promising therapeutic entry point for restoring its tumor-suppressive functions [209,248,256].

1.18- Numb and main pathways regulation.

1.18.1- Numb and Notch.

The Notch signaling pathway is a highly conserved developmental network involved in cell fate determination, homeostasis and regulation of the proliferative/differentiative balance during development and in adult tissue homeostasis [58,75,108,145,146,257].

During mammalian neurogenesis, cell fate decisions are tightly regulated by the interplay between Notch signaling, Hes transcriptional dynamics, and Numb-mediated inhibition [75,146,258].

Notch signaling functions as an essential mechanism to direct cell fate decisions of neighboring cells through cell-cell physical interactions, it binds directly to ligands of the DSL family (Delta, Serrate, Lag-2; DLL1, DLL2, DLL3, Jagged 1/2 in human, located as integral membrane proteins, on the opposing signal-sending cell 2. Receptor-ligand engagement triggers a cascade of proteolytic cleavage events that concludes with the cleavage of Notch [3,92,259,260]. Activation of Notch in progenitor cells results in nuclear translocation of the Notch intracellular domain (NICD), which associates with the CSL/RBPJk transcription complex to induce expression of hes genes (e.g., hes1, hes5) [58,260,261]. Hes proteins act as transcriptional repressors of proneural genes such as *Neurog2* and *Ascl1*, thereby maintaining progenitor identity [262]. Notably, Hes expression is oscillatory, creating transient periods during which proneural genes can be expressed, allowing progenitors to remain flexible in their differentiation potential (FIG 1.9). Numb, asymmetrically segregated during mitosis, modulates this system by promoting NICD degradation and inhibiting Notch receptor recycling [263-265]. In the Numb-positive daughter cell, reduced NICD levels lead to decreased Hes expression, relieving repression on proneural genes and enabling neuronal differentiation. In contrast, the Numb-negative cell retains high Notch activity and Hes oscillations, preserving progenitor fate [73,89]. This coordinated mechanism ensures that asymmetric division produces one differentiating neuron while maintaining a progenitor pool, with Hes oscillations providing temporal control over the precise timing of proneural gene activation (FIG 9) [125,266].

Through these mechanisms, Numb functions as a molecular sensor that fine-tunes Notch activity. This regulation is particularly relevant during asymmetric cell divisions of stem and progenitor cells, where Numb partitioning ensures that one daughter cell remains responsive to Notch while the other does not, thereby establishing distinct cell fates [28,73,89,142,158,166,267].

Beyond its developmental role, dysregulation of the Numb-Notch axis is implicated in multiple cancers, including colon, pancreatic, lung, breast, acute myeloid leukemia, and glioblastoma, highlighting Numb's tumor suppressor function in mammals [158,268-270]. Together, these findings emphasize that precise control of Notch signaling by Numb I essential for proper cell fate specification and tissue homeostasis, although many context-dependent aspects remain to be fully elucidated.

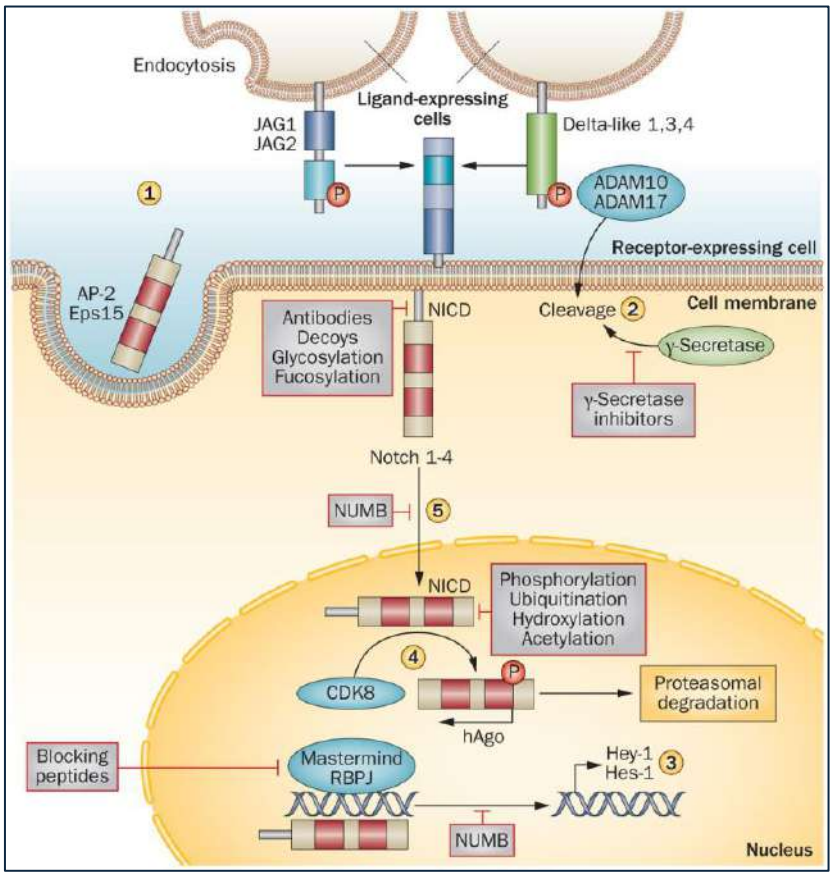

Figure 9: Inhibition of Notch pathway by Numb [102].

Numb interacts with AP-2 and Eps15 to disrupt endocytosis of Notch ligands and receptors (1). The bind ng of ligands (Delta, Jagged [JAG]) to Notch transmembrane receptors 1–4 triggers a series of proteolytic cleavages by ADAM family proteins (ADAM 10, ADAM 17) and a γ–secretase complex that led to the release of the Notch intracellular domain (NICD) (2). The NICD is translocated into the nucleus, interacts with the recombining binding protein suppressor of hairless (RBPJ) transcription factor and the transcriptional activator protein Mastermind to regulate target genes such as Hes-1 and Hey-1. Numb might disturb this transcriptional machinery and inhibit Notch-dependent gene expression (3). Phosphorylation of NICD by CDK8 leads to hAgo-dependent proteasomal degradation of NICD (4). Numb prevents translocation of NCID into the nucleus (5). Strategies under development for the therapeutic inhibition of the Notch pathway are indicated in boxes.

1.18.2- Numb and p53-MDM2.

MDM2 (HDM2 in humans) is an oncogenic E3 ubiquitin ligase that targets the tumor suppressor p53 for proteasomal degradation, thereby promoting tumorigenesis [271]. Beyond its canonical role in p53 regulation, MDM2 can also bind Numb, forming a trimeric Numb-MDM2-p53 complex in epithelial cells (FIG 10) [181,272]. Within this complex, Numb enhances p53 stability by inhibiting its ubiquitination, effectively prolonging its half-life from approximately 60 minutes to 120 minutes and augmenting its transcriptional activity [101,112,143,181,273]. This protective interaction has significant biological consequences: experimental depletion of Numb using short hairpin RNA (shRNA) or small interfering RNA (siRNA) achieving 80-90% reduction in Numb protein levels decreased p53 half-life from ~60 minutes to ~20 minutes and diminished total p53 protein abundance by two-fold [181,274]. Notably, conditional knockouts of Numb-like (Numbl) did not alter p53 stability, indicating that this function is specific to Numb and cannot be compensated by its paralog [275]. Conversely, overexpression of Numb increased p53 half-life from ~60 minutes to 120 minutes and enhanced its transcriptional activity, highlighting Numb's capacity to stabilize and functionally activate this critical tumor suppressor [101,112,143,181,273].

Despite these findings, the molecular mechanism underlying Numb's stabilizing effect on p53 remains incompletely resolved. It is unclear whether Numb acts primarily through direct physical interaction with p53, thereby sterically blocking MDM2 access to ubiquitination sites on p53, or whether it functions indirectly by sequestering MDM2 away from p53, reducing the frequency of MDM2-p53 encounters [181-183,271,272]. Additional complexity arises from reports indicating that activated Notch signaling can stabilize p53 in vitro through Hey1-mediated binding to an MDM2 enhancer, leading to transcriptional repression of MDM2 itself. However, evidence suggests that Notch does not directly participate in the Numb-mediated stabilization of p53, indicating that p53 homeostasis can be controlled through both Notch-dependent and Notch-independent pathways, with Numb operating within the latter [276,277].

In aged skeletal muscle, satellite cells, the resident muscle stem cells exhibit decreased Notch signaling, elevated MDM2 expression, and correspondingly reduced p53 levels [278-280]. Loss of p53 due to increased MDM2 activity contributes to defective spindle assembly and mitotic catastrophe, a form of cell death that occurs when mitosis fails to produce viable daughter cells, ultimately impairing the regenerative capacity of aged muscle [276,281]. Pharmacological activation of p53 using Nutlin-3, a small-molecule inhibitor that disrupts the p53-MDM2 interaction without affecting Numb, successfully reduced mitotic catastrophe and restored the proliferative capacity of satellite cells in aged muscle, demonstrating that restoring p53 activity is critical for maintaining stem cell function during aging [282]. These observations underscore the broader physiological relevance of the Numb-MDM2-p53 regulatory axis, extending its importance beyond cancer biology to encompass tissue homeostasis, stem cell maintenance, and age-related regenerative decline [142,159,181-183].

.

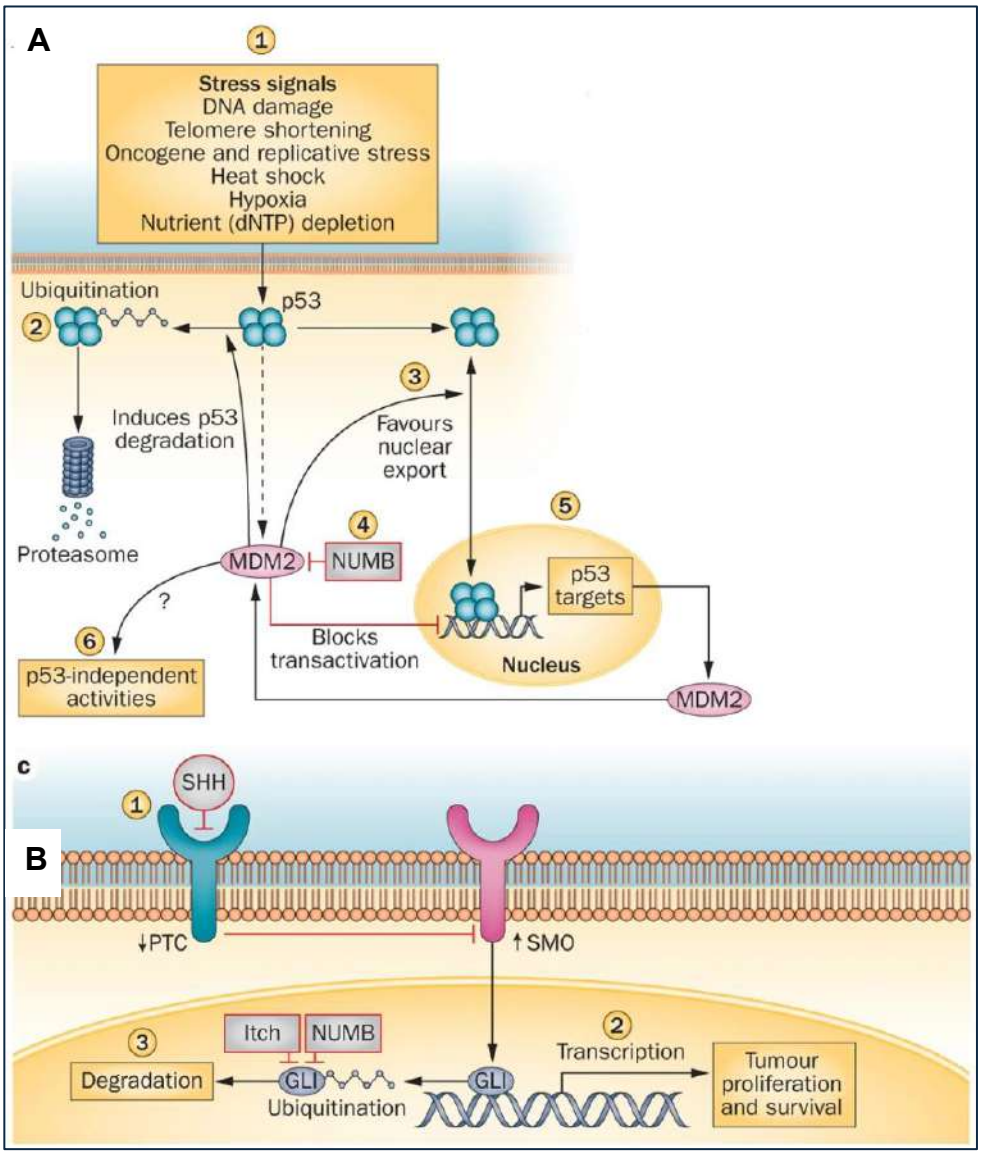

Figure 10: Control of p53 activity by Numb [102].

A) The negative regulatory feedback loop controls p53: p53-dependent transcription of MDM2 promotes p53 degradation (2). MDM2 also inhibits p53 activity by blocking p53 transcriptional activity and favoring p53 nuclear export (3). By inhibiting MDM2 activity, Numb amplifies p53 activity (4). Transcription of target genes promotes p53 tumor-suppressor properties (5). NUMB-MDM2 interaction might also alter p53-independent MDM2 activities (6). B) Regulation of the Hedgehog/Gli pathway by Numb. Sonic hedgehog (SHH) inhibits the repression of Smoothened (SMO) by Patched (PTC) (1). Activation of SMO transmits the signal intracellularly and triggers the nuclear action of the Gli proteins. Gli proteins regulate target genes that participate in tumor proliferation and survival (2). Numb interacts with Itch to promote ubiquitination and degradation of Gli (3). In prostate cancer cells, GLI proteins bind to the androgen receptor and affect androgen signaling.

1.19- Numb and Numb-like (Numbl).

1.19.1- Numb-like.

Numb-like (Numbl) is a paralog of Numb that arose through gene duplication early in vertebrate evolution, sharing significant structural homology including conserved phosphotyrosine-binding (PTB) and proline-rich region (PRR) domains that enable interactions with key signaling molecules and endocytic machinery [42,156,158,267]. Functionally, Numbl acts as a regulator of cell fate decisions, particularly during development, by modulating pathways such as Notch signaling [267]. While Numb and Numbl exhibit overlapping roles in maintaining progenitor pools and controlling differentiation as evidenced by their combined requirement for proper neural tube architecture and cortical lamination in double knockout models, they also possess distinct, non-redundant functions in neurogenesis and other developmental processes [177]. Notably, Numbl exhibits a more restricted expression pattern compared to the ubiquitous distribution of Numb, being preferentially enriched in postmitotic neurons and specific brain regions and shows distinct temporal dynamics during differentiation [267]. These expression differences suggest tissue-specific and stage-specific division of labor between the two paralogs, with Numb specializing in early progenitor maintenance and asymmetric divisions, and Numbl contributing more prominently to neuronal maturation, axonal trafficking, and synaptic function [93].

Phylogenetic and sequence analyses reveal that mouse Numb shares strong sequence similarity (76% identity) with the N-terminal portion of mouse Numbl (amino acids 42-331), while both proteins exhibit 63.7% identity to *Drosophila* Numb (dNumb), indicating evolutionary conservation of core functional domains across invertebrates and vertebrates [6,85].

In addition, its expression is different during development, with ubiquitous Numb expression and more restricted expression of Numbl in the central nervous system [6,85,86,97]. In neurodevelopment, Numb and Numbl antagonize Notch signaling and coordinate the inheritance of fate determinants during asymmetric division, thereby balancing progenitor maintenance with neuronal differentiation [85,93]. Their functions extend beyond development, Numb and Numbl regulate clathrin-mediated endocytosis and trafficking of receptors such as Notch, integrins, and growth factor receptors, processes equally relevant in stem cell biology and tumorigenesis. Dysregulation of either protein disrupts these pathways, contributing to neurodevelopmental disorders, neurodegeneration, and cancer, underscoring their pivotal roles at the intersection of cell fate, signaling, and disease [42,69,94,100,112,156,158,222,228,267,283].

Numb and Numbl have been characterized as tumor suppressor genes as well [267,284], leading to Notch signaling pathway inhibition [267,285] or p53 stabilization [112,178,181,286] . Numb inhibits the Notch pathway through its interaction with ITCH and NICD, labeling NICD for ubiquitination and degradation [102,147,285]. Although this is one of the most known roles of Numb, this protein has also been linked to the Wnt pathway, promoting β-catenin degradation through polyubiquitination [267,287-289].

Previous results obtained by Numbl knockdown by shRNA, with no changes in Numb levels, showed an increment in tumorigenic properties and increased resistance to chemotherapy, with a worse prognosis in breast, lung and colorectal tumors [267]. Importantly, the downregulation of Numbl also triggers Notch pathway activation, further increasing the epithelia-mesenchymal transition (EMT), cancer stem cell (CSC) transcriptional markers and CSC-like phenotypes[180,197,250,267,289,290]. Although both proteins share overlapping functions in maintaining neural progenitors, Numbl alone cannot fully compensate for the loss of Numb, underscoring their partial redundancy and functional divergence during neurogenesis [68,74,86,163,178,267,291]. Single knockouts underscore this divergence: Numb-deficient mice die early in embryogenesis [151,179], whereas Numbl-null mice survive to adulthood without gross brain abnormalities [86,178].

In contrast, double mutants exhibit severe disruption of progenitor maintenance, neuronal differentiation, and tissue architecture, underscoring their cooperative yet non-equivalent roles [85,178,179,292]. In humans, Numb and Numbl proteins share significant structural and functional similarities, yet they also exhibit distinct differences. Both proteins are involved in cell fate determination and play crucial roles in various cellular processes (TABLE 2).

	Numb	Numb-like (Numbl)
Localization	Membrane associated and nuclear	Cytoplasm
Protein domains	PTB domain and PRR.	PTB and PRR with small variation in sequence.
Expression patterns	Widely expressed in various tissues and critical for asymmetric cell division, particularly in neural progenitors.	Restricted expression pattern, mainly in the nervous system.
Functional roles	Exhibits a key role in maintaining stem cell populations, cell fate determination, and differentiation by regulating Notch signaling and endocytosis.	Shares overlapping functions with Numb but thought to have distinct roles in neuronal differentiation and brain development. Numbl may also compensate for the loss of Numb function in certain contexts.
Redundancy and Compensation	There is functional redundancy between Numb and Numbl. Numbl can partially compensate for the loss of Numb in some, but not all, biological contexts.	

Table 2: General comparison between Numb and Numbl [86,163,178,267].

1.20- Integration of Numb as a scaffold protein.

1.20.1- Numb as an integrator of different pathways.

Numb functions as a cargo-selective endocytic adaptor that integrates multiple signaling pathways to regulate cell fate, polarity, and differentiation (FIG 11) [73,125,126,142,150,153]. Its best characterized role is the negative regulation of Notch signaling, achieved by recruiting the E3 ubiquitin ligase ITCH to promote ubiquitination and degradation of the Notch Intracellular Domain (NICD) at the plasma membrane, thereby preventing its nuclear translocation and the activation of Notch target genes, like Hes/Hey family proteins [73,205,207]. All four Numb isoforms suppress Notch1 transcriptional activity but appear to have little or no effect on Notch2 or Notch3 [205].

Furthermore, Numb and Notch are also inversely expressed during the progression of oligodendrocyte differentiation, with higher Numb expression in mature oligodendrocytes [293]. In the developing neocortex, Numb and Notch are expressed in the ventricular zone of progenitors, while Numb-like (Numbl) is expressed in postmitotic neurons in the cortical zone [85]. Numb also plays a role in the proliferation of cardiomyocytes and trabecular morphogenesis through its interaction with Notch1. However, Numb/Numbl can inhibit Notch2 signaling to control heart myocardial compaction [294].

Isoform-specific differences add further complexity: Numb isoforms containing the PRR^{S} suppress Notch signaling, whereas those with the PRR^{L} enhance it [70,93]. Consistent with its inhibitory role, Numb expression inversely correlates with Notch1 in non–small cell lung cancer (NSCLC), where its loss promotes tumorigenesis. In progenitor cells, Numb also acts as a target and modulator of canonical Wnt signaling, being transcriptionally induced by β-catenin to suppress Notch activity and promote differentiation [150]. This Numb-mediated Wnt–Notch regulatory loop is further controlled by androgen receptors, and its disruption contributes to breast and colorectal cancer progression [109,150].

In addition, Numb inhibits the Hedgehog pathway by repressing Gli1 activity in cerebellar granule progenitor cells, thereby limiting stem cell proliferation and promoting differentiation (FIG 11) [295,296]. Interestingly, the Numb paralog Numbl exerts opposite effects, acting as an inhibitor of both Wnt and Hedgehog signaling, suggesting functional divergence following gene duplication [267,288,289,297].

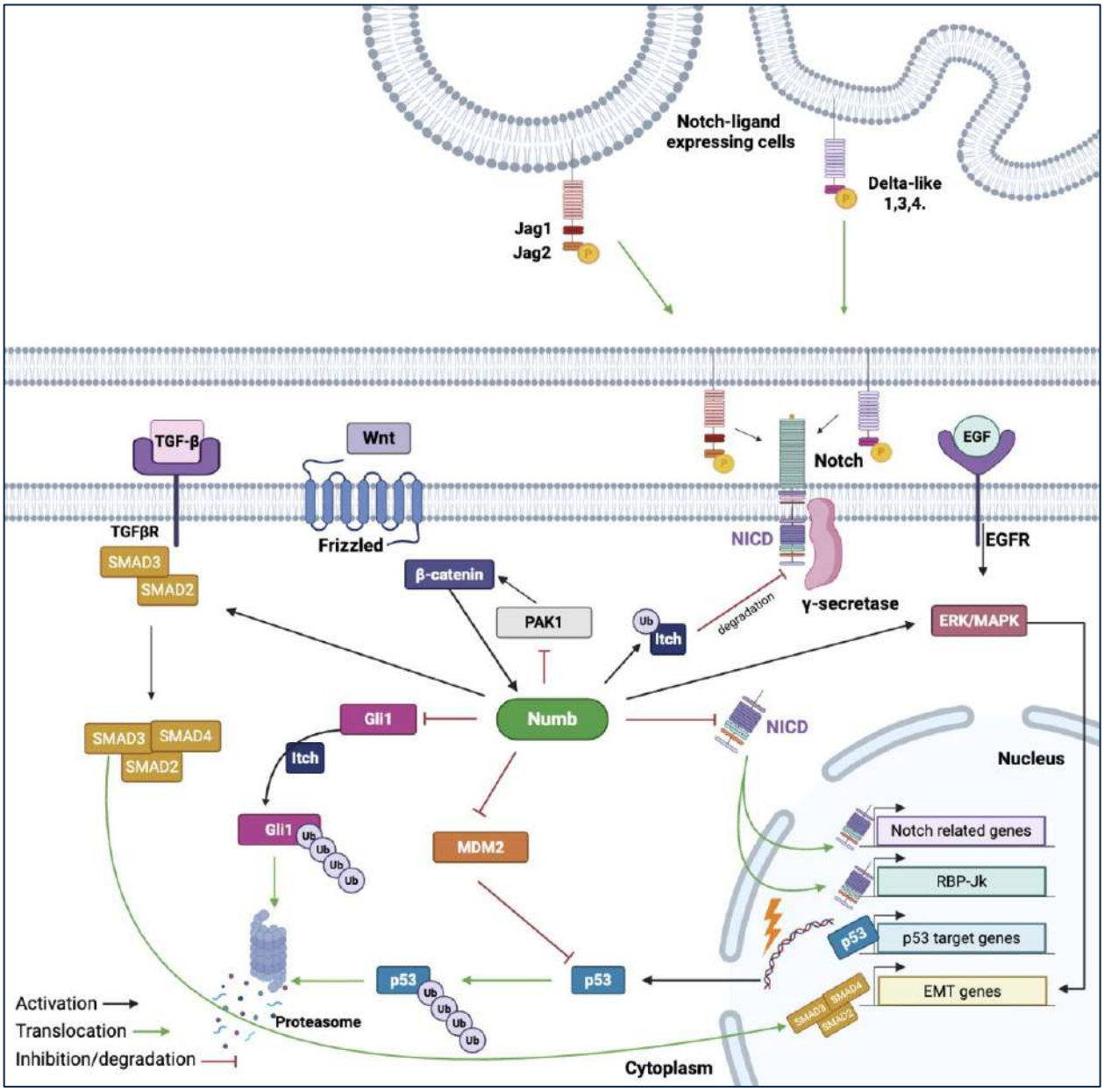

Figure 11: Numb acts as an adaptor protein in multiple signaling pathways.

Numb inhibits Notch signaling by interacting with NICD. Additionally, the interaction between Numb and MDM2 increases p53 stability, allowing transcription of genes related to DNA-damage repair. Furthermore, the PRR^{L} Numb isoform promotes ERK/MAPK signaling and the formation of a SMAD complex, leading to transcription of genes related to EMT. In addition, Numb promotes the ubiquitination and subsequent degradation of both Numb and ITCH through Gli1.

Beyond these developmental pathways, Numb also regulates the stability and activity of the tumor suppressor p53 by forming a tricomplex with p53 and the E3 ligase MDM2, preventing p53 ubiquitination and degradation and thereby sustaining its transcriptional activity [143,181,272,274,277,279,286]. This protective mechanism requires exon 3, which encodes the long PTB^{L} present only in certain Numb isoforms [157,177,219]. Dysregulation of the Numb/p53/MDM2 complex has been implicated in the pathogenesis of several cancers, including breast, kidney, and pancreatic tumors [108,220,221]. Moreover, Numb's stabilization of p53 also promotes asymmetric mammary stem cell divisions, linking its developmental and tumor-suppressive functions [143,222,228,298]. Collectively, these findings highlight Numb as a central node in cellular signaling networks, coordinating receptor endocytosis and degradation with transcriptional regulation to fine-tune the balance between proliferation, differentiation, and tissue homeostasis.

1.21- Numb and epigenetic regulation.

Emerging evidence indicates that Numb may interface with epigenetic regulators to fine-tune gene expression programs during neurodevelopment and stem cell differentiation [295,299-303]. Traditionally recognized as a cell fate determinant acting through endocytic and signaling regulation, Numb's functions now appear to extend into the realm of chromatin control and transcriptional regulation [303-305].

One of the most well-characterized examples of this interplay arises from Numb's capacity to modulate p53 stability. By forming a trimeric complex with p53 and MDM2, Numb prevents p53 ubiquitination, thereby stabilizing and prolonging its activity [181,272]. Since p53 has well-established roles in regulating the transcription of genes involved in chromatin remodeling, DNA methylation, and histone modification, Numb-mediated control of p53 levels may represent an indirect mechanism through which Numb influences the epigenetic landscape of developing cells [78,295,299-303].

In parallel, Numb's crosstalk with the Notch signaling pathway provides another axis through which it may modulate epigenetic states. Notch activation leads to the nuclear translocation of the NICD (Notch intracellular domain), which recruits Mastermind-like (MAML) coactivators and histone acetyltransferases (HATs) to Notch-responsive promoters, activating transcription of target genes such as Hes and Hey [3,58,306,307] . Numb antagonizes this pathway by promoting NICD ubiquitination and degradation, thus indirectly restraining Notch-dependent transcriptional activation [6,85,108,111,124]. Given that Notch signaling impacts chromatin accessibility and histone acetylation at lineage-specific loci, Numb's antagonism may help preserve a transcriptionally poised chromatin state in neural progenitors, allowing appropriate timing of neurogenic gene expression [3,58,306-309].

Furthermore, Numb's influence appears to intersect with the Polycomb Repressive Complex 2 (PRC2), a key epigenetic regulator that deposits the repressive histone mark H3K27me3 through the methyltransferase activity of EZH1 and EZH2 [77,299,310]. PRC2 plays crucial roles in maintaining neural progenitor identity and repressing premature neuronal differentiation [77,311-313]. Preliminary studies have suggested that Numb may modulate PRC2 function indirectly either through Notch-p53 interactions or via the regulation of transcriptional repressors and chromatin-modifying enzymes associated with Polycomb activity [314-317].

For instance, p53 can repress or activate PRC2 target genes depending on cellular context, and Numb's stabilization of p53 may therefore alter PRC2-mediated repression at neurogenic loci, but this relation between Numb-PRC2 hasn't been shown yet [101,112,143,181,183,273-275].

Collectively, these findings point toward a possible multilayered relationship between Numb and epigenetic regulation, in which Numb acts as a signaling integrator that bridges cell fate determinants, transcriptional control, and chromatin-based memory. By coordinating the activity of signaling pathways with chromatin regulators, Numb may ensure that neural progenitors transition through defined transcriptional and epigenetic states, safeguarding the balance between self-renewal and differentiation during neurodevelopment.

1.22- Numb dysregulation.

Numb dysregulation has profound implications for both neurodevelopmental disorders and tumorigenesis, reflecting its central role in controlling cell fate decisions, polarity, and signaling balance [75,112,288,289,297,318-322]. Under physiological conditions, Numb ensures the asymmetric segregation of cell fate determinants during mitosis and the proper modulation of signaling pathways such as Notch, p53, and Wnt, which are essential for maintaining neural progenitor pools and for the ordered progression of neurogenesis [112,181,183,274]. Perturbations in Numb expression, localization, or isoform balance can therefore result in aberrant differentiation, loss of polarity, and uncontrolled proliferation hallmarks shared by both developmental and neoplastic contexts [42,69,94,100,112,156,158,222,228,267,283].

During neurodevelopment, Numb expression is tightly regulated in a spatiotemporal manner. Studies in mammalian neural progenitors show that Exon 9 containing isoforms (Numb Ex9in) are enriched in apical progenitor cells and promote proliferative divisions, whereas Exon 9–skipping isoforms (Numb Ex9sk) predominate in differentiating neurons, favoring neurogenic divisions [109,166]. Disruption of this balance can alter the ratio of symmetric to asymmetric divisions, leading to aberrant neuronal layering, cortical dysplasia, or microcephaly-like phenotypes. Indeed, Numb deficiency or mis-splicing has been linked to defective Notch signaling repression, resulting in prolonged progenitor self-renewal and delayed neuronal differentiation [155,203,217,220,224]. Moreover, because Numb also interacts with proteins involved in vesicular trafficking and endocytosis, its dysregulation may impair receptor turnover, further disturbing the homeostatic control of key neurogenic cues [166,173,196,229,323,324].

Numb’s role extends beyond development into the maintenance of neural homeostasis. Altered Numb expression has been observed in neurodevelopmental and psychiatric disorders, including autism spectrum disorder (ASD) and schizophrenia, where transcriptomic analyses reveal disrupted Numb-related signaling networks [93,325-327]. In these contexts, Numb dysfunction may compromise neuronal polarity and synaptic connectivity, potentially through aberrant Notch and Wnt activity or through disrupted

endocytic recycling of neurotransmitter receptors [142,222,224,328]. Furthermore, Numb's regulatory connection to p53 and epigenetic modifiers such as PRC2 suggests that Numb loss could impact chromatin states critical for neuronal gene expression and plasticity [295,299-305].

In cancer, Numb frequently acts as a context-dependent tumor suppressor [238,239]. Its downregulation has been reported in breast, lung, colorectal, and brain tumors, where loss of Numb leads to enhanced Notch signaling, reduced p53 stability, and increased stemness and proliferation [158,166,183]. In breast cancer, particularly in triple-negative and basal-like subtypes, Numb expression is markedly reduced, correlating with poor prognosis and higher tumor grade [159,228,250]. Mechanistically, Numb loss results in the degradation of p53 through MDM2 activation, suppression of apoptosis, and uncontrolled cell cycle progression [158,159,181]. Conversely, in certain contexts, such as hepatocellular carcinoma or glioblastoma, specific Numb isoforms can acquire oncogenic-like properties, promoting proliferation or migration indicating that Numb's role in cancer is isoform- and context-dependent [103,247,251].

Notably, Numb dysregulation may also affect cancer stem cell (CSC) maintenance, as Numb's control of asymmetric division is crucial for maintaining the balance between CSC self-renewal and differentiation [125,158,329]. Loss of Numb shifts divisions toward symmetry, expanding the stem-like population and contributing to tumor heterogeneity and resistance to therapy [3,100,104,158,329,330]. These effects are often reinforced by the epigenetic rewiring driven by aberrant Notch and Wnt activation, positioning Numb as a molecular hub linking developmental signaling, stemness, and oncogenic transformation [331-333].

These findings underscore those Numb functions as a dual safeguard in both neural development and tumor suppression. Its dysregulation disrupts the delicate equilibrium between proliferation and differentiation, leading to neurodevelopmental abnormalities or malignant transformation depending on the cellular and epigenetic context. Understanding how Numb expression and isoform regulation are altered in disease will be essential to identify therapeutic strategies that restore proper cell fate decisions and signaling balance.

1.23- Numb therapeutics.

Numb has emerged as a promising therapeutic target due to its central role in balancing key signaling pathways that govern cell fate, proliferation, and survival. By antagonizing Notch activity, stabilizing p53, and modulating endocytic trafficking [75,101,112,157,181,183,273]. Numb functions as a critical tumor suppressor in several cancers [158,166,183]. At the same time, its context-dependent actions where certain isoforms or post-translational modifications can promote oncogenic signaling highlight the complexity of targeting Numb [158,159,181] . These dual roles position Numb as both a potential biomarker and a therapeutic node, where strategies aimed at restoring its tumor-suppressive functions or selectively modulating isoform activity could open new avenues for cancer treatment and regenerative medicine [102,222,224,225,237,242,247,297].

Neurodevelopmental disorders (NDDs) and cancer, though clinically distinct, share common biological underpinnings involving disruptions in cell growth, proliferation, and differentiation [318,322] . Both conditions are influenced by mutations in key signaling pathways such as PI3K/mTOR, MAPK, Wnt, and Notch, as well as by transcription factors and chromatin remodelers that regulate gene accessibility during development [75,112,288,289,297,318-321]. Large-scale genetic studies reveal that cancer driver genes are enriched in damaging de novo variants in NDD patients, and de novo mutations are disproportionately found in cancer-related genes [320]. Epidemiological evidence further supports this overlap, with several cohorts showing increased cancer risk in individuals with NDDs, though findings are not always consistent. Taken together, these data suggest that the same genetic and molecular pathways, depending on context, may bias cells toward uncontrolled proliferation in cancer or impaired differentiation in NDDs, highlighting a fundamental mechanistic link between the two disease groups [318,320,322].

Beyond NDDs, given that EAAT3/SLC1A1 is one of the strongest and most consistently replicated genetic risk factors for obsessive compulsive disorder (OCD), the identification of Numb as a key regulator of EAAT3 endocytosis offers a new mechanistic framework for therapeutic investigation [334-336]. By binding the *YxNxxF* sorting motif of EAAT3, Numb controls the balance between intracellular retention and surface availability of this glutamate transporter, an especially relevant process in postsynaptic neurons where EAAT3 uptake of glutamate and cysteine shapes synaptic excitability and redox homeostasis [173,229,336,337]. Dysregulated EAAT3 trafficking has been proposed to alter glutamatergic tone, a central neurobiological feature of OCD [334,335]. Therefore, targeting Numb or modulating its interaction with EAAT3 may represent a novel therapeutic strategy, either by enhancing surface EAAT3 to increase glutamate clearance or by correcting aberrant endocytic cycling associated with disease variants. Using Numb as an entry point to manipulate EAAT3 localization and function could thus provide a powerful experimental approach to dissect glutamate-driven circuitry changes in OCD and identify new intervention points for restoring synaptic homeostasis.

This duality emphasizes the importance of dissecting isoform-specific and context-dependent functions before any clinical translation [166]. Modulating Numb activity either restoring its tumor-suppressive roles in cancers where it is lost, or inhibiting its pro-tumorigenic functions where it is overexpressed represents a promising but challenging therapeutic strategy [101,158,159,181,228,288,289]. In parallel, its role in maintaining neural progenitors and regulating neurogenic niches suggests potential applications in regenerative medicine, where fine-tuning Numb activity could influence stem cell balance and tissue repair. Collectively, these insights position Numb, and potentially its paralog Numbl, as attractive yet complex therapeutic targets across cancer, neurodevelopmental disorders, and degenerative disease [14,19,22,29,42,68,338,339].

Some work in placental biology exemplifies the importance of isoform discovery and functional characterization for therapeutic translation [160]. For the first time, Numb expression was characterized in the human placenta and invasive extra villous trophoblasts (EVTs), leading to the identification of three novel isoforms (Numb 7-9) [160]. Isoform-specific assays revealed distinct functional consequences: p72-Numb1 promoted EVT migration, p66 and p65 enhanced apoptosis and constrained invasion, while others such as Numb8 appeared neutral [160].

These findings highlight how Numb isoforms fine-tune the balance between proliferation, migration, and survival, not only during placental morphogenesis but potentially also in other developmental systems [158,160,166]. From a therapeutic perspective, the ability to selectively modulate isoform activity could allow targeted interventions in conditions ranging from pregnancy-related disorders to neurodevelopmental disease [69,72,155,156,160,225,297].

Isoform divergence also shapes tumor biology. In medulloblastoma (MB), Numb p66 and p72 were found to have opposing functions: p66 promotes neural differentiation and suppresses stemness, whereas p72 sustains proliferation and EMT traits [252]. This isoform imbalance contributes to MB subgroup heterogeneity, with p66 loss reinforcing Hedgehog pathway hyperactivation in SHH MB [112,252,340]. Importantly, the splicing regulator RBFOX3/NEUN drives the p72-to-p66 switch during differentiation, establishing a feedback loop that could be harnessed therapeutically [206]. Restoring or mimicking p66 activity may counteract Hedgehog-driven tumorigenesis, while inhibiting p72 could limit proliferation. These results highlight the potential of isoform-targeted therapies to overcome the limitations of current pathway inhibitors [252,269,341] .

Beyond cancer, Numb has also been implicated in viral neuropathogenesis [342,343]. During Zika virus (ZIKV) infection, Numb is degraded through the ubiquitin-proteasome pathway, impairing neurogenesis and contributing to congenital Zika syndrome. Mechanistically, Numb loss disrupts Notch, Hedgehog, and WNT signaling, destabilizes p53, and ultimately compromises neural progenitor maintenance. Protecting or restoring Numb stability through proteasome inhibition, blocking viral capsid Numb interaction, or regulating Numb splicing emerges as a potential strategy to mitigate ZIKV-induced developmental defects. This highlights how Numb centered therapeutics could extend beyond oncology into infectious and developmental medicine [342].

Finally, Numb's involvement in a novel Rab4a-Numb-Notch1-Rac1-Sox2 axis further emphasizes its centrality in cancer stemness regulation [344]. Here, Numb acts not only as a regulator of Notch degradation but also as a transcriptional controller of Notch1, placing it at the core of an oncogenic program linking vesicular trafficking to stem cell identity. Intervening at the level of Numb within this pathway offers the possibility to simultaneously dampen Notch, Rac1, and Sox2 driven self-renewal a unique approach to targeting cancer stem cells and reshaping the tumor microenvironment [344,345].

In conclusion, Numb isoforms act as a molecular switch between tumor suppression and oncogenesis, neuroprotection and neurotoxicity, invasion and constraint. Their diversity and regulation by alternative splicing make them promising-yet complex therapeutic targets. Future strategies will require isoform-specific precision, balancing restoration of tumor-suppressive and differentiation-promoting functions with inhibition of pro-tumorigenic or pathogenic activities. This paradigm situates Numb at the forefront of next-generation therapeutics, bridging oncology, developmental biology, regenerative medicine, and virology.

Despite our growing understanding of the cellular and molecular mechanisms governing mammalian neurogenesis, the precise roles of key cell fate determinants during cortical neuronal differentiation remain incompletely understood. Among these determinants, the evolutionarily conserved protein Numb, and its alternatively spliced isoforms have emerged as critical regulators of asymmetric cell division and cell fate specification [6,58,105-108,166]. Originally identified as an intrinsic determinant segregating asymmetrically during mitosis, Numb functions as an endocytic adaptor protein that modulates multiple signaling pathways, including Notch, Hedgehog, and p53, thereby influencing progenitor maintenance versus differentiation decisions [142,158,166,194,329]. However, the relevance of human Numb during neural commitment or neural differentiation, the specific contributions of individual Numb isoforms to cortical neurogenesis, their temporal expression patterns during the transition from NECs to RGPs to IPCs and neurons, and their functional interplay in regulating neuronal differentiation remain largely unexplored.

This doctoral thesis aims to investigate the role of Numb and its isoforms during cortical neuronal differentiation, addressing fundamental questions about how Numb functions contribute to cell fate decisions, neuronal subtype specification, and the temporal progression of corticogenesis. Through a combination of molecular, cellular, and developmental approaches, this work seeks to elucidate the mechanisms by which Numb isoforms coordinate the balance between progenitor proliferation and neuronal differentiation within the complex microenvironment of the developing cerebral cortex.

CHAPTER 2

II.- HIPOTHESIS AND OBJECTIVES.

HIPOTHESIS.

Numb contributes to the regulation of human embryonic stem cell maintenance and cortical neurogenesis through mechanisms that may involve isoform-specific functions and dynamic subcellular localization.

GENERAL OBJECTIVE.

To elucidate the molecular mechanisms governing Numb-dependent cell fate decisions during human cortical neurogenesis.

SPECIFIC OBJECTIVES.

To define the expression and subcellular localization of endogenous Numb across cellular contexts, from hESC-derived neural populations at distinct stages of cortical differentiation, and to assess how these features are modulated by cell density and developmental state

To determine the epigenetic regulatory landscape of the Numb locus across pluripotent and differentiated neuronal states, and to assess its contribution to Numb expression dynamics during cortical differentiation.

To define the differential roles of human Numb variants by analyzing isoform dynamics during neurogenesis

To establish the functional requirement of Numb during human neurogenesis through the implementation of inducible degradation systems that allow precise temporal control of protein depletion

CHAPTER 3

III.- MATERIALS AND METHODS.

3.1- General Experimental system.

All experiments were performed using human embryonic stem cells (hESCs, H9/WA09) and HEK293T cells as complementary model systems. hESCs were maintained under feeder-free conditions and differentiated into cortical neurons using a modified Dual-SMAD inhibition protocol. HEK293T cells were cultured under standard conditions and used for method optimization and validation experiments.

Cell culture, passaging, and cryopreservation procedures were performed following established protocols to ensure reproducibility and consistency across experiments.

3.1.1- Human Embryonic Kidney 293T (Hek293T) cell culture.

Human Embryonic Kidney 293T (HEK293T) cells were utilized as a model system to establish and optimize basic tissue culture handling techniques, as well as to perform preliminary assays for antibody expression and validation. Cells were cultured in Dubelcco's modified Eagle's medium (DMEM) (GIBCO, Invitrogen, USA), supplemented with 10% (v/v) heat-inactivated Fetal bovine serum (FBS), 100 U/ml penicillin and 100 µg/mL streptomycin.

3.1.2- Human Embryonic Stem Cell (hESC) culture and maintenance.

Human embryonic stem cell (hESC) lines, including WA09 (H9), Hes5::GFP, and DLL1::GFP, were obtained from the ReinbergLab These reporter lines were originally generated by the PlacatonakisLab at New York University (NYU).

Human embryonic stem cells (hESCs) were cultured on plates coated with Matrigel (Corning, Cat. No. 354234) in Nutristem (NS) medium (Sartorius, Cat. No. 05-100-1A) under feeder-free conditions. To prepare the coating solution, Matrigel (10 mg/mL) was thawed overnight at 4°C and diluted 1:20 in cold DMEM/F12 medium, yielding a final concentration of approximately 0.5 mg/mL. The diluted solution was aliquoted and stored at –20°C until use. Prior to coating, Matrigel aliquots were thawed on ice and further diluted 1:1 with DMEM/F12 to obtain a working concentration of 0.25 mg/mL (equivalent to a 1:40 dilution). 10 cm plates were coated with 4 mL; 15 cm plates were coated with 7 mL of diluted Matrigel and incubated for 1 hour at 37°C. The coating solution was then aspirated, and plates were rinsed once with 2 mL of DMEM/F12 before seeding. It is important to note that Matrigel concentrations may require optimization depending on the cell line or differentiation protocol used.

For cell thawing, frozen hESC vials were rapidly thawed and resuspended in 3 mL of pre-warmed Nutristem supplemented with the ROCK inhibitor Y-27632 (Tocris, Cat. No. 1254) at a final concentration of 10 µM (1:1000). The cells were centrifuged at 1100 rpm for 3 minutes, the supernatant was removed, and the pellet was resuspended gently in 1 mL of Nutristem.

The suspension was plated dropwise onto the Matrigel-coated 10 cm dishes containing 7 mL of Nutristem with ROCK inhibitor. The medium was replaced daily, gradually increasing the volume of Nutristem according to cell confluence. Typically, cultures at 70–80% confluence required 13 mL of fresh medium. hESCs were passaged every 4–7 days, depending on the cell line, confluence, and experimental purpose.

3.1.3- Passaging and cryopreservation of hESCs.

At 80–90% confluence, cells were passaged using TrypLE Express (ThermoFisher Scientific, Cat. No. 12604-013) or Dispase (Stemcell Technologies, Cat. No. 07923). The choice of reagent depended on the experimental purpose: for neural differentiation, cells were typically split 1:1 or used directly from the existing plate; for chromatin immunoprecipitation sequencing (ChIP-seq) experiments, cells were split 1:4 using TrypLE to promote expansion; and for routine maintenance, splits ranging from 1:5 to 1:7 were performed.

For TrypLE-based passaging, culture medium was removed, and 1 mL of TrypLE Express containing ROCK inhibitor (Rocki) (1:1000) was added per 10 cm plate. Plates were incubated at 37°C and gently agitated every few minutes. After approximately 10 minutes, most cells had dissociated into single cells. The cells were then collected with 3 mL of DMEM/F12, and the plate was rinsed with an additional 4 mL of DMEM/F12 to recover remaining cells. The combined cell suspension was centrifuged at 1200 rpm for 4 minutes. The resulting pellet was gently resuspended in NutriStem supplemented with ROCK inhibitor and replated at the desired density, typically 4×10^6 cells per 15 cm plate or 1×10^6 cells per 10 cm plate.

For Dispase passaging, 1 mL of Dispase solution (1 U/mL) containing ROCK inhibitor (1:1000) was added per 10 cm plate (helping to promote single colonies formation) and incubated at 37°C, gently agitating every 10 minutes. After 30 minutes, partially detached colonies were rinsed off with DMEM/F12 and transferred to a 15 mL conical tube.

The cell suspension was allowed to settle by gravity for 2 minutes, after which the supernatant was aspirated. The colonies were washed once more with 10 mL of DMEM/F12 and allowed to settle again. The pellet was then resuspended in 2 mL of Nutristem and gently pipetted to break colonies into small clusters resembling fine particulate matter. Cells were typically split 1:6 for passaging or cryopreserved as needed.

For cryopreservation, hESCs were resuspended in Nutrifreeze (Sartorius, Cat. No. 05-713-1C) at approximately 0.5-0.7 mL per vial, corresponding to one-half of a confluent 10 cm plate per vial. Vials were stored in a controlled-rate freezing container at –80°C overnight before transfer to liquid nitrogen for long-term storage.

3.1.4- Differentiation of Human Embryonic Stem Cells (hESCs) into cortical neurons.

Human embryonic stem cells (hESCs) were prepared at approximately 70% confluency prior to differentiation. Plates were pre-coated with freshly diluted Matrigel (1:100 in DMEM/F12 with GlutaMAX) (Gibco,10565042) and incubated at 37°C for 1 hour, using 200 µL for 24-well plates, 1.2 mL for 6-well plates, and 5.5 mL for 10-cm dishes. hESCs were passaged at ~85% confluency to avoid overgrowth, typically splitting one 10-cm plate into three 6-well plates. For passaging, cells were washed once with PBS, incubated with 3 mL TrypLE Express for 3 minutes at 37°C, and resuspended in hESC medium supplemented with ROCK inhibitor (Rocki). Cells were collected, centrifuged at 1000 rpm for 3 minutes, and replated at a 1:12 to 1:18 ratio for maintenance or at 1:3 from a 10-cm plate into 6-well plates for neuronal differentiation. Each 6-well received 3 mL of medium, refreshed the following day, and was cultured for two days before initiating differentiation.

3.1.4.1- Neural induction.

For neural induction (Day 0-9), cells were washed twice with PBS or pre-warmed DMEM/F12 (GlutaMAX) and cultured in 3 mL of N2B27 medium composed of equal parts Neurobasal medium (ThermoFisher, 10888022) (with B27 supplement at a final 1:100 dilution) (ThermoFisher, 12587010) and DMEM/F12 (GlutaMAX) with N2 supplement (final 1:200 dilution) (ThermoFisher, 17502048), supplemented with 1:1000 β-mercaptoethanol (Sigma, 21-985-023).
The medium was further enriched with SB431542 (Tocris, 1614) (10 µM, 1:1000), LDN193189 (Tocris, 6053) (1 µM, 1:1000), and XAV939 (Tocris, 3748) (3 µM, 1:2000). On days 2 and 4, cells were washed and fed with the same N2B27-based medium containing these small molecules. On day 6, XAV939 was withdrawn, and medium was

replaced with N2B27 supplemented with SB431542 (10 µM, 1:1000) and LDN193189 (250 nM, 1:4000). On day 8, 3 mL of fresh N2B27 medium was added to generate conditioned medium, which was collected the following day (Day 9).

3.1.4.2- Neural progenitors and early neurons.

For the transition from neural stem cells (NSCs) to Neural progenitor stage (Day 9-20), Matrigel-coated plates were prepared by incubation at 37°C for 1 hour. On Day 9, conditioned medium was collected, supplemented with Rocki, and cells were washed with PBS before adding 2 mL TrypLE Express per 6-well plate. Cells were incubated at 37°C for 3-4 minutes until partial detachment and gently resuspended in 2 mL of pre-warmed DMEM/F12 (GlutaMAX) per well. The cell suspension was centrifuged at 1000 rpm for 3 minutes, and pellets were resuspended in 1.5 mL of conditioned medium. Cell density was adjusted to 1×10^6 cells/mL in conditioned medium containing Rocki. Cells were plated by carefully pipetting 400 µL per 6-well plate within a pre-drawn circular area using a 5 mL serological pipette and incubated for 15 minutes at 37°C. During this period, differentiation medium was prepared by diluting conditioned medium 1:3 with fresh N2B27 and supplementing with ascorbic acid (Millipore Sigma, 57803) (0.2 mM, 1:1000), BDNF (R&D system, 248-BDB-010) (10 ng/mL, 1:2000), and DAPT (Stem cell technologies, 72082) (10 µM, 1:1000). After 15 minutes, 2 mL of this differentiation medium was gently added to each well. On days 11 and 13, medium was refreshed with N2B27 supplemented with ascorbic acid, BDNF, and DAPT. Cells typically began exhibiting neuronal morphology between days 20-23, and after day 30-35+, mature neurons it can be observed, indicating successful differentiation into cortical neurons.

3.1.4.3- Mature cortical neurons.

In order to obtain a robust population of mature cortical neurons, a few modifications experience-based were made in this protocol. Between days 8-12, basic Fibroblast Growth Factor 2 (FGF2) 20 ng/mL (ThermoFisher, 100-18B) it was added, ascorbic acid it was decreased to 0.1 nM and DAPT it was added immediately after day 20.

3.2- Objective 1: Numb expression and subcellular localization across cellular contexts and neural differentiation

To determine how Numb expression and subcellular localization vary across cell types and cellular contexts, endogenous Numb protein levels and distribution were analyzed in HEK293T cells, human embryonic stem cells (hESCs), and hESC-derived neural populations at different stages of cortical differentiation. Cells were examined under multiple conditions, including varying cell densities and defined differentiation time points, to capture context-dependent changes in Numb expression and localization throughout the transition from pluripotency to neural commitment and maturation.

3.2.1- Immunofluorescence staining.

For immunofluorescence analysis, cells were plated on plates and glass coverslips pre-coated with Matrigel for human embryonic stem cells (hESCs). Once the desired experimental conditions were achieved, culture medium was removed, and cells were fixed with 4% paraformaldehyde (PFA) (Fischer Scientific, 15710) in PBS pH 7.4 (1X) (Gibco, 10010-023) at room temperature for 10–15. Following fixation, cells were washed twice with PBS and permeabilized/blockaded in PBS containing 10% fetal bovine serum (FBS) (ThermoFisher Scientific, 16140071) 1% bovine serum albumin (BSA; filtered) (Sigma Aldrich, 3117332001), and 0.1% Triton X-100 (Sigma, T8787) (PBT solution) for 30 minutes at room temperature. Primary antibodies were diluted in PBT to test different concentrations and incubated with the samples at 4C overnight (ON) in a humidity chamber. The next day, after 3 PBS washes, cells were incubated with the appropriate fluorophore-conjugated secondary antibody (typically 1:500 dilution; Invitrogen) prepared in PBS containing 5% FBS and 1% BSA for 60-90 minutes at room temperature. Nuclei were counterstained with DAPI for 10 minutes during the final PBS wash. Samples were mounted and analyzed. If staining appeared weak or non-specific, antibody concentrations and incubation times were optimized.

3.2.2- Western Blot.

3.2.2.1- Gel preparation.

To resolve proteins of interest, a 10% bis-tris resolving gel was prepared, as this concentration provides optimal separation for proteins in the mid-molecular weight range approximately 20-100 kDa. Gel solutions were freshly mixed using acrylamide/bis-acrylamide (Biorad, 1610156), Bis-Tris buffer, ammonium persulfate (APS) (Sigma, A3678-100G), and TEMED (Biorad, 161-0800). The resolving gel was poured into the casting apparatus and overlaid with isopropanol to ensure a level surface and prevent oxygen inhibition during polymerization.

Following polymerization, the overlay was removed, and a 4% stacking gel was prepared and cast above the resolving gel with a comb inserted to form wells. Degassing of acrylamide solutions and the use of freshly prepared APS/TEMED were employed to ensure consistent polymerization and reproducibility across experiments.

The Bis-Tris gels for protein electrophoresis were prepared as follow:

Component	Stock	8% run	10% run	12.5% run	stacking
1.25 M bis/tris pH 6.7	3.5x	14.3 mL	14.3 mL	18 mL	5.7 mL
Bis/acrylamide	0.8%/30%	13.3 mL	16.6 mL	23.3 mL	3.5 mL
H2O	-	22 mL	18.7 mL	8.1 mL	10.5 mL
APS	10%	450 µL	450 µL	562 µL	200 µL
TEMED	-	50 µL	50 µL	62.5 µL	20 µL
Total		50 µL	50 mL	50 mL	20 µL

3.2.2.2- Sample preparation.

Protein lysates were prepared from cells or tissues using RIPA buffer supplemented with protease and phosphatase inhibitors to prevent degradation.

RIPA buffer			
Component	**Volume**	**Inhibitors**	
HEPES 25 mM	1.25 mL	**Components**	**Volume (1µL)**
NaCl 150 mM	7.5 mL	Pepstatin 1X	1 µL
EDTA 5 mM	0.5 mL	Leupeptin 1X	1 µL
SDS 0.1%	0.5 mL	Aprotinin 1X	1 µL
Deoxycholate	2.5 mL	PMSF 1mM	10 µL
Triton X-100 1%	0.5 mL		
H2O	37.25 mL		
Total	50 mL		

Cells were harvested directly from culture plates using a cell scraper and cold 1X PBS. Lysates were maintained on ice with 1 mL of cold 1X PBS to preserve protein integrity and centrifuged at 1,000 × g for 15 minutes. The resulting pellet was resuspended in 100 µL of RIPA buffer at a 1:1 ratio, mixed gently, and incubated on ice for 10 minutes. Samples were then centrifuged at 13,000 rpm for 5 minutes. The supernatant was transferred to a new microcentrifuge tube, and protein concentration was determined using the Bradford assay (Bio-Rad, catalog #5000205) according to the manufacturer's instructions.

Protein concentrations were determined using a bicinchoninic acid (BCA) assay (ThermoFisher, A53225), and equal amounts of protein were loaded per lane to ensure comparability across samples. Samples were denatured, followed by heating at 95°C for five minutes. This step ensured complete denaturation and linearization of proteins, allowing separation based solely on molecular weight during electrophoresis.

3.2.2.3- Electrophoresis.

The polymerized gels were assembled into the electrophoresis apparatus and filled with (2-(N-morpholino) ethanesulfonic acid) buffer (MES 1X) running buffer. Protein samples and a prestained molecular weight ladder were carefully loaded into the wells. Electrophoresis was conducted at 150 V to allow proteins to migrate through the stacking gel for 1 hour. The run was terminated once the dye front approached the bottom of the gel if extra time it was needed.

3.2.2.4- Protein transfer.

Following electrophoresis, proteins were transferred onto a polyvinylidene difluoride (PVDF) membrane, selected for its high protein-binding capacity and durability. The transfer buffer it was prepared with 20mM Tris pH8, 150 nM of glycine, and 10% of methanol. Prior to assembly, PVDF membranes were activated in methanol and equilibrated in transfer buffer.

The gel and membrane were sandwiched between filter papers and sponges to form the transfer stack, ensuring no air bubbles were present. Transfers were performed using a wet transfer system at 4°C for 90-120 minutes under 100 volts.

3.2.2.5- Immunoblotting.

Membranes were blocked in 2.5% nonfat dry milk prepared in TBST (Tris-buffered saline with Tween-20) for 30 minutes on a rocker at room temperature (RT) for 30 minutes to reduce nonspecific antibody binding. Membranes were incubated with primary antibodies diluted in blocking buffer overnight at 4°C with gentle agitation (see antibody list). After three washes in TBST, secondary antibodies were added (see antibody list) for 60 minutes at room temperature. Membranes were incubated with horseradish peroxidase (HRP)-conjugated. Excess antibody was removed by repeated washes in TBST to reduce background signal.

3.2.2.6- Detection.

Protein bands were visualized using Pierce™ ECL Western Blotting Substrate (ECL) (ThermoFisher, 32106) substrate, which reacts with HRP to produce a luminescent signal. 15 seconds after ECL it was added, membranes were exposed to imaging systems capable of capturing signals within a linear dynamic range. Multiple exposures were taken to avoid signal saturation and ensure accurate quantification. In cases requiring multiplex detection, fluorescently labeled secondary antibodies were used, and membranes were scanned using a fluorescence imager with appropriate filters. Housekeeping proteins such as GAPDH, β-actin and vinculin (see antibody list) were probed as loading controls.

3.3- Objective 2: Epigenetic regulation of Numb

To determine whether Numb is transcriptionally regulated during cortical differentiation, we analyzed chromatin states at the Numb locus.

3.3.1- ChIPseq protocol.

Standard crosslinked ChIP-seq workflows generally require on the order of 10–20 million cells per ChIP reaction to obtain sufficient chromatin for robust immunoprecipitation, particularly for low-abundance factors. To accommodate limited material, a modified low-input protocol using the Diagenode kit (Diagenode, C010101320) it was implemented, which it was optimized for reduced starting cell numbers (100000 cells).

3.3.1.1- Cell culture and differentiation.

Human embryonic stem cells (hESCs), Parental Line (H9) were cultured under feeder-free conditions on Matrigel-coated plates using NutriStem medium. Cells were maintained at 37 °C in a humidified atmosphere with 5% CO_2. The stemness it was confirmed with markers as OCT4.

To generate cortical neurons, hESCs were differentiated following the Differentiation of Human Embryonic Stem Cells (hESCs) into Cortical Neurons (Methods 3.4). Neural progenitors were expanded and matured over ~35 days to obtain a robust cortical neuron population. Neuronal identity was confirmed by markers such as NeuN.

3.3.1.2- Double crosslinking and cell harvesting (Modified from the original protocol).

To stabilize both protein–protein and protein-DNA interactions prior to chromatin immunoprecipitation (ChIP-M), a double crosslinking strategy was employed using disuccinimidyl glutarate (DSG) (Fisher Scientific, C1104) followed by formaldehyde (FA). All reagents were prepared fresh prior to use.

Cells were cultured under standard conditions until reaching approximately 70-80% confluency. For the first crosslinking step, DSG was dissolved in PBS 1X to a final

concentration of 20 mM. The culture medium was aspirated, and cells were incubated with DSG solution at 37 °C for 45 minutes. Following incubation, the DSG solution was removed, and cells were washed once with PBS to eliminate residual crosslinker.
Immediately thereafter, formaldehyde was added directly to the cells at a final concentration of 1% in pre-warmed culture medium. Crosslinking with FA was carried out at room temperature for 10 minutes. The reaction was quenched by the addition of glycine to a final concentration of 125 mM, followed by a 5-minute incubation at room temperature.
Cells were then washed twice with ice-cold PBS, harvested by scraping, and pelleted by centrifugation at 500 × g for 5 minutes at 4 °C. The resulting cell pellets were either processed immediately for chromatin extraction and fragmentation or stored at −80C for later use and 4C to use immediately.

3.3.1.3- Cell lysis and chromatin shearing.

The supernatant was aspirated carefully to avoid disturbing the pellet. Chromatin was then sheared by sonication using the Bioruptor Plus (Diagenode, B01020014). When samples had been processed in standard 1.5-mL tubes, they were transferred into sonication tubes compatible with the device prior to shearing.

After test different conditions of sonication, samples were sonicated for 20 cycles of 30 seconds ON and 30 seconds OFF at High power. After sonication, samples were briefly centrifuged for 15 seconds to collect condensate. The material was transferred into fresh 1.5-mL tubes and centrifuged at 16,000 × g for 10 minutes at 4C. The supernatant containing the sheared chromatin was collected and transferred into new 1.5 mL tubes.

The size distribution of sheared chromatin was assessed using a Fragment analyzer, Agilent High Sensitivity D1000 ScreenTape on a TapeStation. Briefly, 1-2 µL of purified DNA was mixed with the appropriate sample buffer and loaded onto the ScreenTape according to the manufacturer's instructions. Samples and ladder were run using the High Sensitivity DNA protocol. Fragment size was determined from the resulting electropherogram and gel image, with the desired range being 300-600 bp, ensuring efficient immunoprecipitation and library preparation (FIG 15).

The resulting chromatin was used immediately for immunoprecipitation (or stored at –80C). Repeated freeze-thaw cycles were avoided to preserve chromatin integrity.

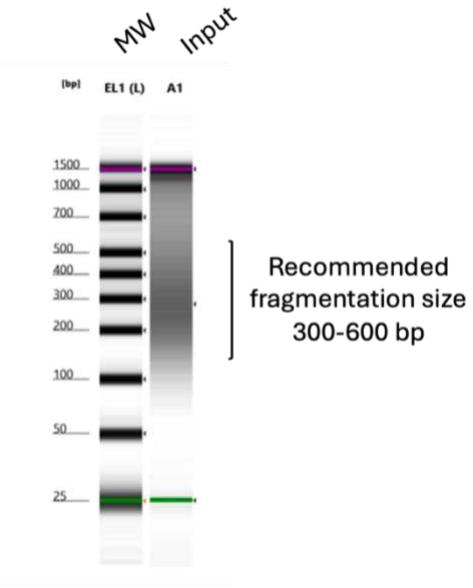

Figure 12: Representative fragment analyzer output.

The expected amplicon size for the targeted Numb region ranges between 300 and 600 bp.

3.3.1.4- Magnetic immunoprecipitation (IP).

The number of IP reactions to be performed, including negative and positive control IPs, was determined. The required volume of DiaMag Protein A-coated magnetic beads was then transferred to a clean 1.5 mL tube, using 10 µL of magnetic beads per reaction.

The beads were washed four times with 50 µL of ice-cold Beads Wash Buffer (tBW1) per reaction. For each wash, tBW1 was added, the beads were resuspended by pipetting up and down several times, and the tubes were placed in the magnetic rack. After allowing 1 minute for magnetic capture, the supernatant was removed. This wash step was repeated three additional times.
After the final wash, the beads were resuspended in Beads Wash Buffer (tBW1) by adding the original bead volume (10 µL per IP). The immunoprecipitation mix was then prepared in 1.5 mL tubes as described in the table below.

Component	Volume per reaction
Shared chromatin	100 µL
ChIP Buffer tC1	100 µL
200X Protease Inhibitor cocktail	0.75 µL

A 20-µL aliquot was set aside as the input sample and kept at 4°C. The specific antibody was then added to each tube, in example, *Drosophila* spike-in was included to provide a baseline expression control for normalization. Furthermore, stemness markers and cortical neuron markers were integrated into the analyses to validate lineage specificity, and activation and repression markers were added to assess transcriptional regulatory states. Subsequently, 10 µL of the washed magnetic beads were added to each reaction. Samples were incubated overnight at 4°C on a rotator.

For the washing steps, the tubes were briefly centrifuged and placed on the 1.5 mL Diagenode magnetic rack. After 1 minute, the supernatant was removed. Then, 100 µL of Wash Buffer tW1 was added, and the beads were gently resuspended by shaking. The samples were incubated for 5 minutes on the rotator at 4C. This washing procedure was repeated once each with Wash Buffers tW2, tW3, and tW4, respectively.

3.3.1.5- Elution, decrosslinking and DNA purification.

After the final wash buffer was removed, 100 µL of Elution Buffer iE1 was added to the beads. The bead pellet was resuspended and incubated for 30 minutes at room temperature on the rotator. The tubes were then briefly centrifuged and placed on the magnetic rack. The supernatant was transferred to a new tube, and 4 µL of Elution Buffer tE2 was added. In parallel, 80 µL of Elution Buffer iE1 and 4 µL of Elution Buffer iE2 were added to the 20 µL input sample. All samples were incubated for 4 hours (or overnight) in a thermomixer at 1,300 rpm and 65C.

Following incubation, the tubes were briefly centrifuged, and 500 µL of ChIP DNA Binding Buffer was added to each sample and mixed gently. The mixture was transferred to the provided spin column placed in a collection tube. Columns were centrifuged at 10,000 × g for 30 seconds, and the flowthrough was discarded.

Next, 200 µL of DNA Wash Buffer was added to each column, followed by centrifugation at ≥10,000 × g for 30 seconds. This wash step was repeated once more. The column was then transferred to a new 1.5 mL microcentrifuge tube, and 10-50 µL of DNA Elution Buffer was added directly to the column matrix. DNA was eluted by centrifugation at ≥10,000 × g for 30 seconds. The DNA concentration was measured, and the samples were stored at 4C for short-term use or at –80C for long-term preservation.

3.3.1.6- Library preparation and sequencing.

Library construction.

DNA was purified from de-crosslinked ChIP samples using the QIAquick PCR Purification Kit and eluted in 31 µL of Elution Buffer (typically yielding ~30 µL). The input DNA (10 µg) was diluted 1:50 following de-crosslinking prior to the start of library preparation.

End-Repair: End-it DNA end generation of the blunt 5' phosphorylated ends.

For 30u ng library	Volume1X (µL)
Decrosslinked sample	13.6
End-repair buffer	2
dNTP 2.5 mM mix	2
ATP 10mM	2
End repair enzyme	0.4
Total	20

Samples were incubated at room temperature for 45 minutes. DNA was subsequently purified using the QIAquick PCR Purification Kit and eluted in 36 µL of Elution Buffer (typically yielding ~34 µL).

Generation of 3' A overhang (Kienow 3'➔ 5').

Component	Volume 1X (µL)
Sample (from step12.1.1)	34
Klenow Buffer	5
dATP 1mM	10
Klenow Exo minus	1
Total	50

Samples were incubated at 37°C for 30 minutes. DNA was then purified and eluted in 14 µL of Elution Buffer.

Adaptor ligation.

The index adapters used in this step were selected carefully to prevent barcode duplication and ensure unambiguous detection across all combinations. As an example, the table below lists the adapter sequences corresponding to one round of ChIP-seq of activation and repression markers analyzed. Every round it was performed in triplicates.

Component	Volume 1X (µL)
Sample (from step 12.1.2)	13
DNA 2X ligase buffer	15
3uM Index mix	0.5
DNA ligase (3U/µL)	1.5
Total	30

	DNA HT Dual Index Kit - 24N (Cat. R400664)				
Libraries	**Barcodes**	**i7 Index name**	**i5 Index name**	**i7 bases for sample sheet**	**i5 bases for sample sheet**
EZH2 hESCs	**1**	N701	S505	TAAGGCGA	GTAAGGAG
H3k27me3 hESCs	**2**	N702	S505	CGTACTAG	GTAAGGAG
H3k27Ac hESCs	**3**	N703	S505	AGGCAGAA	GTAAGGAG
H3K4me3 hESCs	**4**	N704	S505	TCCTGAGC	GTAAGGAG
Spike hESCs	**5**	N701	S506	TAAGGCGA	ACTGCATA
Input hESCs	**6**	N705	S505	GGACTCCT	GTAAGGAG
EZH2 N	**7**	N706	S505	TAGGCATG	GTAAGGAG
H3k27me3 N	**8**	N701	S506	TAAGGCGA	ACTGCATA
H3k27Ac N	**9**	N702	S506	CGTACTAG	ACTGCATA
Spike N	**10**	N702	S507	CGTACTAG	GTAAGAGG
Input N	**11**	N703	S506	AGGCAGAA	ACTGCATA

hESCs: Human Embryonic Stem Cells H9

N: Cortical neurons differentiated from hESCs (H9)

After a 15-minute incubation at room temperature, samples proceeded to AMPure XP bead–based cleanup according to the manufacturer's instructions.

Size selection by AMPure XP beads.

AMPure XP beads were allowed to equilibrate to room temperature for at least 30 minutes prior to use, and fresh 70% ethanol was prepared. DNA samples from Step 12.2.3 were diluted with 70 µL of H_2O. Subsequently, 50 µL of AMPure XP beads (0.5×) were added to each sample, mixed thoroughly by pipetting, and incubated at room temperature for 5 minutes. Samples were placed on a magnetic rack for bead separation (approximately 5 minutes), and the supernatant was transferred to a new tube, discarding the beads. An additional 50 µL of AMPure XP beads (1.0×) was added to the supernatant, mixed by pipetting, and incubated at room temperature for 5 minutes. Samples were again separated on the magnet, washed twice with 70% ethanol, and air-dried for 5 minutes. DNA was eluted in 40 µL of TE buffer and separated from the beads on the magnet.

Post ligation PCR quantification.

4uL of each standard from the KAPA Library Quantification Kit (Roche, KK4824) were used, and the libraries were diluted 1:1000 in the provided dilution buffer prior to quantification. The specific primers were provided by the index kit to detect every adapter.

Component	Volume 1X (µL)
Sample (from step 12.2.4)	4
2X SYBR mix (primers included)	6
H2O	0
Total	10

PCR conditions			
Step	Temperature	Time	Cycles
Initial denaturation	95C	5 min	1
Denaturation	95C	30 s	35
Annealing	60C	30 s	
Extension	60C	15 min	

Library amplification.

The library amplification it was performed according to the following guidelines.

Component	Volume 1X (µL)
Sample (from step 12.2.4)	20
5X Q5 buffer	10
10mM dNTP	1
NEXTflex primer mix	2
Q5 enzyme	0.5
H2O	16.5
Total	50

PCR conditions			
Step	**Temperature**	**Time**	**Cycles**
Initial denaturation	98C	30 s	1
Denaturation	98C	10 s	16
Annealing	65C	20 s	
Extension	72C	20 s	
Final Extension	72C	3 min	1
Hold	4C	∞	

DNA was purified using AMPure XP beads (1.0×) by adding 50 µL of beads to each sample, mixing thoroughly by pipetting, and incubating at room temperature for 5 minutes. Samples were placed on a magnetic rack to separate the beads, washed twice with fresh 70% ethanol, and air-dried for 5 minutes. DNA was eluted in 20 µL of TE buffer, taking care not to carry over beads. The purified libraries were subsequently submitted for sequencing.

Bioinformatic analysis.

Quality control of raw sequencing reads was performed using FastQC. Low-quality reads and adapter sequences were removed using Trimmomatic or Cutadapt. The filtered reads were then aligned to the human reference genome (hg38) using Bowtie2 or BWA. Enriched regions (peaks) were identified with MACS2 using input DNA as the control.

Peak annotation was performed using HOMER or ChIPseeker to identify promoter regions of the Numb gene. Enrichment of transcription factors was visualized using IGV or deepTools. Finally, ChIP-seq data were integrated with RNA-seq datasets to assess the correlation between transcription factor binding and Numb expression levels in human embryonic stem cells and differentiated neurons.

3.4- Objective 3: Isoform dynamic during neurogenesis

To characterize the dynamics of Numb isoform expression during neurodevelopment, we analyzed alternative splicing events across differentiation stages.

3.4.1- Analyzing Numb splicing during hESC/hiPSC to cortical neuron differentiation.

Numb alternative splicing during hESC/hiPSC differentiation into mature cortical neurons using publicly available RNA-seq datasets from two published studies it was performed. The first dataset corresponded to hESCs neuronal differentiation from Leemput *et al.,* 2014 [346], and the second to hiPSC neuronal differentiation from Burke *et al.,* 2020 [347]

3.4.2- Expression of marker genes at different stages.

To validate the differentiation trajectory and characterize the temporal dynamics of lineage commitment, expression profiles of canonical stage-specific marker genes were systematically analyzed across the differentiation time course. A custom visualization function was employed to generate temporal expression plots for key markers representing distinct developmental stages: NANOG (pluripotency marker characteristic of undifferentiated hESCs), SOX1 (neural stem cell marker indicative of early neural commitment), PAX6 (neural progenitor cell marker associated with dorsal telencephalic specification), and SYP (synaptophysin, a mature neuronal marker reflecting synaptic vesicle formation).

Additionally, genes of particular interest to the study, Numb and Numbl (cell fate determinants involved in asymmetric cell division), as well as EZH1 and EZH2 (catalytic subunits of Polycomb Repressive Complex 2 with distinct roles in stem cell maintenance and differentiation), were profiled to investigate their potential regulatory contributions to cortical neurogenesis.

For each gene, normalized expression values were extracted from the DESeq2 object and visualized on both linear and log2 scales to accommodate the dynamic range of expression changes spanning multiple orders of magnitude. Linear scale plots facilitate intuitive interpretation of absolute expression levels and fold-changes, while log2-transformed visualizations enhance the detection of subtle expression shifts in lowly expressed genes and reveal proportional changes more clearly. All generated plots were systematically archived in a designated output directory to maintain a comprehensive record of stage-specific marker validation, providing empirical confirmation that the differentiation protocol successfully recapitulates the expected transcriptional program of cortical neuron development.

3.4.3- Analyzing alternative splicing with a focus on Numb during differentiation from hESCs and iPSCs to cortical neurons.

To investigate post-transcriptional regulation during neuronal differentiation, alternative splicing events were analyzed using rMATS (replicate Multivariate Analysis of Transcript Splicing) output data. Pre-filtered splicing events for the numb gene, encompassing all major splicing event types (exon skipping, alternative 5' splice sites, alternative 3' splice sites, mutually exclusive exons, and retained introns), were systematically retrieved from the rMATS analysis pipeline. Data integrity was verified through programmatic validation of required fields, including event nomenclature, genomic coordinates, and inclusion level values (Percent Spliced In, PSI) across experimental conditions. For each detected splicing event, temporal inclusion profiles were visualized to assess dynamic changes in isoform usage throughout the differentiation time course. A custom plotting function was implemented to generate individual visualizations for each splicing event, displaying PSI values as a function of differentiation stage with appropriate error estimation derived from biological replicates.

To ensure reproducibility and facilitate subsequent analysis, all generated plots were systematically archived in a structured directory hierarchy, with each event assigned a unique identifier corresponding to its genomic position and splicing mechanism. The visualization pipeline incorporated robust error handling to manage events with insufficient read coverage or ambiguous splicing patterns, thereby preventing analysis termination due to individual event failures. This comprehensive splicing analysis enabled the identification of developmentally regulated Numb isoform switches that may contribute to the functional specification of neural progenitors and post-mitotic neurons, complementing the transcriptional profiling data to provide a multi-layered understanding of gene regulatory mechanisms governing cortical neurogenesis.

3.5- Objective 4: Functional requirement of Numb

To determine whether Numb is essential for hESC viability and neurogenesis, we developed inducible degradation systems and performed functional perturbation experiments.

3.5.1- dTAG-Crispr into hESCs.

The key steps are summarized below. For a complete description of the protocol, refer to the original publication from Damhofer *et al.,* 2021 [348,349].

3.5.1.1- Selection of backbones: Expression of Cas9 and donor/cloning vector.

The backbones vectors for sgRNA/Cas9 expression it was px458 and pBlueScript II SK (+) as a cloning or donor vector, were selected and generated as follows in methods (FIG 12).

px458

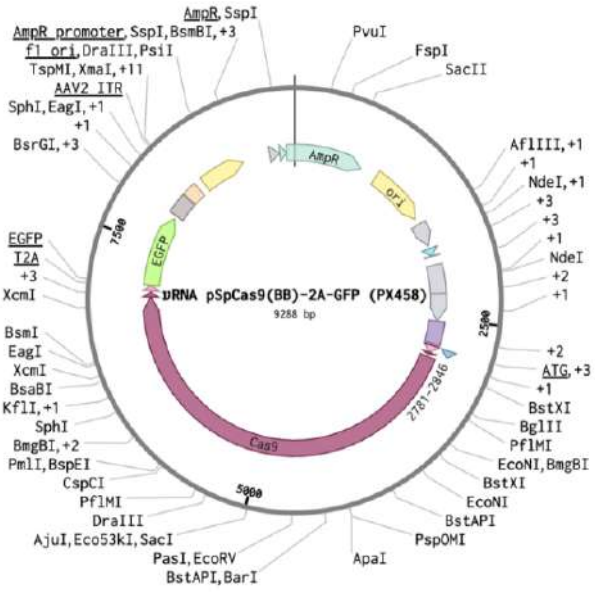

p. Blue Script

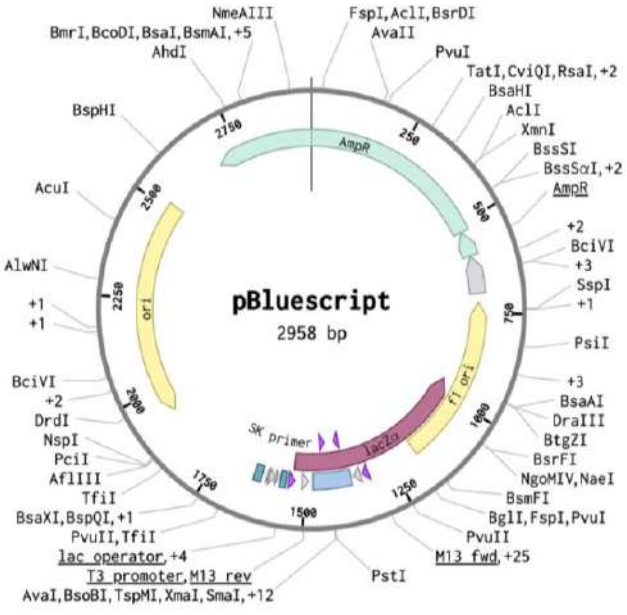

Figure 13: Plasmids used for Crispr reactions.

3.5.1.2- sgRNA design.

All primers in this protocol were designed using the software primer3 (https://primer3.ut.ee/) and IDT resources. The design sgRNAs were performed by IDT, searching the knock-in site, and selecting the appropriate sgRNA according to their score. The insertion site was selected to ensure simultaneous targeting of all Numb isoforms with optimal specificity and efficiency, while preserving the integrity of normal protein translation.

Selection of sgRNA candidates was guided by two primary criteria: efficient cleavage within 10-20 bp of the intended Numb integration site and minimal predicted off-target activity. Based on these parameters, sgRNA-NUMB.1 and sgRNA-NUMB.2 were chosen, each directing Cas9 cutting immediately upstream of the START codon, at the 5′ end of Numb exon 1.

Guide Name	sgRNA sequence (5' -> 3')	PAM	Position	Strand	Efficiency percentile (Doench 2016)	MIT Guide Specificity Score
Exon.1_NUMBdTAG1_sgRNA	GATGAAGAAGGCGTTCGCAC	CGG	chr14:73355648-73355670	minus	69% (56)	97
Exon.1_NUMBdTAG2_sgRNA	TCAATTGGAGCATGCCGGCG	TGG	chr14:73284224-73284246	plus	72% (57)	97

3.5.1.3- Digestion of px458 for sgRNA cloning.

px458 was digested using XhoI and SacI, and the resulting linearized vector backbone was resolved on a 1% agarose gel and purified using the QIAGEN Gel Extraction Kit (Qiagen, 28706). The expected size of the recovered backbone was 9,292 bp (px458-Numb-CCG-Assembly vector). An empty digested vector was processed in parallel to serve as a control.

Component	Volume µL (1X)
10x CutSmart buffer	3
Xho1	1
Sac1	1
10ug of px458	10
ddH2O	15
Total	30

Component	Volume µL (1X)
Oligo mix diluted	2
Pre-cut px458	5
T4 ligase enzyme	1
T4 ligase buffer	1
ddH2O	1
Total	10

3.5.1.4- Oligo annealing and dilution.

The annealing reaction was prepared in a PCR tube, incubated for 5 minutes at the designated annealing temperature, and subsequently cooled to 20 °C at a ramp rate of 5C/min in a thermocycler. Following annealing, the resulting oligo duplexes were diluted 1:20 in nuclease-free water for use in the ligation reaction.

3.5.1.5- Ligation of the annealed oligos into px458 vector.

Once the two sgRNA oligos (ordered from IDT) were annealed, they were ligated into the pre-cut px458 vector, to obtain the px458-Numb-CCG-Assembly vector. The ligation mixture was prepared in a PCR tube, and the reaction was incubated at 20 °C for 2 hours to obtain the px458-Numb-CGG-Assembly plasmid according to the follow steps.

Component	Volume (µL) 1X
sgRNA-NUMB.1 (100 µM)	5
sgRNA-NUMB.2 (100 µM)	1
NEB buffer	1
ddH2O	43
Total	50

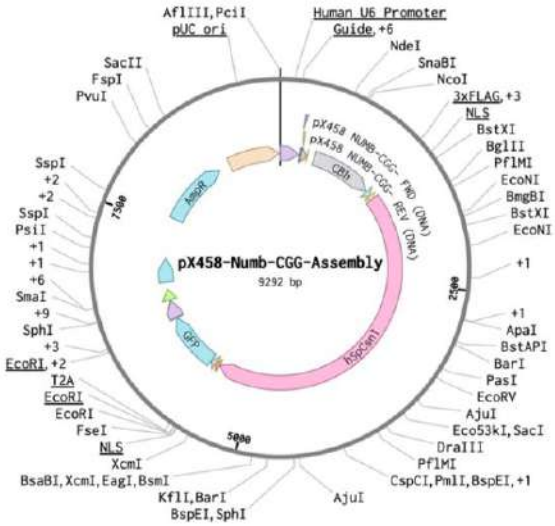

3.5.1.6- Transformation of competent cells.

Chemically competent *E. coli* were transformed with the px458-Numb-CCG-Assembly plasmid by combining plasmid DNA with the cells and incubating the mixture on ice for 30 min. Heat shock was performed at 42 °C for 45-60 s, followed by immediate cooling on ice for 2 min. Cells were then recovered in 300 µL of LB medium at 37 °C with shaking for 1 h to enable expression of the ampicillin-resistance cassette. The transformation was plated onto LB-agar containing ampicillin and incubated overnight at 37 °C. After 24 h, individual colonies were selected, and 50 µL of each culture was supplemented with 50% glycerol and stored at −80 °C to preserve the original clones (FIG 13).

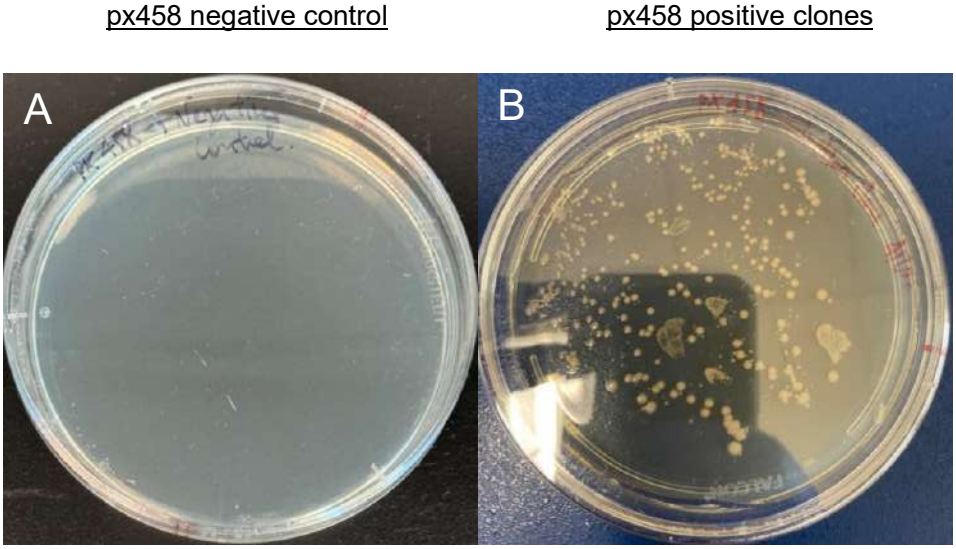

Figure 14: Selection of ampicillin resistant clones (pX458).

(A) Negative control plate seeded with cells carrying px548, which does not confer ampicillin resistance. (B) Colonies transformed with px458, exhibiting ampicillin resistance, and selected for further experiments.

3.5.1.7- Miniprep-Sanger sequencing.

Plasmid DNA was isolated from individual ampicillin-resistant colonies using the QIAGEN Plasmid Miniprep Kit (QIAGEN, 12123) in accordance with the manufacturer's instructions. Briefly, single colonies were inoculated into 5 mL of LB medium supplemented with ampicillin and cultured overnight at 37 °C with agitation. Bacterial cells were harvested by centrifugation, resuspended in resuspension buffer, and subsequently lysed and neutralized. Clarified lysates were applied to silica-based spin columns for plasmid purification. DNA was eluted in nuclease-free water and quantified before downstream applications. Correct insertion of the sgRNA cassette into the px458 backbone was verified by Sanger sequencing using primers annealing to the U6 promoter region of the px458-Numb-CCG-Assembly plasmid

Primers for sequencing
U6F: GATACAAGGCTGTTAGAGAG
U6: CAGTGCAGGGGAAAGAATAGTAGAC

3.5.1.8- Design of the donor sequence for the gBlock system.

The next step involved generating the donor sequence through IDT's gBlock Gene Fragment service. This donor fragment contained the left (L-HA) and right (R-HA) homology arms flanking the FKBP12^{F36V} (dTAG) degron fused to a 2×HA epitope tag, enabling in-frame insertion at the endogenous Numb locus. Homology arms between 400–700 bp are generally recommended for efficient HDR. After testing multiple designs with varying arm lengths and sequence compositions, the configuration that produced the fewest secondary effects consisted of a 445 bp L-HA (blue) and a 501 bp R-HA (green), flanking the FKBP12^{F36V} (black).

This optimized construct constituted the final gBlock-Numb-dTAG donor DNA fragment (FIG 14).

gBlock-Numb-dTAG donor

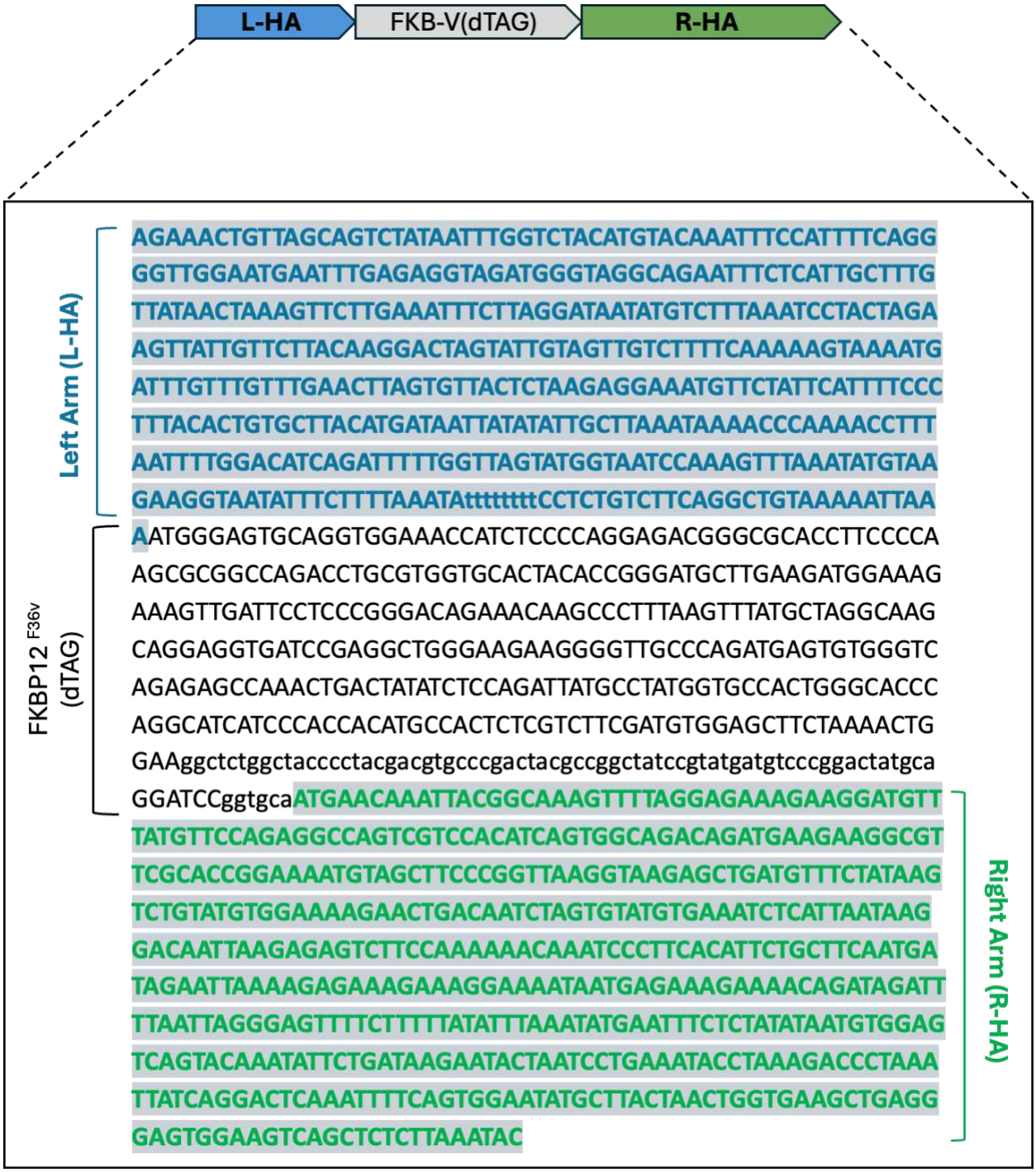

Figure 15: Representative figure of the composition of the donor sequence gBlock-Numb-dTAG.

3.5.1.9- Amplification of the selection cassette.

PCR amplifying the gBlock-Numb-dTAG it was performed according to the following parameters:

PCR primers
NUMB-dTAG-donor-Xho1-F: CGCTCGAGAGAAACTGTTAGCAGTCTATAATTTG
NUMB-dTAG-donor-Sac1-R: CGgagctcGTATTTAAGAGAGCTGACTTCCAC

Component	Volume µL (1X)
dNTPs (10 uM)	1
Taq polymerase	0.5
P1	1.25
P2	1.25
Buffer	5
H2O	16
Total	25

PCR conditions			
Step	Temperature	Time	Cycles
Initial denaturation	95C	3 min	1
Denaturation	95C	15 seg	34
Annealing	60C	15 seg	
Extension	72C	1.20 min	
Final Extension	72C	5 min	1
Hold	12C	∞	

After PCR amplification, the products were resolved on a 1% agarose gel, and the bands were excised, extracted, and purified, using QIAGEN Gel Extraction Kit following the manufacturer guides. The purified fragments were then digested with SacI and XhoI for 2 hours. This digested fragment served as the insert for ligation into the pre-cut pBlueScript vector. The pBlueScript plasmid was treated similarly: digested with SacI and XhoI for 2 hours, resolved on a 1% agarose gel, and the appropriate backbone band was extracted and purified using the recommended kits.

Subsequent cloning steps followed the same procedures as described for px458, including transformation into chemically competent *E. coli*, plating on ampicillin-supplemented agar, and incubation for 24 hours at 37 °C. Plasmid DNA from selected colonies was purified using standard miniprep kits, and the correct insertion was confirmed by Sanger sequencing using the designated primers.

Primers
NUMB-N-dTAG -F: ATTCATTTTCCCTTTACACTGTGC
NUMB-N-dTAG- R: CAGCTCTTACCTTAACCGGGA

3.5.1.10- Delivery of px458 and pBlueScript into the hESCs.

For human embryonic stem cells (hESCs), including the parental line (PL) as well as the reporter lines HES5::GFP and DLL1::GFP, nucleofection via electroporation was chosen to maximize transfection efficiency. For each round of transfection, the following procedure was performed. Cells were first detached using Dispase for approximately 3 minutes to facilitate the generation of single-cell suspensions. Detachment was halted by adding 2 mL of Nutristem medium supplemented with small molecules SB431542 (Tocris, 1614) (10 µM), LDN193189 (Tocris, 6053) (1 µM), and XAV939 (Tocris, 3748) (3 µM) and Rocki. After removing the culture medium, the cells were gently resuspended in the electroporation reaction buffer provided by Neon Transfection kit (Invitrogen, MPK10025R). For each transfection, 4-5 × 10^6 cells per well of a 6-well plate were used. Prior to nucleofection, the residual medium was removed and replaced with 3 mL of nucleofection buffer from the kit. The cell buffer mixture was gently mixed and transferred into a nucleofection tube, ready for electroporation to be performed at 1350v, 30 ms, 1 pulse.

This procedure ensured minimal cell stress while maintaining high viability and single-cell dispersal, both of which are critical for efficient delivery of plasmid DNA or ribonucleoprotein complexes into hESCs. Rocki it was maintained throughout the recovery period to further enhance cell survival and colony formation post-nucleofection.

Mix
1 µg px458
2 µg pBlueScript
250 µL of Nutristem supplemented with small molecules and Rocki
5 million cells

After nucleofection, cells were plated into 6-well plates previously coated with Matrigel for 1 hour. Plates contained pre-warmed Nutristem medium supplemented with Rocki and the small molecules SB431542 10 µM, LDN193189 1 µM and XAV939 3 µM to support cell survival and recovery. The medium was replaced 16 hours post-nucleofection.

Following a recovery period of 3–5 days, ampicillin selection was initiated with gradually increasing concentrations to eliminate untransfected cells and enrich for those expressing the antibiotic-resistance cassette. Once selection was complete, single-cell sorting was performed to isolate cells with the highest GFP expression (top 5%). WT reporter lines (HES5::GFP and DLL1::GFP) were included as controls for GFP baseline expression, while the parental WT line served as a negative control. Sorted cells were replated into 96-well plates coated with Matrigel and containing pre-warmed Nutristem medium supplemented with ROCK inhibitor to promote single-cell survival and colony formation.

3.5.1.11- Screening of the generated clones.

When cells reached approximately 70% confluency, they were trypsinized and resuspended in 100 µL of Nutristem medium supplemented with Rocki and the small molecules SB431542 (Tocris, 1614; 10 µM, 1:1000), LDN193189 (Tocris, 6053; 1 µM, 1:1000), and XAV939 (Tocris, 3748; 3 µM, 1:2000). Genomic DNA was then purified using the QIAGEN Genomic DNA Purification Kit and diluted in TE buffer (10 mM Tris-HCl, pH 8.0; 0.1 mM EDTA). DNA concentration was measured, and PCR was performed to distinguish homozygous and heterozygous clones.

The PCR strategy enabled clear differentiation between tagged and untagged alleles: amplification of the dTAG-integrated allele generated a 574 bp fragment, whereas amplification of the wild-type allele yielded a 350 bp fragment.

The primers selected were:

Primers
P1: ACCCAGGCATCATCCCACCACA
P2: TTCCGGTGCGAACGCCTTCTTC
P3: TGTACAAATTTCCATTTTCAGGGGT

The PCR reaction it was performed as follow

Component	Volume (µL) 1X
10X Taq buffer	2
P1 10 uM	0.5
P2 10 uM	0.5
P3 10 uM	0.5
10 mM dNTPs	0.4
Taq polymerase	0.1
Genomic DNA	2
ddH2O	14
Total	20

PCR conditions			
Step	**Temperature**	**Time**	**Cycles**
Initial denaturation	94C	5 min	1
Denaturation	94C	30 seg	35
Annealing	60C	30 seg	
Extension	72C	3 min	
Final Extension	72C	5 min	1
Hold	4C	∞	

PCR products were resolved on a 1% agarose gel. Homozygous clones were identified by a single band at ~574 bp, while heterozygous clones exhibited two bands corresponding to 350 bp (wild-type) and 574 bp (dTAG-integrated) alleles.

3.5.2 -Inducible Degradation of Numb

Inducible degradation of endogenous Numb was achieved using the dTAG system, in which the protein of interest is fused to the FKBP12^F36V degron and selectively targeted for proteasomal degradation upon treatment with a heterobifunctional small molecule ligand.

hESCs harboring the integration of the FKBP12^F36V tag at the N-terminus of Numb were cultured under standard conditions prior to treatment. For degradation experiments, cells were plated at defined densities to ensure consistent cell confluency across conditions.

The dTAG ligand was prepared as a stock solution in DMSO and diluted in culture medium immediately prior to use. Cells were treated with a range of ligand concentrations, including sub-nanomolar to nanomolar levels, to evaluate dose-dependent effects on Numb degradation. Final DMSO concentration was kept constant across all conditions.

For dose-response experiments, cells were exposed to increasing concentrations of dTAG ligand for a fixed duration. For time-course experiments, cells were treated with a selected concentration of dTAG and harvested at defined time points post-treatment to assess degradation kinetics.

At each condition, cells were collected for protein and imaging analyses. Degradation efficiency was evaluated by Western blot to quantify Numb protein levels relative to untreated controls.

To ensure specificity of the degradation system, parental (non-tagged) hESCs were treated with equivalent concentrations of dTAG ligand as negative controls. Vehicle-only (DMSO) treatments were included to control for solvent effects.

All experiments were performed in biological replicates using independent clones. Treatment durations, concentrations, and cell densities were standardized across experiments to ensure reproducibility.

3.5.3 Rescue Experiments with Numb Isoforms

To assess whether specific Numb isoforms could rescue the phenotype induced by endogenous Numb depletion, individual isoforms (p72, p71, p66, p65) were cloned into lentiviral expression vectors.

3.5.3.1- Lentiviral production and concentration.

Lentiviral particles were produced using a third-generation lentiviral packaging system in Human Embryonic Kidney 293T (HEK293T) cells. This system provides high-efficiency transgene delivery while ensuring replication incompetence through separation of the essential viral components into multiple plasmids. HEK293T cells were maintained in DMEM supplemented with 10% fetal bovine serum (FBS) and 1% Penicillin/Streptomycin and plated in 15-cm dishes to reach 60–70% confluency on the day of transfection. For each 15-cm dish, a total of 21 µg of plasmid DNA was used, consisting of 10 µg of the lentiviral transfer vector (in this case, pLVX-NUMB isoform-SNAP), 5 µg of the envelope plasmid pMD2.G (VSVG), 5 µg of the packaging plasmid psPAX2 (BM10), and 1 µg of pcRev encoding the Rev protein to support gag-pol expression.

Two transfection solutions were prepared using Opti-MEM (Gibco, 31985070) as the base medium. Solution A contained 500 µL of Opti-MEM with the plasmid DNA mixture described above. Solution B contained 500 µL of Opti-MEM with 100 µL of polyethyleneimine (PEI, 1 mg/mL) (ThermoFisher, 040527.22) to achieve a final concentration of approximately 100 µg PEI per transfection. Solutions A and B were combined in an Eppendorf tube, vortexed briefly for 10 seconds, and incubated at room temperature for 15 minutes to allow DNA-PEI complex formation. The transfection mixture was then added dropwise to the 15-cm plate containing HEK293T cells in 15 mL of fresh DMEM.

After 24 hours, the culture medium was replaced with 35 mL of the appropriate medium for the target cell type, in this case, NutriStem medium for subsequent hESC infections to promote optimal viral particle release and reduce PEI toxicity. Viral supernatant was collected 60-72 hours post-transfection and clarified by filtration through a 0.45 µm poly ether sulfone (PES) filter to remove cell debris. The filtered viral suspension was aliquoted and stored at –80°C until use.

3.5.3.2- Lentiviral transduction to hESCs.

Prior to lentiviral transduction, hESCs were cultured on Matrigel-coated plates and allowed to reach approximately 60-80% confluence, ensuring that cells were neither overconfluent nor undergoing spontaneous differentiation. Meanwhile, a single aliquot of the lentiviral stock it was thawed and kept on ice until use. Finally, a stock of Rocki with NutriStem it was prepared to be added during and after transduction to promote the survival of hESCs. The viral particles generated were added directly into the culture plate, containing either each Numb individually or the pool of the 4 of them, including a scramble as an empty vector or control (data not shown). The cells were incubated at 37°C for 16-18 hours (overnight). The media it was changed after 12-24 h to fresh medium with Rocki to remove residual virus/PEI. Puromycin range between 0.5 µg/mL-2 µg/mL it was tested (Invivogen, ant-pr-1) for 36-48 hours post transfection. The positive cells were collected and freeze.

3.5.4- Inducible expression system

Exogenous Numb isoforms were expressed using a doxycycline (DOX)-inducible system based on a tetracycline-responsive transcriptional activation mechanism. In this system, the addition of doxycycline enables the binding of a reverse tetracycline-controlled transactivator (rtTA) to tetracycline response elements (TRE), thereby inducing transcription of the gene of interest.

hESCs were transduced with lentiviral vectors encoding individual Numb isoforms under the control of a TRE promoter. Following transduction, stable cell populations were established and maintained under standard culture conditions.

Doxycycline was added to the culture medium at defined concentrations to induce isoform expression. To achieve controlled expression levels, doxycycline concentration was titrated across a defined range, allowing modulation of protein abundance. Induction time points were standardized across experiments to ensure reproducibility.

Expression of Numb isoforms was validated and compared to endogenous Numb levels in untreated cells. Immunofluorescence was used to assess subcellular localization of the induced proteins and basal expression in the absence of doxycycline was evaluated to assess potential leakiness of the system.

To coordinate exogenous isoform expression with endogenous Numb depletion, the inducible system was combined with dTAG-mediated degradation in a temporally controlled manner.

Three experimental configurations were implemented:

- **Pre-induction:** Cells were treated with doxycycline for a defined period prior to dTAG addition to allow accumulation of exogenous Numb isoforms before endogenous protein degradation.
- **Simultaneous induction:** Doxycycline and dTAG ligand were added concurrently to induce expression and degradation in parallel.
- **Post-degradation induction:** dTAG treatment was applied prior to doxycycline addition to induce isoform expression after depletion of endogenous Numb.

All conditions were performed using standardized treatment durations and concentrations. Control conditions included cells treated with doxycycline alone, dTAG alone, and untreated cells.

3.5.5- Oscillatory expression strategies

Oscillatory expression of Numb isoforms was implemented using a doxycycline (DOX)-inducible system to generate alternating periods of gene induction and repression. Cells were subjected to sequential cycles of doxycycline addition and withdrawal to modulate temporal expression dynamics.

For induction phases, doxycycline was added to the culture medium at defined concentrations for a specified duration to promote expression of the exogenous Numb isoforms. This was followed by washout steps in which doxycycline-containing medium was replaced with fresh medium lacking the inducer to terminate transcriptional activation.

Multiple oscillatory cycles were performed using standardized timing intervals for induction and repression phases. The duration of each cycle was kept consistent across experiments to ensure reproducibility.

Expression dynamics were monitored by Western blot and/or immunofluorescence at selected time points to confirm induction efficiency and protein persistence following doxycycline removal and control conditions included continuous doxycycline exposure (constant induction), absence of doxycycline (no induction), and non-transduced cells.

3.5.6- Morphological analyses

Cellular morphology was assessed to evaluate structural changes following dTAG-mediated degradation of Numb. Cells were monitored using phase-contrast and brightfield microscopy at defined time points after treatment.

Colony integrity was evaluated based on morphological criteria characteristic of human embryonic stem cells (hESCs), including colony compaction, border definition, and cell

density. Changes in colony organization were recorded as loss of defined edges, decreased compaction, and increased intercellular spacing.

Cell detachment was assessed by monitoring the presence of floating cells in the culture medium and reduction in adherent cell density. Detached cells were identified based on rounded morphology and refractile appearance under phase-contrast microscopy.

Apoptotic-like morphology was evaluated based on established criteria, including cell rounding, shrinkage, and membrane blebbing.

Images were acquired using identical microscopy settings across all conditions to ensure comparability. Analyses were performed across multiple biological replicates and independent clones.

Untreated controls and parental (non-edited) cells exposed to dTAG ligand were included to control for potential off-target effects.

3.6- Supporting experimental procedures

3.6.1- Cell cycle arrest protocols for hESCs.

To synchronize human embryonic stem cells (hESCs) at specific phases of the cell cycle, cells were first passaged at a 1:4 ratio from a 15 cm plate at approximately 90% confluence using TrypLE Express and replated into four new 15 cm plates. Media (NutriStem, NS) was changed daily, gradually increasing the volume up until the cells reached 90% confluence, typically within 4-6 days.

S-phase arrest.

Cells were incubated with 22 mL NS supplemented with 1.8 mL of 100 mM thymidine (Sigma, T9250) in phosphate-buffered saline pH 7.4 1X (PBS) (Gibco, 10010-023) (final concentration 7.5 mM; After 20 hours, the medium was removed, and cells were washed twice with 5 mL DMEM/F12, followed by 6 hours in fresh NS. A second thymidine block was applied by adding 1.8 mL of 100 mM thymidine (final 7.5 mM) for 18 hours, until the next day. Cells were then processed as follows:

S-phase early: Media was replaced (without washing) with 16 mL NS with or without SLX (hESCs) treatment for 2 hours before fixation.

S-phase late: Media was removed and cells washed twice with 5 mL DMEM/F12, then incubated with 16 mL NS for 2 hours, followed by 1 mL NS with or without SLX (hESCs) for an additional 2 hours before fixation, totaling 4 hours from thymidine release.

G2 phase: Cells were washed twice with 5 mL DMEM/F12, incubated in 16 mL NS for 4 hours, then treated with 1 mL NS with or without SLX (hESCs) for 2 hours before fixation (6 hours total from thymidine release).

Mitosis and G1 arrest.

Cells were treated with 22 mL NS containing 1.8 mL of 100 mM thymidine (final 7.5 mM) for 20 hours. The following day, the medium was removed, and cells were washed twice with 5 mL DMEM/F12, followed by incubation in 20 mL NS for 4 hours. Nocodazole was added at a final concentration of 100 ng/mL (Sigma M1404; 1:1000 dilution of 100 µg/mL stock) for hESCs, to induce mitotic arrest. After 12 hours cells were processed as follows:

Prometaphase: Cells were treated with 1 mL NS with or without SLX (hESCs) for 2 hours before fixation.

Anaphase-Telophase: Cells were treated with 1 mL NS with or without SLX, then washed twice with 5 mL DMEM/F12 and incubated in 16 mL NS for 20 minutes. Following this, Blebbistatin (Sigma B0560) was added at a final concentration of 5 µM (1:1000 dilution of 5 mM stock) and maintained for 30 minutes (hESCs) before fixation.

G1-phase early: After Nocodazole release, cells were washed twice with 5 mL DMEM/F12 and incubated with 16 mL NS for 2 hours with or without SLX before fixation.

G1-phase late: After Nocodazole release, cells were washed twice with 5 mL DMEM/F12 and incubated with 16 mL NS for 2 hours, followed by 1 mL NS with or without SLX for an additional 2 hours before fixation (total 4 hours from Nocodazole release).

The cells obtained in the different set points were fixated to Immunofluorescence staining.

3.6.2- Electroporation.

For electroporation of Hek293T or hESCs, cells were seeded one day prior to transfection to reach approximately 80% confluency. On the day of electroporation, cells were harvested by removing the culture medium, washing with PBS, and detaching with TrypLE Express for 2-3 minutes at 37°C. Detached cells were neutralized with DMEM supplemented with 10% FBS, centrifuged at 300 × g for 5 minutes, and the supernatant was removed. The cell pellet was resuspended in Buffer R (Neon Transfection Kit) (ThermoFisher, MPK10025) at a density of 5×10^6 cells/mL. For the transfection mix, 1-5 µg of plasmid DNA or 50-100 nM siRNA was combined with the resuspended cells and mixed carefully to avoid air bubbles. Electroporation was performed using the Neon Transfection System, with the 10 µL tip used for 1×10^5 cells and the 100 µL tip for 5×10^5 cells per reaction. Suggested parameters for Hek293T and hESCs were tested. The optimization results in 1150 V, 20 ms pulse width, and 2 pulses, as a best result in terms of effectiveness and safety. Immediately after electroporation, cells were transferred into pre-warmed, antibiotic-free DMEM with 10% FBS (HEK293T) and Nutristem pre-coated plates with Rocki (hESCs) and incubated at 37°C with 5% CO_2. Antibiotics were omitted for the first 24 hours to minimize cellular stress, and transfection efficiency was assessed 24-48 hours post-electroporation using fluorescence or puromycin screening.

IV.- RESULTS.

4.1 Numb expression and subcellular localization across cellular contexts and neural differentiation

4.1.2- Hek293 and Human Embryonic Stem Cells (hESCs) express endogenous Numb.

The aim of this thesis was to elucidate the role of the different Numb isoforms during human neural differentiation, using human embryonic stem cells (hESCs) WA09, also known as H9 as a model base.

As a first approach, Hek293 cells were used to standardize Numb antibodies concentration and observe the endogenous expression of Numb at first by Western Blot The antibodies tested are in Table 3 (TABLE 3).

Antibody anti-Numb	Host type	Dilution 1st antibody	Dilution 2nd antibody	Target
Numb ab4147	Goat Polyclonal	1-2 µg/mL	1:2000 to 1:5000	Synthetic peptide within 600 aa into C-terminus of human Numb.
Numb ab155415	Rabbit Polyclonal	0.5-2 µg/mL	1:2000 to 1:5000	Recombinant fragment within 1-250 aa of human Numb.
Numb PA1-32452	Rabbit Polyclonal	1-3 µg/mL **(discontinued)**	1:2000 to 1:5000	Synthetic peptide within 600-653 aa into C-terminal of human Numb
Numb AF4338	Sheep Polyclonal	1-3 µg/mL	1:2000 to 1:5000	Recombinant fragment within Thr356-Leu592 of human Numb.

Table 3: First batch of primary Anti-Numb antibodies evaluated in this study.

In Hek293 cells, the Numb protein plays as an endocytic adaptor that controls several signaling pathways, especially by influencing the degradation and trafficking of the Notch receptor and the stabilization of the tumor suppressor p53. Numb protein is endogenously expressed in Hek293 cells (FIG 16).

Hek293 cells are highly valued in research for their consistent growth, genetic stability, and exceptional ease of manipulation. They exhibit high transfection efficiency, readily incorporating foreign DNA through a variety of methods, which makes them ideal for gene expression and functional studies. Their robust protein expression capacity allows for high-yield production of recombinant proteins, positioning Hek293 cells as a preferred system for generating biotherapeutics, vaccines, and viral vectors used in both basic and translational research. As a human-derived cell line, they also provide physiologically relevant post-translational modifications, such as glycosylation, which are often lacking in non-human systems like Chinese hamster ovary (CHO) cells. Furthermore, Hek293 cells are adaptable and can be cultured either as adherent monolayers or in suspension, supporting both small-scale laboratory experiments and large-scale industrial production. Importantly, the Numb protein is not essential for Hek293 cell survival or proliferation, which makes this line an excellent model for genetic manipulation studies involving Numb knockout or degradation systems.

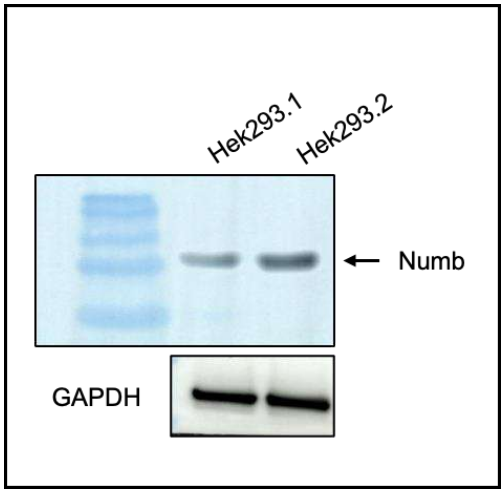

Figure 16: Western blot analysis showing endogenous Numb levels in Hek293 cells.

Lane 1 corresponds to the molecular weight marker; Lanes 2 and 3 represent biological duplicates of Hek293 lysates. A clear Numb-specific band is detected at approximately 75 kDa, confirming robust endogenous expression in this cell line.

One of the main challenges in detecting the human Numb protein lies in the limited specificity of commercially available antibodies toward its distinct isoforms. Most commercial antibodies are raised against epitopes located within regions common to all isoforms, meaning they primarily recognize the full-length Numb p72 protein. Consequently, it is theoretically difficult to discriminate among the four human Numb isoforms (Numb1-4) using these antibodies alone. Nevertheless, some studies have reported by Western blot the detection of two distinct Numb protein bands one migrating around 75 kDa and another around 70 kDa corresponding to two groups of isoforms.

These bands can be categorized based on the presence of alternative phosphotyrosine-binding (PTB) domains: Numb1 (p72) and Numb2 (p66) contain the long PTB domain (PTB^{L}) and migrate at approximately 75 kDa, whereas Numb3 (p71) and Numb4 (p65) possess the short PTB domain (PTB^{S}) and migrate at approximately 70 kDa. Unfortunately, we could obtain at this time, those expecting 2 bands.

The WA09 human embryonic stem cell (hESC) line, also known as H9, is among the most extensively characterized and widely used pluripotent stem cell lines in biomedical research. This line serves as an exceptional model for investigating early human development, lineage specification, differentiation mechanisms, and disease modeling. WA09 cells maintain a stable karyotype over extended passages and exhibit robust self-renewal capacity when cultured under defined, feeder-free conditions. They consistently express the canonical pluripotency markers OCT4 (POU5F1), SOX2, and NANOG, confirming their undifferentiated state. Importantly, H9 cells retain the ability to differentiate into cell types of representatives of all three germ layers ectoderm, mesoderm, and endoderm which makes them particularly valuable for studying human neurogenesis and lineage commitment in vitro.

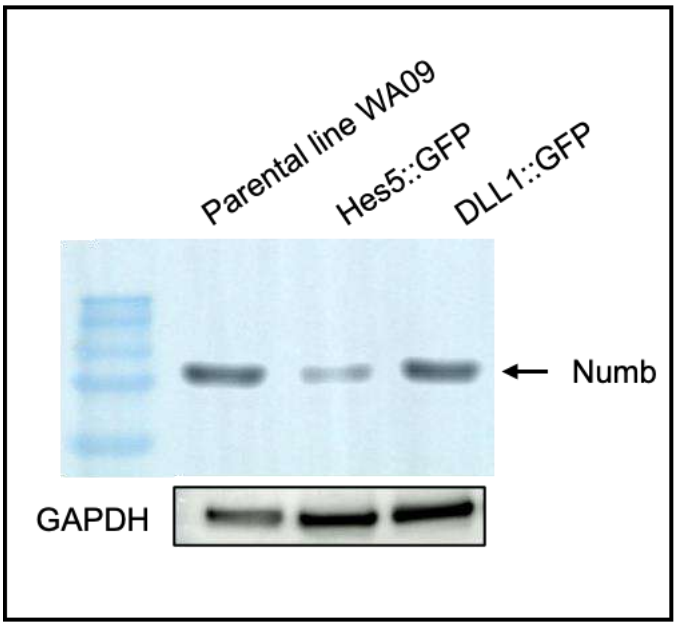

***Figure 17: Endogenous Numb expression in human embryonic stem cell lines*.**

Western blot analysis assessing endogenous Numb levels across multiple hESC backgrounds. Lane 1 shows the molecular weight marker; Lane 2 corresponds to the Parental WA09 (H9) Line; Lane 3 to the Hes5::GFP reporter line; and Lane 4 to the DLL1::GFP reporter line. A distinct Numb band is observed at ~75 kDa in all samples, confirming consistent endogenous expression across these hESC derivatives.

In this study, the WA09 parental line and its DLL1::GFP and HES5::GFP reporter derivatives exhibited comparable levels of endogenous Numb protein expression, suggesting that Numb abundance is not significantly altered by the integration of the reporter constructs. Using the same Numb antibody (ab4145, Abcam), Western blot analysis of undifferentiated hESC cultures revealed a single prominent Numb band (FIG 17). This finding contrasts with reports describing two distinct bands corresponding to different Numb isoform groups, indicating that in hESCs either a predominant isoform is expressed, or the antibody is unable to resolve the isoform-specific differences under the tested conditions.

4.1.3- hESCs Parental Line WA09 (H9): Cell cycle arrest protocols.

To investigate how specific cell cycle phases influence the expression of Numb-related factors and components of the Notch signaling pathway, a cell synchronization protocol was employed. Given that Numb is known to regulate asymmetric cell division and the balance between progenitor self-renewal and differentiation, understanding how it signaling partners vary across cell cycle stages provides key mechanistic insight into neural progenitor behavior.

Parental cell lines WA09 (H9) were synchronized using a double thymidine block to achieve precise arrest and release, allowing controlled progression through distinct cell cycle phases. Samples were collected at representative time points corresponding to prometaphase, S phase, and anaphase–telophase. These stages were chosen because they encompass major checkpoints where fate determinants, including Numb and Notch effectors, are asymmetrically distributed or transcriptionally regulated. Following synchronization, immunofluorescence staining was performed to visualize and quantify the expression and localization patterns of Numb, Hes5, and DLL1 during cell cycle progression. The progression followed the expected pattern described in the literature, with approximately 70% of the cells successfully transitioning through the different stages of the cell cycle, confirming the efficiency and reproducibility of the synchronization protocol.

During neurogenesis, Hes5 and DLL1 serve as complementary markers of the dynamic activity of the Notch pathway, which orchestrates the balance between progenitor maintenance and neuronal commitment. Hes5, a basic helix–loop–helix (bHLH) transcriptional repressor, is a direct target of Notch activation and is typically expressed at high levels in neural progenitor cells (NPCs). Its sustained expression in proliferating progenitors maintains them in an undifferentiated state by repressing proneural genes such as *Ascl1* and *Neurog2*. As the cell cycle progresses toward the G2/M transition and

mitosis, Hes5 expression tends to decrease, coinciding with the onset of differentiation signals. In contrast, DLL1, a canonical Notch ligand, is expressed in cells that are exiting the progenitor state and beginning neuronal differentiation. DLL1's expression increases during late S phase and G2, marking cells preparing to differentiate, and peaks as these cells undergo asymmetric division when one daughter cell retains progenitor identity (via Notch activation through Hes5), and the other initiates a neuronal program.

Preliminary data revealed that Numb localization becomes increasingly polarized as cells progress from prometaphase to anaphase–telophase, consistent with its established role in directing asymmetric partitioning of cell fate determinants. Meanwhile, Hes5 displayed nuclear enrichment during early stages (S phase), suggesting active Notch signaling in proliferating progenitors, whereas DLL1 expression became more prominent at the cell membrane in cells progressing toward cytokinesis, indicating the onset of neuronal commitment (FIG 18).

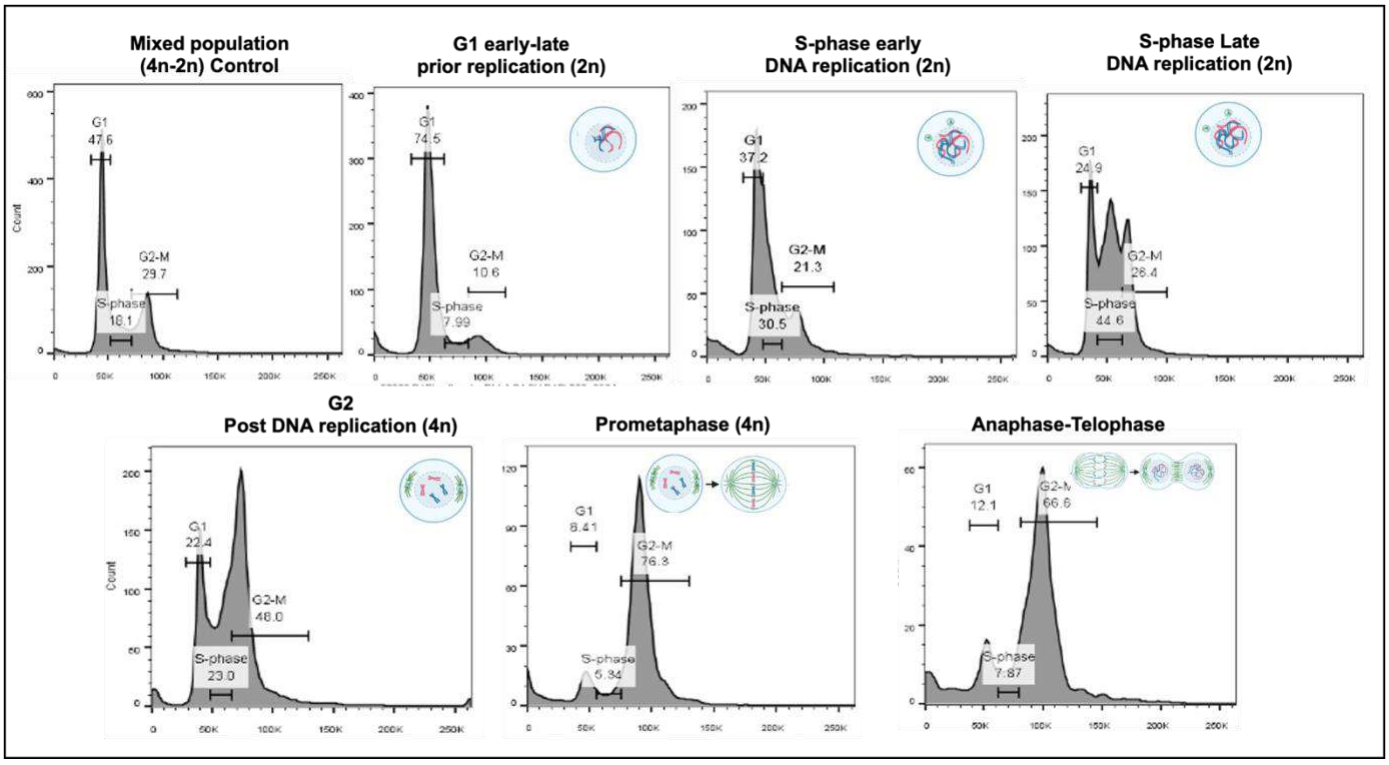

Figure 18: Cell cycle progression of WA09 (H9) hESCs after double-thymidine synchronization.

Flow cytometry analysis of the Parental Line WA09 (H9) following synchronization using a double-thymidine block. The profile illustrates the distribution of cells across G1, S, and G2/M phases.

Following release from the block, the cells progressed synchronously through the subsequent cell cycle phases, as described in the literature. Flow cytometry and microscopy analyses confirmed that approximately 70% of the cell population transitioned through the expected stages of the cell cycle, demonstrating the efficiency and reproducibility of the synchronization procedure.

To examine the relationship between cell cycle progression and neurogenic markers, we evaluated the expression of Hes5, a well-recognized marker of stemness and maintenance of the undifferentiated state, and DLL1, which marks early neuronal commitment. The differential expression of these markers across cell cycle stages provided insight into the dynamic balance between self-renewal and lineage specification.

Consistent with Western blot analyses, multiple anti-Numb antibodies were tested under various experimental conditions (TABLE 4), including different antibody dilutions, fixation methods, and mounting media, to optimize detection by immunofluorescence. Despite these optimizations, antibody performance it could not detect Numb protein using Immunofluorescence assays, underscoring the importance of validation when studying Numb localization and expression during specific cell cycle transitions (Data no shown).

This table summarizes the different Numb antibodies and experimental conditions tested to establish optimal immunofluorescence staining (TABLE 4).

Anti-Numb antibody	Company	Dilutions	Fixation FA%	Mounting media	
ab4147	Abcam	1:50	4%, 5%, 8%	Prolong Dako mounting media	**5-10 µg/mL**
ab155415	Abcam	1:100			
PA1-32452	ThermoFisher	1:200			
AF4338	RD systems	1:500			

		1:1000			

Table 4: Optimization of Numb antibodies for immunofluorescence (IF).

Immunofluorescence failed to reliably detect Numb during the analyzed cell-cycle stages, likely due to the low endogenous expression of Numb in hESCs compared with cancer cell lines, where the antibodies had been originally validated.

DLL1 and Hes5, both tagged with GFP were pretty helpful to identify the transition between different steps. Using as a background marker, Laminin beta 2 (Lmnb2) encodes the β2 chain of Laminin, a heterotrimeric extracellular matrix (ECM) glycoprotein. In hESCs, Lmnb2 expression and deposition are tightly regulated by extracellular cues, cell adhesion receptors, and pluripotency-associated signaling pathways and it can be observed during cell cycle stages.

During the S phase and prometaphase, neural progenitor cells are largely proliferative, maintaining an undifferentiated state. In this context, Notch signaling is active, leading to high Hes5 expression, which represses proneural transcription factors (*Ascl1*, *Neurog2*) and prevents premature neuronal differentiation. Hes5, as a transcriptional repressor, ensures that progenitors remain in the cell cycle and maintain their stem-like identity.

As cells transition through mitosis (anaphase–telophase), particularly in asymmetric divisions, Notch signaling becomes differentially inherited. One daughter cell retains active Notch–Hes5 signaling, preserving progenitor features, while the other cell, which downregulates Notch signaling, begins to express DLL1. DLL1, a Notch ligand, is upregulated in differentiating cells and acts in a lateral inhibition manner to activate Notch in neighboring progenitors, reinforcing their undifferentiated state (FIG 19).

Thus, throughout the cell cycle, Hes5 expression correlates with progenitor proliferation and S-phase activity, while DLL1 expression emerges as cells exit mitosis and commit to neuronal differentiation. Monitoring DLL1 and Hes5 expression across these phases can therefore reveal the timing of Notch pathway modulation that links cell cycle dynamics to neurogenic fate decisions.

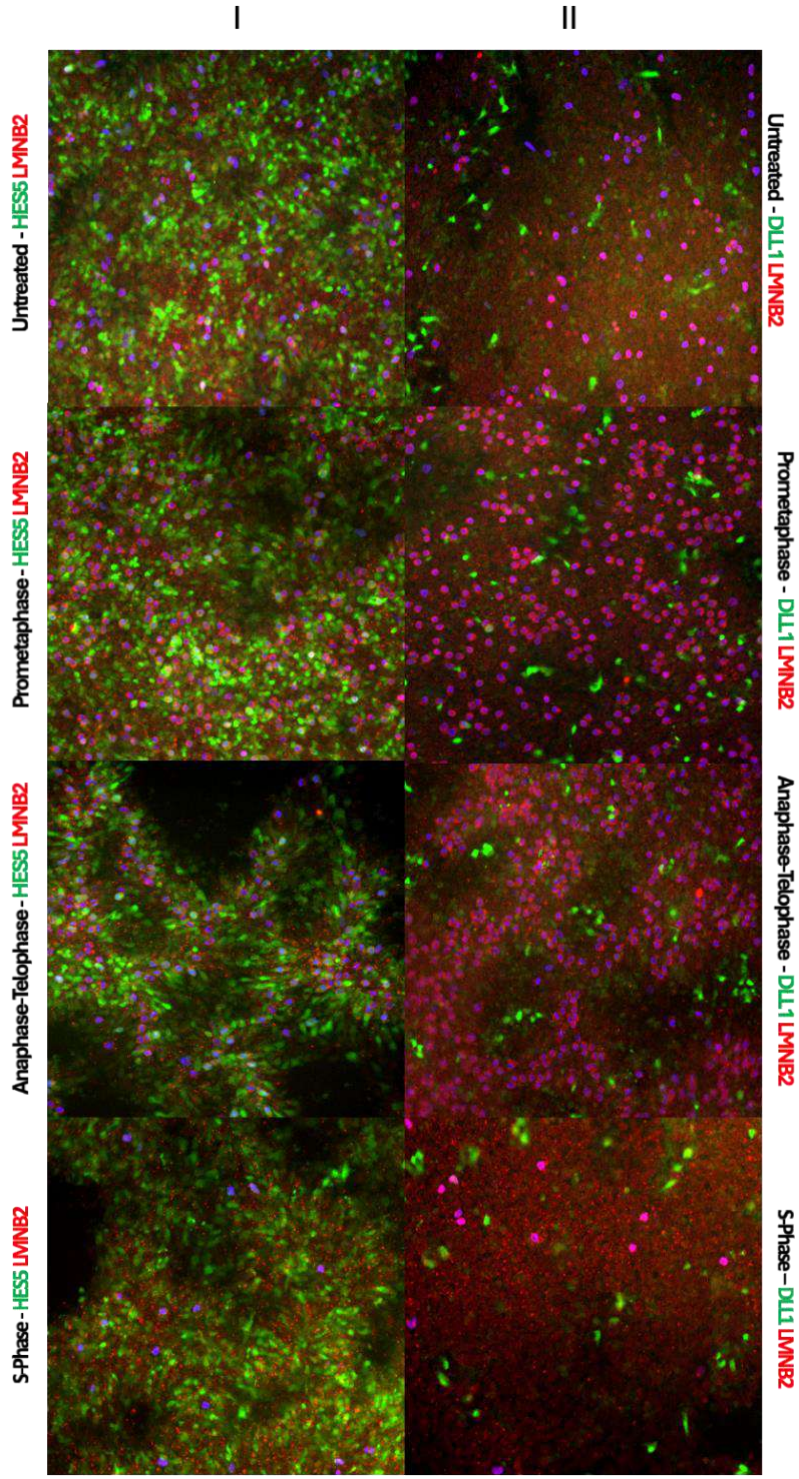

Figure 19: Immunofluorescence of Notch pathway markers during cell cycle modulation.

Immunofluorescence analysis of Notch pathway components Hes5 and DLL1 under cell cycle arrest conditions. Panel I depicts Hes5 expression in proliferating neural progenitors, while Panel II highlights a subset of cells initiating DLL1 expression, indicative of early neural commitment. Lmnb2 was used as a nuclear/chromatin marker to delineate nuclear morphology.

4.1.4- Endogenous Numb expression and localization detected by Immunofluorescence (IF) in Hek293 and hESCs.

A new antibody against Numb became available during the course of this work, and it was tested its ability to detect Numb protein in Hek293 cells and H9 (WA09) human embryonic stem cells (hESCs) by Immunofluorescence (TABLE 5).

Antibody anti-Numb	Host type	Dilution 1st antibody	Dilution 2nd antibody	Target
Numb C29G11	Rabbit Monoclonal	1:50 1:100 1:200 1:500	1:2000 to 1:5000	Synthetic peptide within Ala570 of human Numb.

Table 5: Optimization of Numb monoclonal antibody C29G11 for immunofluorescence.

Using a dilution of 1:50, the antibody successfully detected Numb in both Hek293 cells and hESCs. In Hek293 cells, Numb displayed a predominantly cytoplasmic localization, consistent with previous reports describing Numb as a cytoplasmic adaptor and scaffold protein involved in endocytic trafficking and signaling regulation (FIG 20).

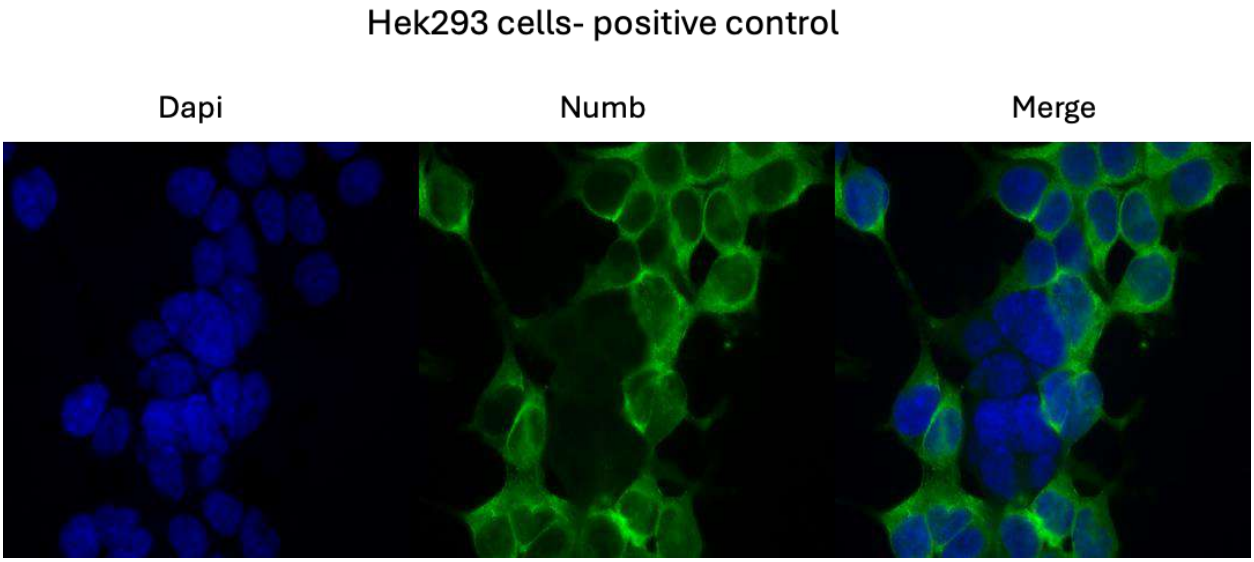

Figure 20: Subcellular localization of endogenous Numb by Immunofluorescence in Hek293 cells.

Immunofluorescence analysis of endogenous Numb expression in human cells. Numb signal (green) is predominantly cytoplasmic, while nuclei are counterstained with DAPI (blue). This staining pattern highlights the cytoplasmic distribution of Numb under basal conditions.

In hESCs, including the parental WA09 line and the Hes5::GFP and DLL1::GFP reporter lines, Numb exhibited a more ubiquitous pattern of distribution, with the majority of the fluorescence signal localized in the cytoplasm, although nuclear staining was also evident in a subset of cells. This broader subcellular localization suggests that Numb may operate in multiple compartments depending on the cellular state or developmental stage (FIG 21).

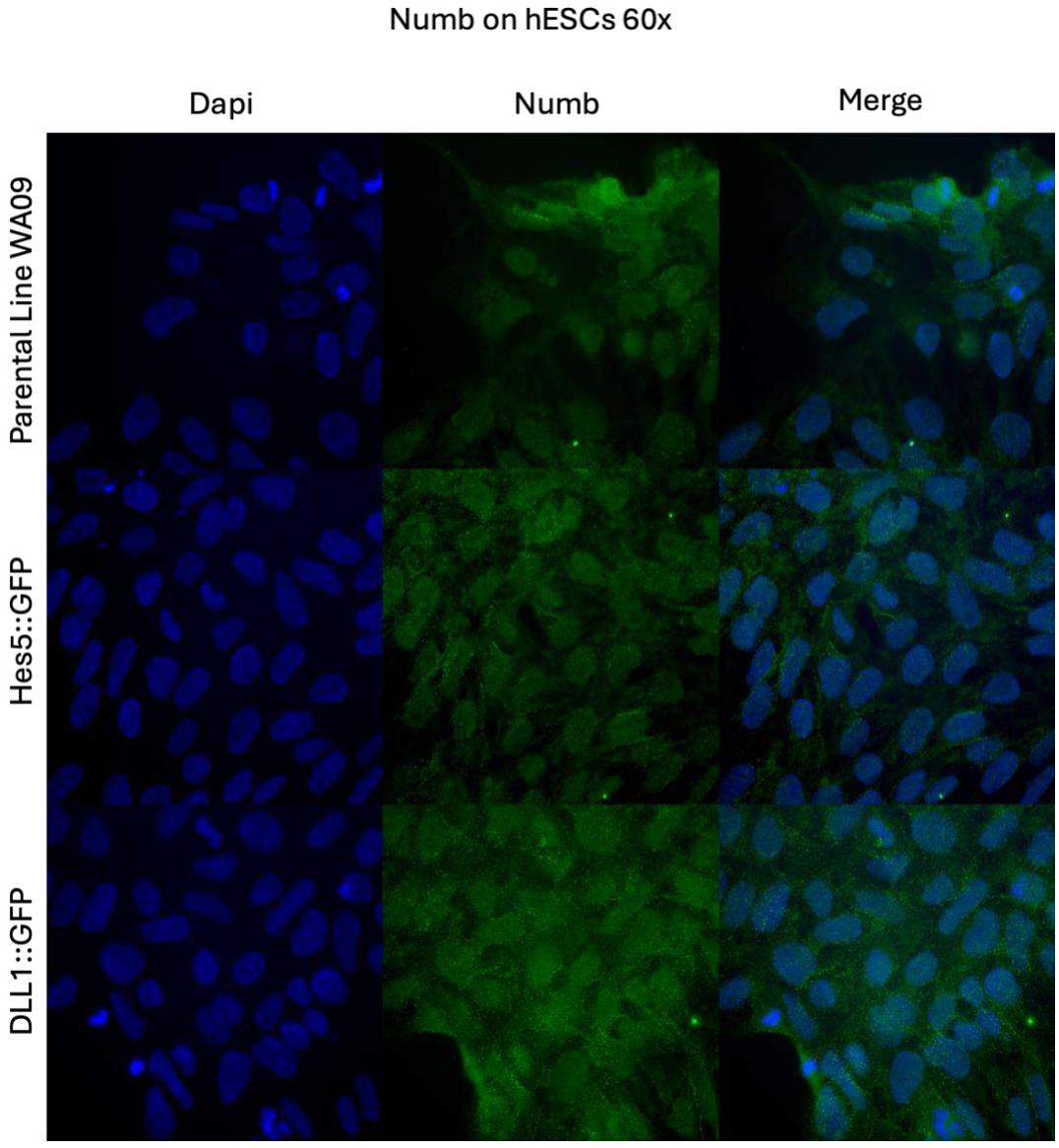

Figure 21: Endogenous Numb expression in human embryonic stem cells.

Immunofluorescence analysis of human embryonic stem cells (hESCs) reveals endogenous Numb expression. Numb signal (green) is primarily cytoplasmic, with detectable nuclear localization. Nuclei are counterstained with DAPI (blue). This pattern demonstrates the dual subcellular distribution of Numb in pluripotent stem cells.

Given its role as a multifunctional scaffold protein, cytoplasmic localization provides Numb the spatial advantage to interact with diverse signaling pathways, including Notch, p53, and integrin-related signaling. The presence of Numb in the nucleus, however, is particularly interesting, as previous studies have linked specific Numb isoforms to distinct subcellular distributions and biological functions. Notably, p72 and p66 isoforms are reported to localize primarily in the cytoplasm, while p71 and p65 isoforms are more enriched in the nucleus, where they may influence transcriptional programs or chromatin-associated processes [124,127].

The coexistence of cytoplasmic and nuclear pools of Numb in hESCs therefore likely reflects isoform-specific expression and dynamic regulation during cell fate transitions, emphasizing Numb's versatility as a key integrator of signaling and structural cues in pluripotent and differentiating cells.

4.1.5- Numb subcellular localization is influenced by cell density.

Interestingly, the expression pattern of Numb was not uniform among cells culture. In some cells, Numb was predominantly cytoplasmic, while in others it showed a more nuclear or perinuclear localization when Numb colocalized with DLL1 in early neurons (from day 18-25 of neuron differentiation). This heterogeneity adds a new layer of complexity to the characterization of Numb in pluripotent cells (FIG 22 A-D). Upon closer observation, it became clear that cell density and confluency were major determinants of Numb's localization, or the number of cells attached to the slide. When hESCs were cultured at high confluency, Numb was mainly confined to the cytoplasm, consistent with its known role in endocytic trafficking and receptor regulation (FIG 22D-Panel I) In contrast, when cells were plated at lower density or at earlier stages of colony growth, Numb displayed a more nuclear localization pattern (FIG 22D-Panel II).

This context-dependent distribution suggests that Numb's subcellular localization may shift according to the cell's physiological state, possibly reflecting changes in cell polarity, adhesion, or signaling activity as cultures reach confluence. This observation aligns with reports from other systems where Numb localization is dynamically regulated by cell-cell contact, integrin signaling, or mechanical tension although such confluency-dependent regulation has not previously been described in neurodevelopmental or pluripotent stem cell models.

These findings indicate that Numb's localization in hESCs is not static, but rather responsive to the microenvironment and culture conditions, suggesting that its functional role, cytoplasmic versus nuclear, may vary depending on the state of cell-cell communication or differentiation potential. This insight provides a valuable consideration

for future experiments aiming to dissect Numb's specific functions during early neural commitment or Notch pathway regulation in human stem cells [269].

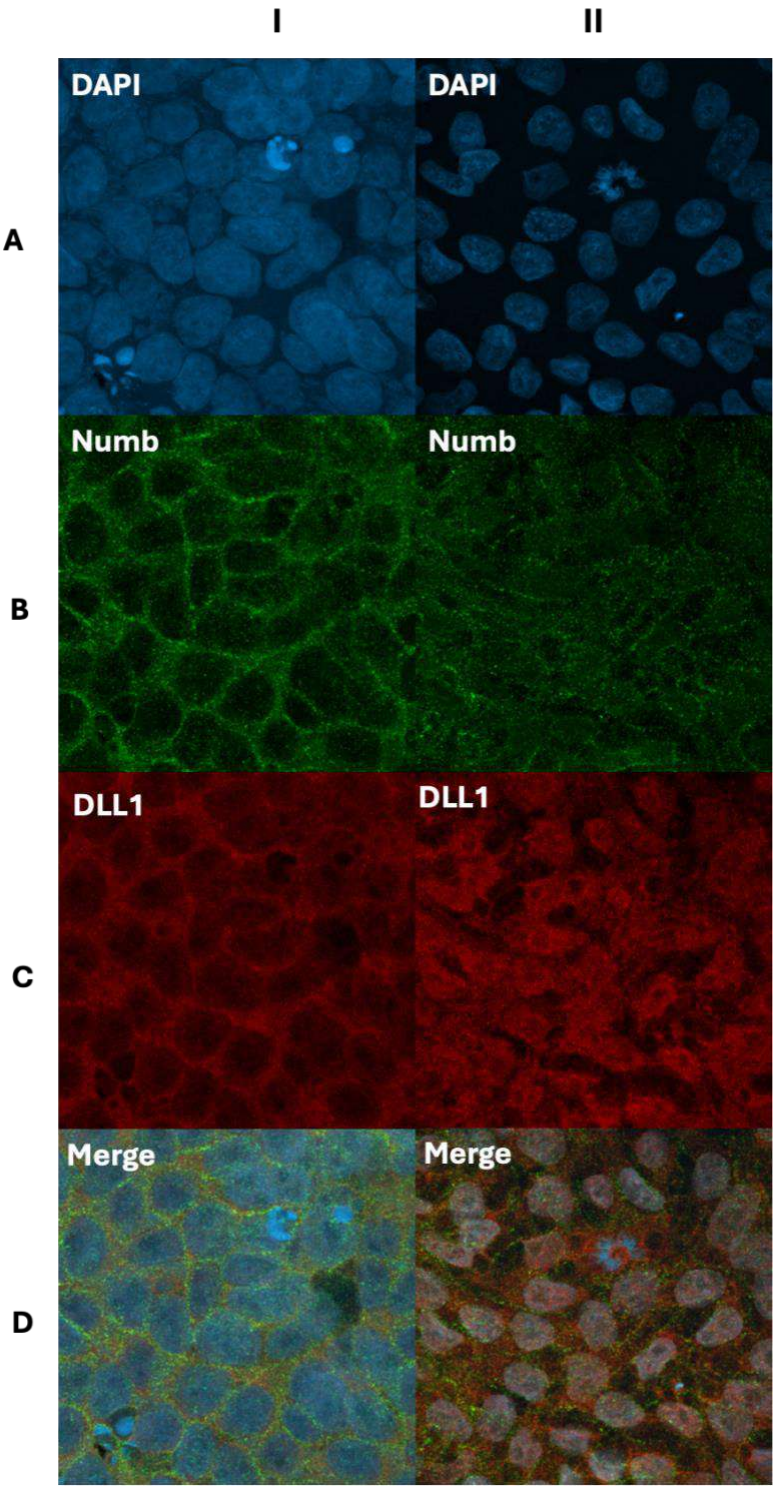

Figure 22: Co-localization of Numb and DLL1 during cortical neuron differentiation.

Immunofluorescence analysis at Day 20 of cortical neuron differentiation demonstrates the spatial relationship between Numb (green) and DLL1 (red). In Panel I, Numb and DLL1 exhibit prominent cytoplasmic expression. Panel II shows a more diffuse distribution of both proteins throughout the cell. Nuclei are counterstained with DAPI (blue).

4.1.6- Modified Dual-SMAD Inhibition protocol generates a robust cortical neuron population.

Using the established cortical neuron differentiation protocol, cortical neurons were successfully obtained after approximately 35 days of differentiation from hESCs. Although the differentiation process led to the appearance of neuronal populations expressing canonical markers, the efficiency and morphological maturity of the resulting neurons were suboptimal (FIG 23A). The cultures displayed a heterogeneous composition, with a relatively low proportion of mature neurons and the presence of cells that appeared to remain at progenitor or intermediate differentiation stages.

To improve the overall yield, purity, and neuronal phenotype, the differentiation protocol was systematically modified and optimized. Adjustments were made in key parameters such as growth factor timing, cell plating density, and duration of dual-SMAD inhibition to better mimic the developmental cues guiding cortical neurogenesis. Additional refinements included extending the neuronal maturation phase, optimizing substrate composition (e.g., laminin or poly-L-ornithine coating), and fine-tuning media supplementation to promote neuronal survival and axonal elongation (TABLE 6).

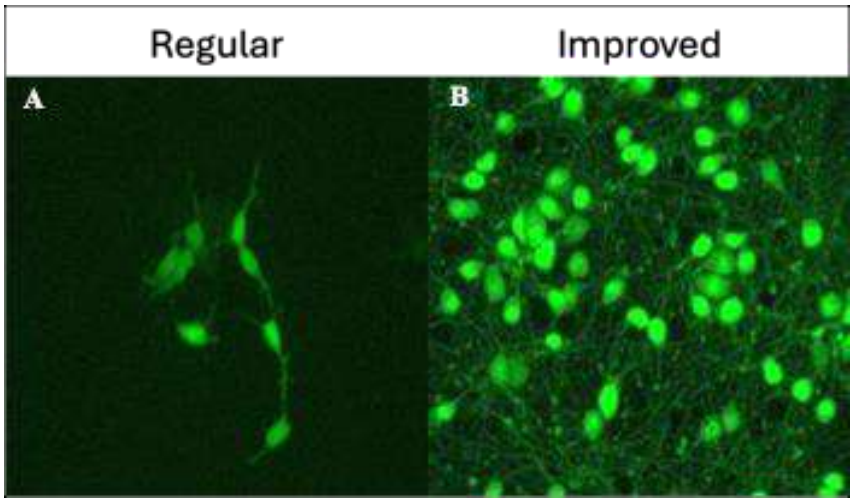

Figure 23: Comparison of cortical neuron differentiation protocols.

Immunofluorescence comparison of cortical neuron differentiation outcomes using standard versus optimized Dual SMAD inhibition protocols. Panel A shows neurons derived with the regular protocol, while Panel B illustrates enhanced neuronal differentiation and network formation achieved with the optimized protocol. NEUN (red) was used as a neuronal marker, highlighting mature neuronal populations and improved differentiation efficiency in the modified protocol.

Steps	Regular protocol	Improved version
Day 1-2 **Induction of Neural Differentiation**	SB431542 LDN193189 XAV939	SB431542 LDN193189 XAV939
Day 3-7 **Rise of Neural progenitors**	SB431542 LDN193189	SB431542 LDN193189
Day 8-20 **Enrichment and Expansion of NPCs**	Ascorbic Acid BDNF DAPT	FGF2 (Day 8-12) BDNF ↓ Ascorbic acid DAPT after day 20
25+ days **Rise of neurons**	Ascorbic Acid BDNF DAPT	Ascorbic Acid BDNF DAPT
35+ days **Mature neurons**	Ascorbic Acid BDNF DAPT	Ascorbic Acid BDNF DAPT

Table 6: Comparison of standard and optimized Dual SMAD inhibition protocols for cortical neuron differentiation.

To enhance neuronal differentiation efficiency and improve cortical neuron yield, FGF2 was supplemented between days 8 and 12 to promote neural progenitor proliferation and survival, supporting the expansion of early neuroepithelial populations. The γ-secretase inhibitor DAPT, which suppresses Notch signaling, was initially withdrawn from early stages of differentiation to prevent excessive inhibition of the pathway, since complete Notch blockade at this point can impair progenitor maintenance and compromise overall neuronal output. Additionally, the concentration of ascorbic acid was reduced to minimize potential cytotoxic effects observed during early neuronal commitment.

Instead, DAPT was reintroduced at later stages of differentiation between days 16 and 25+ when neural progenitors begin to transition toward postmitotic neurons. This timing allowed for a more physiologically relevant downregulation of Notch activity, facilitating neuronal maturation rather than premature differentiation.

With these modifications, the cultures exhibited a more homogeneous and robust population of cortical neurons by the end of the differentiation period, characterized by well-developed neuronal networks, increased neuronal marker expression (NeUN), and reduced variability across replicates. These results suggest that fine-tuning the temporal modulation of FGF and Notch signaling is critical for achieving efficient and reproducible cortical neurogenesis from hESCs (FIG 23B).

4.1.7- Morphological features of hESCs during cortical neuron differentiation.

At the starting point, hESCs exhibit a compact, epithelial-like morphology. They grow as tight, flat colonies with well-defined edges and high nuclear-to-cytoplasmic ratios. Individual cells are small, with round nuclei, prominent nucleoli, and scant cytoplasm. Cell–cell junctions are strong, supported by E-cadherin–based adherent junctions, maintaining colony integrity. The colonies display uniform refractive borders under phase contrast microscopy, and spontaneous differentiation is minimal when pluripotency conditions (FGF2, TGF-β/Activin A) are maintained (FIG 24A).

Morphologically, NPCs (days 15 to 20) form radially arranged, columnar cells surrounding a central lumen-like space. These rosettes are characterized by apico-basal polarity, with tight junctions at the apical surface (marked by ZO-1, N-cadherin, and Par3). NPCs display elongated, spindle-shaped bodies, and their nuclei align radially around the rosette lumen, reflecting interkinetic nuclear migration behavior typical of neuroepithelial cells in vivo. This stage its known as neural rosettes formation (FIG 24B).

As differentiation progresses, NPCs gradually transition from neuroepithelial cells to radial glia-like progenitors, which are slightly more elongated and migratory. They express PAX6, SOX1, and Nestin, marking their neural identity and commitment to a cortical

lineage. During this period, mitotic activity remains high, and cells often retain rosette or sheet-like arrangements before spreading into a more bipolar, migratory phenotype.

Following further differentiation cues (e.g., withdrawal of FGF and addition of neurotrophic factors such as BDNF and GDNF), NPCs begin to exit the cell cycle and acquire neuronal morphology. Cells become smaller and more phase-bright, with a bipolar or unipolar shape at first, extending thin neurites that later branch into multiple processes. Within days, neurons begin to form dense networks, showing clear axon-dendrite polarization. Early neurons express βIII-tubulin (Tuj1), DCX, and MAP2, markers of immature neuronal differentiation (not shown). Axons start to elongate, and growth cones are evident at their distal tips. Morphologically, the culture transitions from uniform sheets of progenitors to a web-like network of interconnected cells with extended processes. Over several weeks (typically 30-50 days or more), neurons undergo progressive maturation characterized by increased neurite complexity, synaptogenesis, and electrophysiological activity. Morphologically, mature cortical neurons exhibit large, polarized somas with distinct axons and highly branched dendritic arbors. Dendritic spines begin to appear along the processes, reflecting synaptic specialization. The nuclei become eccentrically located within the soma, and the cytoplasm is enriched in Nissl substance (FIG 24C).

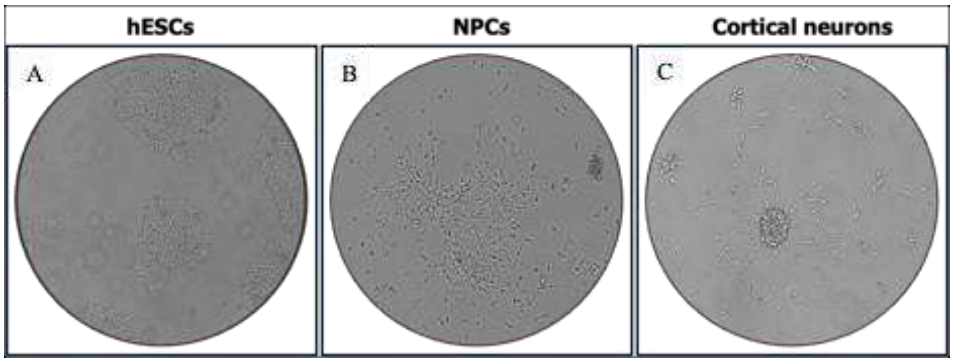

Figure 24: Morphological changes of hESCs upon cortical neuron differentiation.

A) Human embryonic stem cells (hESCs) exhibit a compact, high–nucleus-to–cytoplasm morphology, forming tightly packed colonies with smooth edges and prominent nucleoli. B) In contrast, neural progenitor cells (NPCs) display an elongated, bipolar or radial morphology, often forming rosette-like structures characteristic of early neuroepithelium. C) Mature neurons show highly polarized morphology, including a defined soma, extensive dendritic arborization, and a single long axon, reflecting the acquisition of functional neuronal architecture

4.1.8- Numb expression slightly declines during cortical neuron differentiation.

To investigate the dynamics of the Numb-Notch signaling axis during cortical neuron differentiation, protein expression levels of Numb, DLL1, and Hes5 were analyzed by Western blot at 4-day intervals throughout the differentiation timeline. As internal controls, SOX2 was used as a marker of undifferentiated and neural progenitor cells, NeuN as a marker of mature neurons, and β-actin as a loading control. This approach allowed us to monitor how these key regulators change in abundance during the progressive transition from pluripotent stem cells to differentiated cortical neurons.

As expected, DLL1, a canonical Notch ligand, displayed a pronounced increase in expression around day 15, corresponding to the onset of neuronal commitment when cells begin to exit the cell cycle and initiate neurite outgrowth. The elevated DLL1 levels at this stage are consistent with its role in lateral inhibition, where differentiating neurons signal to neighboring progenitors to maintain their undifferentiated state, ensuring a balanced production of neurons and progenitor cells.

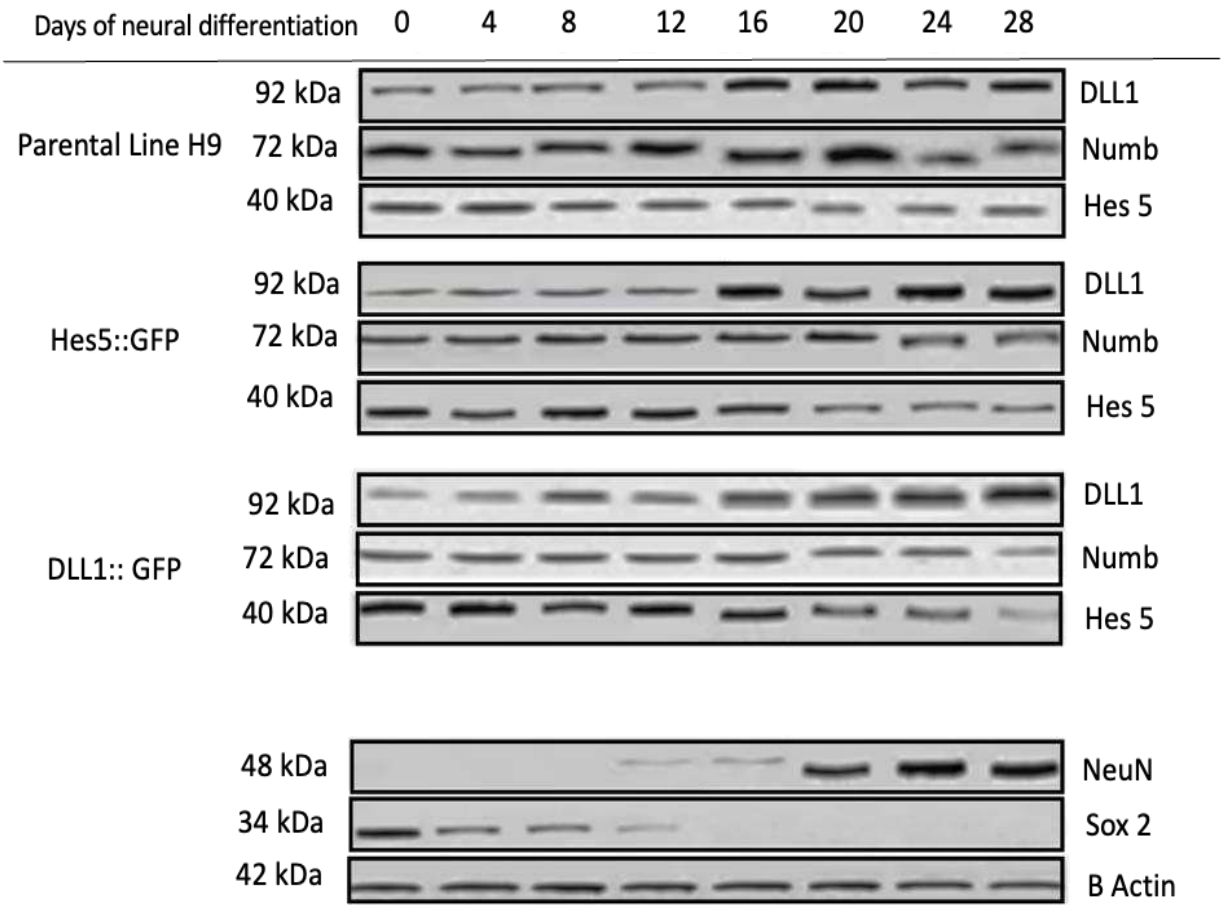

Figure 25: Dynamics of Numb and Notch pathway components during hESC differentiation.

Temporal expression analysis of Numb, Hes5, and DLL1 during cortical neuron differentiation in WA09 (H9) parental cells, Hes5::GFP, and DLL1::GFP reporter lines. Across all three lines, Hes5 expression peaks between days 12–28 before decreasing, DLL1 expression rises following the neural progenitor cell stage, and Numb shows a modest decline in fully differentiated neurons (+28 days).

Hes5, a direct transcriptional target of Notch signaling and a hallmark of neural progenitor identity, showed a modest increase in expression from day 0 through day 12, peaking between days 8 and 12 coinciding with the neural progenitor cell (NPC) stage. This transient upregulation likely reflects active Notch signaling maintaining the progenitor pool during early neurogenesis, followed by a gradual decline as cells commit to neuronal fates.

In contrast, Numb protein levels exhibited a gradual decrease after day 20, suggesting a developmental downregulation once the majority of progenitors have differentiated. This reduction supports the notion that Numb is primarily required during earlier stages of neural development, where it promotes asymmetric cell division and regulates the balance between progenitor maintenance and differentiation by antagonizing Notch signaling. However, the persistent, albeit reduced, presence of Numb in later stages implies additional functions beyond progenitor regulation potentially related to endocytosis, vesicle trafficking, and synaptic maturation in postmitotic neurons (FIG 25).

Overall, these results illustrate a coordinated temporal pattern in which DLL1 and Hes5 activity peak during neural commitment and early progenitor maintenance, while Numb expression declines as cells acquire a mature neuronal phenotype, reflecting a shift in its functional role from cell fate determination to neuronal maintenance and intracellular trafficking in cortical neuron development.

4.1.9- hESCs (H9) endogenously express all four Numb isoforms: p72, p71, p66, and p65.

To assess endogenous Numb isoform expression, Western blot (WB) analyses were performed using a modified protocol optimized for resolving closely sized isoforms. Briefly, protein lysates from hESCs and neural progenitor cells (NPCs) were separated on a 15% Bis-Tris resolving gel, which was hand-cast to enhance separation of the 65-75 kDa isoform range. Gels were electrophoresed for 2.5 hours at a constant 75 V to maximize band resolution. Under these conditions, all four known human Numb isoforms p72, p71, p66, and p65 were consistently detected.

In agreement with prior reports, WB analyses revealed two major bands: an upper band corresponding to the grouped long-PTB isoforms (p72/p71) and a lower band corresponding to the short-PTB isoforms (p66/p65). Notably, an increased intensity of the lower band (p66/p65) was observed upon differentiation into the NPC stage, indicating a shift in isoform abundance during lineage progression (FIG 26).

These results confirm that hESCs maintain the full complement of Numb isoforms, demonstrating that alternative splicing of Numb is active even at the pluripotent stage. The co-expression of both long (exon 9-containing) and short (exon 9-skipping) isoforms suggests that hESCs preserve significant molecular flexibility, likely enabling context-dependent modulation of pathways such as Notch signaling. This balanced isoform repertoire may support early cell fate decisions, consistent with observations in other developmental systems.

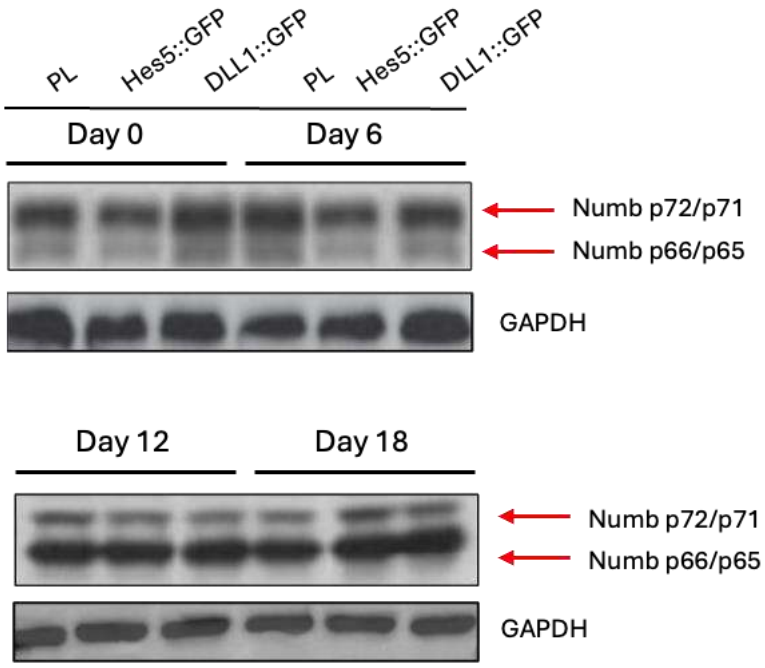

Figure 26: Expression of Numb isoforms during hESC differentiation.

Western Blot of human embryonic stem cells (hESCs) and neural progenitor cells (NPCs) reveals expression of all four human Numb isoforms. Numb isoforms are detected during the stem cell stage (Days 0–6) and NPC stage (Days 12–18). The red arrow indicates the combined expression pattern of Numb isoforms grouped according their PTB domain.

4.2- Epigenetic regulation of Numb

4.2.1- H3K27Ac is enrich in Numb promoter previous Dual SMAD inhibition for cortical neuron differentiation.

After observing that Numb protein levels decrease slightly during differentiation, the next logical question was to identify the possible molecular players responsible for downregulating Numb during cortical neuron differentiation. To address this, chromatin immunoprecipitation sequencing (ChIP-seq) analyses. Given that the Polycomb Repressive Complex 2 (PRC2) is widely recognized as a key transcriptional repressor during neurodevelopment, we hypothesized that EZH2, the catalytic subunit of PRC2, could be mediating repression of Numb upon differentiation. To test this, samples were collected at two key time points: Day 0, representing pluripotent stem cells, and Day 35 or later, representing mature cortical neurons, and processed according to standard ChIP-seq protocols.

Comparison with publicly available differentiation datasets confirmed the reliability of our protocol: for instance, we observed the expected decrease in H3K27ac enrichment at the POU5F1 (OCT4) locus upon differentiation, consistent with the known silencing of pluripotency genes reported in the literature. These observations not only validate the differentiation protocol but also provide a solid framework to interrogate potential EZH2-mediated repression of Numb during human cortical neuron maturation (FIG 27).

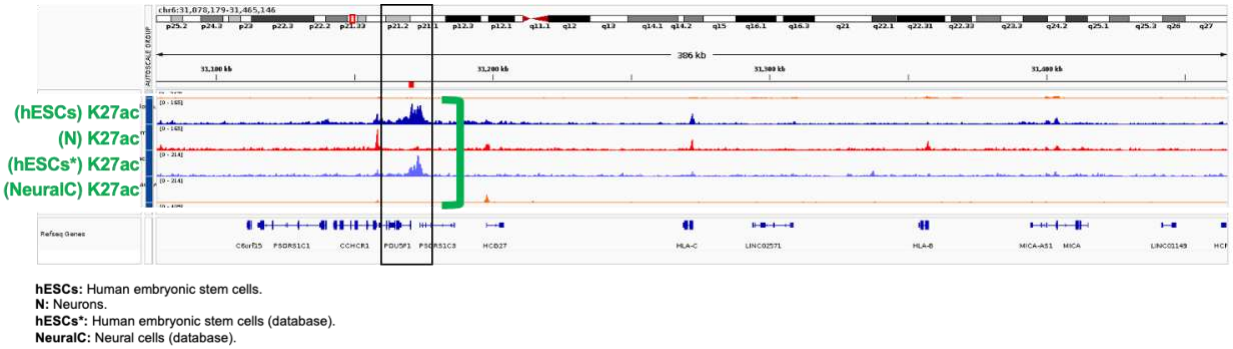

Figure 27: ChIP analysis shows enrichment of the active histone mark H3K27Ac at the Numb promoter.

In human embryonic stem cells, indicating transcriptional activation in the stem cell state. This enrichment is lost in mature cortical neurons, consistent with successful neural differentiation and downregulation of Numb promoter activity during neuronal maturation.

4.2.2- PRC2-mediated epigenetic regulation of Notch components, DLL1 and Hes5, during cortical neuron differentiation.

After double checking the differentiation protocol worked. The next question it was, what's the role of PRC2 with Notch components, Hes5 and DLL1. This relation has been well described compared to Numb.
To investigate the epigenetic mechanisms regulating Notch pathway activity during neural differentiation, we performed ChIP-seq analysis for H3K27me3, the repressive histone mark catalyzed by PRC2, in human embryonic stem cell–derived neural progenitors and differentiated neurons.

The results revealed a clear enrichment of H3K27me3 at multiple Notch pathway components, including DLL1and Hes5, in progenitor cells compared to differentiated neurons. This enrichment correlated with high expression of EZH2, the catalytic subunit of PRC2, and reduced transcriptional activity of Notch targets, consistent with an epigenetic repression of the pathway.

ChIP-seq analysis revealed a dynamic chromatin switch at the DLL1 promoter during neuronal differentiation. In neural progenitors, the promoter is enriched for EZH2 and H3K27me3, consistent with PRC2-mediated transcriptional repression that maintains progenitor identity by limiting premature Notch ligand expression. As cells commit to differentiation, EZH2 and H3K27me3 levels decrease, while H3K27ac levels increase, reflecting the replacement of a repressive mark with an active histone modification. This acetylation is associated with an open chromatin conformation that facilitates transcription factor binding, leading to upregulation of DLL1. Functionally, this epigenetic switch enables differentiating neurons to express Notch ligands, promoting lateral inhibition and coordinating the balance between differentiation and progenitor maintenance (FIG 28).

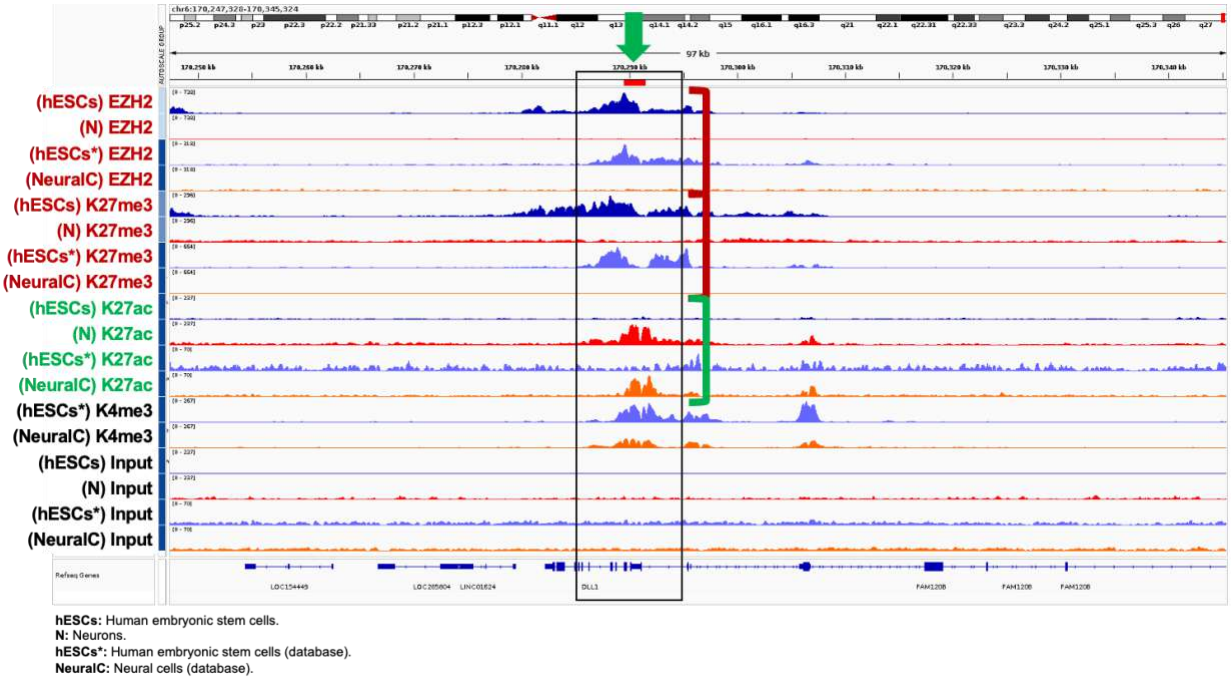

Figure 28: Epigenetic Regulation of DLL1 and Numb During Neural Differentiation.

ChIP-seq analysis of DLL1 regulatory regions shows dynamic epigenetic changes during differentiation. At DLL1 promoters, levels of the repressive mark H3K27me3 and the PRC2 component EZH2 decrease, while the activating mark H3K27Ac increases. These changes correlate with transcriptional activation and highlight coordinated epigenetic regulation of DLL1 and Numb promoters during neural differentiation.

This dynamic modulation indicates that PRC2 activity defines a chromatin-restrictive window that constrains Notch signaling in neural progenitors to ensure proper timing of differentiation. In line with this, progenitors with high Notch activity exhibited reduced H3K27me3 at Hes5, whereas forced PRC2 activation restored the repressive mark and downregulated Notch target expression.

Similar to DLL1, ChIP-seq analysis revealed a dynamic chromatin remodeling at the Hes5 promoter during neural differentiation. In neural progenitors, the locus is marked by EZH2 and H3K27me3, reflecting PRC2-mediated repression that maintains progenitor plasticity by limiting excessive Notch effector activity. Upon differentiation, EZH2 and H3K27me3 levels decrease while H3K27ac levels increase, establishing an open chromatin state that facilitates transcription factor and NICD–RBPJ complex recruitment.

Unlike DLL1, which primarily propagates Notch signaling as a ligand, the activation of Hes5 fine-tunes the feedback dynamics of the pathway, ensuring progenitors maintain a balanced pool capable of responding to differentiation cues. This gene-specific chromatin switch highlights how PRC2 repression differentially modulates Notch pathway components, coordinating both ligand expression and effector activity to preserve the proper timing and balance between progenitor maintenance and neuronal differentiation (FIG 29).

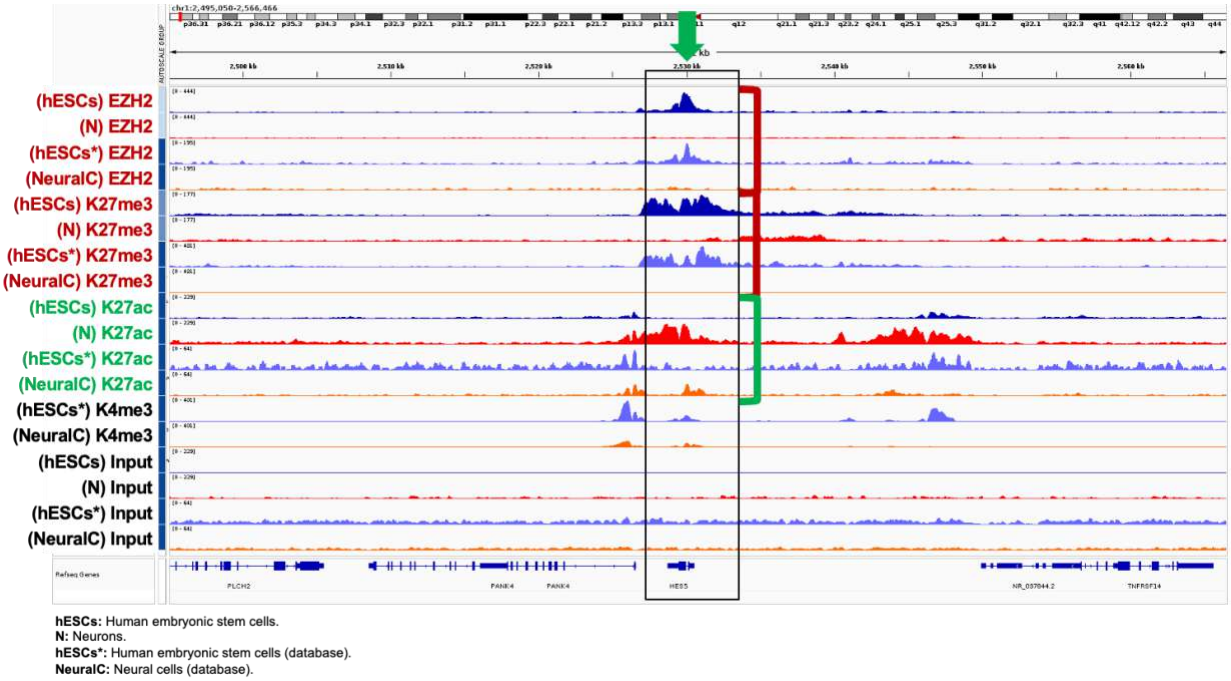

Figure 29: Epigenetic modulation of Hes5 and Numb during neural differentiation.

ChIP-seq analysis of the HES5 locus reveals dynamic epigenetic remodeling during differentiation. Levels of the repressive mark H3K27me3 and the PRC2 component EZH2 at the HES5 promoter decrease, while the activating mark H3K27Ac increases.

Together, these findings demonstrate that PRC2 represses Notch signaling at the chromatin level, establishing an epigenetic barrier that controls the balance between neural stem cell maintenance and neuronal differentiation.

4.2.3- The Numb promoter is enriched for active Chromatin marks and misplays minimal EZH2 or H3K27me3 occupancy.

Chromatin profiling at the Numb promoter suggests that its regulation is primarily influenced by transcriptional activation factors rather than repressive epigenetic marks. The ChIP-seq analysis performed across the Numb promoter region revealed an enrichment of active chromatin signatures, such as H3K27ac and H3K4me3, together with the presence of transcriptional co-activators, indicating an open and transcriptionally permissive chromatin state. In contrast, the levels of canonical repressive marks, including H3K27me3, deposited by PRC2 and H3K9me3 (not shown), were markedly reduced or absent. These findings support the notion that Numb expression is maintained or induced by the balance of activating histone modifications and the recruitment of transcriptional activators, rather than by Polycomb-mediated repression. This epigenetic profile is consistent with Numb's functional role as a determinant of cell fate and supports the hypothesis that its transcriptional regulation is tightly coupled to the transition from pluripotency to neural lineage commitment (FIG 30).

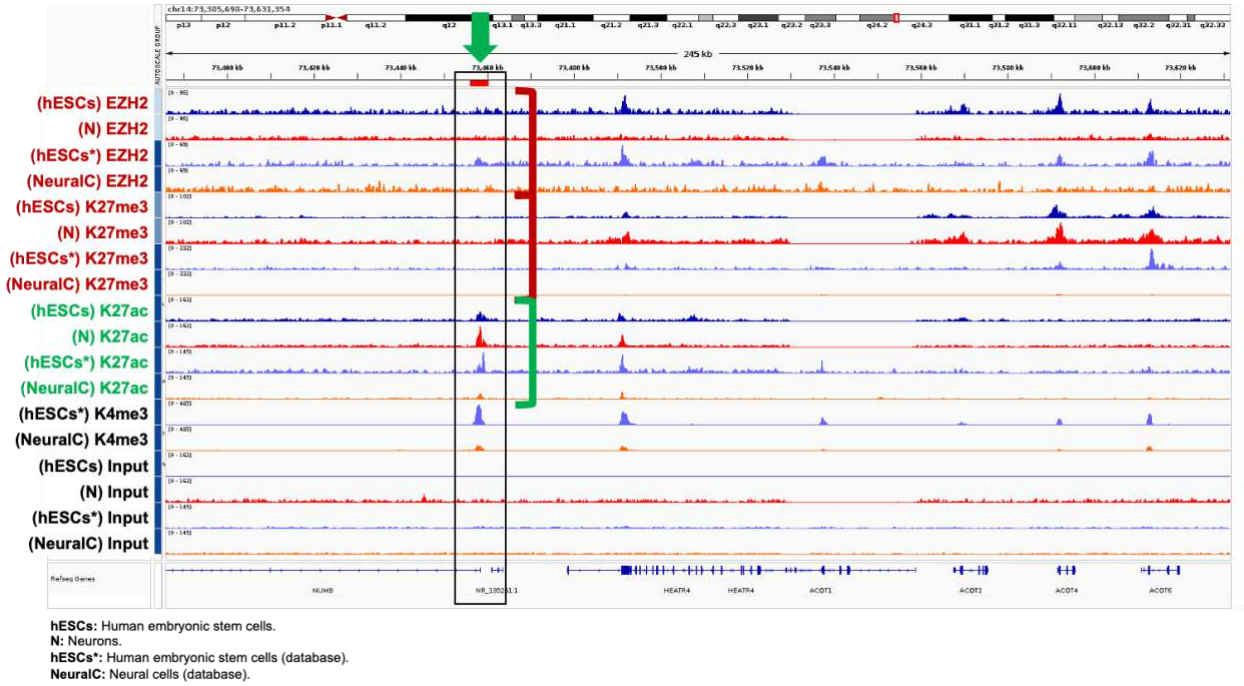

Figure 30: Epigenetic landscape of the numb promoter during neural differentiation.

ChIP-seq tracks of the Numb promoter reveal low occupancy of the repressive mark H3K27me3 and the PRC2 component EZH2 (red), alongside enrichment of the activating mark H3K27Ac (green). This pattern indicates an open, transcriptionally active chromatin state at the NUMB promoter, consistent with its regulation during differentiation.

4.2.4- Numb downregulation during cortical neuron differentiation correlates with loss of H3K4me3.

According to the available datasets suitable for comparison with our results, only ChIP-seq data generated in H1 cells were accessible. Importantly, H1 and H9 hESC lines are highly comparable, as they exhibit similar pluripotency features, differentiation capacities, and overall transcriptional profiles, making H1 a reliable reference for our analyses.

The ChIP-Seq data and expression analysis together demonstrate that Numb expression decreases significantly upon differentiation of H1 human embryonic stem cells (hESCs). H1 into neural cells, corresponding with notable changes in histone modification patterns. In undifferentiated hESCs, the K4me3 mark associated with active transcription is strongly enriched at the Numb locus, consistent with high mRNA expression levels. However, during neural differentiation, this K4me3 signal is markedly reduced, correlating with a sharp decrease in Numb transcript abundance.

This loss of the active histone mark suggests transcriptional repression of Numb in neural cells. In parallel, the presence of EZH2 and increased H3K27me3 levels, both linked to Polycomb-mediated gene silencing, indicate an epigenetic transition from an active to a repressed chromatin state. Together, these data suggest that the downregulation of Numb expression during differentiation is driven by chromatin remodeling, involving the loss of activating histone marks and potential recruitment of repressive complexes such as PRC2 (FIG 31).

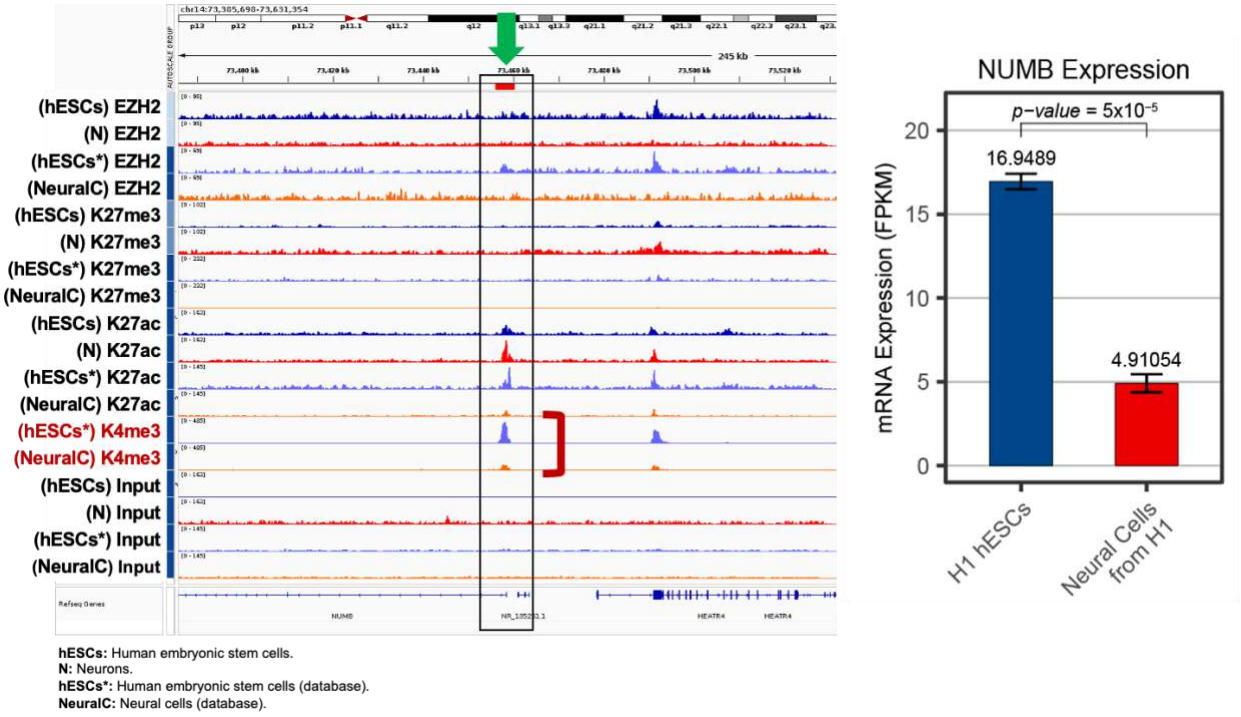

Figure 31: ChIP-seq analysis demonstrates that Numb expression declines during differentiation.

Numb decrease coinciding with a reduction in the activating histone mark H3K4me3 (red) at its promoter. This epigenetic change reflects decreased transcriptional activity of Numb as cells progress toward a mature neuronal state.

4.2.5- Mouse embryonic stem cells harbor a poised Numb promoter as an example of the mammalian context of cortical neuron differentiation.

To further understand the epigenetic regulation of Numb we explored publicly available chromatin datasets from mouse embryonic stem cells, as the mouse model provides a well-characterized and highly conserved framework for studying early developmental gene regulation.

The Numb locus and its promoter architecture are evolutionarily conserved between mouse and human, particularly in regions containing CpG islands and key transcription factor binding motifs, making the mouse system an appropriate comparative model for dissecting chromatin dynamics and transcriptional control mechanisms.

Analysis of mouse ChIP-seq and accessibility datasets revealed that EZH2 occupancy and H3K27me3 enrichment at the Numb promoter are very low, suggesting that PRC2-mediated repression does not play a major role in regulating this gene in pluripotent or early differentiating states.

In contrast, the promoter region displayed strong enrichment for H3K4me3, H3K9ac, H3K27ac, H3K56ac, H3K64ac, and H3K122ac, together with prominent peaks in ATAC-seq and DNase-seq profiles, indicating a highly accessible and transcriptionally active chromatin environment. This combination of active histone modifications and chromatin accessibility marks supports the notion that Numb expression is driven by activating rather than repressive epigenetic mechanisms. These findings align with our observations in human embryonic stem cells, reinforcing the idea that Numb regulation is predominantly controlled through transcriptional activation pathways, rather than through canonical Polycomb-dependent silencing, during early developmental stages (FIG 32).

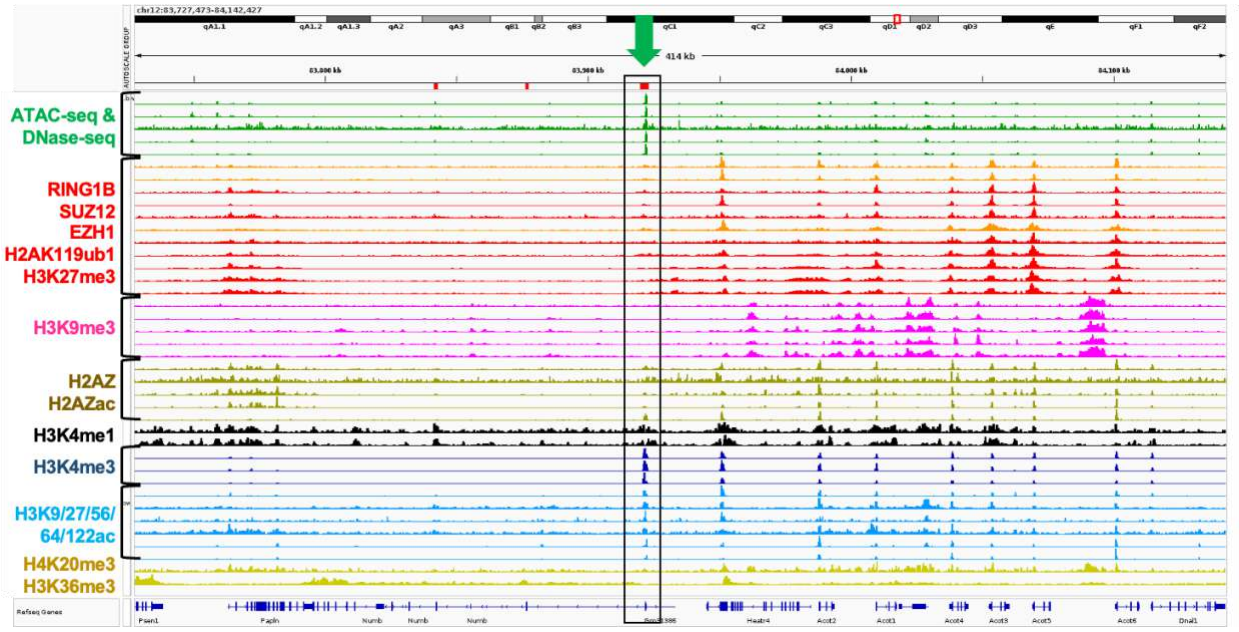

Figure 32: Epigenetic status of the Numb promoter in mouse embryonic stem cells.

ChIP-seq analysis of the Numb promoter in mouse embryonic stem cells (mESCs) shows minimal occupancy of PRC2 components, including EZH2, and low levels of the repressive mark H3K27me3 (red). These data suggest that the Numb promoter is in a largely permissive chromatin state in mESCs.

The ATAC-seq signal at the Numb promoter (highlighted region) shows a strong enrichment peak, indicating high chromatin accessibility a hallmark of open chromatin and transcriptional activity.

Several transcription factors (TFs) such as KLF4, E2F1, and EP400, along with co-activator complexes (BRD4, MED1, MED12, NELF, and NIPBL), display pronounced peaks at the Numb promoter region. This pattern suggests active recruitment of transcriptional regulators involved in gene activation and enhancer-promoter communication.

Moreover, components of the cohesin complex (RAD21) and CTCF, known for establishing chromatin looping and higher-order structure, are enriched at or near the Numb promoter, potentially facilitating long-range interactions with distal regulatory elements. The chromatin remodelers (CHD family: CHD1–CHD9, BRG1, ADNP) also

exhibit strong occupancy, indicating that nucleosome remodeling is actively maintaining the accessible state of the promoter. This open configuration allows for dynamic binding of transcriptional machinery.

In contrast, heterochromatin-associated proteins (HP1α, HP1β, SUV39H1/2, SETDB1) and histone deacetylases (HDAC1/2) show minimal enrichment at the Numb promoter, consistent with the active and transcriptionally permissive chromatin environment observed. So Numb promoter is highly open chromatin (FIG 33).

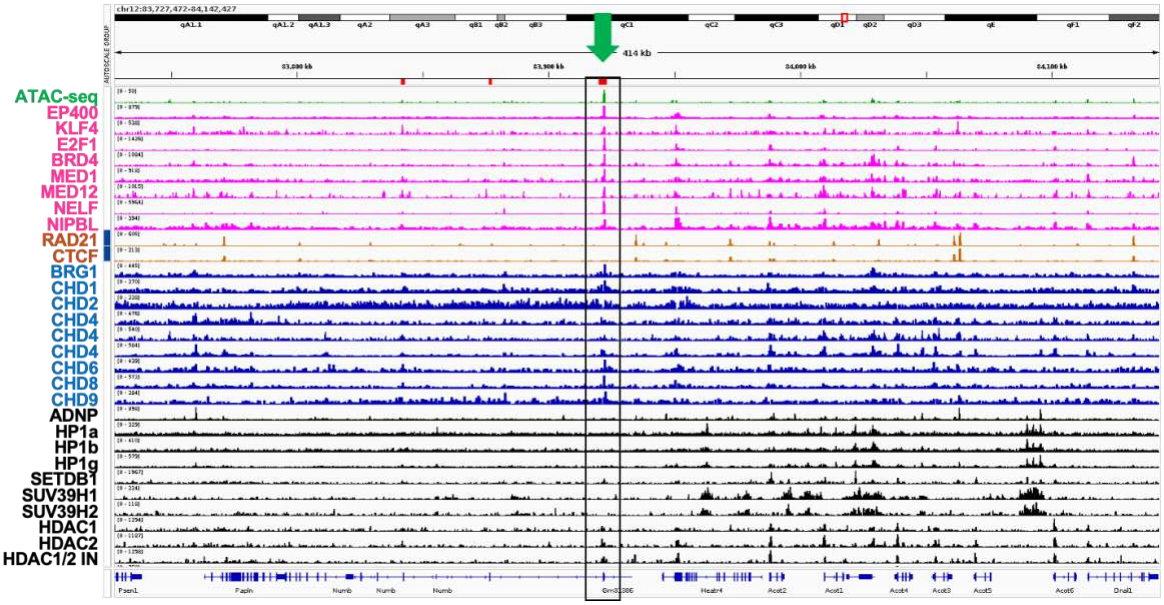

Figure 33: Open chromatin state of the Numb promoter on mESCs.

ChIP-seq analysis indicates that the Numb promoter exists in a highly open chromatin configuration. This accessible state facilitates the binding of multiple transcription factors and chromatin remodelers, as highlighted within the black rectangle, supporting active transcriptional potential. The Numb gene promoter in mESCs appears to be in an open chromatin state, as evidenced by the enrichment of many TFs and possibly chromatin remodelers. Open chromatin is typically associated with transcriptionally active genes or genes poised for activation. This suggests that the Numb gene is not being repressed by mechanisms like Polycomb-mediated silencing in the cells used for this experiment.

The observation that many transcription factors (TFs) are enriched at the Numb promoter but EZH2 and SUZ12 are absent or show low enrichment is intriguing. EZH2 and SUZ12 are part of the Polycomb Repressive Complex 2 (PRC2), which is associated with gene silencing through trimethylation of histone H3 at lysine 27 (H3K27me3). The absence of EZH2 and SUZ12 at the Numb promoter suggests that Numb may be in an active state of transcription and is not being silenced by the Polycomb complex in this context (FIG 34).

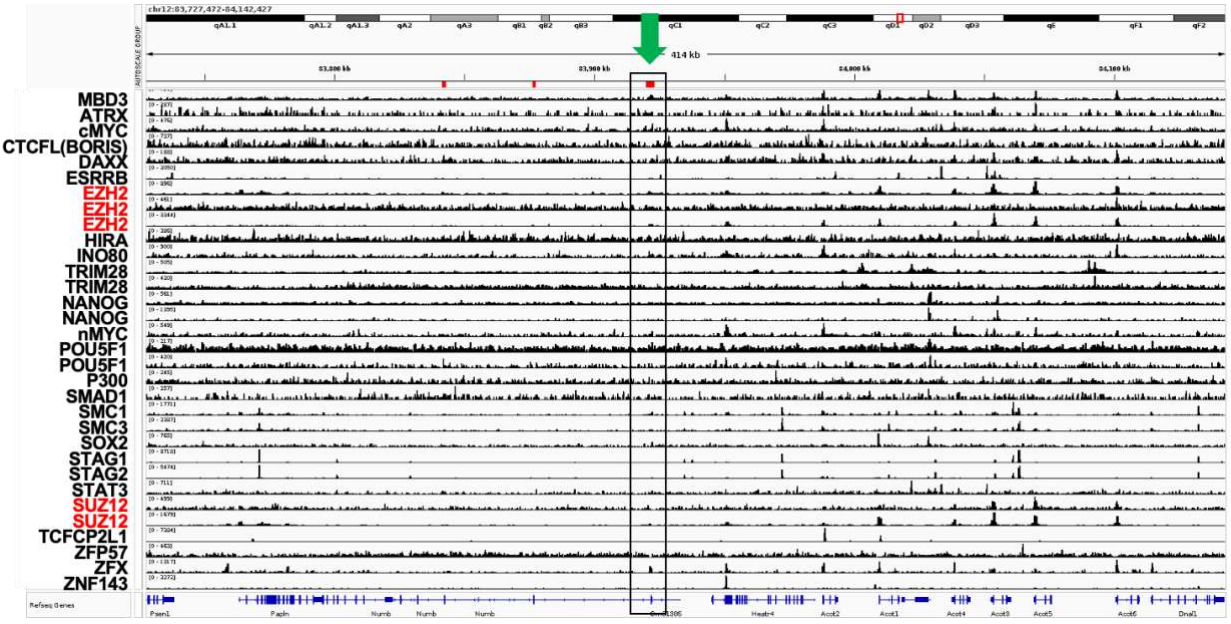

***Figure 34: Open chromatin and factor occupancy at the Numb promoter on mESCs*.**

ChIP-seq analysis reveals that the Numb promoter adopts a highly open chromatin state, allowing enrichment of various transcription factors and chromatin remodelers (black). In contrast, PRC2 components, including EZH2 and H3K27me3 (red), are present at very low levels, indicating minimal repressive regulation at this promoter

4.3 Isoform dynamic during neurogenesis

4.3.1- Inclusion of Numb isoforms containing Exons 3 and 9 dramatically decreases during cortical neuron differentiation.

Knowing that Numb levels decrease upon differentiation, our next question was whether there is available data to analyze the expression of Numb isoforms during human cortical neuron differentiation and how their expression changes throughout this process.

We analyze the alternative splicing of Numb during hESC/hiPSC to cortical neuron differentiation using data from two published studies. One on hESC neuronal differentiation from Leemput *et al.,* 2014 [346] and the other on hiPSC neuronal differentiation from Burke *et al.,* 2020 [347].
First of all, several markers were analyzed to check the stemness o neural commitment of the population of cells included in both studies (TABLE 7).

Marker	Expressed by
NANOG	Undifferentiated or pluripotent cells
SOX1	Early neural progenitor cells
PAX6	Neural progenitor
SYP	Mature cortical neurons

Table 7: Potency markers for tracking Numb Exon 3 and Exon 9 splicing during cortical neuron differentiation datasets.

4.3.2- hESC to cortical neuron differentiation: Analysis of Leemput et al. (2014) dataset.

From the dataset provided by van de Leemput *et al.* (2014) [346], the temporal expression profile of key developmental markers clearly delineates the progression from pluripotency to neural commitment and neuronal maturation. NANOG, a core pluripotency marker, exhibited high expression levels between days 2 and 7, consistent with the maintenance of an undifferentiated stem cell state. After day 7, NANOG expression sharply declined to nearly undetectable levels, indicating the exit from pluripotency and the onset of lineage specification. Correspondingly, SOX1 expression showed a pronounced peak around day 7, marking the transition toward the neuroectodermal and early neural progenitor cell (NPC) stages. PAX6, a canonical NPC marker, became highly expressed from days 12-15 onward, confirming the establishment of the neural progenitor population. Its expression gradually decreased as differentiation progressed into more mature cortical neuron stages. In parallel, SYP (Synaptophysin), a marker of mature and synaptically active neurons, showed a progressive increase beginning around day 26 and continuing through day 77, the final stage analyzed, reflecting neuronal maturation and synapse formation (FIG 35).

Regarding Numb expression, its transcript levels remained relatively stable throughout the differentiation process, suggesting a persistent requirement for Numb function across multiple stages of neural development from progenitor maintenance to neuronal maturation. Similarly, Numb-like (Numbl) expression also appeared sustained, with minor fluctuations between days 10 and 60. These subtle variations may reflect population heterogeneity, as differentiating cultures contain a dynamic mix of progenitors and maturing neurons, each potentially expressing different Numb and Numb isoforms. This sustained expression pattern implies that both Numb and Numbl maintain essential roles

throughout neurogenesis, possibly ensuring the fine-tuning of Notch signaling and the balance between proliferation and differentiation across developmental stages.

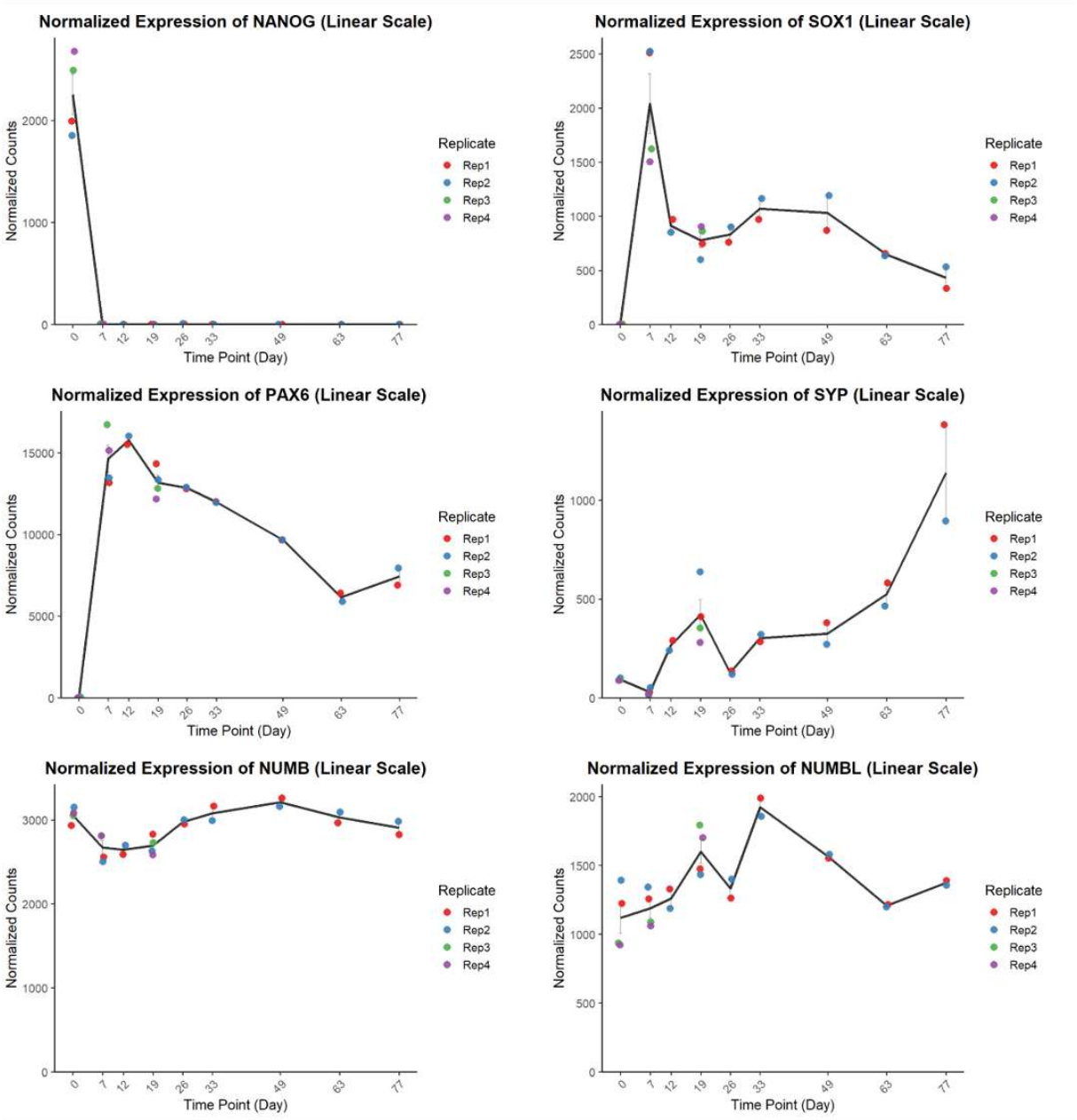

Figure 35: Expression of pluripotency, neuronal, Numb, and Numbl markers.

Analysis of published data from Leemput et al. (2014) showing expression profiles of pluripotency markers, neuronal markers, and the Numb family proteins (Numb and Numbl) during neural differentiation.

4.3.3- Exon 3 and Exon 9 containing Numb isoforms decline during hESC-derived cortical neuron differentiation (Leemput et al. 2014).

Exons 4 and 7were used as internal controls because they are constitutively included in all Numb transcripts and are not subjected to alternative splicing events. Their consistent detection across all differentiation time points confirms the reliability of the assay and the stability of Numb transcript expression during neural differentiation. In contrast, the analysis of alternative exons revealed dynamic regulation linked to neural lineage progression. Specifically, the inclusion of exon 3 decreased dramatically from day 3 to neural progenitor cell (NPC) stage around day 20, reaching nearly undetectable levels. This finding indicates that exon 3–containing isoforms (Ex3in), corresponding to the long PRR variants p66 and p72, are progressively downregulated and ultimately silenced as cells commit to the NPC fate. A similar temporal pattern was observed for exon 9 inclusion.

The expression of exon 9-containing isoforms, which give rise to the p72 and p71 variants, declined steadily from day 3 through day 20 just before the emergence of neurons and continued to decrease thereafter. This coordinated loss of both exon 3 and exon 9 inclusion suggests a developmental switch in Numb splicing during neurogenesis, favoring the expression of isoforms lacking these exons (Ex3Δ/Ex9Δ) like p65 (Numb4). Such a transition likely reflects functional adaptation, as shorter Numb isoforms have been associated with neuronal differentiation and maturation, whereas the longer isoforms are more characteristic of undifferentiated or proliferative states (FIG 36).

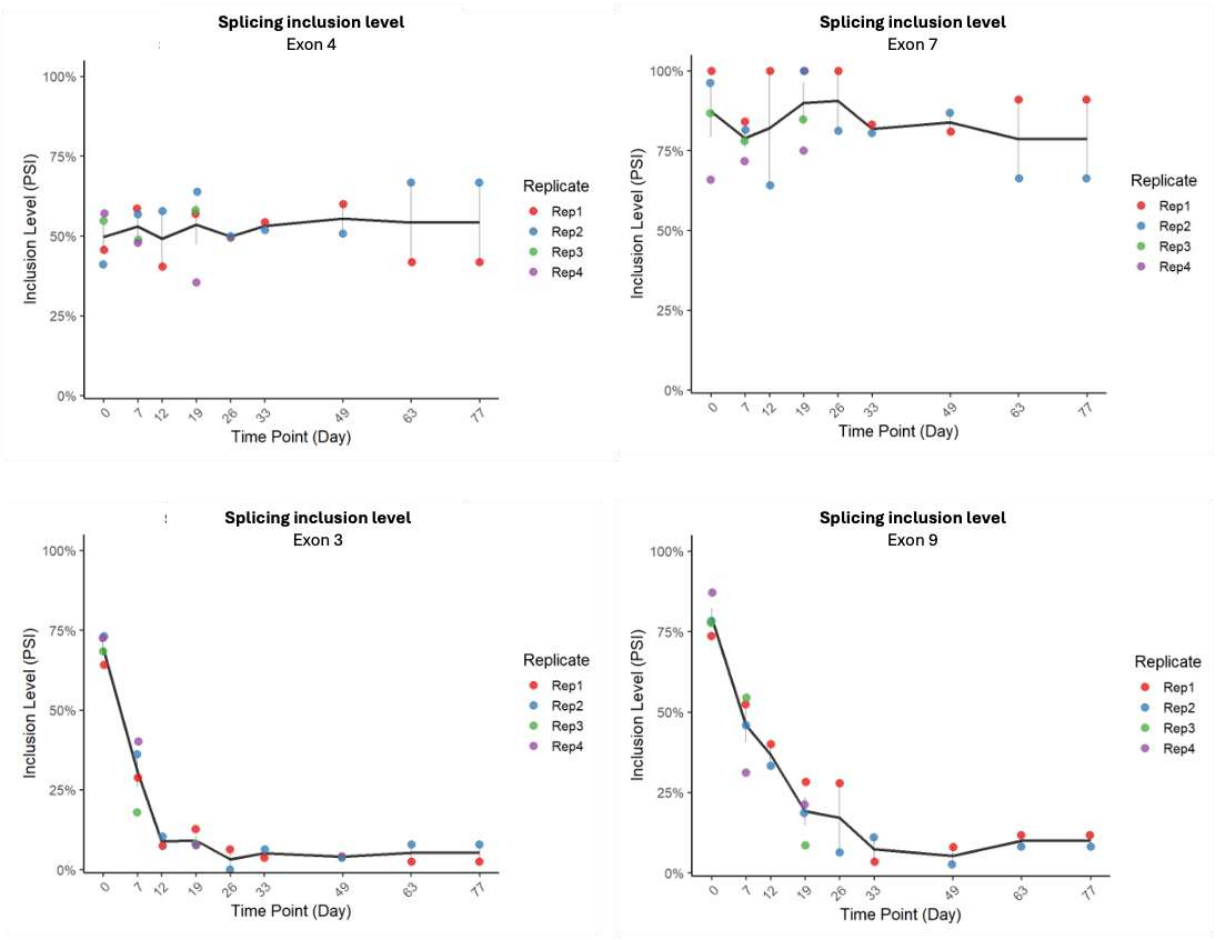

Figure 36: Dynamic exon usage during cortical neuron differentiation. Analysis based on Leemput et al. (2014).

It shows that while exons 4 and 7 used as controls and not subject to alternative splicing remain consistently included, the inclusion of Numb exons 3 and 9 markedly decreases after Day 12 of cortical neuron differentiation.

4.4.4- iPSC to cortical neuron differentiation: Analysis of Burke et al. (2020) dataset.

In a similar manner to the previous dataset derived from hESC differentiation, neural lineage progression from human induced pluripotent stem cells (iPSCs) was examined by analyzing the temporal expression of canonical developmental markers (FIG 37).

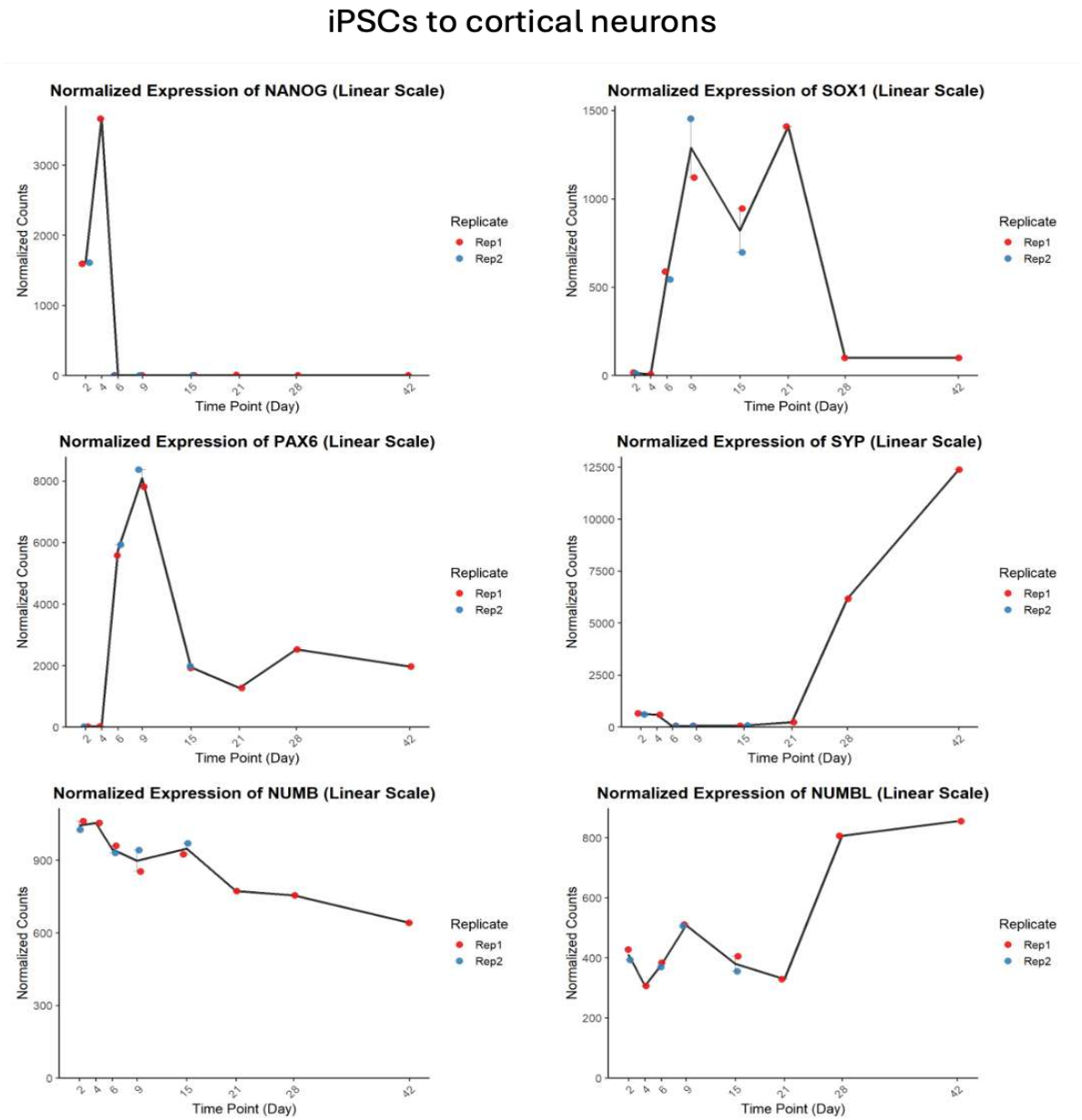

Figure 37: Expression profiles of pluripotency, neuronal, Numb, and NumbI markers. Analysis based on Burke et al. (2020).

It shows the temporal expression of pluripotency markers, neuronal markers, and Numb family proteins (Numb and Numbl) during neural differentiation.

NANOG, a key pluripotency factor, exhibited a pronounced peak in expression around days 2-3, corresponding to the undifferentiated iPSC stage. Following this period, NANOG expression sharply declined, marking the transition out of the pluripotent state and the onset of neural induction. SOX1, an early neuroectodermal and pre-neural progenitor marker, increased in expression immediately after the loss of NANOG, confirming the initiation of neural specification. Interestingly, compared to hESC differentiation, SOX1 downregulation in iPSC-derived cultures occurred more gradually, suggesting a slightly extended or asynchronous transition between pluripotent and progenitor stages, possibly reflecting epigenetic variability or residual somatic memory intrinsic to iPSCs.

PAX6, a hallmark of neural progenitor identity, showed a robust increase in expression from day 0 through day 12, reaching its maximum during the establishment of the earliest NPC population. Subsequently, its levels gradually declined as differentiation progressed toward more mature neuronal phenotypes. Consistent with this trajectory, SYP (Synaptophysin), a marker of synaptic vesicle proteins and neuronal maturation, began to rise significantly after day 26, reflecting the appearance of mature, postmitotic neurons and synaptic network formation in the culture.

In terms of Numb and Numb-like (Numbl) expression, both genes displayed sustained expression throughout the differentiation timeline, closely mirroring the trends observed in hESC-derived systems. This persistence suggests that Numb and Numbl play continuous and essential roles throughout neurogenesis, from progenitor maintenance to neuronal maturation. The consistent expression may reflect their involvement in fine-tuning signaling pathways such as Notch, which orchestrates the balance between self-renewal and differentiation in developing neural populations. Minor fluctuations observed during intermediate stages could arise from population heterogeneity or the coexistence of multiple Numb isoforms with distinct regulatory functions, further emphasizing the dynamic regulation of Numb alternative splicing during iPSC-derived neural differentiation.

4.4.5- Exon 3 and Exon 9–containing Numb isoforms decline during iPSC-derived cortical neuron differentiation (Burke et al. 2020).

Following the same approach used for the dataset from Leemput et al. (2014), exon 4 and exon 7 were included as internal controls, since both are not subject to alternative splicing events. The expression pattern observed was consistent with the previous dataset, supporting the reliability of the analysis [346].

In contrast, exons 3 and 9 exhibited dynamic regulation during differentiation, with their inclusion levels significantly decreasing as the cells transitioned from undifferentiated stem cells to neural progenitor cells (NPCs). Specifically, exon 3 inclusion showed a dramatic decline starting at day 3, reaching nearly undetectable levels by day 12, coinciding with the NPC stage. This reduction in exon 3 inclusion likely reflects the downregulation of isoforms containing exon 3, such as the long PRR variants p66 and p72, which are progressively silenced as cells commit to the neural lineage. Similarly, exon 9 inclusion followed a comparable trajectory, steadily decreasing from day 3 through day 20, just before the emergence of mature neurons, and continuing to decline thereafter (FIG 38). The coordinated loss of exon 3 and exon 9 inclusion during neural differentiation suggests a key regulatory switch in Numb splicing that favors the expression of isoforms lacking these exons (Ex3Δ/Ex9Δ), such as the shorter p65 variant.

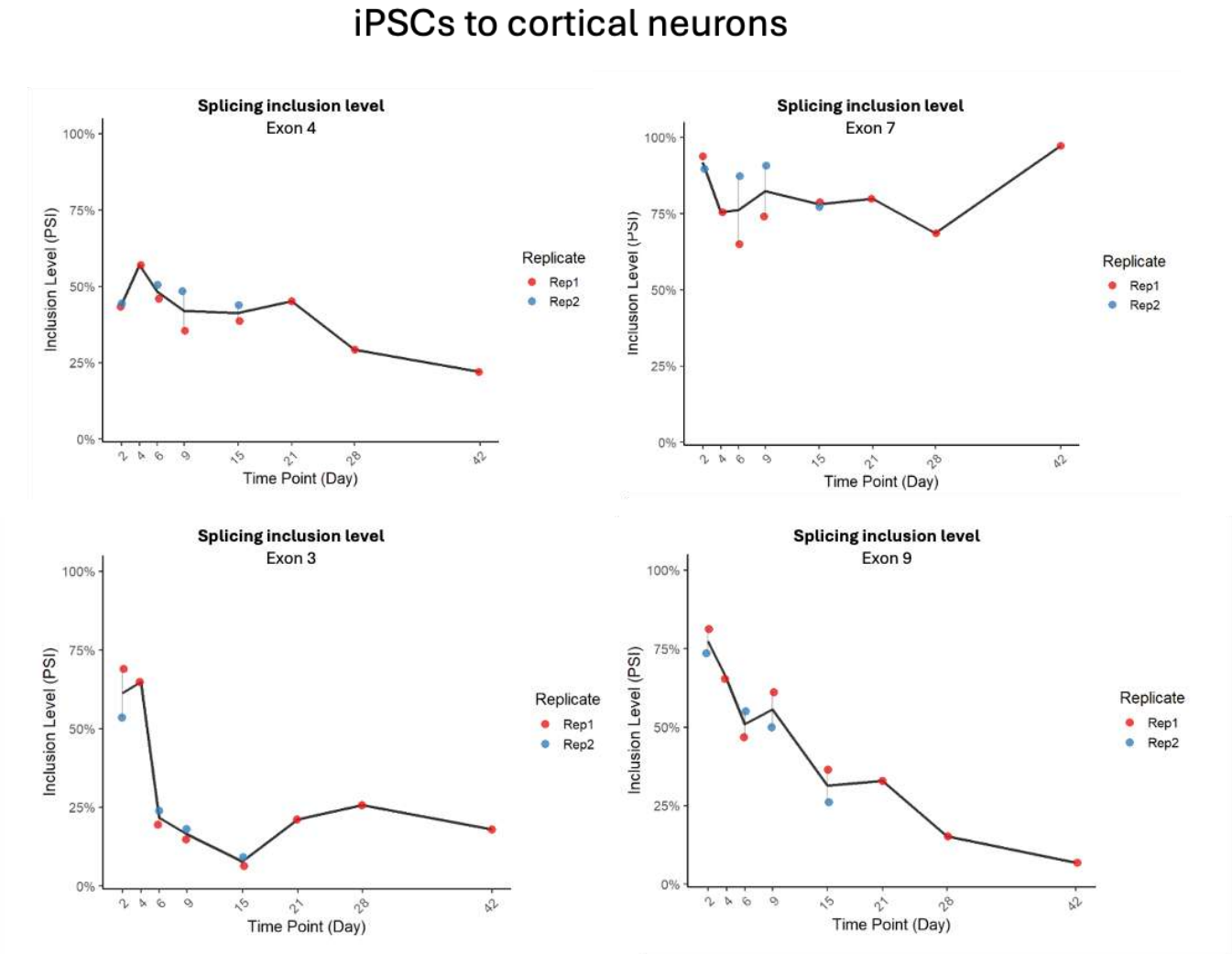

***Figure 38: Stage-specific alternative splicing of Numb exons during cortical differentiation. Based on Burke et al. (2020*).**

It shows that while exons 4 and 7 used as controls and not subject to alternative splicing remain consistently included, the inclusion of Numb exons 3 and 9 markedly decreases after Day 12 of cortical neuron differentiation.

This shift is consistent with findings that shorter Numb isoforms are associated with neuronal differentiation and maturation, while the longer isoforms are more prevalent in undifferentiated or proliferative states. Therefore, the progressive exclusion of exons 3 and 9 may reflect an essential splicing mechanism driving the transition from proliferative neural progenitors to differentiated neurons.

4.5- Functional requirement of Numb

4.5.1- Degradation systems: Comparison of OsTIR1 and dTAG approaches.

We compared the efficiency of Numb degradation in human embryonic stem cells using two orthogonal degradation systems: the OsTIR1/auxin-inducible degron (AID) system and the dTAG system. The OsTIR1 system operates via a two-step mechanism, in which the target protein is first tagged with an AID domain and subsequently recognized by the plant-derived F-box protein OsTIR1 in the presence of auxin, leading to ubiquitination and proteasomal degradation. In contrast, the dTAG system functions as a one-step process: the target protein is fused to a $FKBP12^{F36V}$ domain, and upon addition of the dTAG small molecule, the fusion protein is directly recruited to endogenous E3 ligases for rapid degradation. In our hands, the dTAG system achieved faster depletion of Numb, with a more immediate reduction in protein levels, whereas the OsTIR1 system exhibited a slightly delayed response, likely reflecting the requirement for two sequential steps. Both systems achieved robust and specific degradation, but the single step dTAG approach provides a more streamlined and temporally precise tool for acute protein depletion in human embryonic stem cells.

To compare degradation systems in human embryonic stem cells, we evaluated the OsTIR1/auxin-inducible degron (AID) system versus the dTAG system. Their differences could be observed in FIG 39 and Table 8.

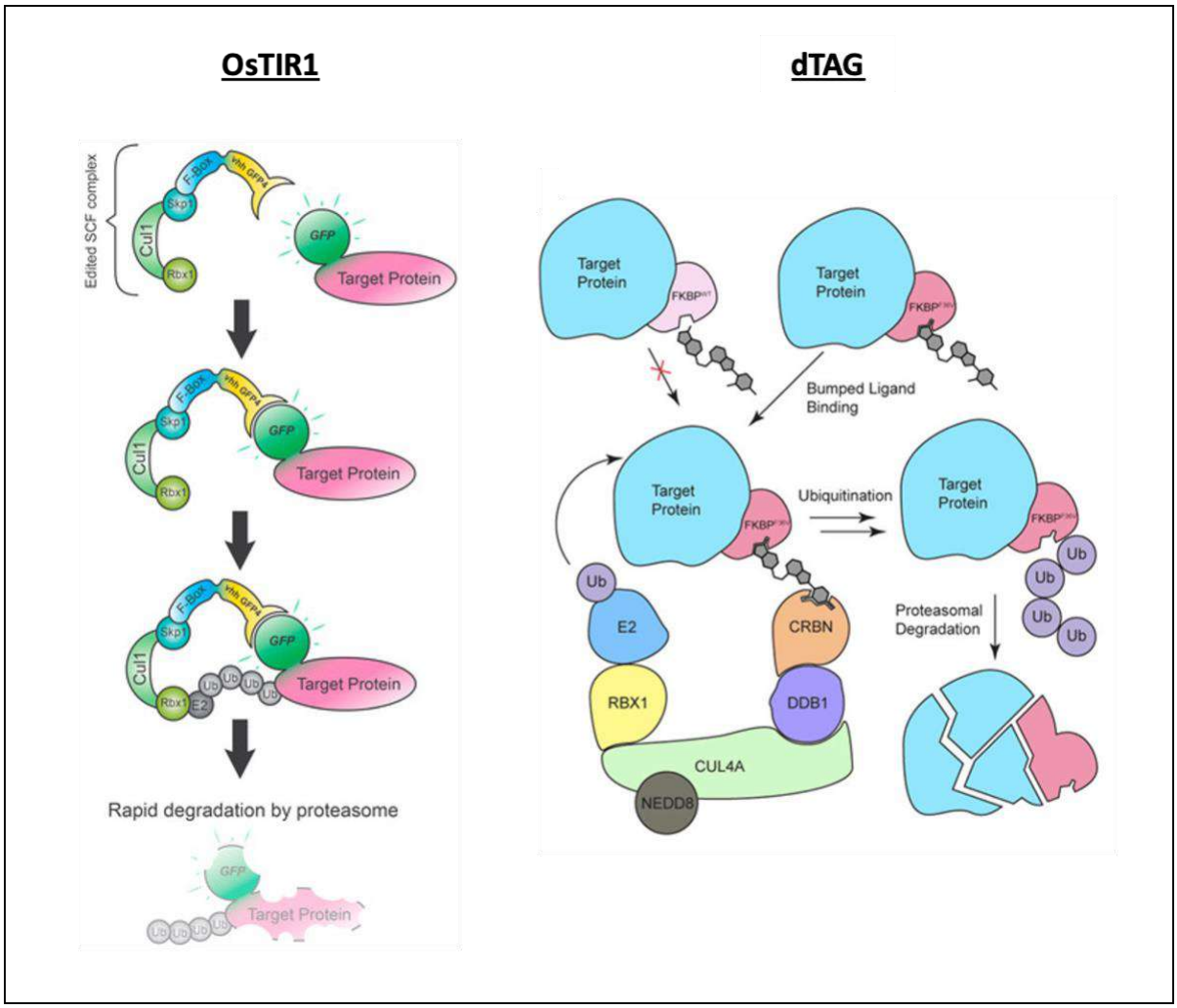

Figure 39: Comparison of OSTR1 and dTAG protein degradation systems.

Schematic comparison of two widely used targeted protein degradation platforms: the OSTR1 and dTAG systems. Key mechanisms of action are highlighted in the scheme.

Electroporation of the two components required for the OsTIR1 system resulted in extensive cell lethality, indicating that this system it might be toxic to human embryonic stem cells (hESCs). Although the OsTIR1 system was previously established and successfully used in mouse embryonic stem cells (mESCs) within the laboratory, following the same protocol failed to yield viable hESCs after electroporation. Moreover, because OsTIR1 relies on a two-step integration process, the efficiency of obtaining correctly modified cells is considerably reduced (FIG 40). This added complexity, together with the observed cytotoxicity, makes the system particularly challenging to apply in hESCs.

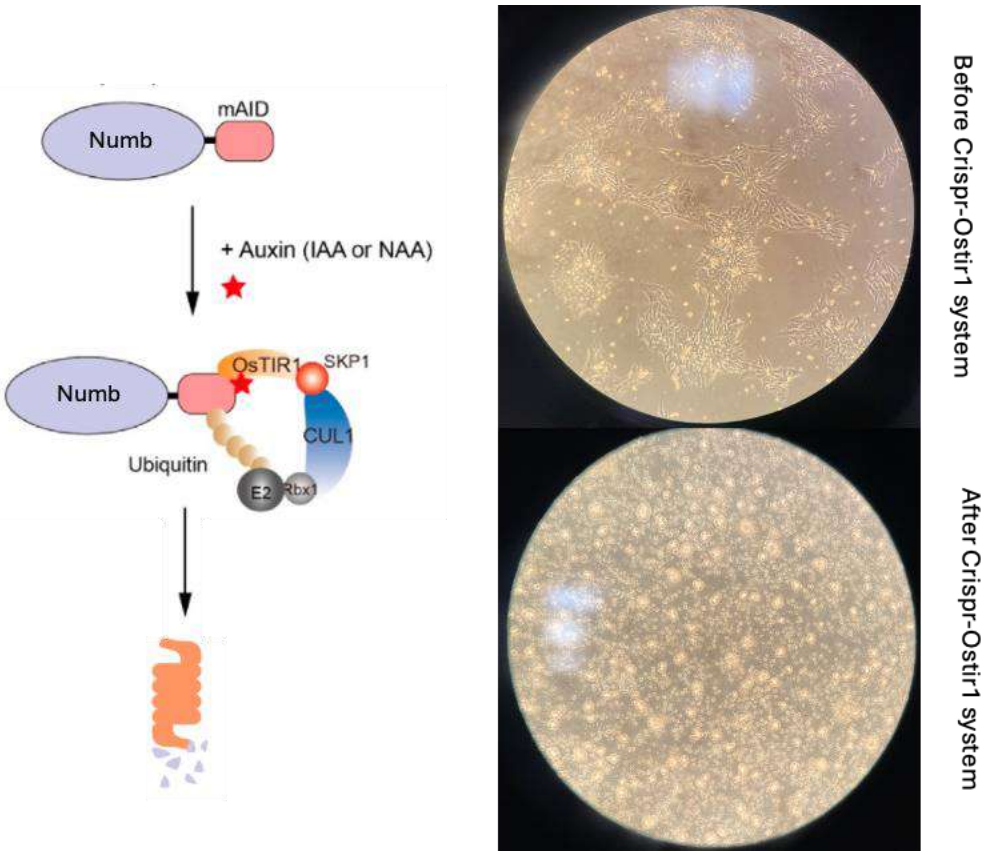

Figure 40: Limitations of the OSTR1 system in CRISPR-modified cells.

Following CRISPR-mediated genome editing, the OSTR1 degradation system was unable to preserve cellular viability. This highlights potential cytotoxic effects or incompatibility of the system in cells harboring essential gene modifications.

	dTAG	OsTIR1
Mechanism	Uses a synthetic small molecule ligand to bind a target protein tagged with $FKBP12^{F36V}$ and an E3 ligase, triggering degradation.	An F-box protein that, when combined with a degron tag on a target protein, uses the plant hormone auxin to trigger degradation.
Inducer	Synthetic small molecule ligand (e.g., dTAG-v1).	Auxin (e.g., indole-3-acetic acid).
Application	Commonly used in mammalian cells to study gene function.	Used in various organisms, including yeast, plants, and mammalian cells, often requiring the expression of OsTIR1 protein and the degron tag.
Complexity	Requires only one genetic element (the $FKBP12^{F36V}$-tagged protein) for the system to work in some applications.	Requires two genetic elements (the OsTIR1 protein and the degron-tagged protein).
Reversibility	Reversible: degradation stops when the ligand is removed.	Reversible: protein levels recover after auxin is removed from the medium.

Table 8: Mechanistic comparison of OSTR1 and dTAG degradation systems.

Even though, the dTAG and OsTIR1/AID systems both enable conditional protein degradation through ligand-induced recruitment of an E3 ubiquitin ligase, yet they differ significantly in design, kinetics, and suitability for human embryonic stem cells (hESCs).

One of the main advantages of the dTAG system in hESCs is its genetic simplicity. Only the degron-tagged allele must be generated, since the endogenous ubiquitin-proteasome machinery is sufficient for degradation. In contrast, the OsTIR1/AID system requires the introduction of both the AID tag and the OsTIR1 transgene, increasing the genetic burden on pluripotent cells. This difference is particularly relevant in hESCs, where maintaining genomic stability and pluripotency is essential. The introduction of a plant-derived protein such as OsTIR1 can sometimes alter gene expression networks or cell cycle behavior, leading to variability or loss of pluripotency.

A key advantage of the dTAG system is its compatibility with mammalian cellular physiology. The dTAG ligands are small, cell-permeable molecules with minimal off-target effects, and the system does not rely on exogenous pathways. In contrast, the auxin-inducible degron system introduces a heterologous plant pathway into mammalian cells, which can lead to unwanted interactions or altered signaling. Auxin itself can be less stable in culture and sensitive to medium pH, further contributing to variability.

From a technical perspective, both systems use relatively small tags (roughly 10-12 kDa), but dTAG achieves degradation more consistently and with fewer background effects. The dTAG system also performs better in hESCs due to the uniform accessibility of its ligand and the absence of the need for exogenous transgene expression.

Functionally, the dTAG system has proven particularly powerful for studying developmental regulators in pluripotent cells. Its rapid and reversible control allows researchers to deplete key transcriptional or epigenetic factors transiently, capturing early or reversible changes during lineage commitment. The OsTIR1/AID system, while still useful in some contexts especially where shared OsTIR1-expressing lines exist tends to be less predictable in pluripotent systems due to these biological and technical constraints.

In summary, for human embryonic stem cells, the dTAG system offers a clear advantage. It provides fast, reversible, and precise protein depletion without perturbing pluripotency networks or requiring additional transgenes. The OsTIR1/AID system remains a valid alternative, particularly for multiplexed tagging when a stable OsTIR1 line is already available, but overall, dTAG is generally preferred for hESC applications due to its simplicity, clean background, and superior performance in pluripotent contexts.

4.5.2- sgRNA targeting Exon 1 of endogenous Numb.

The dTAG system is designed around a bifunctional small molecule that enables highly specific and efficient targeted protein degradation. This molecule contains two functional arms: the left arm binds with high affinity to the engineered $FKBP12^{F36V}$ domain fused to the protein of interest, while the right arm recruits an endogenous E3 ubiquitin ligase, such as CRBN or VHL, to initiate ubiquitination and subsequent proteasomal degradation. Degradation occurs only when both interactions are established, ensuring stringent specificity, minimal off-target effects, and precise temporal control of protein depletion.

To generate an inducible degradation system for Numb, several genomic loci were tested for the insertion of the $FKBP12^{F36V}$ degron tag. The first strategy targeted exon 1, which is shared by all four human Numb isoforms. Tagging at this position allows the simultaneous and complete depletion of all isoforms, thus eliminating isoform-specific bias an essential feature when studying Numb's global function in stem cell maintenance and differentiation. In addition, exon 1 is located before the onset of alternative splicing, simplifying the editing process and minimizing the risk of disrupting regulatory splicing events.

An alternative strategy targeted exon 10, the last coding exon of Numb, which shows a high degree of sequence conservation among isoforms. The rationale for this approach was to maintain the integrity of the upstream regulatory regions while enabling isoform-inclusive tagging. However, this design proved technically challenging due to the large intronic regions flanking exon 10, which significantly reduced the efficiency of homology-directed repair (HDR). Furthermore, the small guide RNAs (sgRNAs) designed for this region exhibited low on-target scores, resulting in poor cutting efficiency and a limited recovery of correctly targeted clones. Consequently, despite its theoretical advantages, exon 10 was deemed unsuitable for precise editing in hESCs due to the complex genomic architecture surrounding the locus (FIG 41).

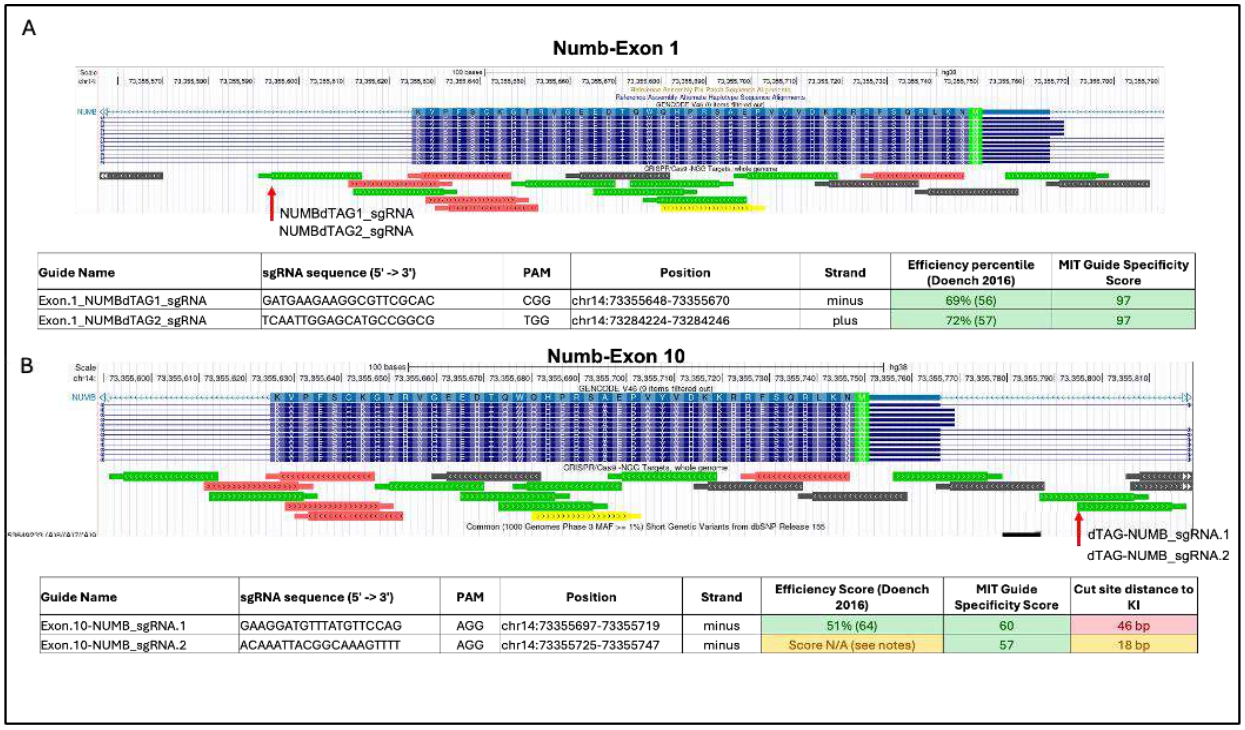

Guide Name	sgRNA sequence (5' -> 3')	PAM	Position	Strand	Efficiency percentile (Doench 2016)	MIT Guide Specificity Score
Exon.1_NUMBdTAG1_sgRNA	GATGAAGAAGGCGTTCGCAC	CGG	chr14:73355648-73355670	minus	69% (56)	97
Exon.1_NUMBdTAG2_sgRNA	TCAATTGGAGCATGCCGGCG	TGG	chr14:73284224-73284246	plus	72% (57)	97

Guide Name	sgRNA sequence (5' -> 3')	PAM	Position	Strand	Efficiency Score (Doench 2016)	MIT Guide Specificity Score	Cut site distance to KI
Exon.10-NUMB_sgRNA.1	GAAGGATGTTTATGTTCCAG	AGG	chr14:73355697-73355719	minus	51% (64)	60	46 bp
Exon.10-NUMB_sgRNA.2	ACAAATTACGGCAAAGTTTT	AGG	chr14:73355725-73355747	minus	Score N/A (see notes)	57	18 bp

Figure 41: Design of sgRNAs targeting human Numb exons.

Small guide RNAs (sgRNAs) designed to target Exon 1 and Exon 10 of the human Numb gene. The sgRNAs were selected based on predicted on-target efficiency and minimal off-target effects to facilitate CRISPR-mediated genome editing.

Other exons, such as exon 4 and exon 5, were also evaluated as potential insertion sites for the FKBP12^{F36V} domain. Similar to exon 10, these regions are embedded within extensive intronic sequences, complicating targeted integration and yielding low sgRNA efficiency scores (data not shown). Moreover, targeting internal exons carries an additional risk of disrupting isoform-specific splicing, which could alter Numb expression or produce nonfunctional variants.

Ultimately, targeting exon 1 emerged as the most robust and efficient strategy. The combination of this strategic tagging site with a well-balanced homology arm design in the donor construct enabled high HDR efficiency and the generation of stable hESC lines expressing the FKBP12^{F36V}tagged Numb protein.

Upon validation, these cells displayed normal morphology, proliferation, and differentiation potential, confirming that the integration of the dTAG system at exon 1 is both functionally neutral and biologically compatible. This configuration allows rapid, reversible, and isoform-independent depletion of Numb in hESCs, providing a reliable platform for dissecting its role in early human development (FIG 42).

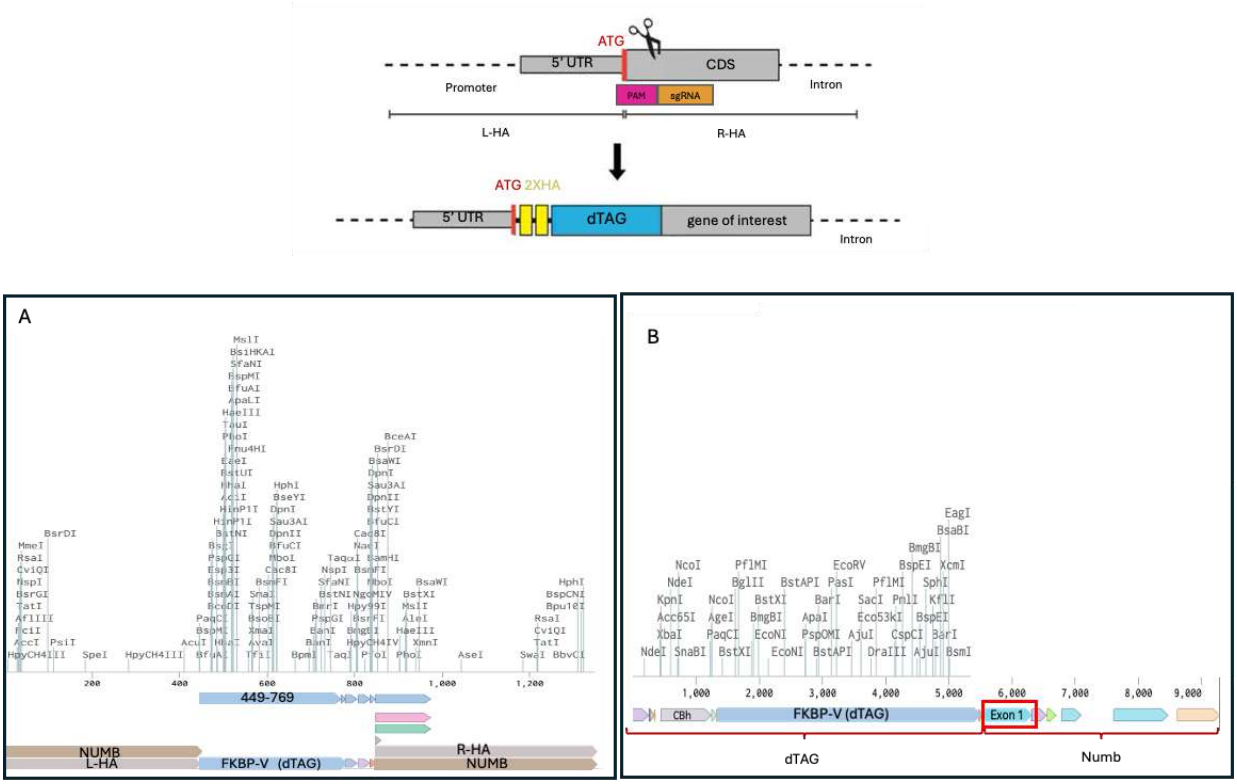

Figure 42: Schematic of dTAG integration into the Numb locus.

Representative diagram illustrating the dTAG construct design for CRISPR-mediated tagging of Numb. The construct includes a left homology arm (L-HA) and right homology arm (R-HA) flanking the FKBP-V(dTAG) degron, which is fused in-frame to the first exon of Numb.

4.5.3- Clone 210 exhibits homozygous integration of the dTAG cassette in the parental line.

After CRISPR-mediated integration of the FKBP12^{F36V} degron tag (dTAG) into the Numb locus, it was essential to determine whether the modification occurred in one or both alleles. Distinguishing between heterozygous and homozygous clones is a crucial validation step, as it directly impacts the efficiency and interpretation of downstream degradation experiments. Only homozygous integration guarantees that all Numb alleles are tagged with the FKBP12^{F36V} degron, enabling complete and uniform depletion of the protein upon treatment with the dTAG ligand. In contrast, heterozygous clones, which retain one wild-type allele, continue to express untagged Numb isoforms, leading to only partial degradation and potentially masking phenotypic consequences associated with complete Numb loss. Thus, confirming zygosity was necessary to ensure the fidelity of subsequent functional analyses in human embryonic stem cells (hESCs).

To discriminate between homozygous and heterozygous integrations, specific primer sets were designed to amplify regions spanning both the endogenous Numb sequence and the inserted dTAG cassette. One set of primers recognized sequences within the FKBP12^{F36V} degron, while another set targeted endogenous regions of Numb flanking the insertion site. The PCR strategy allowed clear differentiation between tagged and untagged alleles: amplification of the dTAG-integrated allele produced a fragment of 574 base pairs (bp), whereas amplification of the wild-type allele yielded a 350 bp product (FIG 43).

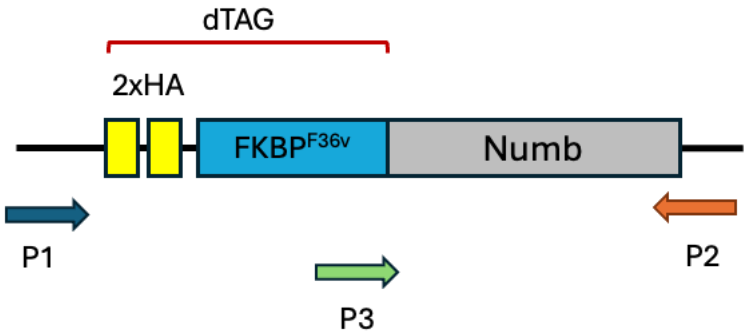

Figure 43: Primer design for validation of Numb-dTAG fusion.

Following screening of over 900 individual clones, the vast majority exhibited the presence of both PCR bands, indicating heterozygous integration of the dTAG cassette. Remarkably, only a single clone designated Clone 210 displayed the exclusive 574 bp band, confirming homozygous insertion of the FKBP12^{F36V} degron into both Numb alleles, using a Parental Line WT as a control. This clone was therefore selected for all subsequent characterization and degradation assays, ensuring that all Numb isoforms could be uniformly degraded upon dTAG ligand addition and that the observed effects truly reflected the complete loss of Numb function in hESCs (FIG 44).

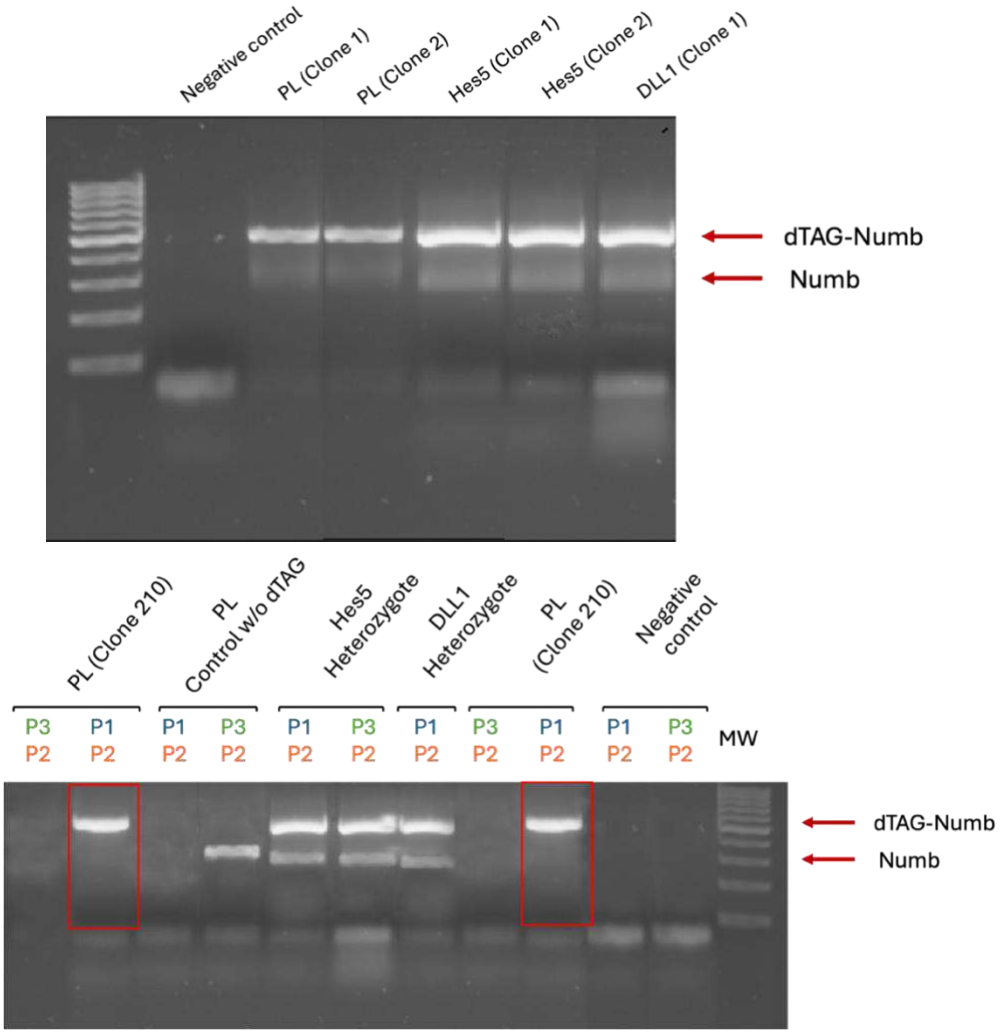

Figure 44: PCR-based screening of Numb-dTAG clones.

PCR screening was performed to distinguish homozygous and heterozygous Numb-dTAG clones. (A) Representative gel showing clone identification based on expected band sizes. (B) Representative gel highlighting the sole homozygous clone (Clone 210) compared to wild-type control (WT), heterozygous clones, and a negative control.

4.5.4- dTAG integration is non-toxic in both heterozygous and homozygous clones during cortical neuron differentiation.

After confirming the successful insertion of the dTAG sequence and determining the zygosity (heterozygous or homozygous), the next question was whether the modified cells retained their ability to differentiate, and whether the incorporation of the dTAG system introduced any potential toxicity. For this analysis, the selected cell lines included the Parental Line clone 210 (the only homozygous clone identified) and the heterozygous DLL1 and Hes5 clones. At day 0 of Neural differentiation, all the cell lines expressed OCT4 as a nuclear marker of pluripotency or stemness (FIG 45).

The incorporation of the dTAG system into all three human embryonic stem cell (hESC) lines via electroporation did not impair their ability to undergo neural differentiation. Following selection and expansion, the modified hESCs retained their typical pluripotent morphology and differentiation capacity, confirming that the introduction of the $FKBP12^{F36V}$ degron tag and associated elements was non-toxic and did not interfere with key cellular processes required for lineage specification.

At the pluripotent stem cell stage, around day 12-15 at NPC stage, all three lines expressed both Hes5 (red) and Numb (green). Confocal imaging revealed that Hes5, a transcription factor downstream of the Notch pathway, was predominantly localized in the nucleus, where it appeared as bright punctate signals corresponding to active transcriptional foci. In contrast, Numb showed a mainly cytoplasmic distribution, consistent with its role as an endocytic adaptor and regulator of membrane signaling, although a fraction of Numb signal was also detected in the nucleus. The merged fluorescence images displayed overlapping regions of red and green, visualized as yellow puncta, indicating partial co-localization of Numb and Hes5 within specific cellular compartments (FIG 46).

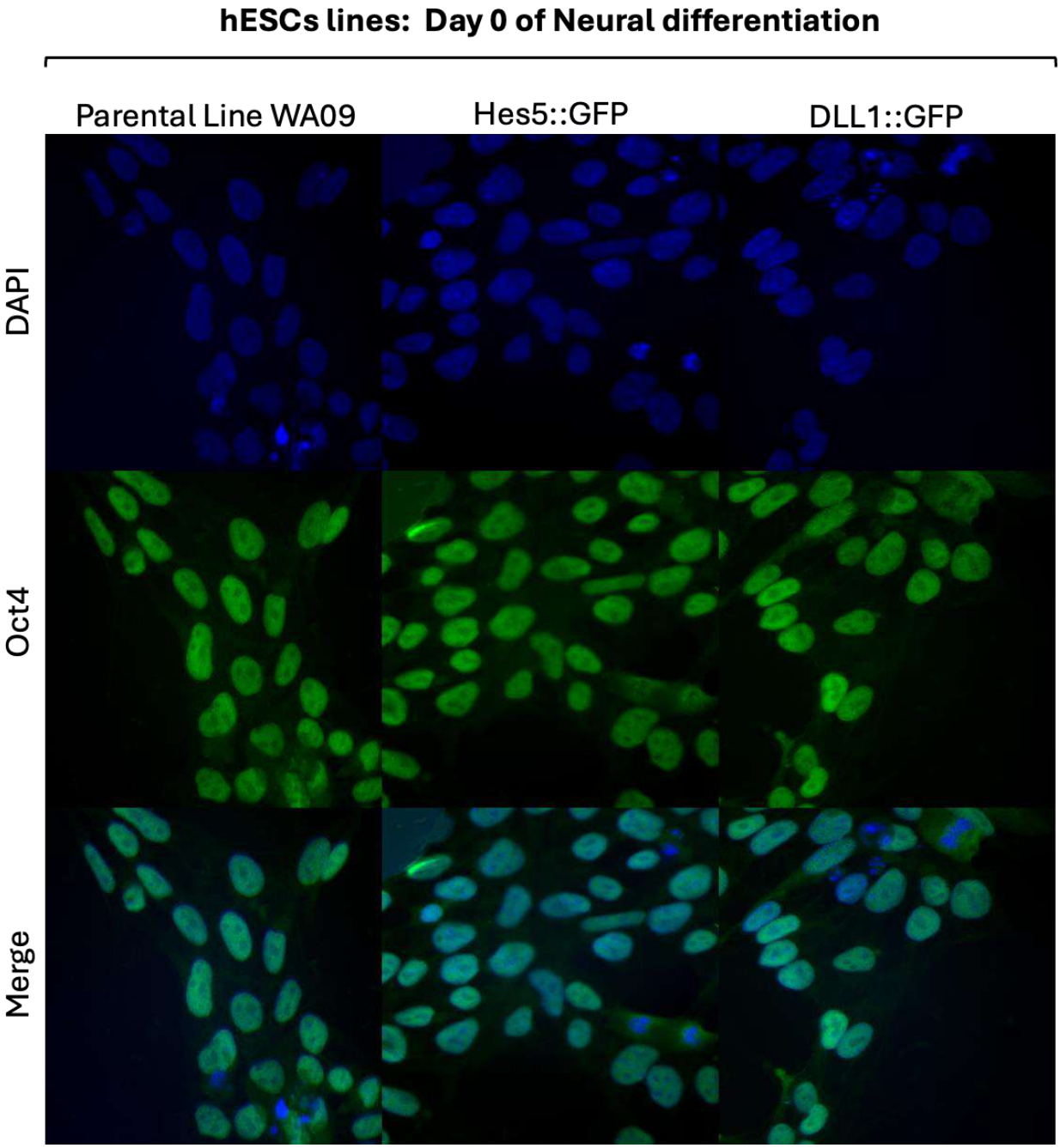

Figure 45: Nuclear OCT4 expression in hESCs.

Immunofluorescence analysis of human embryonic stem cells (hESCs) Parental WA09 (H9), He5::GFP, and DLL1::GFP lines demonstrates expression of the pluripotency marker OCT4 in the stem cell state. OCT4 signal (green) is localized to the nucleus, as confirmed by colocalization with DAPI (blue), indicating maintenance of pluripotent identity in all lines.

Upon induction of neural differentiation, the modified cells efficiently progressed into neural progenitor cells after (NPCs), displaying the typical elongated, polarized morphology characteristic of early neuroepithelial identity. At this stage, the expression pattern of Numb changed markedly compared to the stem cell state, with Numb remaining largely cytoplasmic. In contrast, DLL1 (red) a canonical Numb ligand and Notch pathway component became strongly expressed and was restricted to the cytoplasm and plasma membrane of NPCs, particularly between days 15 and 20 of cortical neuron differentiation, when the first neuron appears. The co-localization of Numb and DLL1 was evident by the appearance of yellow fluorescence, reflecting their close spatial association and potential molecular interaction during early neurogenesis (FIG 47).

These results demonstrate that integration of the dTAG system does not perturb the intrinsic developmental potential or molecular identity of hESCs. The presence of the degron tag and exposure to the dTAG ligand (dTAG v1) did not induce cytotoxicity or alter the expression of key developmental regulators such as Hes5, Numb, or DLL1. Collectively, these findings confirm that the dTAG system is biologically inert and compatible with human pluripotent cells, allowing precise, reversible, and temporally controlled degradation of target proteins without compromising cell viability, proliferation, or differentiation potential. This establishes dTAG as a powerful and versatile platform for dissecting protein function during early human neurodevelopment, enabling real-time interrogation of signaling dynamics and cell fate transitions under physiological conditions.

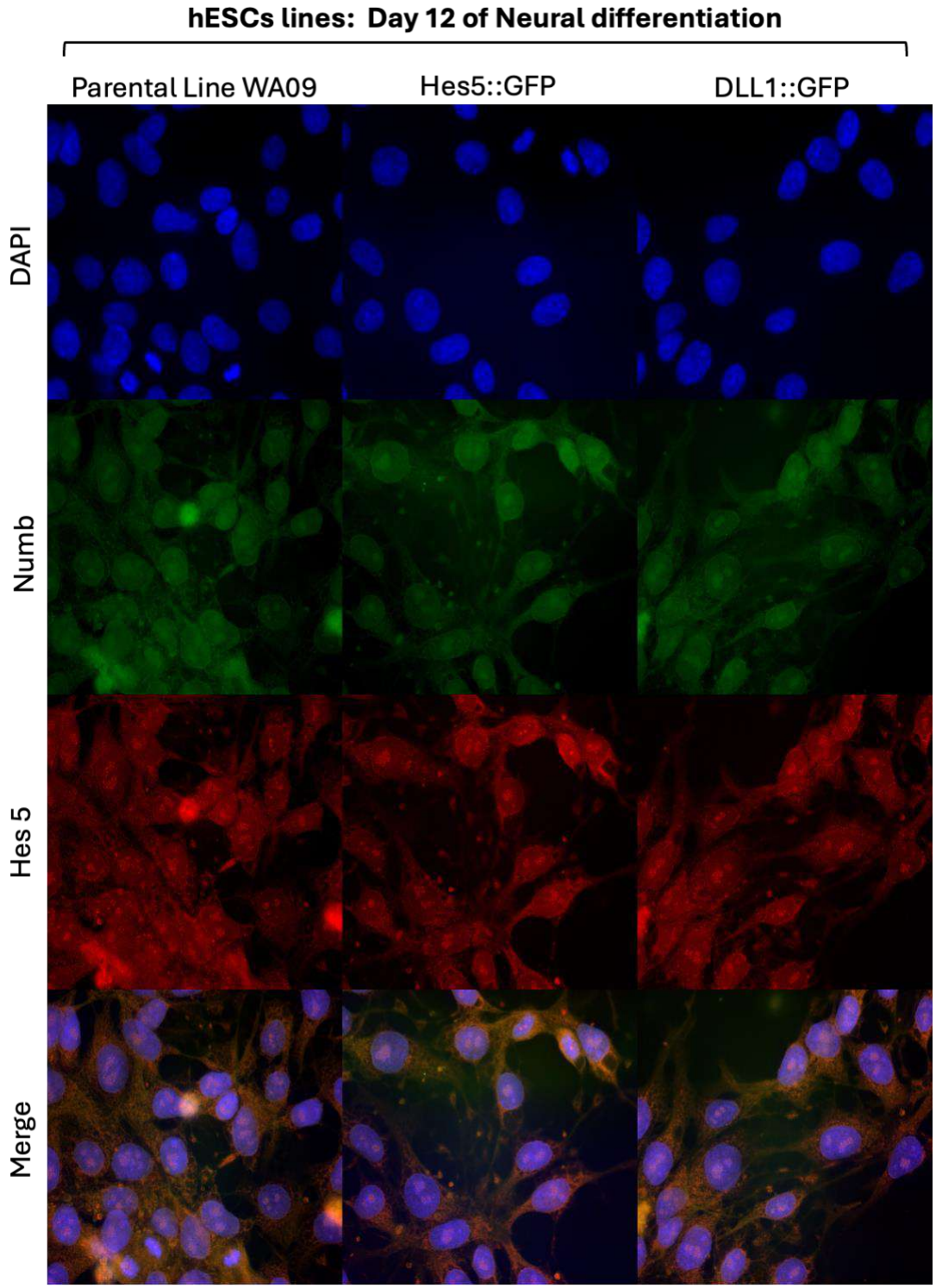

Figure 46: Numb and Hes5 Localization in hESC-dTAG lines during neural differentiation.

Immunofluorescence analysis of hESC-dTAG lines parental WA09 (H9), Hes5::GFP, and DLL1::GFP at Day 12 of cortical neuron differentiation. Numb (green) and HES5 (red) show overlapping expression (yellow) in the cytoplasm, with peak (brightness) accumulation observed in the nuclei.

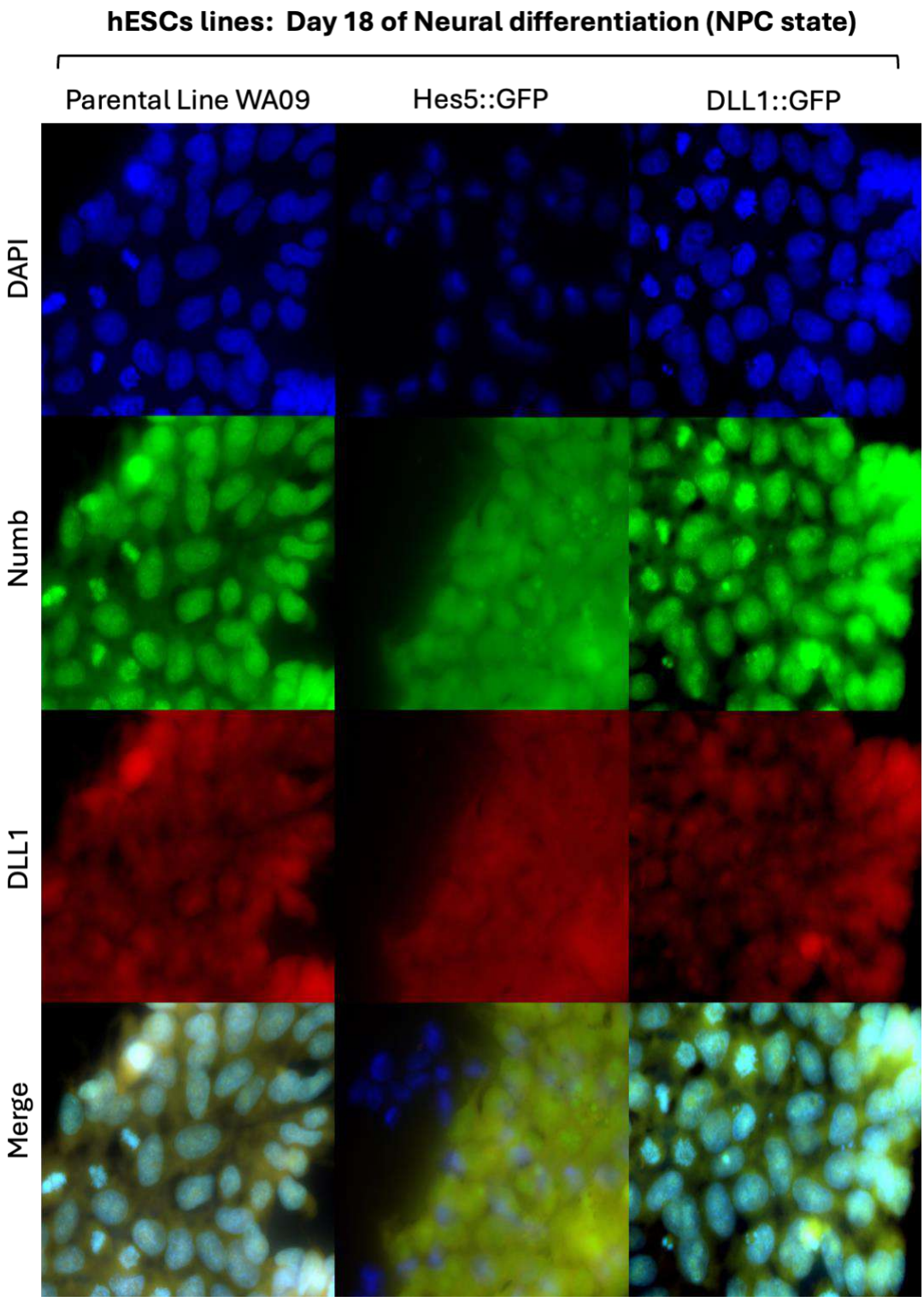

Figure 47: Numb and DLL1 localization in hESC-dTAG lines at the neural progenitor stage.

Immunofluorescence analysis of hESC-dTAG lines. Parental WA09 (H9), Hes5::GFP, and DLL1::GFP at Day 18 of cortical neuron differentiation, corresponding to the neural progenitor cell (NPC) stage. Numb (green) and DLL1 (red) exhibit overlapping cytoplasmic expression, as shown in the merged images (yellow).

4.5.5- hESCs are highly susceptible to Numb degradation dTAG-mediated.

After confirming that the insertion of the dTAG system was not cytotoxic and did not interfere with the ability of the cells to differentiate through cortical neural lineage, the next step was to determine the optimal concentration of the dTAGv1 ligand. Establishing this concentration is critical to achieve precise and reproducible control over the extent and kinetics of Numb degradation. Because the dTAG system operates through a small-molecule-induced interaction between the degron-tagged protein and an E3 ubiquitin ligase, ligand concentration directly dictates both the efficiency and speed of protein degradation. Testing a range of concentrations allows identification of the minimal effective dose required for complete and rapid Numb depletion while minimizing off-target effects or cytotoxic responses. Moreover, characterizing degradation kinetics across different doses provides insight into the temporal dynamics of protein turnover, which is particularly important when investigating the immediate versus sustained effects of Numb loss during neural differentiation.

To assess this, degradation was induced within a defined time window suitable for monitoring the impact of Numb loss on neural commitment during cortical neuron differentiation. The experimental setup included PL-dTAG (Clone 210), heterozygous Hes5-dTAG and DLL1-dTAG lines, their respective wild-type control. The first concentration series tested consisted of 75 nM, 50 nM, 25 nM, 10 nM, 7.5 nM, and 2.5 nM of dTAGv1, using vinculin as a loading control to evaluate degradation efficiency. Based on published data, a 9–12-hour treatment window was considered optimal to induce measurable protein depletion and to rescue the phenotype in subsequent functional assay [348].

In all tested cell lines, the addition of dTAGv1 triggered a rapid depletion of Numb protein, with total degradation observed as less than three hours post-treatment (Data not shown), promoting the cells goes to death. This rapid response indicates that the system is effective but particularly sensitive to Numb loss.

The early onset of degradation suggests that the dTAGv1 ligand efficiently penetrates the cells and promptly induces the formation of the ternary complex required for ubiquitination and proteasomal degradation. Such fast kinetics not only confirm the functional efficiency of the dTAG system in these lines but also highlight the critical dependence of these cells on Numb levels, as even short-term depletion may rapidly alter downstream signaling and cellular behavior. Cell lines control was tested with 2.5nM of dTAGv1, concentration considered High considering the result showing with the cells lines targeted by Crispr (FIG 48).

Given the pronounced sensitivity of the cells upon Numb depletion, the next step was to evaluate whether lower concentrations of dTAGv1 could induce a more controlled degradation without compromising cell viability. To this end, a new dilution range was tested, from 0.05 nM to 0.5 nM, across PL-dTAG, Hes5-dTAG, and DLL1-dTAG cell lines, using their respective WT controls cell lines of degradation of Numb. Despite the substantial reduction in ligand concentration, the outcome remained consistent with previous observations: cells exhibited marked morphological deterioration within 3 hours of treatment and complete cell death by 6 hours with 0.05 nM of dTAG, while the others concentration tested, showed a complete Numb degradation between 3-6 hours. These results indicate that even minimal levels of dTAGv1 are sufficient to trigger near-complete Numb degradation, leading to a loss of essential cellular functions required for survival. This extreme sensitivity underscores the critical dependence of these cell lines on Numb for maintaining cellular homeostasis and suggests that Numb plays a non-redundant role in sustaining viability during the early stages of neural commitment.

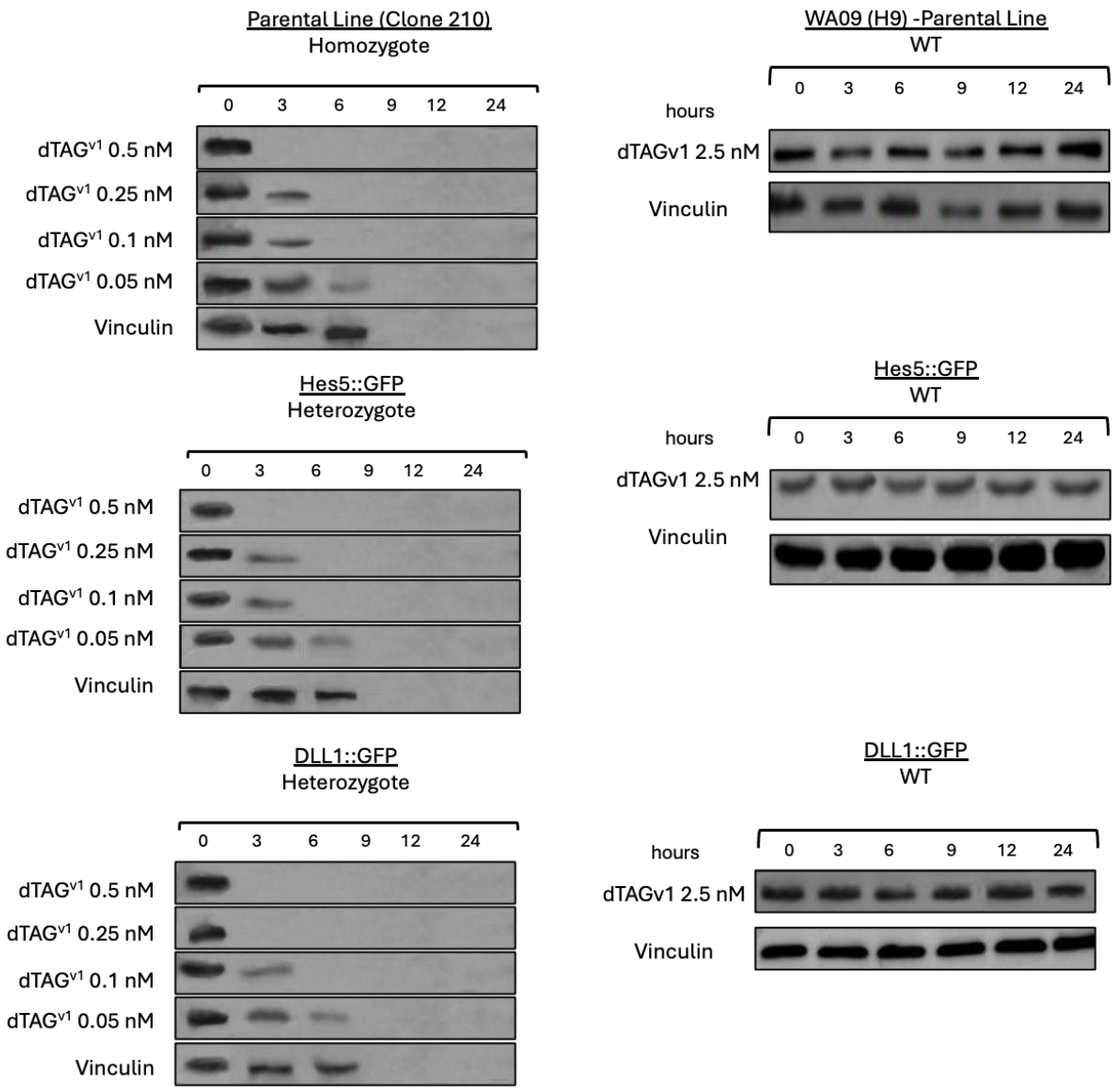

***Figure 48: Rapid Numb degradation using the dTAG system*.**

Western blot analysis demonstrating fast degradation of Numb via the dTAG system. Left panels show dTAG-treated Numb-dTAG clones: Parental Clone 210 (homozygous) and Hes5::GFP and DLL1::GFP (heterozygous) treated with low dTAG concentrations (0.05–0.5 nM). Right panels depict wild-type (WT) cells treated with 2.5 nM dTAG as controls.

4.5.6- Inducible expression of Numb isoforms fails to rescue cell death triggered by dTAG-mediated degradation of endogenous Numb.

Taking these results into account, it became clear that endogenous Numb is extremely sensitive to dTAGv1-mediated degradation, with complete loss observed even at concentrations as low as 0.1 nM and 0.05 nM. To counteract this rapid depletion and assess whether exogenous expression could rescue the phenotype, each Numb isoform or the pool of them it was independently reintroduced using our pLVx expression plasmids (FIG 49). The goal was to restore Numb function and buffer the effects of acute degradation, recognizing that transcriptional activation and protein synthesis occur at a slower rate than proteasomal degradation. To minimize stress and off-target effects typically associated with electroporation, lentiviral transduction was selected as the delivery method for stable expression.

To verify proper system functionality, the plasmids were transfected and analyzed by Western blot using an anti-SNAP-tag antibody, confirming successful induction of SNAP-tagged Numb isoforms (FIG 4.35). Doxycycline (DOX) was applied at three concentrations, 20 ng/ml, 100 ng/ml and 1 µg/m1 to determine the expression efficiency and dose-responsiveness of the inducible system (FIG 50).

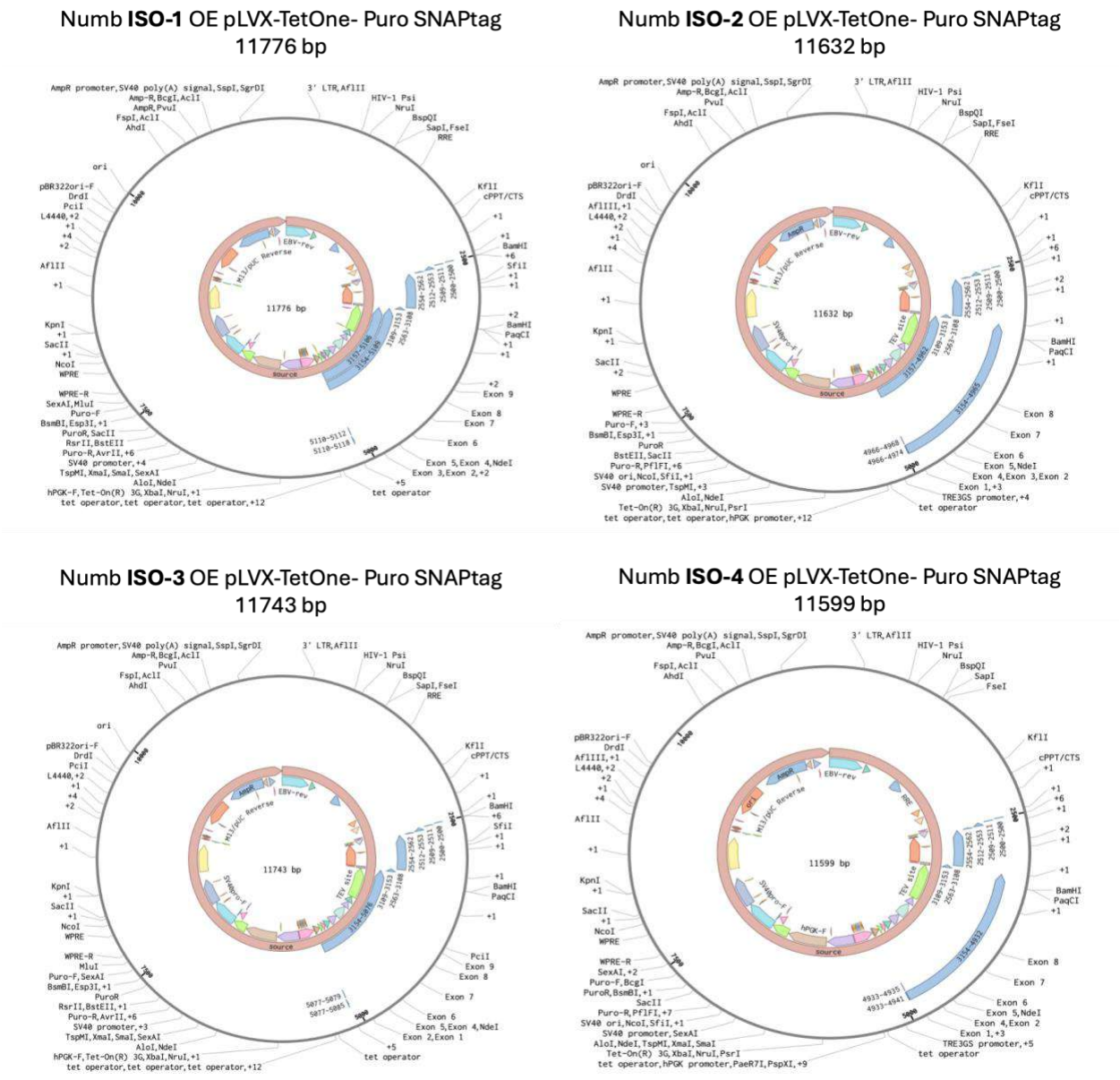

Figure 49: Schematic of pLVX plasmids encoding human Numb isoforms.

Diagram illustrating the pLVX plasmid constructs used to express individual human Numb isoforms. Each plasmid contains the coding sequence for a specific Numb isoform, enabling isoform-specific expression studies in transfected cells.

For example, cells grown to approximately 80% confluence were treated with 0.1 nM dTAGv1 to induce Numb degradation. After 10 hours of treatment, doxycycline (DOX) was added to the culture medium to initiate expression of the SNAP-tagged Numb isoforms. Three different DOX concentrations were tested) to evaluate the dose-dependent induction of exogenous Numb and its potential to counteract or rescue the effects of endogenous Numb depletion (TABLE 9).

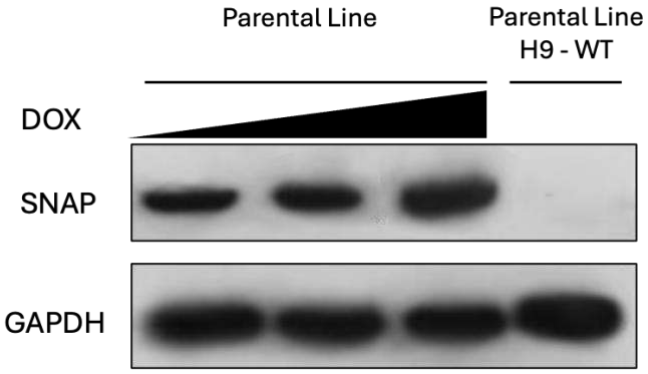

Figure 50: DOX-Inducible expression of Numb isoforms.

In Parental line clone 210 and WT were transfected with a plasmid encoding a pool of Numb isoforms fused to a SNAP tag. Expression was induced by increasing concentrations of doxycycline (DOX), and GAPDH was used as a loading control.

Doxycycline (DOX)	
Concentration	Results
1µg/mL	Strong or robust induction
100 ng/mL	Moderate induction
20 ng/mL	Low induction

Table 9: Evaluation of SNAP-DOX induction system robustness.

Across all tested concentrations, SNAP-tag expression was clearly detected and correlated with the applied DOX dose, demonstrating that the inducible system effectively drives isoform-specific Numb expression in a tunable manner (FIG 51). These findings establish a functional platform for subsequent rescue experiments aimed at dissecting isoform-dependent differences in Numb stability, degradation resistance, and their ability to sustain cell viability during neural differentiation.

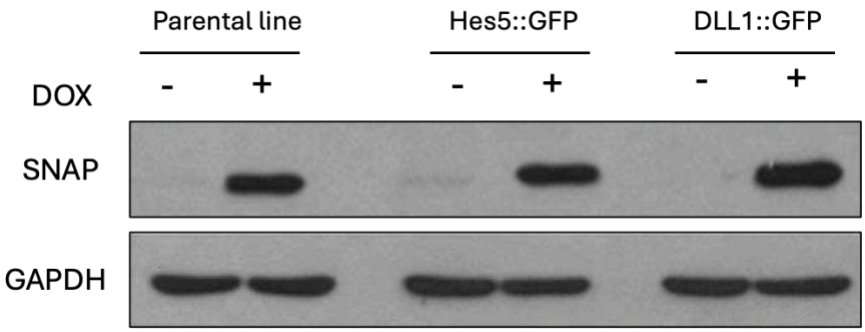

Figure 51: DOX-inducible Numb isoform expression in dTAG clones.

Western blot analysis of Numb expression in Parental Line homozygote Clone 210), Hes5-dTAG, and DLL1-dTAG heterozygotes cells treated with or without 1 mg/mL doxycycline (DOX). GAPDH was used as a loading control.

After confirming that the inducible expression system was functional (FIG 51), the next objective was to determine whether exogenous expression of the Numb isoforms could rescue the rapid degradation triggered by the dTAG system. This was tested in PL (Clone 210), Hes5-dTAG, and DLL1-dTAG cell lines, all carrying the endogenous Numb fused to the $FKBP12^{F36V}$ degron. Considering that transcriptional activation and protein synthesis occur on a slower timescale than proteasomal degradation, different timing strategies were established to optimize rescue efficiency. Doxycycline (DOX) induction of the SNAP-tagged Numb isoforms was applied either before, after, or simultaneously with dTAGv1 treatment, allowing assessment of how timing can influence the ability of exogenous Numb to compensate for endogenous loss. All experiments were performed in triplicate to ensure reproducibility and statistical robustness. The specific conditions tested included various DOX concentrations combined with corresponding dTAGv1 treatments, designed to capture both immediate and delayed rescue responses across the three cell lines (TABLE 10).

Added 1st	Time (hours)	Added 2nd
dTAG 0.05 nM **dTAG 0.1 nM**	6-8-12-24-48	DOX 1 µg/ml DOX 100 ng/ml DOX 20 ng/ml
DOX 1 µg/ml **DOX 100 ng/ml** **DOX 20 ng/ml**	6-8-12-24-48	dTAG 0.05 nM dTAG 0.1 nM
dTAG 0.05 nM + DOX 1 µg/ml **dTAG 0.05 nM + DOX 100 ng/mL** **dTAG 0.05 nM + DOX 20 ng/mL**	6-8-12-24-48	-
dTAG 0.1 nM + DOX 1 µg/ml **dTAG 0.1 nM + DOX 100 ng/mL** **dTAG 0.1 nM + DOX 20 ng/mL**	6-8-12-24-48	-

Table 10: Workflow for rescue of Numb degradation.

Unfortunately, none of the tested conditions were able to rescue the cells or promote survival once the dTAG-induced degradation of endogenous Numb was initiated. Across all timing strategies, DOX added before, after or simultaneously with dTAGv1 and across all tested concentrations, the cells consistently underwent rapid cell death. This was observed in 100% of the experimental replicates (data no shown), indicating that the exogenous expression of Numb isoforms was insufficient to compensate for the acute loss of endogenous Numb. These results highlight the extreme sensitivity of these cell lines to Numb depletion and suggest that even transient or partial loss of Numb function cannot be buffered by inducible overexpression, emphasizing the non-redundant, essential role of endogenous Numb in maintaining cell viability during neural commitment.

4.5.7- Inducible expression of Numb isoforms in an oscillatory way fails to rescue cell death triggered by dTAG-mediated degradation of endogenous Numb.

Knowing this negative result rescuing the phenotypes caused by Numb disruption by the dTAGv1, maybe the proper expression of Numb and it related factors are under control of the oscillatory dynamics between Notch signaling and its regulators, including Numb, has been observed to govern the timing and balance of cell fate transitions across multiple developmental contexts. Through asymmetric segregation and feedback regulation, Numb periodically inhibits Notch activity, creating temporal fluctuations in pathway output that coordinate transitions between progenitor maintenance and differentiation.

For example, in neural progenitors, fluctuating expression of *Hes1* and *Ascl1* maintained cells in a progenitor state, whereas dampening of these oscillations preceded neuronal commitment.
Similarly, in the presomitic mesoderm, periodic activation of Notch and Wnt pathways established the segmentation clock required for somite formation. Comparable rhythmic Notch activity was also detected in epithelial and stem cell niches, such as the hair follicle and intestinal crypt, where oscillations supported self-renewal while permitting intermittent differentiation. These findings indicate that temporal modulation of Notch activity, often tuned by Numb-mediated feedback, provides a mechanism by which progenitor populations dynamically balance renewal and lineage specification.

Taking these observations into consideration, the next step was to investigate if oscillatory dynamics of Notch target genes, modulated by Numb, could be leveraged to test dTAG-mediated degradation in a frequency-dependent manner. Specifically, we aimed to determine whether the exogenous expression of individual Numb isoforms or the pool of them, fused to the SNAP tag and induced by DOX, could rescue the phenotype when DOX was added either before or after the induction of endogenous Numb degradation. All experiments were performed in triplicate to ensure reproducibility. To address this, a series of experimental conditions were designed. For example, cells at ~80% confluency were treated with 0.05 nM dTAGv1 for 1 hour, followed by three washes with 1X PBS and an 8-hour rest period.

A second pulse of 0.05 nM dTAGv1 was then applied for 1 hour, again followed by three PBS washes, and cell viability and phenotype were subsequently assessed. In parallel, DOX was added either before or after both dTAG pulse, to evaluate the capacity of SNAP-tagged Numb isoforms to compensate for the loss of endogenous protein. The experimental setup included multiple conditions to systematically test timing, concentration, and isoform-specific rescue potential. The table below summarizes the experimental runs, including cell line, dTAG treatment timing, DOX addition, and sampling timepoints (TABLE 11).

	DOX	1st dTAG	DOX	Waiting time (hours)	Wash	Waiting time (hours)	DOX	2nd dTAG	DOX	Waiting time (hours)	Wash	Waiting time	Check cells
1	1 µg/ml	0.05 nM	-	1 hour	X3	8 hours	1 µg/ml	0.05 nM	-	1 hour	X3	8 hours	X
2	-	0.05 nM	1 µg/ml	1 hour	X3	8 hours	-	0.05 nM	1 µg/ml	1 hour	X3	8 hours	X
3	1 µg/ml	0.1 nM	-	1 hour	X3	8 hours	1 µg/ml	0.1 nM	-	1 hour	X3	8 hours	X
4	-	0.1 nM	1 µg/ml	1 hour	X3	8 hours	-	0.1 nM	1 µg/ml	1 hour	X3	8 hours	X
5	1 µg/ml	0.05 nM	-	1 hour	X3	6 hours	1 µg/ml	0.05 nM	-	1 hour	X3	6 hours	X
6	-	0.05 nM	1 µg/ml	1 hour	X3	6 hours	-	0.05 nM	1 µg/ml	1 hour	X3	6 hours	X
7	1 µg/ml	0.1 nM	-	1 hour	X3	6 hours	1 µg/ml	0.1 nM	-	1 hour	X3	6 hours	X
8	-	0.1 nM	1 µg/ml	1 hour	X3	6 hours	-	0.1 nM	1 µg/ml	1 hour	X3	6 hours	X
9	1 µg/ml	0.05 nM	-	30 min	X3	3 hours	1 µg/ml	0.05 nM	-	30 min	X3	3 hours	X
10	-	0.05 nM	1 µg/ml	30 min	X3	3 hours	-	0.05 nM	1 µg/ml	30 min	X3	3 hours	X
11	1µg/ml	0.1 nM	-	30 min	X3	3 hours	1 µg/ml	0.1 nM	-	30 min	X3	3 hours	X
12	-	0.1 nM	1 µg/ml	30 min	X3	3 hours		0.1 nM	1 µg/ml	30 min	X3	3 hours	X
13	1 µg/ml	0.05 nM	-	30 min	X3	1 hour	1 µg/ml	0.05 nM	-	30 min	X3	1 hour	X
14	-	0.05 nM	1 µg/ml	30 min	X3	1 hour	-	0.05 nM	1 µg/ml	30 min	X3	1 hour	X
15	1 µg/ml	0.1 nM	-	30 min	X3	1 hour	1 µg/ml	0.1 nM	-	30 min	X3	1 hour	X
16	-	0.1 nM	1 µg/ml	30 min	X3	1 hour	-	0.1 nM	1 µg/ml	30 min	X3	1 hour	X
17	1 µg/ml	0.05 nM	-	15 min	X3	1 hour	1 µg/ml	0.05 nM	-	15 min	X3	1 hour	X
18	-	0.05 nM	1 µg/ml	15 min	X3	1 hour	-	0.05 nM	1 µg/ml	15 min	X3	1 hour	X
19	1 µg/ml	0.1 nM	-	15 min	X3	1 hour	1 µg/ml	0.1 nM	-	15 min	X3	1 hour	X
20	-	0.1 nM	1 µg/ml	15 min	X3	1 hour	-	0.1 nM	1 µg/ml	15 min	X3	1 hour	X

Table 11: Oscillatory rescue of Numb degradation.

After carefully evaluating all the experimental conditions tested, none of them were able to rescue the phenotype or prevent cell death, further emphasizing the critical role of Numb during this process. Regardless of the timing of doxycycline (DOX) induction whether added before or after dTAGv1 treatment, the cells were unable to survive following endogenous Numb degradation. The onset of cell death was consistently characterized by progressive cell detachment, ultimately leading to the complete loss of the culture (FIG 52).

A

DOX	1st dTAG	DOX	Waiting time (hours)	Wash	Waiting time (hours)	DOX	2nd dTAG	DOX	Waiting time (hours)	Was h	Waiting time
1 ug/ml	0.05 nM	-	1 hour	X3	8 hours	1 ug/ml	0.05 nM	-	1 hour	X3	8 hours

1st round dTAG | 2nd round dTAG

B

DOX	1st dTAG	DOX	Waiting time (hours)	Wash	Waiting time (hours)	DOX	2nd dTAG	DOX	Waiting time (hours)	Wash	Waiting time
-	0.05 nM	1 ug/ml	1 hour	X3	6 hours	-	0.05 nM	1 ug/ml	1 hour	X3	6 hours

1st round dTAG | 2nd round dTAG

C

DOX	1st dTAG	DOX	Waiting time (hours)	Wash	Waiting time (hours)	DOX	2nd dTAG	DOX	Waiting time (hours)	Wash	Waiting time
1 ug/ml	0.1 nM	-	30 min	X3	1 hour	1 ug/ml	0.1 nM	-	30 min	X3	1 hour

1st round dTAG | 2nd round dTAG

***Figure 52: Cell viability across dTAG concentrations*.**

Analysis of cell death under varying dTAG concentrations (0.05–0.1 nM) across different experimental conditions.

As shown in Figure 52A, forcing the expression of SNAP-tagged Numb isoforms with 1 µg/mL DOX, followed by treatment with 0.05 nM dTAGv1 for 1 hour, PBS washing (3×), and an 8-hour rest period, resulted in massive cell death. Nearly the entire cell population was lost after the first round of dTAG treatment, and the few remaining cells displayed severe morphological abnormalities such as cytoplasmic shrinkage and membrane blebbing. Upon the second round of dTAG treatment, the remaining cells completely detached and died. A similar outcome was observed in Figure 52B, where DOX was added after dTAGv1-induced degradation, with a 6-hour delay between treatments resulting again in 100% cell death.

A shorter exposure protocol was also tested, using 0.05 nM dTAGv1 for 30 minutes, followed by PBS washing and a 1-hour rest period (Figure 52C). Despite the reduced incubation time, approximately 20% of the cells were already dead after the first treatment, and surviving cells exhibited clear signs of stress, including membrane irregularities and cytoplasmic condensation. After the second round of dTAG treatment, the majority of the remaining cells also underwent cell death. Importantly, these effects were independent of both the timing of DOX induction and the concentration of dTAG used, reinforcing the conclusion that Numb depletion is incompatible with cell survival in this context.

4.5.8- Morphological analyses after Numb's degradation.

Detailed morphological analysis throughout the degradation process revealed a reproducible sequence of cellular changes (FIG 53A). Initially, cell borders appeared brighter and more refractive, consistent with early detachment (FIG 53B). This was followed by the appearance of apoptotic bodies (red arrows and circles, FIG 53C), which progressively accumulated over time until nearly the entire culture surface was populated by dying cells (FIG 53D). Collectively, these results demonstrate that the loss of Numb, even in the presence of forced expression of SNAP-tagged isoforms, leads to irreversible cell death, underscoring its essential role in maintaining cell integrity and survival.

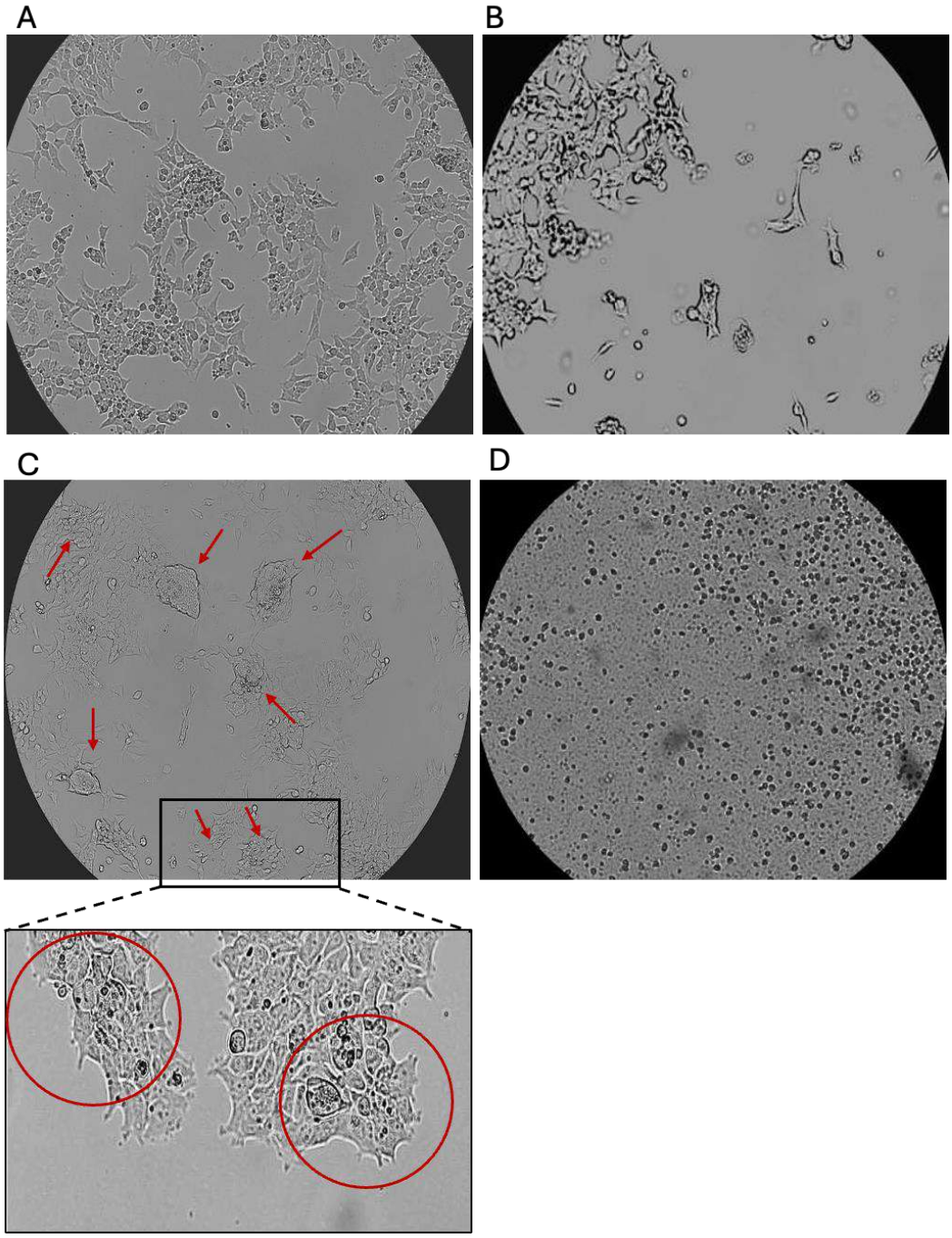

Figure 53: Morphological changes following dTAG treatment:

Representative images showing hESCs cultures after dTAG addition. Red arrows and circles highlight apoptotic bodies and areas of extensive cell detachment.

4.5.9- Numb depletion in mature cortical neurons induces morphological defects without affecting cell viability

To assess the functional requirement of Numb in differentiated neural cells, homozygous dTAG-PL C210 hESC-derived cortical neurons were treated with dTAG ligand to induce degradation of endogenous Numb. In contrast to the rapid and pronounced lethality observed in stem cells, mature cortical neurons did not exhibit overt cell death upon Numb depletion when compared to untreated controls.

However, morphological analysis revealed clear alterations in neuronal architecture. Treated neurons displayed disrupted network organization, characterized by an unstable and less interconnected neuronal network in culture. Neuronal morphology appeared markedly affected, with evident structural abnormalities compared to control conditions.

Western blot analysis confirmed that dTAG treatment led to a reduction in Numb protein levels, although depletion was not complete, as residual Numb expression remained detectable. This partial reduction suggests that, while Numb levels are decreased, they may not reach a threshold sufficient to induce cell death in mature neurons.

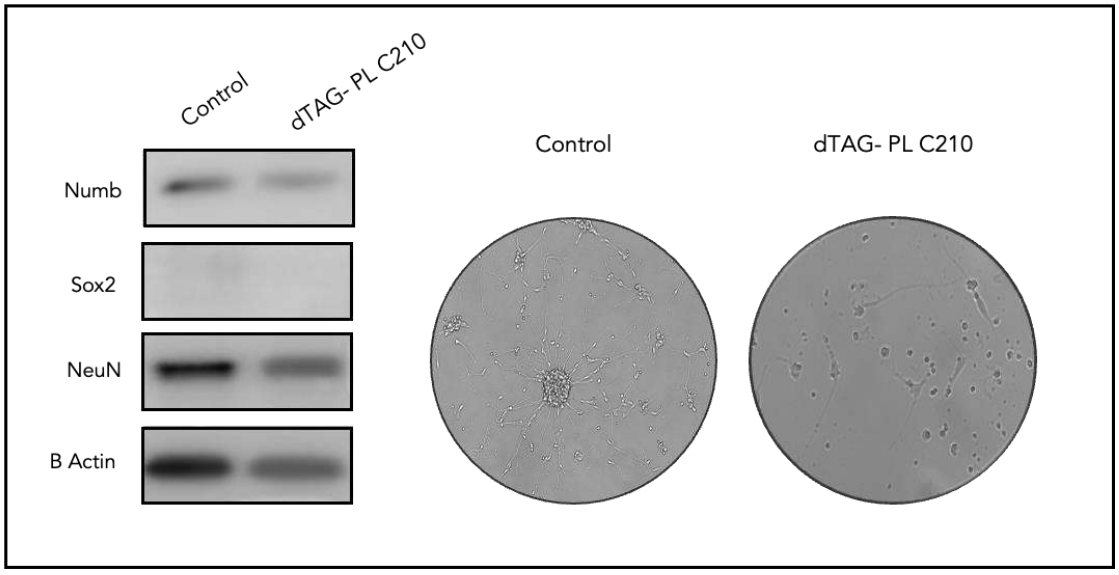

Figure 54: Degradation of Numb in mature cortical neurons

Left panel: Western blot showing dTAG-mediated depletion of Numb in the homozygous parental line compared to control. SOX2 and NeuN were used as lineage markers, while β-actin was used as a loading control

Right panel: Representative images of cortical neurons in culture showing altered morphology following Numb degradation.

CHAPTER 5

V.- DISCUSSION.

The investigation of Numb function during human cortical neurogenesis has revealed a complex regulatory landscape that challenges several prevailing assumptions about this critical cell fate determinant. Our comprehensive approach, integrating CRISPR-mediated genetic manipulation, inducible degradation systems, chromatin profiling, and differentiation analyses, has uncovered fundamental insights into Numb's essentiality, isoform-specific dynamics, and context-dependent regulation during neural development. However, these findings also expose significant technical challenges and biological complexities that warrant careful consideration.

One of the most striking observations from our study is the extreme sensitivity of human embryonic stem cells (hESCs) to Numb depletion, as evidenced by the rapid and complete cell death following dTAG-mediated degradation. Even at concentrations as low as 0.05 nM dTAGv1, endogenous Numb degradation triggered irreversible cellular collapse within 3-6 hours, characterized by progressive membrane blebbing, cytoplasmic condensation, formation of apoptotic bodies, and ultimately complete detachment of the culture. This phenotype was observed consistently across multiple cell lines, including the parental WA09 line and the DLL1::GFP and Hes5::GFP reporter derivatives, indicating that the lethality is not an artifact of a specific genetic background but rather reflects a fundamental requirement for Numb in maintaining hESC viability. Importantly, our attempts to rescue this phenotype through exogenous expression of SNAP-tagged Numb isoforms proved unsuccessful regardless of the timing of doxycycline induction, whether added before, after, or simultaneously with dTAGv1 treatment. We systematically tested various temporal windows (from 15 minutes to 48 hours), multiple doxycycline concentrations (20 ng/mL to 1 µg/mL), and different degradation kinetics (single pulse versus oscillatory treatment protocols designed to mimic the known oscillatory dynamics

of Notch signaling), yet none of these strategies prevented cell death. This failure to rescue suggests that the rate of transcriptional activation and protein synthesis of exogenous Numb simply cannot compensate for the rapid proteasomal degradation of the endogenous protein, highlighting a critical temporal mismatch between protein turnover and de novo expression that appears insurmountable in this system.

Moreover, the absolute dependence of hESCs on endogenous Numb despite forced overexpression of individual isoforms or pools thereof implies that Numb may possess non-redundant structural or regulatory functions that cannot be complemented by ectopically expressed variants, possibly due to differences in post-translational modifications, subcellular localization, or integration into pre-existing protein complexes that are disrupted upon acute depletion.

The technical challenges encountered during the generation of dTAG-tagged Numb lines further underscore the complexity of targeting this locus. The human Numb gene spans a genomic region characterized by exceptionally large intronic sequences separating individual coding exons, particularly surrounding exons 3 and 9, which are subject to alternative splicing and encode functionally distinct protein domains (FIG 54) [6,350]. These extensive intronic regions, often exceeding several kilobases, posed significant obstacles for homology-directed repair (HDR)-based gene editing strategies. Initial attempts to insert the $FKBP12^{F36V}$ degron tag at exon 10, the terminal coding exon shared by all isoforms, were hampered by low HDR efficiency, likely due to the difficulty of delivering sufficiently long homology arms flanking such large intronic sequences and the reduced accessibility of guide RNAs (gRNAs) designed to target this region. Indeed, multiple gRNA designs for exon 10 exhibited suboptimal on-target cutting scores, resulting in limited recovery of correctly targeted clones and frequent off-target integration events. Similarly, targeting internal exons such as exon 4 or exon 5 proved impractical, as these loci are embedded within comparably expansive intronic contexts and carry the additional risk of disrupting isoform-specific splicing events, which could generate nonfunctional truncated variants or alter the relative abundance of individual isoforms in unpredictable ways.

Ultimately, we achieved successful and efficient tagging by targeting exon 1, the first coding exon common to all four major human Numb isoforms (p72, p71, p66, and p65). This N-terminal tagging strategy ensured that all splice variants would be uniformly modified, enabling isoform-inclusive degradation upon dTAGv1 treatment while minimizing interference with downstream regulatory elements. Nevertheless, the laborious screening of over 900 individual clones yielded only a single homozygous integration event (Clone 210), highlighting the inherent inefficiency of HDR-based approaches in hESCs and the critical importance of patient, large-scale screening efforts when working with complex, intron-rich loci such as Numb.

These technical constraints have broader implications for the field, as they emphasize that not all developmental regulators are equally amenable to CRISPR-based functional dissection, particularly those encoded by genes with fragmented genomic architectures or subject to extensive alternative splicing.

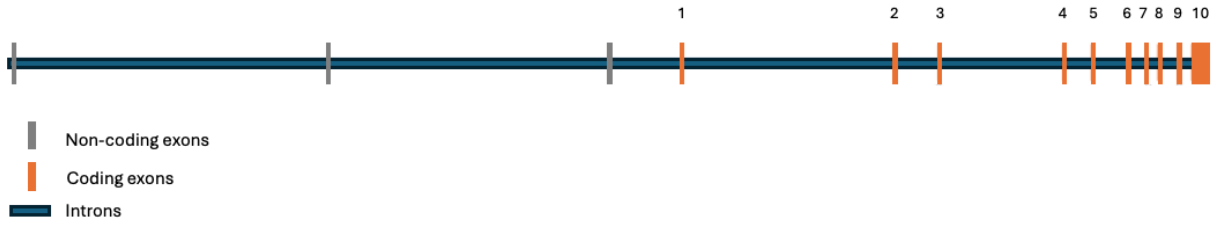

Figure 55: Structure of the human numb gene.

This gene consists of 13 exons, which the first 3 are non-coding exons, separated by 12 introns. Boxes indicate exons, and lines indicate introns and intergenic regions [6].

Our epigenetic analyses, incorporating ChIP-seq profiling of key histone modifications (H3K27me3, H3K27ac, H3K4me3) and Polycomb Repressive Complex 2 (PRC2) components (EZH2, SUZ12), revealed an unexpected chromatin landscape at the Numb promoter that diverges from classical models of developmental gene regulation [351,352]. Contrary to our initial hypothesis that Numb downregulation during cortical neuron differentiation might be mediated by PRC2-dependent H3K27me3 deposition, a canonical silencing mechanism widely employed during lineage specification [353,354], we observed that the Numb promoter remains largely devoid of repressive chromatin marks throughout the differentiation timeline. Specifically, EZH2 and SUZ12 occupancy at the Numb *locus* was minimal or absent in both undifferentiated hESCs and differentiated neural progenitor cells (NPCs), and H3K27me3 levels remained low even at late stages of cortical neuron maturation (day 35 and beyond). Instead, the promoter displayed persistent enrichment for active histone marks, including H3K27ac, H3K4me3, H3K9ac, and multiple acetylation variants (H3K56ac, H3K64ac, H3K122ac), together with pronounced peaks in ATAC-seq and DNase-seq profiles, indicative of sustained chromatin accessibility and transcriptional competence. This "open chromatin" configuration was further corroborated by the robust binding of numerous transcription factors (e.g., KLF4, E2F1, EP400) and chromatin remodeling complexes (e.g., CHD1-CHD9, BRG1, ADNP) at the Numb promoter, as evidenced by publicly available ChIP-seq datasets from mouse embryonic stem cells (mESCs), which share a highly conserved promoter architecture with human Numb [355,356] .

Notably, components of the cohesin complex (RAD21) and CTCF were also enriched at this *locus*, suggesting the formation of chromatin loops that may facilitate long-range enhancer-promoter interactions and maintain the promoter in a poised or active state CTCF were also enriched at this *locus*, suggesting the formation of chromatin loops that may facilitate long-range enhancer-promoter interactions and maintain the promoter in a poised or active state [357,358]. In stark contrast, heterochromatin-associated proteins (HP1α, HP1β, SUV39H1/2, SETDB1) and histone deacetylases (HDAC1/2) exhibited minimal enrichment, confirming the absence of stable repressive chromatin structures [359,360]. These findings indicate that Numb transcriptional downregulation during neural differentiation is not driven by canonical Polycomb-mediated silencing but rather by alternative regulatory mechanisms that operate post-transcriptionally or through the withdrawal of activating signals.

One compelling hypothesis emerging from our data is that Numb protein levels are regulated primarily through post-transcriptional mechanisms, including microRNA-mediated translational repression and targeted proteolysis, rather than through transcriptional repression at the chromatin level [78,243-245,287,361]. The observation that Numb mRNA expression remains relatively stable throughout cortical differentiation as confirmed by RNA-seq analyses from both our dataset and published studies from Leemput *et al.,* 2014 and Burke *et al.,* 2020 [346,347] yet Numb protein levels decline progressively after day 20, strongly supports a model in which protein stability or translation efficiency, rather than transcript abundance, is the primary determinant of Numb expression during neurogenesis. Several microRNAs (miRNAs) known to target Numb transcripts, including miR-31, miR-146, miR-543, miR-335, and miR-9, have been implicated in promoting oncogenicity by antagonizing Numb function in various cancer contexts, and their upregulation during neural differentiation could similarly dampen Numb protein synthesis in developing neurons [42,78,243-245,287,310,322,362].

Additionally, ubiquitin-proteasome-mediated degradation pathways, potentially involving E3 ubiquitin ligases such as ITCH (which interacts with Numb to regulate Notch degradation) or other, yet-to-be-identified enzymes, may actively destabilize Numb protein as cells transition from proliferative progenitors to postmitotic neurons [69,111,194,295,363]. This notion is consistent with the rapid kinetics of Numb depletion observed upon dTAGv1 treatment, which suggests that endogenous Numb turnover is already primed for rapid degradation and that the dTAG system merely accelerates a pre-existing proteolytic pathway. Furthermore, the failure of exogenous Numb isoforms to rescue dTAG-induced lethality may reflect the inability of these constructs to recapitulate the precise stoichiometry, subcellular localization, or post-translational modification state of endogenous Numb, all of which could be critical for its proper function. Collectively, these observations point toward a multilayered regulatory network in which chromatin accessibility maintains transcriptional competence at the Numb *locus*, while post-transcriptional and post-translational mechanisms dynamically modulate protein abundance in response to developmental cues [364].

Another intriguing dimension of Numb regulation uncovered by our study is the context-dependent subcellular localization of Numb protein, which appears to be influenced by cell density and, potentially, by the relative expression of specific isoforms [269]. Using a newly validated monoclonal anti-Numb antibody (C29G11), we successfully detected endogenous Numb protein by immunofluorescence in both HEK293 cells and hESCs, revealing distinct localization patterns depending on culture conditions. In Hek293 cells, Numb displayed a predominantly cytoplasmic distribution, consistent with its established role as a cytoplasmic adaptor protein involved in endocytic trafficking and receptor regulation [365]. However, in hESCs, Numb exhibited a more heterogeneous distribution, with some cells showing primarily cytoplasmic localization and others displaying nuclear or perinuclear enrichment. Critically, this variability was not random but correlated strongly with cell density: at high confluency, Numb was largely confined to the cytoplasm, whereas at lower density or during early colony formation, nuclear localization became more prominent.

This observation suggests that Numb's subcellular distribution is dynamically regulated by cell-cell contact, adhesion signaling, or mechanical tension factors known to influence the activity of polarity complexes such as PAR3/PAR6/aPKC, which phosphorylate and regulate Numb localization during asymmetric cell division in Drosophila and mammalian neural progenitors [180,269,366,367]. The differential localization of Numb isoforms may also reflect functional specialization: isoforms containing the long phosphotyrosine-binding (PTB) domain (PTB^{L}; p72 and p66) preferentially localize to the plasma membrane and endosomal compartments due to their enhanced affinity for membrane-associated proteins such as Notch, EPS15, and α-adaptin, whereas isoforms with the short PTB domain (PTB^{S}; p71 and p65) are more enriched in the nucleus, where they may contribute to transcriptional regulation or chromatin-associated processes [69,75,124,127,143,153,156,160]. This notion is supported by previous reports indicating that PTB^{S} isoforms can interact with nuclear factors such as p53 and MDM2, forming a trimeric complex that stabilizes p53 and enhances its tumor-suppressive functions [69,71,117,124,272,286]. In our hESCs cultures, the coexistence of cytoplasmic and nuclear Numb pools likely reflects the simultaneous expression of multiple isoforms with distinct regulatory properties, and the shift in localization observed with increasing cell density may represent a developmental adaptation in which cells modulate Numb function according to their physiological state balancing signaling control at the membrane with transcriptional or epigenetic regulation in the nucleus. This context-dependent localization has important implications for interpreting Numb's role during differentiation, as it suggests that Numb may exert distinct functions at different stages of neural commitment, transitioning from a membrane-associated regulator of Notch and integrin signaling in proliferative progenitors to a nuclear effector of gene expression programs in differentiating neurons.

The isoform-specific dynamics of Numb expression during cortical neuron differentiation provide additional layers of complexity to our understanding of this protein's developmental roles. By analyzing publicly available RNA-seq datasets from both hESC-derived from Leemput *et al.,* 2014 [346] and iPSC-derived from Burke *et al.,* 2020 [347] cortical differentiation protocols, we systematically quantified the inclusion or exclusion of exons 3 and 9, which define the four major Numb isoforms through alternative splicing. Our analyses revealed a striking developmental transition in isoform usage: in undifferentiated hESCs and early neural progenitors, isoforms containing exon 9, corresponding to the long proline-rich region, PRR^{L}, found in p72 and p71) predominated, whereas isoforms lacking exon 9, corresponding to PRR^{S}, found in p66 and p65, became progressively enriched as cells transitioned into postmitotic neurons. Specifically, the inclusion of exon 9 declined dramatically from day 3 to day 20, coinciding with the neural progenitor cell (NPC) stage and continued to decrease thereafter, ultimately reaching nearly undetectable levels in mature cortical neurons (day 35 and beyond) (FIG 55).

A parallel but less pronounced shift was observed for exon 3 inclusion, which also decreased during differentiation, though with somewhat slower kinetics. These temporal patterns were remarkably consistent across both hESC and iPSC datasets, despite known differences in epigenetic memory and differentiation efficiency between the two cell types, suggesting that the developmental switch in Numb isoform expression represents a highly conserved and robust mechanism of lineage progression in human cortical neurogenesis. Functionally, the predominance of PRR^{L} isoforms in undifferentiated and proliferative states is consistent with prior studies showing that these isoforms sustain progenitor self-renewal and antagonize differentiation, possibly by maintaining moderate levels of Notch signaling or by promoting integrin-mediated adhesion and extracellular matrix interactions that support stem cell niche architecture. Conversely, the enrichment of PRR^{S} isoforms in differentiating neurons aligns with their reported capacity to drive neuronal maturation and neurite outgrowth, likely through enhanced antagonism of Notch signaling via more efficient endocytic degradation of the Notch intracellular domain (NICD) and through distinct interactions with cytoskeletal and trafficking machinery that facilitate axonal and dendritic extension.

The observation that exons 4 and 7 constitutively included control exons not subject to alternative splicing remained stable throughout differentiation confirms the integrity of our splicing analyses and indicates that the changes in exon 3 and exon 9 inclusion reflect genuine developmental regulation rather than global transcriptional instability or RNA degradation artifacts. Importantly, the coordinated downregulation of both exon 3 and exon 9 inclusion as cells commit to neuronal fates implies a convergent splicing program that progressively favors the shortest Numb isoform (p65; Ex3Δ/Ex9Δ) in mature neurons, potentially reflecting a terminal differentiation state in which Numb's function shifts from regulating progenitor maintenance to supporting neuronal homeostasis and synaptic function.

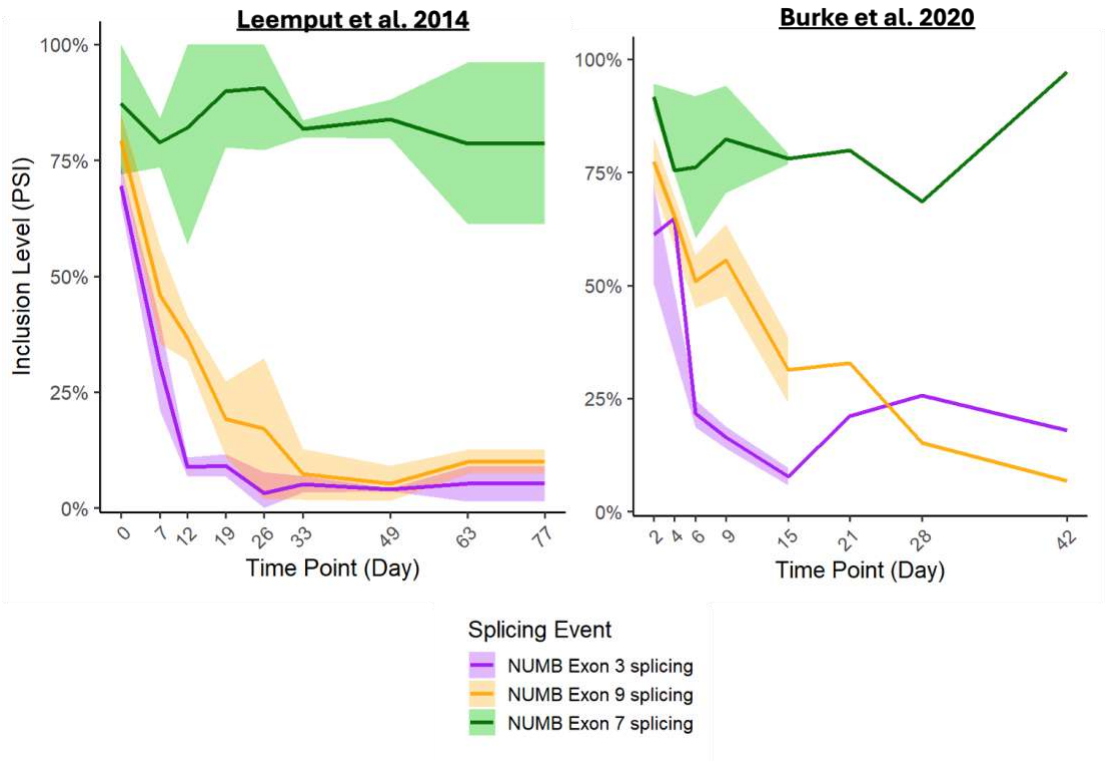

Figure 56: The inclusion of exons 3 and 9 decreases upon differentiation in both datasets.

Numb isoforms p72, p71 and p66 likely function primarily at early stages of differentiation, during the proliferative and early neurogenic phases. In contrast, Numb p65 appears to play more prominent roles from the NPC stage through neuronal maturation.

The regulation of Numb alternative splicing during neural differentiation appears to be governed by a complex interplay of RNA-binding proteins (RBPs) and splicing factors that dynamically interpret developmental signals and translate them into isoform-specific outcomes[127,154,159,203,205,206,215,244,254]. Multiple splicing regulators orchestrate the inclusion or skipping of Numb exons, thereby shaping isoform-specific functions during development and disease. RBM4 promotes exon 3 inclusion and suppresses exon 9 inclusion, generating neuronal isoforms essential for proper Mash1 expression, neurite extension, and maturation; loss of RBM4 disrupts these processes but can be partially rescued by reintroducing p66 or p65 [203,216-218,221]. In contrast, SRSF9 favors exon 9 retention especially in ovarian cancer by binding non-m6A-modified Numb transcripts and promoting oncogenic isoform production that sustains Notch activity [248,368]. m6A deposition near exon 10 counters this by recruiting HNRNPA2B1, which blocks SRSF9 and shifts splicing toward exon 9 skipping, revealing an epitranscriptomic layer of Numb regulation [234,248]. Additional factors such as PTBP1 [218,251], promoting exon 9 inclusion and QKI-5 [253,254], promoting exon 9 skipping, act in a competitive manner and are implicated in both neurodevelopment and cancer. Their developmental expression patterns, including the decline of PTBP1 during embryogenesis [369], correlate with the transition from PRR^{L} to PRR^{S} isoforms in neurons[69,124]. Consistent with these mechanisms, our cortical differentiation system, the progressive enrichment of exon9 skipped isoforms from day 20 onward likely reflects the upregulation of splicing repressors (such as QKI-5 or NONO) and/or the downregulation of splicing enhancers (such as SRSF9 or PTBP1) as cells exit the cell cycle and commit to neuronal fates [218,248,251,369]. However, the precise identity and temporal dynamics of the splicing factors responsible for this transition in human cortical neurogenesis remain incompletely characterized and represent a critical area for future investigation.

The extreme sensitivity of hESCs to Numb depletion, as revealed by our dTAG experiments, raises fundamental questions about the non-redundant functions of Numb during early human development and the extent to which its paralog, Numb-like (Numbl), can compensate for its loss [74,85,86,93,163,178]. In Drosophila, Numb is encoded by a single gene and functions as an essential regulator of asymmetric cell division and Notch antagonism during sensory organ development, with complete loss-of-function mutations leading to dramatic cell fate transformations [6,105,107,109]. In mammals, Numb underwent gene duplication early in vertebrate evolution, giving rise to two paralogs, Numb and Numbl that share significant sequence homology in their PTB and PRR domains and exhibit overlapping expression patterns in developing tissues, particularly in the central nervous system [74,85,86,163,178]. This evolutionary duplication initially suggested the possibility of functional redundancy, and indeed, single knockout studies in mice have revealed that Numb-null embryos die around E11.5 due to severe neural tube closure defects and placental abnormalities, whereas Numbl-null mice are viable and fertile with only subtle phenotypes, indicating that Numbl alone cannot fully compensate for Numb loss during embryonic development [74,292].

However, combined loss of both Numb and Numbl achieved through conditional knockout strategies in neural progenitors results in catastrophic disruption of cortical neurogenesis, including loss of apico-basal polarity, premature cell cycle exit, depletion of neural progenitor pools, and aberrant cortical lamination, demonstrating that the two proteins share essential, partially redundant functions in maintaining progenitor identity and regulating asymmetric divisions [163,370]. Despite this functional overlap, several lines of evidence indicate that Numb and Numbl are not interchangeable and possess distinct, non-redundant activities in specific contexts [93]. For example, Numbl is preferentially enriched in postmitotic neurons and exhibits a more restricted expression pattern in the CNS compared to the ubiquitous expression of Numb, suggesting tissue-specific or stage-specific division of labor between the two paralogs [85,93]. Moreover, Numb and Numbl display distinct phosphorylation hotspots and post-translational modification profiles such as Numb-S438 and Numbl-S370 phosphorylation that differentially regulate their stability, localization, and interaction networks [320], indicating that they integrate into partially distinct signaling pathways.

In our hESCs system, the inability of exogenous Numb isoforms to rescue dTAG-induced lethality suggests that Numbl expression alone is insufficient to maintain viability in the acute absence of Numb. This observation implies that Numb performs critical, time-sensitive functions during the early stages of neural commitment that cannot be compensated by Numbl, possibly due to differences in protein stoichiometry, subcellular localization, or binding partner specificity. Alternatively, the rapid kinetics of dTAG-mediated degradation may create a physiological "shock" that overwhelms the cell's capacity to adapt, preventing Numbl from upregulating or relocating to the appropriate subcellular compartments to assume Numb's functions. Importantly, the controversy surrounding Numb and Numbl function extends to cancer biology, where conflicting reports describe Numbl as both a tumor suppressor (e.g., in glioma, breast, lung, and colorectal cancers, where its downregulation enhances migration, invasion, and stemness) and, paradoxically, as a promoter of metastatic progression in advanced lung cancer, where it maintains cancer-initiating cells [267,288,320,362].

These context-dependent and sometimes opposing roles highlight the complexity of Numb/Numbl signaling and emphasize the importance of considering tissue type, developmental stage, genetic background, and signaling microenvironment when interpreting their functions. In the context of our study, the absolute requirement for Numb in hESCs, despite Numbl expression, underscores the conclusion that Numb is a non-redundant, essential regulator of early human neural development, and that understanding its precise mechanisms of action including isoform-specific functions, post-translational regulation, and interactions with other cell fate determinants will require continued investigation using refined genetic tools and systems that allow for more gradual or conditional depletion strategies.

The comparative analysis of Numb expression patterns across human tissues, as demonstrated by resources such as the Human Protein Atlas [371] , offers valuable context for interpreting our findings and underscores the notably low and context-dependent expression of Numb in the adult human brain compared to other organs. Notably, the placenta exhibits the capacity to express specific Numb isoforms during gestation, introducing an additional layer of complexity to Numb's functional network [160]. This placenta-derived expression suggests a nuanced feedback mechanism between maternal and fetal environments, where Numb may play a role in regulating fetal development through maternal-fetal signaling pathways.

According to publicly available RNA-seq and immunohistochemistry data, Numb mRNA and protein are expressed at relatively high levels in tissues characterized by active cell turnover and stem cell activity, such as the gastrointestinal tract, testis, skin, and hematopoietic organs, where Numb likely plays ongoing roles in maintaining progenitor pools and regulating asymmetric divisions. In contrast, Numb expression in the adult cerebral cortex and other brain regions is substantially lower, with only a subset of neuronal populations exhibiting detectable Numb protein by immunostaining (FIG 56).

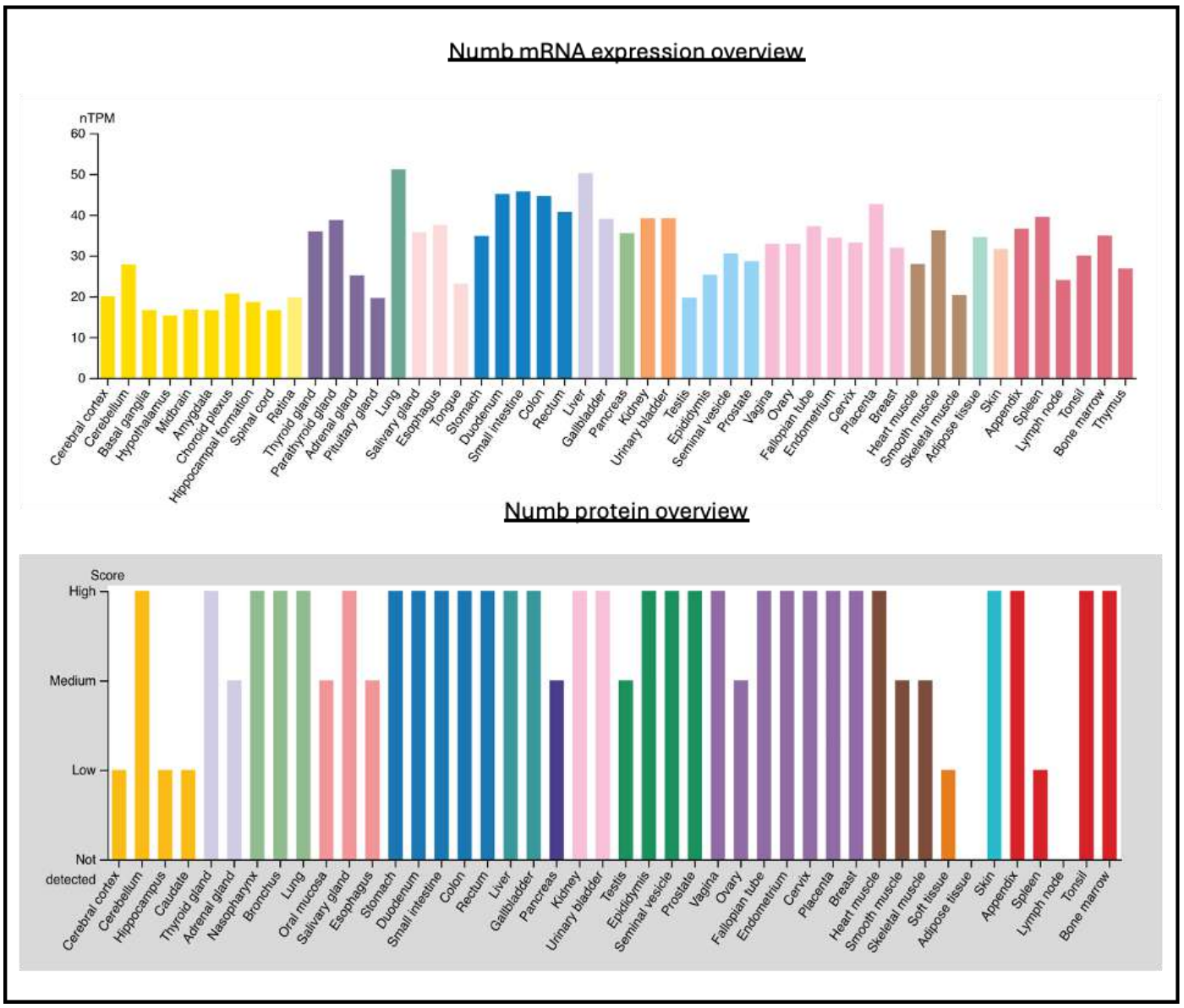

Figure 57: Numb protein and mRNA expression overview.

Upper panel: Protein-level analyses show that Numb is most highly expressed in tissues such as lung, liver, kidney, and stomach/tract. Lower panel: mRNA expression profiles reveal strong Numb transcription in cerebellum, testis, lung, placenta, and additional tissues, highlighting tissue-specific differences between protein abundance and transcriptional activity.

The elevated Numb expression observed in the cerebellum compared to other cerebral tissues likely reflects a convergence of several developmental and cellular processes unique to this brain region. First, the cerebellum undergoes an extended period of postnatal neurogenesis, during which granule cell precursors continue to proliferate and undergo asymmetric divisions events in which Numb is a well-established regulator. In addition, multiple cerebellar cell types naturally exhibit high Numb levels, including Bergmann glia, which guide neuronal migration, and immature granule neurons, which require precise control of Notch and endocytic signaling during their maturation [337,372].

Numb may also play an important role in modulating Shh pathway activity, a key driver of granule precursor proliferation, and in maintaining tumor-suppressive mechanisms that protect against medulloblastoma formation [185,275,291,296,373]. Beyond early development, Numb could contribute to synaptic plasticity, dendritic remodeling, and long-term circuit refinement within cerebellar networks [42,53]. Together, these features help explain why Numb expression is particularly pronounced in the cerebellum and underscore how its functions are highly context-dependent across brain regions and developmental stages. More broadly, this pattern highlights the cerebellum as an especially informative model in which to dissect Numb’s roles in proliferation, differentiation, migration, and the long-term maintenance of neural circuitry.

The downregulation in postmitotic neurons is consistent with our differentiation studies, which show progressive decline in Numb protein levels as cortical neurons mature and suggests that Numb's primary function in the brain is restricted to developmental stages particularly during neurogenesis, gliogenesis, and early circuit formation rather than in maintaining the homeostasis of mature neural networks.

However, residual Numb expression in specific neuronal subtypes, such as interneurons or layer-specific projection neurons, raises the possibility that Numb retains specialized functions in adult neurons, potentially related to synaptic plasticity, receptor trafficking, or neuroprotection [61,85,374]. Indeed, recent studies have implicated Numb in regulating Tau homeostasis and protecting against Tau-induced neurodegeneration in tauopathy models, with the long isoform Numb-p72 rescuing dendritic morphology, synaptic responses, and neuronal viability in the presence of toxic Tau oligomers [155,222,224].

This finding links Numb's developmental role in progenitor fate decisions to its potential neuroprotective functions in postmitotic neurons, suggesting a continuum of Numb activity throughout the lifespan of a neuron. The low baseline expression of Numb in adult brain tissue also has practical implications for the detection and validation of Numb antibodies, as many commercially available antibodies have been optimized and validated primarily in cancer cell lines or peripheral tissues where Numb is more abundantly expressed. This technical limitation may explain the difficulties we encountered in detecting endogenous Numb by immunofluorescence in early hESC cultures, even with antibodies that performed well in Western blots, and underscores the need for continued efforts to develop and validate reagents specifically tailored for studying Numb in pluripotent stem cells and differentiating neural populations.

A broader interpretation of our findings must also consider the inherent differences between human embryonic stem cells (H9/WA09 line) and induced pluripotent stem cells (iPSCs), particularly with respect to epigenetic memory, differentiation efficiency, and baseline expression of developmental regulators such as Numb. H9 hESCs are derived directly from the inner cell mass of human blastocysts and maintain a stable, "naïve" epigenetic landscape that closely resembles the in vivo embryonic state, making them a gold-standard model for studying fundamental developmental mechanisms. In contrast, iPSCs are reprogrammed from somatic cells (often fibroblasts or blood cells) and, despite acquiring pluripotency markers and differentiation capacity, frequently retain residual epigenetic memory of their tissue of origin, which can bias differentiation trajectories, alter the kinetics of lineage commitment, and introduce variability in gene expression profiles [375]. This epigenetic memory, together with differences in X-chromosome inactivation status (in female lines), mitochondrial function, and baseline stress responses, can influence the efficiency and reproducibility of neural differentiation protocols and the expression dynamics of key regulators such as Numb [375,376]. In our comparative splicing analyses, we observed remarkably consistent isoform transitions during cortical differentiation in both H9-derived and iPSC-derived datasets [346,347], suggesting that the developmental switch from PRR^{L} to PRR^{S} isoforms is highly robust and conserved across pluripotent cell types. However, subtle differences in the timing and magnitude of these transitions such as the slightly more gradual downregulation of SOX1 in iPSC-

derived NPCs compared to H9-derived NPCs may reflect the influence of residual somatic memory or reprogramming-induced epigenetic heterogeneity.

These considerations are particularly relevant when interpreting the absolute requirement for Numb in hESCs revealed by our dTAG experiments, as it remains formally possible that iPSC-derived lines with different reprogramming histories or genetic backgrounds might exhibit differential sensitivity to Numb depletion or altered capacity for Numbl-mediated compensation. Nevertheless, the convergence of our H9-based functional studies with published transcriptomic and splicing analyses from multiple independent iPSC lines strongly supports the conclusion that the developmental regulation of Numb isoforms represents a fundamental and conserved mechanism of human cortical neurogenesis, rather than a cell line-specific artifact.

To gain a broader perspective on why Numb may be essential during early developmental stages, its expression dynamics were examined using the *scDevDB* resource (https://scdevdb.deepomics.org). Analysis across human developmental stages reveals a striking enrichment of Numb expression at the zygote stage and in pluripotent stem cells, strongly supporting the idea that Numb is critically required at the onset of human development. This pattern is consistent with RNA-seq datasets showing a pronounced early peak of Numb expression [377]. Such enrichment suggests that Numb may participate in establishing the first lineage decisions, supporting pluripotency, or priming cells for forthcoming asymmetric divisions. As development proceeds, the progressive decrease in Numb expression highlights its predominant contribution to the earliest molecular programs that precede and shape subsequent lineage specification (FIG 57).

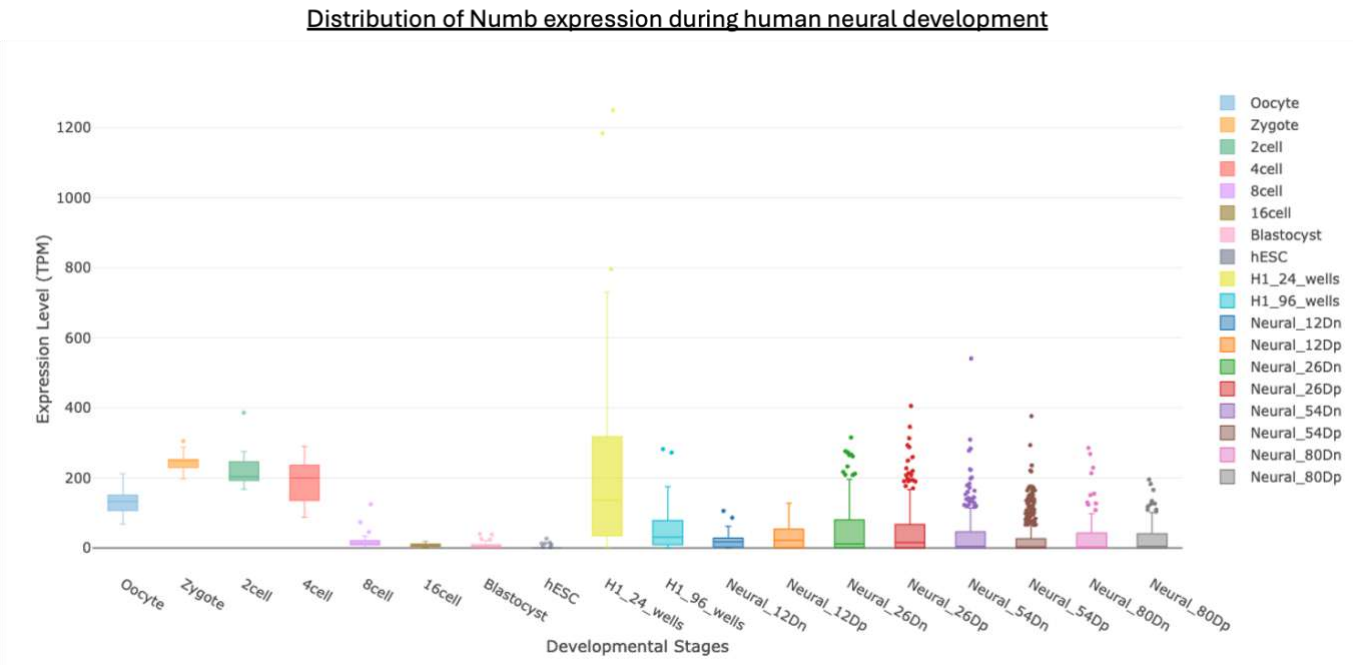

Figure 58: Numb expression during human neural development.

Numb expression exhibits two major peaks: one at the zygote stage and another during the embryonic stem cell state. https://scdevdb.deepomics.org [377].

Over the course of this thesis, several previously uncharacterized Numb isoforms were partially discovered during the process of human corticogenesis, as part of a collaborative initiative originally launched by a former postdoctoral researcher in the Reinberg Lab.

These newly discovered isoforms were consistently expressed at various stages of neurodevelopment. Each isoform was sequenced, cloned into a pLvX vector, and stored at -80°C for future experimental use. Although these isoforms have not been previously described in the literature, their existence introduces an additional layer of complexity to the neurodevelopmental system, especially given the context-dependent and tightly regulated expression patterns observed during corticogenesis. These variants, designated as Clones N1, N2, N3, N4, and N5, expand the known repertoire of Numb isoforms. Their gene structures, along with comparisons to the four canonical Numb isoforms, are detailed in Table 12 (TABLE 12).

Canonical human Numb isoforms described in neurodevelopment	
Name	**Characteristics**
p72	Full length, al exons
p71	Exon 3 spliced
p66	Exon 9 spliced
p65	Exon 3 and 9 spliced
New isoforms	
Name	**Characteristics**
N1	Exon 9 and part of exon 7 spliced
N2	Exon 3, part of exon 10, part of exon1-2 spliced
N3	Exon 7 spliced
N4	Exon 9 and part of exon 8-9 spliced
N5	Exon 4 spliced

Table 12: General comparison between canonical and new Numb isoforms during the context of neurodevelopment.

CHAPTER 6

VI.- CONCLUSSION.

In conclusion, our comprehensive investigation of Numb function and regulation during human cortical neuron differentiation has revealed a multifaceted and context-dependent regulatory landscape that challenges several prevailing models of Numb biology. The extreme sensitivity of hESCs to Numb depletion, as demonstrated by rapid and irreversible cell death following dTAG-mediated degradation, underscores the non-redundant and essential role of this protein in maintaining pluripotent cell viability and supporting the earliest stages of neural commitment functions that cannot be rescued by exogenous isoform expression or compensated by the paralog Numbl under conditions of acute endogenous loss. The failure to achieve phenotypic rescue through forced expression of SNAP-tagged Numb isoforms, despite systematic optimization of timing, dosage, and delivery methods, highlights fundamental constraints imposed by the kinetics of protein turnover and suggests that Numb's critical functions are exquisitely dependent on its endogenous expression levels, subcellular localization, and integration into pre-existing signaling networks. Our chromatin profiling studies have demonstrated that Numb transcriptional regulation deviates from classical PRC2-mediated silencing paradigms, with the Numb promoter remaining in an open, transcriptionally permissive state throughout cortical differentiation, as evidenced by persistent enrichment of active histone marks (H3K27ac, H3K4me3), chromatin accessibility (ATAC-seq, DNase-seq), and absence of repressive Polycomb components (EZH2, SUZ12, H3K27me3). These finding redirects attention toward post-transcriptional and post-translational mechanisms including microRNA-mediated translational repression, ubiquitin-proteasome-mediated degradation, and isoform-specific alternative splicing as the primary determinants of Numb protein abundance during neural development. The dynamic, context-dependent subcellular localization of Numb, which shifts between cytoplasmic and nuclear

compartments in a confluency-dependent manner, further emphasizes the functional plasticity of this protein and suggests that different isoforms may be preferentially deployed in distinct cellular contexts to balance membrane-associated signaling regulation with nuclear transcriptional control. The developmental switch in Numb isoform expression characterized by progressive exclusion of exons 3 and 9 as cells transition from proliferative progenitors to postmitotic neurons represents a highly conserved and robust mechanism that fine-tunes Numb's interactions with Notch, integrin, and cytoskeletal pathways to orchestrate the balance between self-renewal and differentiation. The technical challenges encountered during CRISPR-mediated targeting of the Numb *locus*, imposed by extensive intronic regions and complex splicing architecture, highlight the inherent difficulty of dissecting the functions of developmentally regulated genes with fragmented genomic structures and underscore the importance of careful experimental design and patient, large-scale screening efforts. Finally, the integration of our findings with published studies of Numb and Numbl function in mammalian neurodevelopment and cancer reveals a complex picture of partial functional redundancy, context-dependent specialization, and divergent signaling outputs that depend critically on tissue type, developmental stage, isoform composition, and post-translational modification status.

Collectively, these observations position Numb as a central, non-redundant coordinator of early human neural development operating at the intersection of chromatin regulation, alternative splicing, post-translational control, and membrane trafficking. Moreover, the identification of novel Numb isoforms whether functioning independently or through cooperative mechanisms introduces an additional layer of complexity to the regulation of neurogenesis, potentially uncovering new modulatory axes that influence cortical neuron differentiation. This expanding isoform diversity underscores the necessity for continued investigation using refined genetic tools, isoform-specific functional assays, and systems-level analyses to fully elucidate the molecular mechanisms by which Numb integrates developmental signals to govern cell fate decisions during human corticogenesis.

CHAPTER 7

VII.- RECOMMENDATIONS.

Based on the findings presented in this thesis, future investigations should explore new approaches to fully elucidate Numb's role in human cortical neurogenesis. First, microRNA and degradation pathway analysis is essential to resolve the paradox of declining Numb protein levels despite maintained transcriptional activity and open chromatin configuration at the Numb promoter. Identifying the specific microRNAs (miR-9, miR-31, miR-146, miR-335, miR-543) and E3 ubiquitin ligases responsible for isoform-specific degradation and ubiquitin-proteomic approaches will explain how post-transcriptional mechanisms govern the temporal dynamics of Numb abundance during differentiation.

Second, a systematic RNA-binding protein (RBP) perturbation screen is critical to identify the master regulators driving the developmentally conserved transition from exon 9-containing (PRR^{L}) to exon 9-skipping (PRR^{S}) isoforms. CRISPR-based knockdown of candidate splicing factors (PTBP1, QKI-5, RBM4, SRSF9, NONO), combined with enhanced CLIP sequencing to map direct binding sites on Numb pre-mRNA, will reveal the regulatory networks that coordinate isoform switching with neural commitment and establish whether manipulation of these RBPs can predictably alter differentiation trajectories.

Third, structure-function analysis through domain swapping is imperative to understand why exogenous Numb expression fails to rescue dTAG-mediated lethality. Generating chimeric constructs that interchange PTB domains ($PTB^{L}\leftrightarrow PTB^{S}$) and PRR domains ($PRR^{L} \leftrightarrow PRR^{S}$) between isoforms, coupled with point mutations disrupting specific protein-protein interactions and proximity labeling to map context-dependent interactomes, will identify which structural features are essential at defined developmental stages and explain the molecular basis for rescue failure.

Finally, single-cell multi-omics approaches are necessary to capture the cellular heterogeneity masked by bulk measurements. Integrating single-cell RNA-seq with protein quantification (CITE-seq), chromatin accessibility profiling (scATAC-seq), and long-read sequencing to resolve full-length Numb transcripts will reveal cell-type specific isoform expression patterns, identify rare transitional populations with unique splicing profiles, and enable trajectory inference modeling to predict how isoform dynamics govern individual cell fate decisions during the progenitor-to-neuron transition. Collectively, these research directions will provide mechanistic clarity on when, where, and how Numb isoform functions, transforming our understanding from demonstrating essentiality to defining the precise molecular logic underlying Numb-dependent regulation of human brain development.

VIII.- FUNDINGS.

National Agency for Research and Development (ANID) / Doctorado Becas Chile/2020 – 21200568.

Scholarship Pasantía Doctoral en el Extranjero / ANID-Chile 2022.

HHMI, University of Miami Miller School of Medicine and Sylvester Comprehensive Cancer Center, ReinbergLab and grants from NCI (7R01CA199652-20) and NIH (5R01NS100897-05).

IX.- PUBLICATIONS.

Gonzalez R, Reinberg D. The Notch pathway: A guardian of cell fate during neurogenesis. Curr Opin Cell Biol. 2025. doi: 10.1016/j.ceb.2025.102543. Epub 2025 Jun 2. PMID: 40450792; PMCID: PMC12278768.

The Numb Paradox: One Protein, multiple Isoforms, opposing Functions (2026). In revision.

X.- NOMENCLATURE.

ACD: Asymmetric Cell Division.
ADAM: A Disintegrin And Metalloproteinase.
ALK: Anaplastic Lymphoma Kinase.
APC: Astrocyte Precursor Cell.
aPKC: Atypical Protein Kinase C.
APS: Ammonium Persulfate.
ASD: Autism Spectrum Disorder.
ATAC-seq: Assay for Transposase-Accessible Chromatin sequencing.
BAPTA-AM: 1,2-bis(o-aminophenoxy) ethane-N,N,N',N'-tetraacetic acid acetoxymethyl ester.
BC: Breast Cancer.
BCA: Bicinchoninic Acid.
BDNF: Brain-Derived Neurotrophic Factor.
BV: Blood Vessel.
CDC42: Cell Division Control protein 42 homolog.
ChIP: Chromatin Immunoprecipitation.
ChIP-seq: Chromatin Immunoprecipitation Sequencing.
cKO: Conditional Knockout.
CNS: Central Nervous System.
CP: Cortical Plate.
C-R: Cajal-Retzius.
CSC: Cancer Stem Cell.
CTCF: CCCTC-binding factor.
DAPT: N-[N-(3,5-Difluorophenacetyl)-L-alanyl]-S-phenylglycine t-butyl ester.
DL: Deep Layer.
DMEM: Dulbecco's Modified Eagle's Medium.

dNumb: Drosophila Numb.

DNase-seq: DNase I hypersensitive sites sequencing.

DOX: Doxycycline.

DPF: Aspartic acid-Proline-Phenylalanine motif.

DSG: Disuccinimidyl Glutarate.

dTAG: Degradation TAG.

E: Embryonic day.

ECL: Enhanced Chemiluminescence.

ECM: Extracellular Matrix.

EH: Eps15 Homology.

EMT: Epithelial-Mesenchymal Transition.

EPHB2: Ephrin type-B receptor 2.

EPS15: Epidermal growth factor receptor pathway substrate 15.

EVT: Extravillous Trophoblast.

EZH1/2: Enhancer of Zeste Homolog ½.

FA: Formaldehyde.

FBS: Fetal Bovine Serum.

FGF-2/FGF2: Fibroblast Growth Factor 2.

FKBP12 ^{F36V}: FK506 Binding Protein 12 F36V variant.

GAPDH: Glyceraldehyde 3-Phosphate Dehydrogenase.

GFP: Green Fluorescent Protein.

GMC: Ganglion Mother Cell.

GW: Gestational Week.

HAT: Histone Acetyltransferase.

HDAC: Histone Deacetylase.

HDR: Homology-Directed Repair.

HEK293T: Human Embryonic Kidney 293T cells.

hESC: Human Embryonic Stem Cell.

HRP: Horseradish Peroxidase.

IF: Immunofluorescence.

IGF-1: Insulin-like Growth Factor 1.

IPC: Intermediate Progenitor Cell.

iPSC: Induced Pluripotent Stem Cell.

IQGAP1: IQ motif-containing GTPase-Activating Protein 1.

ITGB5: Integrin beta-5.

IZ: Intermediate Zone.

JAG: Jagged.

KLF4: Krüppel-Like Factor 4.

LB: Luria-Bertani.

LECA: Last Eukaryotic Common Ancestor.

Lgl: Lethal giant larvae.

L-HA: Left Homology Arm.

LMNB2: Laminin Beta 2.

MAML: Mastermind-Like.

MAPK: Mitogen-Activated Protein Kinase.

MB: Medulloblastoma.

MDM2: Mouse Double Minute 2 homolog.

MES: 2-(N-morpholino)ethanesulfonic acid.

miRNA/miR: MicroRNA.

mRNA: Messenger RNA.

mTOR: Mammalian Target of Rapamycin.

MZ: Marginal Zone.

NB: Neuroblast.

NEC: Neuroepithelial Cell.

NICD: Notch Intracellular Domain.

NPC: Neural Progenitor Cell.

NPF: Asparagine-Proline-Phenylalanine motif.

NS: NutriStem.

NSC: Neural Stem Cell.

NSCLC: Non-Small Cell Lung Cancer.

Numbl: Numb-like.

OC: Ovarian Cancer.

OCD: Obsessive Compulsive Disorder.

oRGC: Outer Radial Glial Cell.

PAR3/PAR6: Partitioning defective 3/6.

PAX6: Paired box gene 6.

PBS: Phosphate-Buffered Saline.

PBT: PBS with BSA and Triton.

PCR: Polymerase Chain Reaction.

PCW: Post-conception week.

PEI: Polyethyleneimine.

PES: Poly Ether Sulfone.

PFA: Paraformaldehyde.

PI3K: Phosphoinositide 3-Kinase.

PL: Parental Line.

PM: Plasma Membrane.

PNS: Peripheral Nervous System.

PQBP1: Polyglutamine-binding protein 1.

PRC2: Polycomb Repressive Complex 2.

pre-OPC: Pre-Oligodendrocyte Precursor Cell.

PRR: Proline-Rich Region.

PSI: Percent Spliced In.

PTB: Phosphotyrosine-Binding domain.

PTBP1: Polypyrimidine tract binding protein 1.

PVDF: Polyvinylidene Difluoride.

QKI-5: Quaking-5.

RBM4: RNA-Binding Motif protein 4.

RBP: RNA-Binding Protein.

RBPJ: Recombination Signal Binding Protein for Immunoglobulin Kappa J Region.

Rocki: ROCK inhibitor.

RGC/RGP: Radial Glial Cell/Radial Glial Progenitor.

R-HA: Right Homology Arm.

rMATS: replicate Multivariate Analysis of Transcript Splicing.

RNA-seq: RNA sequencing.

RT: Room Temperature.

RT-PCR: Reverse Transcription Polymerase Chain Reaction.

SCF: Skp, Cullin, F-box.

SH3: Src Homology 3.

shRNA: Short Hairpin RNA.

siRNA: Small Interfering RNA.

SNAP: SNAP-tag protein.

SOP: Sensory Organ Precursor.

SOX1/SOX2: SRY-Box Transcription Factor ½.

SP: Subplate.

SRSF9: Serine/arginine-rich splicing factor 9.

SRM: Selected Reaction Monitoring.

Su(H): Suppressor of Hairless.

SUZ12: Suppressor of Zeste 12.

SVZ: Subventricular Zone.

SYP: Synaptophysin.

TBST: Tris-Buffered Saline with Tween-20.

TEMED: Tetramethylethylenediamine.

TF: Transcription Factor.

TGF-β: Transforming Growth Factor Beta.

tRGC: Truncated Radial Glial Cell.

UL: Upper Layer.

VEGF: Vascular Endothelial Growth Factor.

VGCC: Voltage-Gated Calcium Channel.

VZ: Ventricular Zone.

WB: Western Blot.

WT: Wild Type.

ZIKV: Zika Virus.

XI.- REFERENCES.

1. Cainelli E, Stramucci G, Bisiacchi P: **A light in the darkness: Early phases of development and the emergence of cognition**. *Developmental Cognitive Neuroscience* 2025, **72**:101527.
2. Saglam-Metiner P, Devamoglu U, Filiz Y, Akbari S, Beceren G, Goker B, Yaldiz B, Yanasik S, Biray Avci C, Erdal E, et al.: **Spatio-temporal dynamics enhance cellular diversity, neuronal function and further maturation of human cerebral organoids**. *Communications Biology* 2023, **6**:173.
3. Sachan N, Sharma V, Mutsuddi M, Mukherjee A: **Notch signalling: multifaceted role in development and disease**. *The FEBS Journal* 2024, **291**:3030-3059.
4. Khodosevich K, Sellgren CM: **Neurodevelopmental disorders—high-resolution rethinking of disease modeling**. *Molecular Psychiatry* 2023, **28**:34-43.
5. Jha NK, Chen WC, Kumar S, Dubey R, Tsai LW, Kar R, Jha SK, Gupta PK, Sharma A, Gundamaraju R, et al.: **Molecular mechanisms of developmental pathways in neurological disorders: a pharmacological and therapeutic review**. *Open Biol* 2022, **12**:210289.
6. Zhong W, Feder JN, Jiang M-M, Jan LY, Jan YN: **Asymmetric Localization of a Mammalian Numb Homolog during Mouse Cortical Neurogenesis**. *Neuron* 1996, **17**:43-53.
7. Vasistha NA, García-Moreno F, Arora S, Cheung AF, Arnold SJ, Robertson EJ, Molnár Z: **Cortical and Clonal Contribution of Tbr2 Expressing Progenitors in the Developing Mouse Brain**. *Cereb Cortex* 2015, **25**:3290-3302.
8. Sessa A, Mao CA, Hadjantonakis AK, Klein WH, Broccoli V: **Tbr2 directs conversion of radial glia into basal precursors and guides neuronal amplification by indirect neurogenesis in the developing neocortex**. *Neuron* 2008, **60**:56-69.
9. Haubensak W, Attardo A, Denk W, Huttner WB: **Neurons arise in the basal neuroepithelium of the early mammalian telencephalon: a major site of neurogenesis**. *Proc Natl Acad Sci U S A* 2004, **101**:3196-3201.
10. Uzquiano A, Gladwyn-Ng I, Nguyen L, Reiner O, Götz M, Matsuzaki F, Francis F: **Cortical progenitor biology: key features mediating proliferation versus differentiation**. *Journal of Neurochemistry* 2018, **146**:500-525.
11. Miyata T, Kawaguchi A, Saito K, Kawano M, Muto T, Ogawa M: **Asymmetric production of surface-dividing and non-surface-dividing cortical progenitor cells**. *Development* 2004, **131**:3133-3145.

12. Noctor SC, Martínez-Cerdeño V, Ivic L, Kriegstein AR: **Cortical neurons arise in symmetric and asymmetric division zones and migrate through specific phases**. *Nature Neuroscience* 2004, **7**:136-144.
13. Espinós A, Fernández-Ortuño E, Negri E, Borrell V: **Evolution of genetic mechanisms regulating cortical neurogenesis**. *Dev Neurobiol* 2022, **82**:428-453.
14. Llorente V, Velarde P, Desco M, Gómez-Gaviro MV: **Current Understanding of the Neural Stem Cell Niches**. *Cells* 2022, **11**.
15. Micali N, Kim S-K, Diaz-Bustamante M, Stein-O'Brien G, Seo S, Shin J-H, Rash BG, Ma S, Wang Y, Olivares NA, et al.: **Variation of Human Neural Stem Cells Generating Organizer States In Vitro before Committing to Cortical Excitatory or Inhibitory Neuronal Fates**. *Cell Reports* 2020, **31**:107599.
16. Cayouette M, Raff M: **Asymmetric segregation of Numb: a mechanism for neural specification from Drosophila to mammals**. *Nat Neurosci* 2002, **5**:1265-1269.
17. Roegiers F, Jan YN: **Asymmetric cell division**. *Curr Opin Cell Biol* 2004, **16**:195-205.
18. Cahalane DJ, Charvet CJ, Finlay BL: **Modeling local and cross-species neuron number variations in the cerebral cortex as arising from a common mechanism**. *Proc Natl Acad Sci U S A* 2014, **111**:17642-17647.
19. Matsubara S, Matsuda T, Nakashima K: **Regulation of Adult Mammalian Neural Stem Cells and Neurogenesis by Cell Extrinsic and Intrinsic Factors**. In *Cells*. Edited by; 2021. vol 10.]
20. Guo R, Han D, Song X, Gao Y, Li Z, Li X, Yang Z, Xu Z: **Context-dependent regulation of Notch signaling in glial development and tumorigenesis**. *Sci Adv* 2023, **9**:eadi2167.
21. Zhang L, Wei X: **The Roles of Par3, Par6, and aPKC Polarity Proteins in Normal Neurodevelopment and in Neurodegenerative and Neuropsychiatric Disorders**. *J Neurosci* 2022, **42**:4774-4793.
22. Kon E, Cossard A, Jossin Y: **Neuronal Polarity in the Embryonic Mammalian Cerebral Cortex**. *Frontiers in Cellular Neuroscience* 2017, **Volume 11 - 2017**.
23. Casas Gimeno G, Paridaen J: **The Symmetry of Neural Stem Cell and Progenitor Divisions in the Vertebrate Brain**. *Front Cell Dev Biol* 2022, **10**:885269.
24. Kadowaki M, Nakamura S, Machon O, Krauss S, Radice GL, Takeichi M: **N-cadherin mediates cortical organization in the mouse brain**. *Developmental Biology* 2007, **304**:22-33.
25. Franco SJ, Müller U: **Shaping our minds: stem and progenitor cell diversity in the mammalian neocortex**. *Neuron* 2013, **77**:19-34.
26. Sunchu B, Cabernard C: **Principles and mechanisms of asymmetric cell division**. *Development* 2020, **147**.
27. Piroli ME, Blanchette JO, Jabbarzadeh E: **Polarity as a physiological modulator of cell function**. *Front Biosci (Landmark Ed)* 2019, **24**:451-462.
28. Bhat KM: **Notch signaling acts before cell division to promote asymmetric cleavage and cell fate of neural precursor cells**. *Sci Signal* 2014, **7**:ra101.
29. Paridaen JT, Huttner WB: **Neurogenesis during development of the vertebrate central nervous system**. *EMBO reports* 2014, **15**:351-364.

30. Lazutkin A, Podgorny O, Enikolopov G: **Modes of division and differentiation of neural stem cells**. *Behavioural Brain Research* 2019, **374**:112118.
31. Knoblich JA: **Mechanisms of asymmetric stem cell division**. *Cell* 2008, **132**:583-597.
32. Qian X, Shen Q, Goderie SK, He W, Capela A, Davis AA, Temple S: **Timing of CNS cell generation: a programmed sequence of neuron and glial cell production from isolated murine cortical stem cells**. *Neuron* 2000, **28**:69-80.
33. Lu MS, Johnston CA: **Molecular pathways regulating mitotic spindle orientation in animal cells**. *Development* 2013, **140**:1843-1856.
34. Chou FS, Li R, Wang PS: **Molecular components and polarity of radial glial cells during cerebral cortex development**. *Cell Mol Life Sci* 2018, **75**:1027-1041.
35. Andrews MG, Subramanian L, Salma J, Kriegstein AR: **How mechanisms of stem cell polarity shape the human cerebral cortex**. *Nat Rev Neurosci* 2022, **23**:711-724.
36. Hatanaka Y, Hirata T: **How Do Cortical Excitatory Neurons Terminate Their Migration at the Right Place? Critical Roles of Environmental Elements**. *Front Cell Dev Biol* 2020, **8**:596708.
37. Homem CC, Repic M, Knoblich JA: **Proliferation control in neural stem and progenitor cells**. *Nat Rev Neurosci* 2015, **16**:647-659.
38. Chini M, Hanganu-Opatz IL: **Prefrontal Cortex Development in Health and Disease: Lessons from Rodents and Humans**. *Trends in Neurosciences* 2021, **44**:227-240.
39. Díaz-Piña DA, Rivera-Ramírez N, García-López G, Díaz NF, Molina-Hernández A: **Calcium and Neural Stem Cell Proliferation**. *International Journal of Molecular Sciences* 2024, **25**:4073.
40. Zahr SK, Kaplan DR, Miller FD: **Translating neural stem cells to neurons in the mammalian brain**. *Cell Death Differ* 2019, **26**:2495-2512.
41. Ruan X, Kang B, Qi C, Lin W, Wang J, Zhang X: **Progenitor cell diversity in the developing mouse neocortex**. *Proc Natl Acad Sci U S A* 2021, **118**.
42. Kuo CT, Mirzadeh Z, Soriano-Navarro M, Rašin M, Wang D, Shen J, Šestan N, Garcia-Verdugo J, Alvarez-Buylla A, Jan LY, et al.: **Postnatal Deletion of Numb/Numblike Reveals Repair and Remodeling Capacity in the Subventricular Neurogenic Niche**. *Cell* 2006, **127**:1253-1264.
43. Silbereis JC, Pochareddy S, Zhu Y, Li M, Sestan N: **The Cellular and Molecular Landscapes of the Developing Human Central Nervous System**. *Neuron* 2016, **89**:248-268.
44. Cárdenas A, Villalba A, de Juan Romero C, Picó E, Kyrousi C, Tzika AC, Tessier-Lavigne M, Ma L, Drukker M, Cappello S, et al.: **Evolution of Cortical Neurogenesis in Amniotes Controlled by Robo Signaling Levels**. *Cell* 2018, **174**:590-606.e521.
45. Rakic P: **Evolution of the neocortex: a perspective from developmental biology**. *Nat Rev Neurosci* 2009, **10**:724-735.
46. Corbin JG, Nery S, Fishell G: **Telencephalic cells take a tangent: non-radial migration in the mammalian forebrain**. *Nat Neurosci* 2001, **4 Suppl**:1177-1182.

47. Ma T, Wang C, Wang L, Zhou X, Tian M, Zhang Q, Zhang Y, Li J, Liu Z, Cai Y, et al.: **Subcortical origins of human and monkey neocortical interneurons**. *Nat Neurosci* 2013, **16**:1588-1597.
48. Paredes MF, James D, Gil-Perotin S, Kim H, Cotter JA, Ng C, Sandoval K, Rowitch DH, Xu D, McQuillen PS, et al.: **Extensive migration of young neurons into the infant human frontal lobe**. *Science* 2016, **354**.
49. Shi Y, Wang M, Mi D, Lu T, Wang B, Dong H, Zhong S, Chen Y, Sun L, Zhou X, et al.: **Mouse and human share conserved transcriptional programs for interneuron development**. *Science* 2021, **374**:eabj6641.
50. Song H, Poo M: **The cell biology of neuronal navigation**. *Nat Cell Biol* 2001, **3**:E81-88.
51. Petanjek Z, Judaš M, Šimic G, Rasin MR, Uylings HB, Rakic P, Kostovic I: **Extraordinary neoteny of synaptic spines in the human prefrontal cortex**. *Proc Natl Acad Sci U S A* 2011, **108**:13281-13286.
52. Zhu Y, Sousa AMM, Gao T, Skarica M, Li M, Santpere G, Esteller-Cucala P, Juan D, Ferrández-Peral L, Gulden FO, et al.: **Spatiotemporal transcriptomic divergence across human and macaque brain development**. *Science* 2018, **362**.
53. Yeung MS, Zdunek S, Bergmann O, Bernard S, Salehpour M, Alkass K, Perl S, Tisdale J, Possnert G, Brundin L, et al.: **Dynamics of oligodendrocyte generation and myelination in the human brain**. *Cell* 2014, **159**:766-774.
54. Masuda T, Sankowski R, Staszewski O, Prinz M: **Microglia Heterogeneity in the Single-Cell Era**. *Cell Rep* 2020, **30**:1271-1281.
55. Cadwell CR, Bhaduri A, Mostajo-Radji MA, Keefe MG, Nowakowski TJ: **Development and Arealization of the Cerebral Cortex**. *Neuron* 2019, **103**:980-1004.
56. Kanton S, Boyle MJ, He Z, Santel M, Weigert A, Sanchís-Calleja F, Guijarro P, Sidow L, Fleck JS, Han D, et al.: **Organoid single-cell genomic atlas uncovers human-specific features of brain development**. *Nature* 2019, **574**:418-422.
57. Iwata R, Casimir P, Vanderhaeghen P: **Mitochondrial dynamics in postmitotic cells regulate neurogenesis**. *Science* 2020, **369**:858-862.
58. Gonzalez R, Reinberg D: **The Notch pathway: A guardian of cell fate during neurogenesis**. *Curr Opin Cell Biol* 2025, **95**:102543.
59. Marchetto MC, Hrvoj-Mihic B, Kerman BE, Yu DX, Vadodaria KC, Linker SB, Narvaiza I, Santos R, Denli AM, Mendes AP, et al.: **Species-specific maturation profiles of human, chimpanzee and bonobo neural cells**. *Elife* 2019, **8**.
60. Sorrells SF, Paredes MF, Velmeshev D, Herranz-Pérez V, Sandoval K, Mayer S, Chang EF, Insausti R, Kriegstein AR, Rubenstein JL, et al.: **Immature excitatory neurons develop during adolescence in the human amygdala**. *Nat Commun* 2019, **10**:2748.
61. Zhou Y, Su Y, Li S, Kennedy BC, Zhang DY, Bond AM, Sun Y, Jacob F, Lu L, Hu P, et al.: **Molecular landscapes of human hippocampal immature neurons across lifespan**. *Nature* 2022, **607**:527-533.
62. Zhong S, Ding W, Sun L, Lu Y, Dong H, Fan X, Liu Z, Chen R, Zhang S, Ma Q, et al.: **Decoding the development of the human hippocampus**. *Nature* 2020, **577**:531-536.

63. Roder AE, Johnson K, Knoll M, Khalfan M, Wang B, Schultz-Cherry S, Banakis S, Kreitman A, Mederos C, Youn JH, et al.: **Optimized Quantification of Intrahost Viral Diversity in SARS-CoV-2 and Influenza Virus Sequence Data**. *bioRxiv* 2022.
64. Perica MI, Luna B: **Impact of stress on excitatory and inhibitory markers of adolescent cognitive critical period plasticity**. *Neuroscience & Biobehavioral Reviews* 2023, **153**:105378.
65. Zhou Y, Song H, Ming G-l: **Genetics of human brain development**. *Nature Reviews Genetics* 2024, **25**:26-45.
66. Heavner WE, Ji S, Notwell JH, Dyer ES, Tseng AM, Birgmeier J, Yoo B, Bejerano G, McConnell SK: **Transcription factor expression defines subclasses of developing projection neurons highly similar to single-cell RNA-seq subtypes**. *Proc Natl Acad Sci U S A* 2020, **117**:25074-25084.
67. Fame RM, Dehay C, Kennedy H, Macklis JD: **Subtype-Specific Genes that Characterize Subpopulations of Callosal Projection Neurons in Mouse Identify Molecularly Homologous Populations in Macaque Cortex**. *Cereb Cortex* 2017, **27**:1817-1830.
68. Rasin MR, Gazula VR, Breunig JJ, Kwan KY, Johnson MB, Liu-Chen S, Li HS, Jan LY, Jan YN, Rakic P, et al.: **Numb and Numbl are required for maintenance of cadherin-based adhesion and polarity of neural progenitors**. *Nat Neurosci* 2007, **10**:819-827.
69. Bani-Yaghoub M, Kubu CJ, Cowling R, Rochira J, Nikopoulos GN, Bellum S, Verdi JM: **A switch in numb isoforms is a critical step in cortical development**. *Developmental Dynamics* 2007, **236**:696-705.
70. Wang G, Zhang Z, Li J, Han J, Lu C: **The PTB and PRR domains of numb regulate neurite outgrowth by influencing voltage-gated calcium channel expression and kinetics**. *Brain Res Bull* 2024, **207**:110876.
71. Lu CB, Fu W, Xu X, Mattson MP: **Numb-mediated neurite outgrowth is isoform-dependent, and requires activation of voltage-dependent calcium channels**. *Neuroscience* 2009, **161**:403-412.
72. Kechad A, Jolicoeur C, Tufford A, Mattar P, Chow RWY, Harris WA, Cayouette M: **Numb is required for the production of terminal asymmetric cell divisions in the developing mouse retina**. *J Neurosci* 2012, **32**:17197-17210.
73. Luo Z, Mu L, Zheng Y, Shen W, Li J, Xu L, Zhong B, Liu Y, Zhou Y: **NUMB enhances Notch signaling by repressing ubiquitination of NOTCH1 intracellular domain**. *J Mol Cell Biol* 2020, **12**:345-358.
74. Li H-S, Wang D, Shen Q, Schonemann MD, Gorski JA, Jones KR, Temple S, Jan LY, Jan YN: **Inactivation of Numb and Numblike in Embryonic Dorsal Forebrain Impairs Neurogenesis and Disrupts Cortical Morphogenesis**. *Neuron* 2003, **40**:1105-1118.
75. Petersen PH, Tang H, Zou K, Zhong W: **The enigma of the numb-Notch relationship during mammalian embryogenesis**. *Dev Neurosci* 2006, **28**:156-168.
76. Chandnani N, Gupta I, Thakkar V, Sarkar K: **Epigenetic regulation of enhancer of zeste homolog 2 (EZH2) -Yin Yang 1 (YY1) axis in cancer**. *Pathol Res Pract* 2023, **251**:154885.

77. Margueron R, Li G, Sarma K, Blais A, Zavadil J, Woodcock CL, Dynlacht BD, Reinberg D: **Ezh1 and Ezh2 maintain repressive chromatin through different mechanisms**. *Mol Cell* 2008, **32**:503-518.
78. Wang X, Yang JY, Cai J, Zhang DJ, Zhao L, Luo LH, Xiong Y, Zhang T, Jin M: **MiR-543/Numb promotes proliferation, metastasis, and stem-like cell traits of prostate cancer cells**. *Am J Transl Res* 2021, **13**:617-631.
79. Ascencio G, Galvan L, Sanchez JM, Nagainis A, Tam C, Goins LM, Riggs B: **miR-190 is a Key Regulator in Establishing Cell Polarity and Specification in the Drosophila Nervous System**. *bioRxiv* 2025.
80. Kim SC, Lee SY, Jung UJ, Kim SR: **Application of Neurotrophic Factors as a Therapeutic Approach for Neurodegenerative Diseases**. *Exp Neurobiol* 2025, **34**:169-199.
81. Teleanu RI, Niculescu AG, Roza E, Vladâcenco O, Grumezescu AM, Teleanu DM: **Neurotransmitters-Key Factors in Neurological and Neurodegenerative Disorders of the Central Nervous System**. *Int J Mol Sci* 2022, **23**.
82. Gao C, Wang Q, Chung SK, Shen J: **Crosstalk of metabolic factors and neurogenic signaling in adult neurogenesis: Implication of metabolic regulation for mental and neurological diseases**. *Neurochemistry International* 2017, **106**:24-36.
83. Santolini E, Puri C, Salcini AE, Gagliani MC, Pelicci PG, Tacchetti C, Di Fiore PP: **Numb is an endocytic protein**. *J Cell Biol* 2000, **151**:1345-1352.
84. Rebeiz M, Miller SW, Posakony JW: **Notch regulates numb: integration of conditional and autonomous cell fate specification**. *Development* 2011, **138**:215-225.
85. Zhong W, Jiang MM, Weinmaster G, Jan LY, Jan YN: **Differential expression of mammalian Numb, Numblike and Notch1 suggests distinct roles during mouse cortical neurogenesis**. *Development* 1997, **124**:1887-1897.
86. Petersen PH, Zou K, Hwang JK, Jan YN, Zhong W: **Progenitor cell maintenance requires numb and numblike during mouse neurogenesis**. *Nature* 2002, **419**:929-934.
87. Song Y, Lu B: **Regulation of cell growth by Notch signaling and its differential requirement in normal vs. tumor-forming stem cells in Drosophila**. *Genes Dev* 2011, **25**:2644-2658.
88. Nian F-S, Hou P-S: **Evolving Roles of Notch Signaling in Cortical Development**. *Frontiers in Neuroscience* 2022, **Volume 16 - 2022**.
89. Tran LN, Loew SK, Franco SJ: **Notch Signaling Plays a Dual Role in Regulating the Neuron-to-Oligodendrocyte Switch in the Developing Dorsal Forebrain**. *J Neurosci* 2023, **43**:6854-6871.
90. Shimojo H, Ohtsuka T, Kageyama R: **Oscillations in Notch Signaling Regulate Maintenance of Neural Progenitors**. *Neuron* 2008, **58**:52-64.
91. Imayoshi I, Shimojo H, Sakamoto M, Ohtsuka T, Kageyama R: **Genetic visualization of notch signaling in mammalian neurogenesis**. *Cell Mol Life Sci* 2013, **70**:2045-2057.
92. Edri R, Yaffe Y, Ziller MJ, Mutukula N, Volkman R, David E, Jacob-Hirsch J, Malcov H, Levy C, Rechavi G, et al.: **Analysing human neural stem cell ontogeny by consecutive isolation of Notch active neural progenitors**. *Nature Communications* 2015, **6**:6500.

93. Huang EJ, Li H, Tang AA, Wiggins AK, Neve RL, Zhong W, Jan LY, Jan YN: **Targeted deletion of numb and numblike in sensory neurons reveals their essential functions in axon arborization**. *Genes Dev* 2005, **19**:138-151.
94. Kyriazis GA, Belal C, Madan M, Taylor DG, Wang J, Wei Z, Pattisapu JV, Chan SL: **Stress-induced switch in Numb isoforms enhances Notch-dependent expression of subtype-specific transient receptor potential channel**. *J Biol Chem* 2010, **285**:6811-6825.
95. Johnson SA, Zitserman D, Roegiers F: **Numb regulates the balance between Notch recycling and late-endosome targeting in Drosophila neural progenitor cells**. *Mol Biol Cell* 2016, **27**:2857-2866.
96. Tang H, Rompani SB, Atkins JB, Zhou Y, Osterwalder T, Zhong W: **Numb proteins specify asymmetric cell fates via an endocytosis- and proteasome-independent pathway**. *Mol Cell Biol* 2005, **25**:2899-2909.
97. Wakamatsu Y, Maynard TM, Jones SU, Weston JA: **NUMB Localizes in the Basal Cortex of Mitotic Avian Neuroepithelial Cells and Modulates Neuronal Differentiation by Binding to NOTCH-1**. *Neuron* 1999, **23**:71-81.
98. Couturier L, Mazouni K, Schweisguth F: **Numb Localizes at Endosomes and Controls the Endosomal Sorting of Notch after Asymmetric Division in Drosophila**. *Current Biology* 2013, **23**:588-593.
99. Yan B: **Numb – From flies to humans**. *Brain and Development* 2010, **32**:293-298.
100. Telerman SB, Hamilton RS, Shaw B, Dimitrov JD, Steventon B, Ferguson-Smith AC: **Post-translational regulation of the Numb/Notch pathway in neurogenesis and cancer by Dlk2**. *bioRxiv* 2023:2023.2007.2020.549453.
101. Siddique HR, Feldman DE, Chen CL, Punj V, Tokumitsu H, Machida K: **NUMB phosphorylation destabilizes p53 and promotes self-renewal of tumor-initiating cells by a NANOG-dependent mechanism in liver cancer**. *Hepatology* 2015, **62**:1466-1479.
102. Belle VA, McDermott N, Meunier A, Marignol L: **NUMB inhibition of NOTCH signalling as a therapeutic target in prostate cancer**. *Nat Rev Urol* 2014, **11**:499-507.
103. Shu Y, Tao Q, Xu Q, Chen Y, Xu Y, Ma T, Zhu Z, Wei X, Liu F, Wu Z, et al.: **Loss of NUMB promotes hepatomegaly and hepatocellular carcinoma through the AKT/glycogen/hippo signaling**. *Oncogene* 2025, **44**:2574-2587.
104. Chao S, Yan H, Bu P: **Asymmetric division of stem cells and its cancer relevance**. *Cell Regen* 2024, **13**:5.
105. Uemura T, Shepherd S, Ackerman L, Jan LY, Jan YN: **numb, a gene required in determination of cell fate during sensory organ formation in Drosophila embryos**. *Cell* 1989, **58**:349-360.
106. Rhyu MS, Jan LY, Jan YN: **Asymmetric distribution of numb protein during division of the sensory organ precursor cell confers distinct fates to daughter cells**. *Cell* 1994, **76**:477-491.
107. Spana EP, Kopczynski C, Goodman CS, Doe CQ: **Asymmetric localization of numb autonomously determines sibling neuron identity in the Drosophila CNS**. *Development* 1995, **121**:3489-3494.
108. Spana EP, Doe CQ: **Numb antagonizes Notch signaling to specify sibling neuron cell fates**. *Neuron* 1996, **17**:21-26.

109. Verdi JM, Schmandt R, Bashirullah A, Jacob S, Salvino R, Craig CG, Program AE, Lipshitz HD, McGlade CJ: **Mammalian NUMB is an evolutionarily conserved signaling adapter protein that specifies cell fate**. *Curr Biol* 1996, **6**:1134-1145.
110. Li SC, Songyang Z, Vincent SJ, Zwahlen C, Wiley S, Cantley L, Kay LE, Forman-Kay J, Pawson T: **High-affinity binding of the Drosophila Numb phosphotyrosine-binding domain to peptides containing a Gly-Pro-(p)Tyr motif**. *Proc Natl Acad Sci U S A* 1997, **94**:7204-7209.
111. Guo M, Jan LY, Jan YN: **Control of daughter cell fates during asymmetric division: interaction of Numb and Notch**. *Neuron* 1996, **17**:27-41.
112. Pece S, Confalonieri S, P RR, Di Fiore PP: **NUMB-ing down cancer by more than just a NOTCH**. *Biochim Biophys Acta* 2011, **1815**:26-43.
113. Skeath JB, Doe CQ: **Sanpodo and Notch act in opposition to Numb to distinguish sibling neuron fates in the Drosophila CNS**. *Development* 1998, **125**:1857-1865.
114. Hutterer A, Knoblich JA: **Numb and alpha-Adaptin regulate Sanpodo endocytosis to specify cell fate in Drosophila external sensory organs**. *EMBO Rep* 2005, **6**:836-842.
115. Li SC, Zwahlen C, Vincent SJ, McGlade CJ, Kay LE, Pawson T, Forman-Kay JD: **Structure of a Numb PTB domain-peptide complex suggests a basis for diverse binding specificity**. *Nat Struct Biol* 1998, **5**:1075-1083.
116. Zwahlen C, Li SC, Kay LE, Pawson T, Forman-Kay JD: **Multiple modes of peptide recognition by the PTB domain of the cell fate determinant Numb**. *Embo j* 2000, **19**:1505-1515.
117. Uhlik MT, Temple B, Bencharit S, Kimple AJ, Siderovski DP, Johnson GL: **Structural and evolutionary division of phosphotyrosine binding (PTB) domains**. *J Mol Biol* 2005, **345**:1-20.
118. Salcini AE, Confalonieri S, Doria M, Santolini E, Tassi E, Minenkova O, Cesareni G, Pelicci PG, Di Fiore PP: **Binding specificity and in vivo targets of the EH domain, a novel protein-protein interaction module**. *Genes Dev* 1997, **11**:2239-2249.
119. Matsuzaki F: **Asymmetric division of Drosophila neural stem cells: a basis for neural diversity**. *Curr Opin Neurobiol* 2000, **10**:38-44.
120. Lai EC, Bodner R, Posakony JW: **The Enhancer of split Complex of Drosophila includes four Notch-regulated members of the Bearded gene family**. *Development* 2000, **127**:3441-3455.
121. Betschinger J, Mechtler K, Knoblich JA: **The Par complex directs asymmetric cell division by phosphorylating the cytoskeletal protein Lgl**. *Nature* 2003, **422**:326-330.
122. Wirtz-Peitz F, Nishimura T, Knoblich JA: **Linking Cell Cycle to Asymmetric Division: Aurora-A Phosphorylates the Par Complex to Regulate Numb Localization**. *Cell* 2008, **135**:161-173.
123. Knoblich JA: **Asymmetric cell division during animal development**. *Nat Rev Mol Cell Biol* 2001, **2**:11-20.
124. Verdi JM, Bashirullah A, Goldhawk DE, Kubu CJ, Jamali M, Meakin SO, Lipshitz HD: **Distinct human NUMB isoforms regulate differentiation vs. proliferation**

in the neuronal lineage. *Proceedings of the National Academy of Sciences* 1999, **96**:10472-10476.
125. Neumüller RA, Knoblich JA: **Dividing cellular asymmetry: asymmetric cell division and its implications for stem cells and cancer**. *Genes Dev* 2009, **23**:2675-2699.
126. Mujizah EY, Kuwana S, Matsumoto K, Gushiken T, Aoyama N, Ishikawa HO, Sasamura T, Umetsu D, Inaki M, Yamakawa T, et al.: **Numb Suppresses Notch-Dependent Activation of Enhancer of split during Lateral Inhibition in the Drosophila Embryonic Nervous System**. *Biomolecules* 2024, **14**.
127. Dho SE, French MB, Woods SA, McGlade CJ: **Characterization of four mammalian numb protein isoforms. Identification of cytoplasmic and membrane-associated variants of the phosphotyrosine binding domain**. *J Biol Chem* 1999, **274**:33097-33104.
128. Shan Z, Tu Y, Yang Y, Liu Z, Zeng M, Xu H, Long J, Zhang M, Cai Y, Wen W: **Basal condensation of Numb and Pon complex via phase transition during Drosophila neuroblast asymmetric division**. *Nat Commun* 2018, **9**:737.
129. Crews ST: **Drosophila Embryonic CNS Development: Neurogenesis, Gliogenesis, Cell Fate, and Differentiation**. *Genetics* 2019, **213**:1111-1144.
130. Corty MM, Coutinho-Budd J: **Drosophila glia take shape to sculpt the nervous system**. *Current Opinion in Neurobiology* 2023, **79**:102689.
131. Penkert RR, LaFoya B, Moholt-Siebert L, Vargas E, Welch SE, Prehoda KE: **The Drosophila neuroblast polarity cycle at a glance**. *Journal of Cell Science* 2024, **137**.
132. Riebli N, Viktorin G, Reichert H: **Early-born neurons in type II neuroblast lineages establish a larval primordium and integrate into adult circuitry during central complex development in Drosophila**. *Neural Dev* 2013, **8**:6.
133. Schmit TL, Nihal M, Ndiaye M, Setaluri V, Spiegelman VS, Ahmad N: **Numb regulates stability and localization of the mitotic kinase PLK1 and is required for transit through mitosis**. *Cancer Res* 2012, **72**:3864-3872.
134. Wu S, Yang Y, Tang R, Zhang S, Qin P, Lin R, Rafel N, Lucchetta EM, Ohlstein B, Guo Z: **Apical-basal polarity precisely determines intestinal stem cell number by regulating Prospero threshold**. *Cell Reports* 2023, **42**.
135. Schweisguth F: **Asymmetric cell division in the Drosophila bristle lineage: from the polarization of sensory organ precursor cells to Notch-mediated binary fate decision**. *Wiley Interdiscip Rev Dev Biol* 2015, **4**:299-309.
136. Salzberg A, D'Evelyn D, Schulze KL, Lee J-K, Strumpf D, Tsai L, Bellen HJ: **Mutations affecting the pattern of the PNS in drosophila reveal novel aspects of neuronal development**. *Neuron* 1994, **13**:269-287.
137. Couturier L, Mazouni K, Corson F, Schweisguth F: **Regulation of Notch output dynamics via specific E(spl)-HLH factors during bristle patterning in Drosophila**. *Nature Communications* 2019, **10**:3486.
138. Song Y, Lu B: **Interaction of Notch signaling modulator Numb with α-Adaptin regulates endocytosis of Notch pathway components and cell fate determination of neural stem cells**. *J Biol Chem* 2012, **287**:17716-17728.
139. Jafar-Nejad H, Norga KK, Bellen HJ: **Numb: "Adapting" Notch for Endocytosis**. *Developmental Cell* 2002, **3**:155-156.

140. Berdnik D, Török T, González-Gaitán M, Knoblich JA: **The Endocytic Protein α-Adaptin Is Required for Numb-Mediated Asymmetric Cell Division in Drosophila**. *Developmental Cell* 2002, **3**:221-231.
141. Heitzler P, Bourouis M, Ruel L, Carteret C, Simpson P: **Genes of the Enhancer of split and achaete-scute complexes are required for a regulatory loop between Notch and Delta during lateral signalling in Drosophila**. *Development* 1996, **122**:161-171.
142. Ortega-Campos SM, García-Heredia JM: **The Multitasker Protein: A Look at the Multiple Capabilities of NUMB**. *Cells* 2023, **12**.
143. Gulino A, Di Marcotullio L, Screpanti I: **The multiple functions of Numb**. *Exp Cell Res* 2010, **316**:900-906.
144. Toriya M, Tokunaga A, Sawamoto K, Nakao K, Okano H: **Distinct functions of human numb isoforms revealed by misexpression in the neural stem cell lineage in the Drosophila larval brain**. *Dev Neurosci* 2006, **28**:142-155.
145. Campos-Ortega JA: **Numb Diverts Notch Pathway Off the Tramtrack**. *Neuron* 1996, **17**:1-4.
146. Chapman G, Liu L, Sahlgren C, Dahlqvist C, Lendahl U: **High levels of Notch signaling down-regulate Numb and Numblike**. *J Cell Biol* 2006, **175**:535-540.
147. Frise E, Knoblich JA, Younger-Shepherd S, Jan LY, Jan YN: **The Drosophila Numb protein inhibits signaling of the Notch receptor during cell-cell interaction in sensory organ lineage**. *Proc Natl Acad Sci U S A* 1996, **93**:11925-11932.
148. Giebel B, Wodarz A: **Notch Signaling: Numb Makes the Difference**. *Current Biology* 2012, **22**:R133-R135.
149. Wang S, Younger-Shepherd S, Jan LY, Jan YN: **Only a subset of the binary cell fate decisions mediated by Numb/Notch signaling in Drosophila sensory organ lineage requires Suppressor of Hairless**. *Development* 1997, **124**:4435-4446.
150. Shen Q, Zhong W, Jan YN, Temple S: **Asymmetric Numb distribution is critical for asymmetric cell division of mouse cerebral cortical stem cells and neuroblasts**. *Development* 2002, **129**:4843-4853.
151. Zhong W, Jiang MM, Schonemann MD, Meneses JJ, Pedersen RA, Jan LY, Jan YN: **Mouse numb is an essential gene involved in cortical neurogenesis**. *Proc Natl Acad Sci U S A* 2000, **97**:6844-6849.
152. Belmonte-Mateos C, Pujades C: **From Cell States to Cell Fates: How Cell Proliferation and Neuronal Differentiation Are Coordinated During Embryonic Development**. *Front Neurosci* 2021, **15**:781160.
153. Dho SE, Jacob S, Wolting CD, French MB, Rohrschneider LR, McGlade CJ: **The mammalian numb phosphotyrosine-binding domain. Characterization of binding specificity and identification of a novel PDZ domain-containing numb binding protein, LNX**. *J Biol Chem* 1998, **273**:9179-9187.
154. Nie J, Li SS, McGlade CJ: **A novel PTB-PDZ domain interaction mediates isoform-specific ubiquitylation of mammalian Numb**. *J Biol Chem* 2004, **279**:20807-20815.
155. Lacomme M, Hales SC, Brown TW, Stevanovic K, Jolicoeur C, Cai J, Bois T, Desrosiers M, Dalkara D, Cayouette M: **Numb regulates Tau levels and**

prevents neurodegeneration in tauopathy mouse models. *Sci Adv* 2022, **8**:eabm4295.
156. Karaczyn A, Bani-Yaghoub M, Tremblay R, Kubu C, Cowling R, Adams TL, Prudovsky I, Spicer D, Friesel R, Vary C, et al.: **Two novel human NUMB isoforms provide a potential link between development and cancer**. *Neural Dev* 2010, **5**:31.
157. Confalonieri S, Colaluca IN, Basile A, Pece S, Di Fiore PP: **Exon 3 of the NUMB Gene Emerged in the Chordate Lineage Coopting the NUMB Protein to the Regulation of MDM2**. *G3 (Bethesda)* 2019, **9**:3359-3367.
158. Choi HY, Seok J, Kang GH, Lim KM, Cho SG: **The role of NUMB/NUMB isoforms in cancer stem cells**. *BMB Rep* 2021, **54**:335-343.
159. Colaluca IN, Basile A, Freiburger L, D'Uva V, Disalvatore D, Vecchi M, Confalonieri S, Tosoni D, Cecatiello V, Malabarba MG, et al.: **A Numb-Mdm2 fuzzy complex reveals an isoform-specific involvement of Numb in breast cancer**. *J Cell Biol* 2018, **217**:745-762.
160. Haider M, Qiu Q, Bani-Yaghoub M, Tsang BK, Gruslin A: **Characterization and role of NUMB in the human extravillous trophopblast**. *Placenta* 2011, **32**:441-449.
161. Kriventseva EV, Koch I, Apweiler R, Vingron M, Bork P, Gelfand MS, Sunyaev S: **Increase of functional diversity by alternative splicing**. *Trends Genet* 2003, **19**:124-128.
162. Ahn HR, Kim GJ: **The ascidian numb gene involves in the formation of neural tissues**. *Dev Reprod* 2012, **16**:371-378.
163. Johnson JE: **Numb and Numblike control cell number during vertebrate neurogenesis**. *Trends Neurosci* 2003, **26**:395-396.
164. Sigismund S, Confalonieri S, Ciliberto A, Polo S, Scita G, Di Fiore PP: **Endocytosis and signaling: cell logistics shape the eukaryotic cell plan**. *Physiol Rev* 2012, **92**:273-366.
165. Burkhardt P: **The origin and evolution of synaptic proteins - choanoflagellates lead the way**. *J Exp Biol* 2015, **218**:506-514.
166. Dho SE, Othman K, Zhang Y, McGlade CJ: **NUMB alternative splicing and isoform-specific functions in development and disease**. *J Biol Chem* 2025, **301**:108215.
167. Picco A, Toret CP, Rivier-Cordey A-S, Kaksonen M: **Mosaic evolution of clathrin-mediated endocytosis in fungi**. *Current Biology* 2025, **35**:3674-3686.e3674.
168. Maupin-Furlow JA: **Prokaryotic ubiquitin-like protein modification**. *Annu Rev Microbiol* 2014, **68**:155-175.
169. Darwin KH: **Prokaryotic ubiquitin-like protein (Pup), proteasomes and pathogenesis**. *Nature Reviews Microbiology* 2009, **7**:485-491.
170. Zerbib E, Schlussel S, Hecht N, Bagdadi N, Eichler J, Gur E: **The prokaryotic ubiquitin-like protein presents poor cleavage sites for proteasomal degradation**. *Cell Reports* 2021, **36**:109428.
171. Ramamurthy V, Jolicoeur C, Koutroumbas D, Mühlhans J, Le YZ, Hauswirth WW, Giessl A, Cayouette M: **Numb regulates the polarized delivery of cyclic nucleotide-gated ion channels in rod photoreceptor cilia**. *J Neurosci* 2014, **34**:13976-13987.

172. Brunet T, King N: **The Origin of Animal Multicellularity and Cell Differentiation**. *Developmental Cell* 2017, **43**:124-140.
173. Nishimura T, Kaibuchi K: **Numb Controls Integrin Endocytosis for Directional Cell Migration with aPKC and PAR-3**. *Developmental Cell* 2007, **13**:15-28.
174. Salinas-Saavedra M, Martindale MQ: **Par protein localization during the early development of Mnemiopsis leidyi suggests different modes of epithelial organization in the metazoa**. *eLife* 2020, **9**:e54927.
175. Gazave E, Lapébie P, Richards GS, Brunet F, Ereskovsky AV, Degnan BM, Borchiellini C, Vervoort M, Renard E: **Origin and evolution of the Notch signalling pathway: an overview from eukaryotic genomes**. *BMC Evol Biol* 2009, **9**:249.
176. Bresciani E, Confalonieri S, Cermenati S, Cimbro S, Foglia E, Beltrame M, Di Fiore PP, Cotelli F: **Zebrafish Numb and Numblike Are Involved in Primitive Erythrocyte Differentiation**. *PLOS ONE* 2010, **5**:e14296.
177. Gao Z, Chi FL, Huang YB, Yang JM, Cong N, Li W: **Expression of Numb and Numb-like in the development of mammalian auditory sensory epithelium**. *Neuroreport* 2011, **22**:49-54.
178. Petersen PH, Zou K, Krauss S, Zhong W: **Continuing role for mouse Numb and Numbl in maintaining progenitor cells during cortical neurogenesis**. *Nat Neurosci* 2004, **7**:803-811.
179. Zilian O, Saner C, Hagedorn L, Lee H-Y, Säuberli E, Suter U, Sommer L, Aguet M: **Multiple roles of mouse Numb in tuning developmental cell fates**. *Current Biology* 2001, **11**:494-501.
180. Wang Z, Li SS: **Numb: A new player in EMT**. *Cell Adh Migr* 2010, **4**:176-179.
181. Colaluca IN, Tosoni D, Nuciforo P, Senic-Matuglia F, Galimberti V, Viale G, Pece S, Di Fiore PP: **NUMB controls p53 tumour suppressor activity**. *Nature* 2008, **451**:76-80.
182. Sheng W, Dong M, Chen C, Wang Z, Li Y, Wang K, Li Y, Zhou J: **Cooperation of Musashi-2, Numb, MDM2, and P53 in drug resistance and malignant biology of pancreatic cancer**. *Faseb j* 2017, **31**:2429-2438.
183. Kim H, Ronai ZA: **Rewired Notch/p53 by Numb'ing Mdm2**. *J Cell Biol* 2018, **217**:445-446.
184. Shao C, Chien SJ, Farah E, Li Z, Ahmad N, Liu X: **Plk1 phosphorylation of Numb leads to impaired DNA damage response**. *Oncogene* 2018, **37**:810-820.
185. Holowacz T, Zeng L, Lassar AB: **Asymmetric localization of numb in the chick somite and the influence of myogenic signals**. *Dev Dyn* 2006, **235**:633-645.
186. Hakanen J, Ruiz-Reig N, Tissir F: **Linking Cell Polarity to Cortical Development and Malformations**. *Front Cell Neurosci* 2019, **13**:244.
187. Wang N, Wang DD, Hou X, Li X, Shen Y: **Different roles of Numb-p72 and Numb-p65 on the trafficking of metabotropic glutamate receptor 5**. *Mol Biol Rep* 2021, **48**:595-600.
188. Sorensen EB, Conner SD: **AAK1 regulates Numb function at an early step in clathrin-mediated endocytosis**. *Traffic* 2008, **9**:1791-1800.
189. Shao X, Liu Y, Yu Q, Ding Z, Qian W, Zhang L, Zhang J, Jiang N, Gui L, Xu Z, et al.: **Numb regulates vesicular docking for homotypic fusion of early**

endosomes via membrane recruitment of Mon1b. *Cell Research* 2016, **26**:593-612.
190. Lau KM, McGlade CJ: **Numb is a negative regulator of HGF dependent cell scattering and Rac1 activation**. *Exp Cell Res* 2011, **317**:539-551.
191. Krieger JR, Taylor P, Gajadhar AS, Guha A, Moran MF, McGlade CJ: **Identification and selected reaction monitoring (SRM) quantification of endocytosis factors associated with Numb**. *Mol Cell Proteomics* 2013, **12**:499-514.
192. Chen X, Liu Z, Shan Z, Yao W, Gu A, Wen W: **Structural determinants controlling 14-3-3 recruitment to the endocytic adaptor Numb and dissociation of the Numb·α-adaptin complex**. *J Biol Chem* 2018, **293**:4149-4158.
193. Zhang L, Wu SL, Rubin CS: **A novel adapter protein employs a phosphotyrosine binding domain and exceptionally basic N-terminal domains to capture and localize an atypical protein kinase C: characterization of Caenorhabditis elegans C kinase adapter 1, a protein that avidly binds protein kinase C3**. *J Biol Chem* 2001, **276**:10463-10475.
194. Zhang Y, McGlade CJ: **Pan tissue analysis of human NUMB alternative splicing**. *bioRxiv* 2023:2023.2009.2026.559629.
195. Yang Y, Zhu R, Bai J, Zhang X, Tian Y, Li X, Peng Z, He Y, Chen L, Ji Q, et al.: **Numb modulates intestinal epithelial cells toward goblet cell phenotype by inhibiting the Notch signaling pathway**. *Experimental Cell Research* 2011, **317**:1640-1648.
196. Shao X, Ding Z, Zhao M, Liu K, Sun H, Chen J, Liu X, Zhang Y, Hong Y, Li H, et al.: **Mammalian Numb protein antagonizes Notch by controlling postendocytic trafficking of the Notch ligand Delta-like 4**. *J Biol Chem* 2017, **292**:20628-20643.
197. Karaczyn AA, Adams TL, Cheng RY, Matluk NN, Verdi JM: **Human NUMB6 Induces Epithelial-Mesenchymal Transition and Enhances Breast Cancer Cells Migration and Invasion**. *J Cell Biochem* 2017, **118**:237-251.
198. O'Bryan JP: **The PTB domain: a modular domain with multiple function**. *Curr Opin Drug Discov Devel* 1999, **2**:505-518.
199. Bork P, Margolis B: **A phosphotyrosine interaction domain**. *Cell* 1995, **80**:693-694.
200. Zhang J, Padarti A, Jiang X, Abou-Fadel J: **Redefining PTB domain into independently functional dual cores**. *Biochem Biophys Res Commun* 2020, **524**:595-607.
201. Miao L, Li J, Li J, Lu Y, Shieh D, Mazurkiewicz JE, Barroso M, Schwarz JJ, Xin H-B, Singer HA, et al.: **Cardiomyocyte orientation modulated by the Numb family proteins–N-cadherin axis is essential for ventricular wall morphogenesis**. *Proceedings of the National Academy of Sciences* 2019, **116**:15560-15569.
202. Sato K, Watanabe T, Wang S, Kakeno M, Matsuzawa K, Matsui T, Yokoi K, Murase K, Sugiyama I, Ozawa M, et al.: **Numb controls E-cadherin endocytosis through p120 catenin with aPKC**. *Mol Biol Cell* 2011, **22**:3103-3119.

203. Tarn WY, Kuo HC, Yu HI, Liu SW, Tseng CT, Dhananjaya D, Hung KY, Tu CC, Chang SH, Huang GJ, et al.: **RBM4 promotes neuronal differentiation and neurite outgrowth by modulating Numb isoform expression**. *Mol Biol Cell* 2016, **27**:1676-1683.
204. Choi S, Cho N, Kim KK: **The implications of alternative pre-mRNA splicing in cell signal transduction**. *Experimental & Molecular Medicine* 2023, **55**:755-766.
205. Lee Y, Rio DC: **Mechanisms and Regulation of Alternative Pre-mRNA Splicing**. *Annu Rev Biochem* 2015, **84**:291-323.
206. Kim KK, Nam J, Mukouyama YS, Kawamoto S: **Rbfox3-regulated alternative splicing of Numb promotes neuronal differentiation during development**. *J Cell Biol* 2013, **200**:443-458.
207. Nishimura T, Yamaguchi T, Tokunaga A, Hara A, Hamaguchi T, Kato K, Iwamatsu A, Okano H, Kaibuchi K: **Role of numb in dendritic spine development with a Cdc42 GEF intersectin and EphB2**. *Mol Biol Cell* 2006, **17**:1273-1285.
208. Liu W, Xie H, Liu X, Xu S, Cheng S, Wang Z, Xie T, Zhang ZC, Han J: **PQBP1 regulates striatum development through balancing striatal progenitor proliferation and differentiation**. *Cell Rep* 2023, **42**:112277.
209. Tao Y, Zhang Q, Wang H, Yang X, Mu H: **Alternative splicing and related RNA binding proteins in human health and disease**. *Signal Transduction and Targeted Therapy* 2024, **9**:26.
210. Liu X, Xie H, Liu W, Zuo J, Li S, Tian Y, Zhao J, Bai M, Li J, Bao L, et al.: **Dynamic regulation of alternative polyadenylation by PQBP1 during neurogenesis**. *Cell Reports* 2024, **43**:114525.
211. Tan YZ, Fei DD, He XN, Dai JM, Xu RC, Xu XY, Wu JJ, Li B: **L-type voltage-gated calcium channels in stem cells and tissue engineering**. *Cell Prolif* 2019, **52**:e12623.
212. Wang Z, Zhao M, Su Y, Zhao Q, Ma Z, Yue Q, Zhu Z, Zhang L, Hou Z, Li H: **The impact of NUMB on chicken abdominal adipogenesis: A comprehensive analysis**. *International Journal of Biological Macromolecules* 2024, **278**:134904.
213. Duquette PM, Lamarche-Vane N: **The calcium-activated protease calpain regulates netrin-1 receptor deleted in colorectal cancer-induced axon outgrowth in cortical neurons**. *J Neurochem* 2020, **152**:315-332.
214. Locatelli F, Soda T, Montagna I, Tritto S, Botta L, Prestori F, D'Angelo E: **Calcium Channel-Dependent Induction of Long-Term Synaptic Plasticity at Excitatory Golgi Cell Synapses of Cerebellum**. *J Neurosci* 2021, **41**:3307-3319.
215. Bechara EG, Sebestyén E, Bernardis I, Eyras E, Valcárcel J: **RBM5, 6, and 10 differentially regulate NUMB alternative splicing to control cancer cell proliferation**. *Mol Cell* 2013, **52**:720-733.
216. Teranishi M, Kurose T, Nakagawa K, Kawahara Y, Yuge L: **Hypergravity enhances RBM4 expression in human bone marrow-derived mesenchymal stem cells and accelerates their differentiation into neurons**. *Regenerative Therapy* 2023, **22**:109-114.
217. Su CH, Hung KY, Hung SC, Tarn WY: **RBM4 Regulates Neuronal Differentiation of Mesenchymal Stem Cells by Modulating Alternative Splicing of Pyruvate Kinase M**. *Mol Cell Biol* 2017, **37**.

218. D D, Hung KY, Tarn WY: **RBM4 Modulates Radial Migration via Alternative Splicing of Dab1 during Cortex Development**. *Mol Cell Biol* 2018, **38**.
219. Shen C-L, Tsai Y-Y, Chou S-J, Chang Y-M, Tarn W-Y: **RBM4-mediated intron excision of Hsf1 induces BDNF for cerebellar foliation**. *Communications Biology* 2024, **7**:1712.
220. Su C-H, D D, Tarn W-Y: **Alternative Splicing in Neurogenesis and Brain Development**. *Frontiers in Molecular Biosciences* 2018, **Volume 5 - 2018**.
221. Kar A, Havlioglu N, Tarn WY, Wu JY: **RBM4 interacts with an intronic element and stimulates tau exon 10 inclusion**. *J Biol Chem* 2006, **281**:24479-24488.
222. Kiani L: **NUMB72 — a therapeutic target for tauopathies?** *Nature Reviews Neurology* 2022, **18**:699-699.
223. Sarnowski C, Ghanbari M, Bis JC, Logue M, Fornage M, Mishra A, Ahmad S, Beiser AS, Boerwinkle E, Bouteloup V, et al.: **Meta-analysis of genome-wide association studies identifies ancestry-specific associations underlying circulating total tau levels**. *Communications Biology* 2022, **5**:336.
224. Zhang X, Wang J, Zhang Z, Ye K: **Tau in neurodegenerative diseases: molecular mechanisms, biomarkers, and therapeutic strategies**. *Translational Neurodegeneration* 2024, **13**:40.
225. Totland MZ, Omori Y, Sørensen V, Kryeziu K, Aasen T, Brech A, Leithe E: **Endocytic trafficking of connexins in cancer pathogenesis**. *Biochim Biophys Acta Mol Basis Dis* 2023, **1869**:166812.
226. Cullen PJ, Steinberg F: **To degrade or not to degrade: mechanisms and significance of endocytic recycling**. *Nat Rev Mol Cell Biol* 2018, **19**:679-696.
227. Pathak C, Vaidya FU, Waghela BN, Jaiswara PK, Gupta VK, Kumar A, Rajendran BK, Ranjan K: **Insights of Endocytosis Signaling in Health and Disease**. *Int J Mol Sci* 2023, **24**.
228. Xian J, Cheng Y, Qin X, Cao Y, Luo Y, Cao Y: **Progress in the research of p53 tumour suppressor activity controlled by Numb in triple-negative breast cancer**. *J Cell Mol Med* 2020, **24**:7451-7459.
229. McGill MA, Dho SE, Weinmaster G, McGlade CJ: **Numb Regulates Post-endocytic Trafficking and Degradation of Notch1***. *Journal of Biological Chemistry* 2009, **284**:26427-26438.
230. Lee S, Uchida Y, Wang J, Matsudaira T, Nakagawa T, Kishimoto T, Mukai K, Inaba T, Kobayashi T, Molday RS, et al.: **Transport through recycling endosomes requires EHD1 recruitment by a phosphatidylserine translocase**. *The EMBO Journal* 2015, **34**:669-688.
231. Mettlen M, Chen P-H, Srinivasan S, Danuser G, Schmid SL: **Regulation of Clathrin-Mediated Endocytosis**. *Annual Review of Biochemistry* 2018, **87**:871-896.
232. Haucke V, Kozlov MM: **Membrane remodeling in clathrin-mediated endocytosis**. *J Cell Sci* 2018, **131**.
233. Zuidema A, Wang W, Kreft M, Te Molder L, Hoekman L, Bleijerveld OB, Nahidiazar L, Janssen H, Sonnenberg A: **Mechanisms of integrin αVβ5 clustering in flat clathrin lattices**. *J Cell Sci* 2018, **131**.
234. Zhang Y, Dho SE, Othman K, Simpson CD, Lapierre J, Bondoc A, McGlade CJ: **Numb exon 9 inclusion regulates Integrinβ5 surface expression and promotes breast cancer metastasis**. *Oncogene* 2022, **41**:2079-2094.

235. Morris SW, Kirstein MN, Valentine MB, Dittmer KG, Shapiro DN, Saltman DL, Look AT: **Fusion of a kinase gene, ALK, to a nucleolar protein gene, NPM, in non-Hodgkin's lymphoma**. *Science* 1994, **263**:1281-1284.
236. Bilsland JG, Wheeldon A, Mead A, Znamenskiy P, Almond S, Waters KA, Thakur M, Beaumont V, Bonnert TP, Heavens R, et al.: **Behavioral and neurochemical alterations in mice deficient in anaplastic lymphoma kinase suggest therapeutic potential for psychiatric indications**. *Neuropsychopharmacology* 2008, **33**:685-700.
237. Mossé YP, Wood A, Maris JM: **Inhibition of ALK signaling for cancer therapy**. *Clin Cancer Res* 2009, **15**:5609-5614.
238. Wei R, Liu X, Voss C, Qin W, Dagnino L, Li L, Vigny M, Li SS: **NUMB regulates the endocytosis and activity of the anaplastic lymphoma kinase in an isoform-specific manner**. *J Mol Cell Biol* 2019, **11**:994-1005.
239. Wei R, Kaneko T, Liu X, Liu H, Li L, Voss C, Liu E, He N, Li SS: **Interactome Mapping Uncovers a General Role for Numb in Protein Kinase Regulation**. *Mol Cell Proteomics* 2018, **17**:2216-2228.
240. Serresi M, Piccinini G, Pierpaoli E, Fazioli F: **A ligand-inducible anaplastic lymphoma kinase chimera is endocytosis impaired**. *Oncogene* 2004, **23**:1098-1108.
241. Bento CF, Renna M, Ghislat G, Puri C, Ashkenazi A, Vicinanza M, Menzies FM, Rubinsztein DC: **Mammalian Autophagy: How Does It Work?** *Annu Rev Biochem* 2016, **85**:685-713.
242. Tomuleasa C, Tigu A-B, Munteanu R, Moldovan C-S, Kegyes D, Onaciu A, Gulei D, Ghiaur G, Einsele H, Croce CM: **Therapeutic advances of targeting receptor tyrosine kinases in cancer**. *Signal Transduction and Targeted Therapy* 2024, **9**:201.
243. Chou CH, Chiang CF, Yang CC, Liu YC, Chang SR, Chang KW, Lin SC: **miR-31-NUMB Cascade Modulates Monocarboxylate Transporters to Increase Oncogenicity and Lactate Production of Oral Carcinoma Cells**. *Int J Mol Sci* 2021, **22**.
244. Dou XQ, Chen XJ, Zhou Q, Wen MX, Zhang SZ, Zhang SQ: **miR-335 modulates Numb alternative splicing via targeting RBM10 in endometrial cancer**. *Kaohsiung J Med Sci* 2020, **36**:171-177.
245. Wang X, Cai J, Zhao L, Zhang D, Xu G, Hu J, Zhang T, Jin M: **NUMB suppression by miR-9-5P enhances CD44(+) prostate cancer stem cell growth and metastasis**. *Sci Rep* 2021, **11**:11210.
246. Kikuchi H, Sakakibara-Konishi J, Furuta M, Kikuchi E, Kikuchi J, Oizumi S, Hida Y, Kaga K, Kinoshita I, Dosaka-Akita H, et al.: **Numb has distinct function in lung adenocarcinoma and squamous cell carcinoma**. *Oncotarget* 2018, **9**:29379-29391.
247. Wu J, Shen SL, Chen B, Nie J, Peng BG: **Numb promotes cell proliferation and correlates with poor prognosis in hepatocellular carcinoma**. *PLoS One* 2014, **9**:e95849.
248. Zuo X, Xu J, Yang D, Yang C, Liu X, Chen N, Wang H, Luo X, Luo Q, Wang Y, et al.: **SRSF9 Forms Phase-separated Condensates to Promote Ovarian Cancer Progression by Inducing RNA Alternative Splicing that is Inhibited by m6A Modification**. *Cancer Research* 2025.

249. Zhang H, Zhu H, Peng H, Sheng Y: **Function of serine/arginine-rich splicing factors in hematopoiesis and hematopoietic malignancies**. *Cancer Cell Int* 2024, **24**:257.
250. Zhang Y, Dho SE, Simpson CD, Othman K, Bondoc A, McGlade CJ: **Isoform-specific functions of Numb in breast cancer progression, metastasis and proteome remodeling**. *bioRxiv* 2021:2021.2002.2001.429237.
251. He Z, Ni Q, Li X, Zhao M, Mo Q, Duo Y: **PTBP1 promotes hepatocellular carcinoma progression by regulating the skipping of exon 9 in NUMB pre-mRNA**. *Heliyon* 2023, **9**:e17387.
252. Abballe L, Mastronuzzi A, Miele E, Carai A, Besharat ZM, Moretti M, De Smaele E, Giangaspero F, Locatelli F, Ferretti E, et al.: **Numb Isoforms Deregulation in Medulloblastoma and Role of p66 Isoform in Cancer and Neural Stem Cells**. *Front Pediatr* 2018, **6**:315.
253. Wang JZ, Fu X, Fang Z, Liu H, Zong FY, Zhu H, Yu YF, Zhang XY, Wang SF, Huang Y, et al.: **QKI-5 regulates the alternative splicing of cytoskeletal gene ADD3 in lung cancer**. *J Mol Cell Biol* 2021, **13**:347-360.
254. Zong FY, Fu X, Wei WJ, Luo YG, Heiner M, Cao LJ, Fang Z, Fang R, Lu D, Ji H, et al.: **The RNA-binding protein QKI suppresses cancer-associated aberrant splicing**. *PLoS Genet* 2014, **10**:e1004289.
255. de Miguel FJ, Pajares MJ, Martínez-Terroba E, Ajona D, Morales X, Sharma RD, Pardo FJ, Rouzaut A, Rubio A, Montuenga LM, et al.: **A large-scale analysis of alternative splicing reveals a key role of QKI in lung cancer**. *Molecular Oncology* 2016, **10**:1437-1449.
256. Kanamori M, Kawaguchi T, Nigro JM, Feuerstein BG, Berger MS, Miele L, Pieper RO: **Contribution of Notch signaling activation to human glioblastoma multiforme**. *J Neurosurg* 2007, **106**:417-427.
257. Lampada A, Taylor V: **Notch signaling as a master regulator of adult neurogenesis**. *Frontiers in Neuroscience* 2023, **Volume 17 - 2023**.
258. Zhou B, Lin W, Long Y, Yang Y, Zhang H, Wu K, Chu Q: **Notch signaling pathway: architecture, disease, and therapeutics**. *Signal Transduction and Targeted Therapy* 2022, **7**:95.
259. Gozlan O, Sprinzak D: **Notch signaling in development and homeostasis**. *Development* 2023, **150**.
260. Zhang R, Engler A, Taylor V: **Notch: an interactive player in neurogenesis and disease**. *Cell and Tissue Research* 2018, **371**:73-89.
261. Păun O, Tan YX, Patel H, Strohbuecker S, Ghanate A, Cobolli-Gigli C, Llorian Sopena M, Gerontogianni L, Goldstone R, Ang SL, et al.: **Pioneer factor ASCL1 cooperates with the mSWI/SNF complex at distal regulatory elements to regulate human neural differentiation**. *Genes Dev* 2023, **37**:218-242.
262. Singh N, Siebzehnrubl FA, Martinez-Garay I: **Transcriptional control of embryonic and adult neural progenitor activity**. *Front Neurosci* 2023, **17**:1217596.
263. Ochi S, Imaizumi Y, Shimojo H, Miyachi H, Kageyama R: **Oscillatory expression of Hes1 regulates cell proliferation and neuronal differentiation in the embryonic brain**. *Development* 2020, **147**.

264. Ivanov D: **Notch Signaling-Induced Oscillatory Gene Expression May Drive Neurogenesis in the Developing Retina**. *Frontiers in Molecular Neuroscience* 2019, **Volume 12 - 2019**.
265. Marinopoulou E, Biga V, Sabherwal N, Miller A, Desai J, Adamson AD, Papalopulu N: **HES1 protein oscillations are necessary for neural stem cells to exit from quiescence**. *iScience* 2021, **24**.
266. Gómez-López S, Lerner RG, Petritsch C: **Asymmetric cell division of stem and progenitor cells during homeostasis and cancer**. *Cell Mol Life Sci* 2014, **71**:575-597.
267. García-Heredia JM, Carnero A: **NUMB and NUMBL differences in gene regulation**. *Oncotarget* 2018, **9**:9219-9234.
268. Knoblich JA: **Asymmetric cell division: recent developments and their implications for tumour biology**. *Nat Rev Mol Cell Biol* 2010, **11**:849-860.
269. Su D, Li Y, Zhang W, Gao H, Cheng Y, Hou Y, Li J, Ye Y, Lai Z, Li Z, et al.: **SPTAN1/NUMB axis senses cell density to restrain cell growth and oncogenesis through Hippo signaling**. *J Clin Invest* 2023, **133**.
270. Jiang X, Xing H, Kim TM, Jung Y, Huang W, Yang HW, Song S, Park PJ, Carroll RS, Johnson MD: **Numb regulates glioma stem cell fate and growth by altering epidermal growth factor receptor and Skp1-Cullin-F-box ubiquitin ligase activity**. *Stem Cells* 2012, **30**:1313-1326.
271. Uldrijan S, Pannekoek WJ, Vousden KH: **An essential function of the extreme C-terminus of MDM2 can be provided by MDMX**. *Embo j* 2007, **26**:102-112.
272. Brooks CL, Gu W: **p53 ubiquitination: Mdm2 and beyond**. *Mol Cell* 2006, **21**:307-315.
273. Faraldo MM, Glukhova MA: **Regulating the regulator: Numb acts upstream of p53 to control mammary stem and progenitor cell**. *J Cell Biol* 2015, **211**:737-739.
274. Carter S, Vousden KH: **A role for Numb in p53 stabilization**. *Genome Biol* 2008, **9**:221.
275. Liu L, Lanner F, Lendahl U, Das D: **Numblike and Numb differentially affect p53 and Sonic Hedgehog signaling**. *Biochem Biophys Res Commun* 2011, **413**:426-431.
276. Liu L, Charville GW, Cheung TH, Yoo B, Santos PJ, Schroeder M, Rando TA: **Impaired Notch Signaling Leads to a Decrease in p53 Activity and Mitotic Catastrophe in Aged Muscle Stem Cells**. *Cell Stem Cell* 2018, **23**:544-556.e544.
277. Huang Q, Raya A, DeJesus P, Chao S-H, Quon KC, Caldwell JS, Chanda SK, Izpisua-Belmonte JC, Schultz PG: **Identification of p53 regulators by genome-wide functional analysis**. *Proceedings of the National Academy of Sciences* 2004, **101**:3456-3461.
278. Memme JM, Oliveira AN, Hood DA: **p53 regulates skeletal muscle mitophagy and mitochondrial quality control following denervation-induced muscle disuse**. *J Biol Chem* 2022, **298**:101540.
279. Mazzaro G, Bossi G, Coen S, Sacchi A, Soddu S: **The role of wild-type p53 in the differentiation of primary hemopoietic and muscle cells**. *Oncogene* 1999, **18**:5831-5835.

280. Aubrey BJ, Kelly GL, Janic A, Herold MJ, Strasser A: **How does p53 induce apoptosis and how does this relate to p53-mediated tumour suppression?** *Cell Death & Differentiation* 2018, **25**:104-113.
281. Gioftsidi S, Relaix F, Mourikis P: **The Notch signaling network in muscle stem cells during development, homeostasis, and disease**. *Skeletal Muscle* 2022, **12**:9.
282. Arya AK, El-Fert A, Devling T, Eccles RM, Aslam MA, Rubbi CP, Vlatković N, Fenwick J, Lloyd BH, Sibson DR, et al.: **Nutlin-3, the small-molecule inhibitor of MDM2, promotes senescence and radiosensitises laryngeal carcinoma cells harbouring wild-type p53**. *British Journal of Cancer* 2010, **103**:186-195.
283. Gibbs BC, Shenje L, Andersen P, Miyamoto M, Kwon C: **β1-integrin is a cell-autonomous factor mediating the Numb pathway for cardiac progenitor maintenance**. *Biochem Biophys Res Commun* 2018, **500**:256-260.
284. Pece S, Serresi M, Santolini E, Capra M, Hulleman E, Galimberti V, Zurrida S, Maisonneuve P, Viale G, Di Fiore PP: **Loss of negative regulation by Numb over Notch is relevant to human breast carcinogenesis**. *J Cell Biol* 2004, **167**:215-221.
285. McGill MA, McGlade CJ: **Mammalian numb proteins promote Notch1 receptor ubiquitination and degradation of the Notch1 intracellular domain**. *J Biol Chem* 2003, **278**:23196-23203.
286. Juven-Gershon T, Shifman O, Unger T, Elkeles A, Haupt Y, Oren M: **The Mdm2 oncoprotein interacts with the cell fate regulator Numb**. *Mol Cell Biol* 1998, **18**:3974-3982.
287. Hwang WL, Jiang JK, Yang SH, Huang TS, Lan HY, Teng HW, Yang CY, Tsai YP, Lin CH, Wang HW, et al.: **MicroRNA-146a directs the symmetric division of Snail-dominant colorectal cancer stem cells**. *Nat Cell Biol* 2014, **16**:268-280.
288. Katoh M, Katoh M: **NUMB is a break of WNT - Notch signaling cycle**. *Int J Mol Med* 2006, **18**:517-521.
289. Cheng C, Huang Z, Zhou R, An H, Cao G, Ye J, Huang C, Wu D: **Numb negatively regulates the epithelial-to-mesenchymal transition in colorectal cancer through the Wnt signaling pathway**. *Am J Physiol Gastrointest Liver Physiol* 2020, **318**:G841-g853.
290. Chhabra G, Singh CK, Ndiaye MA, Su S, Shirley CA, Ahmad N: **Role of PLK1/NUMB/NOTCH in epithelial-mesenchymal transition in human melanoma**. *NPJ Precis Oncol* 2024, **8**:6.
291. Dolique T, Baudet S, Charron F, Ferent J: **A central role for Numb/Nbl in multiple Shh-mediated axon repulsion processes**. *iScience* 2025, **28**:112293.
292. Grisanti L, Corallini S, Fera S, Muciaccia B, Stefanini M, Witke W, Vicini E: **Inactivation of Numb and Numblike in spermatogonial stem cells by cell-permeant Cre recombinase**. *Differentiation* 2009, **78**:131-136.
293. Givogri MI, Schonmann V, Cole R, De Vellis J, Bongarzone ER: **Notch1 and Numb genes are inversely expressed as oligodendrocytes differentiate**. *Dev Neurosci* 2003, **25**:50-64.
294. Miao L, Lu Y, Nusrat A, Abdelnasser HY, Datta S, Zhou B, Schwartz RJ, Wu M: **The Spatiotemporal Expression of Notch1 and Numb and Their Functional Interaction during Cardiac Morphogenesis**. *Cells* 2021, **10**.

295. Di Marcotullio L, Ferretti E, Greco A, De Smaele E, Po A, Sico MA, Alimandi M, Giannini G, Maroder M, Screpanti I, et al.: **Numb is a suppressor of Hedgehog signalling and targets Gli1 for Itch-dependent ubiquitination**. *Nat Cell Biol* 2006, **8**:1415-1423.
296. Liu X, Yam PT, Schlienger S, Cai E, Zhang J, Chen W-J, Torres Gutierrez O, Jimenez Amilburu V, Ramamurthy V, Ting AY, et al.: **Numb positively regulates Hedgehog signaling at the ciliary pocket**. *Nature Communications* 2024, **15**:3365.
297. Hristova DM, Fukumoto T, Takemori C, Gao L, Hua X, Wang JX, Li L, Beqiri M, Watters A, Vultur A, et al.: **NUMB as a Therapeutic Target for Melanoma**. *J Invest Dermatol* 2022, **142**:1882-1892.e1885.
298. Tosoni D, Zecchini S, Coazzoli M, Colaluca I, Mazzarol G, Rubio A, Caccia M, Villa E, Zilian O, Di Fiore PP, et al.: **The Numb/p53 circuitry couples replicative self-renewal and tumor suppression in mammary epithelial cells**. *J Cell Biol* 2015, **211**:845-862.
299. He Y, Ji Z, Gong Y, Fan L, Xu P, Chen X, Miao J, Zhang K, Zhang W, Ma P, et al.: **Numb/Parkin-directed mitochondrial fitness governs cancer cell fate via metabolic regulation of histone lactylation**. *Cell Reports* 2023, **42**.
300. Li L, Chen K, Wang T, Wu Y, Xing G, Chen M, Hao Z, Zhang C, Zhang J, Ma B, et al.: **Glis1 facilitates induction of pluripotency via an epigenome-metabolome-epigenome signalling cascade**. *Nat Metab* 2020, **2**:882-892.
301. Zhang D, Tang Z, Huang H, Zhou G, Cui C, Weng Y, Liu W, Kim S, Lee S, Perez-Neut M, et al.: **Metabolic regulation of gene expression by histone lactylation**. *Nature* 2019, **574**:575-580.
302. Izzo LT, Wellen KE: **Histone lactylation links metabolism and gene regulation**. *Nature* 2019, **574**:492-493.
303. Yao W, Hu X, Wang X: **Crossing epigenetic frontiers: the intersection of novel histone modifications and diseases**. *Signal Transduction and Targeted Therapy* 2024, **9**:232.
304. Zaidi SK, Young DW, Montecino M, Lian JB, Stein JL, van Wijnen AJ, Stein GS: **Architectural epigenetics: mitotic retention of mammalian transcriptional regulatory information**. *Mol Cell Biol* 2010, **30**:4758-4766.
305. Dhami Gurpreet K, Liu H, Galka M, Voss C, Wei R, Muranko K, Kaneko T, Cregan Sean P, Li L, Li Shawn S-C: **Dynamic Methylation of Numb by Set8 Regulates Its Binding to p53 and Apoptosis**. *Molecular Cell* 2013, **50**:565-576.
306. Ferrante F, Giaimo BD, Bartkuhn M, Zimmermann T, Close V, Mertens D, Nist A, Stiewe T, Meier-Soelch J, Kracht M, et al.: **HDAC3 functions as a positive regulator in Notch signal transduction**. *Nucleic Acids Res* 2020, **48**:3496-3512.
307. Channakkar AS, D'Souza L, Kumar A, Kalia K, Prabhu S, Phalnikar K, Reddy PC, Muralidharan B: **LSD1 Regulates Neurogenesis in Human Neural Stem Cells Through the Repression of Human-Enriched Extracellular Matrix and Cell Adhesion Genes**. *Stem Cells* 2024, **42**:128-145.
308. Rogers JM, Mimoso CA, Martin BJE, Martin AP, Aster JC, Adelman K, Blacklow SC: **Notch induces transcription by stimulating release of paused RNA polymerase II**. *Genes Dev* 2024, **38**:965-978.

309. van den Ameele J, Krautz R, Cheetham SW, Donovan APA, Llorà-Batlle O, Yakob R, Brand AH: **Reduced chromatin accessibility correlates with resistance to Notch activation**. *Nature Communications* 2022, **13**:2210.
310. Zhao E, Maj T, Kryczek I, Li W, Wu K, Zhao L, Wei S, Crespo J, Wan S, Vatan L, et al.: **Cancer mediates effector T cell dysfunction by targeting microRNAs and EZH2 via glycolysis restriction**. *Nat Immunol* 2016, **17**:95-103.
311. Corley M, Kroll KL: **The roles and regulation of Polycomb complexes in neural development**. *Cell Tissue Res* 2015, **359**:65-85.
312. Wang W, Cho H, Kim D, Park Y, Moon JH, Lim SJ, Yoon SM, McCane M, Aicher SA, Kim S, et al.: **PRC2 Acts as a Critical Timer That Drives Oligodendrocyte Fate over Astrocyte Identity by Repressing the Notch Pathway**. *Cell Reports* 2020, **32**:108147.
313. Oksuz O, Narendra V, Lee CH, Descostes N, LeRoy G, Raviram R, Blumenberg L, Karch K, Rocha PP, Garcia BA, et al.: **Capturing the Onset of PRC2-Mediated Repressive Domain Formation**. *Mol Cell* 2018, **70**:1149-1162.e1145.
314. Wienken M, Dickmanns A, Nemajerova A, Kramer D, Najafova Z, Weiss M, Karpiuk O, Kassem M, Zhang Y, Lozano G, et al.: **MDM2 Associates with Polycomb Repressor Complex 2 and Enhances Stemness-Promoting Chromatin Modifications Independent of p53**. *Mol Cell* 2016, **61**:68-83.
315. Aoyama K, Shinoda D, Suzuki E, Nakajima-Takagi Y, Oshima M, Koide S, Rizq O, Si S, Tara S, Sashida G, et al.: **PRC2 insufficiency causes p53-dependent dyserythropoiesis in myelodysplastic syndrome**. *Leukemia* 2021, **35**:1156-1165.
316. Cleveland AH, Malawsky D, Churiwal M, Rodriguez C, Reed F, Schniederjan M, Velazquez Vega JE, Davis I, Gershon TR: **PRC2 disruption in cerebellar progenitors produces cerebellar hypoplasia and aberrant myoid differentiation without blocking medulloblastoma growth**. *Acta Neuropathologica Communications* 2023, **11**:8.
317. Espanola SG, Song H, Ryu E, Saxena A, Kim ES, Manegold JE, Nasamran CA, Sahoo D, Oh CK, Bickers C, et al.: **Haematopoietic stem cell-dependent Notch transcription is mediated by p53 through the Histone chaperone Supt16h**. *Nat Cell Biol* 2020, **22**:1411-1422.
318. Nussinov R, Yavuz BR, Arici MK, Demirel HC, Zhang M, Liu Y, Tsai CJ, Jang H, Tuncbag N: **Neurodevelopmental disorders, like cancer, are connected to impaired chromatin remodelers, PI3K/mTOR, and PAK1-regulated MAPK**. *Biophys Rev* 2023, **15**:163-181.
319. Kar R, Jha SK, Ojha S, Sharma A, Dholpuria S, Raju VSR, Prasher P, Chellappan DK, Gupta G, Kumar Singh S, et al.: **The FBXW7-NOTCH interactome: A ubiquitin proteasomal system-induced crosstalk modulating oncogenic transformation in human tissues**. *Cancer Rep (Hoboken)* 2021, **4**:e1369.
320. Zhang Y, Yang H, Liu W, Song Q, Li Y, Zhang J, Zhou D, Li A: **Comprehensive pan-cancer analysis of expression profiles and prognostic significance for NUMB and NUMBL in human tumors**. *Medicine (Baltimore)* 2023, **102**:e34717.
321. Liu XH, Wu Y, Yao S, Levine AC, Kirschenbaum A, Collier L, Bauman WA, Cardozo CP: **Androgens up-regulate transcription of the Notch inhibitor Numb in C2C12 myoblasts via Wnt/β-catenin signaling to T cell factor elements in the Numb promoter**. *J Biol Chem* 2013, **288**:17990-17998.

322. Yavuz BR, Arici MK, Demirel HC, Tsai C-J, Jang H, Nussinov R, Tuncbag N: **Neurodevelopmental disorders and cancer networks share pathways, but differ in mechanisms, signaling strength, and outcome**. *npj Genomic Medicine* 2023, **8**:37.
323. Smith CA, Dho SE, Donaldson J, Tepass U, McGlade CJ: **The cell fate determinant numb interacts with EHD/Rme-1 family proteins and has a role in endocytic recycling**. *Mol Biol Cell* 2004, **15**:3698-3708.
324. Krieger JR, Taylor P, Moran MF, McGlade CJ: **Comprehensive identification of phosphorylation sites on the Numb endocytic adaptor protein**. *PROTEOMICS* 2015, **15**:434-446.
325. Zhang Y, Xiang Z, Jia Y, He X, Wang L, Cui W: **The Notch signaling pathway inhibitor Dapt alleviates autism-like behavior, autophagy and dendritic spine density abnormalities in a valproic acid-induced animal model of autism**. *Progress in Neuro-Psychopharmacology and Biological Psychiatry* 2019, **94**:109644.
326. Wang N, Wang DD, Shen Y: **Numb deficiency causes impaired trafficking of mGlu5 in neurons and autistic-like behaviors**. *Neurosci Lett* 2019, **707**:134291.
327. Wang X, Bey AL, Katz BM, Badea A, Kim N, David LK, Duffney LJ, Kumar S, Mague SD, Hulbert SW, et al.: **Altered mGluR5-Homer scaffolds and corticostriatal connectivity in a Shank3 complete knockout model of autism**. *Nature Communications* 2016, **7**:11459.
328. Ntelios D, Berninger B, Tzimagiorgis G: **Numb and Alzheimer's Disease: The Current Picture**. *Frontiers in Neuroscience* 2012, **Volume 6 - 2012**.
329. Chhabra SN, Booth BW: **Asymmetric cell division of mammary stem cells**. *Cell Division* 2021, **16**:5.
330. Filippone MG, Freddi S, Zecchini S, Restelli S, Colaluca IN, Bertalot G, Pece S, Tosoni D, Di Fiore PP: **Aberrant phosphorylation inactivates Numb in breast cancer causing expansion of the stem cell pool**. *Journal of Cell Biology* 2022, **221**.
331. Wils LJ, Bijlsma MF: **Epigenetic regulation of the Hedgehog and Wnt pathways in cancer**. *Critical Reviews in Oncology/Hematology* 2018, **121**:23-44.
332. Xue C, Chu Q, Shi Q, Zeng Y, Lu J, Li L: **Wnt signaling pathways in biology and disease: mechanisms and therapeutic advances**. *Signal Transduction and Targeted Therapy* 2025, **10**:106.
333. Katoh M, Katoh M: **Precision medicine for human cancers with Notch signaling dysregulation (Review)**. *Int J Mol Med* 2020, **45**:279-297.
334. González LF, Henríquez-Belmar F, Delgado-Acevedo C, Cisternas-Olmedo M, Arriagada G, Sotomayor-Zárate R, Murphy DL, Moya PR: **Neurochemical and behavioral characterization of neuronal glutamate transporter EAAT3 heterozygous mice**. *Biol Res* 2017, **50**:29.
335. Delgado-Acevedo C, Estay SF, Radke AK, Sengupta A, Escobar AP, Henríquez-Belmar F, Reyes CA, Haro-Acuña V, Utreras E, Sotomayor-Zárate R, et al.: **Behavioral and synaptic alterations relevant to obsessive-compulsive disorder in mice with increased EAAT3 expression**. *Neuropsychopharmacology* 2019, **44**:1163-1173.

336. Su JF, Wei J, Li PS, Miao HH, Ma YC, Qu YX, Xu J, Qin J, Li BL, Song BL, et al.: **Numb directs the subcellular localization of EAAT3 through binding the YxNxxF motif**. *J Cell Sci* 2016, **129**:3104-3114.
337. Zhou P, Alfaro J, Chang Eun H, Zhao X, Porcionatto M, Segal Rosalind A: **Numb Links Extracellular Cues to Intracellular Polarity Machinery to Promote Chemotaxis**. *Developmental Cell* 2011, **20**:610-622.
338. Le N, Vu TD, Palazzo I, Pulya R, Kim Y, Blackshaw S, Hoang T: **Robust reprogramming of glia into neurons by inhibition of Notch signaling and NFI factors in adult mammalian retina**. *bioRxiv* 2023.
339. Huilgol D, Levine JM, Galbavy W, Wang B-S, He M, Suryanarayana SM, Huang ZJ: **Direct and indirect neurogenesis generate a mosaic of distinct glutamatergic projection neuron types in cerebral cortex**. *Neuron* 2023, **111**:2557-2569.e2554.
340. Guo Y, Zhang K, Cheng C, Ji Z, Wang X, Wang M, Chu M, Tang DG, Zhu HH, Gao WQ: **Numb(-/low) Enriches a Castration-Resistant Prostate Cancer Cell Subpopulation Associated with Enhanced Notch and Hedgehog Signaling**. *Clin Cancer Res* 2017, **23**:6744-6756.
341. Wang H-Y, Hsieh P-F, Huang D-F, Chin P-S, Chou C-H, Tung C-C, Chen S-Y, Lee L-J, Gau SS-F, Huang H-S: **RBFOX3/NeuN is Required for Hippocampal Circuit Balance and Function**. *Scientific Reports* 2015, **5**:17383.
342. He J, Yang L, Chang P, Yang S, Wang Y, Lin S, Tang Q, Zhang Y: **Zika Virus Induces Degradation of the Numb Protein Required through Embryonic Neurogenesis**. *Viruses* 2023, **15**.
343. Iannolo G, Sciuto MR, Cuscino N, Pallini R, Douradinha B, Vitiani LR, De Maria R, Conaldi PG: **Zika virus infection induces MiR34c expression in glioblastoma stem cells: new perspectives for brain tumor treatments**. *Cell Death & Disease* 2019, **10**:263.
344. Karthikeyan S, Casey PJ, Wang M: **RAB4A is a master regulator of cancer cell stemness upstream of NUMB-NOTCH signaling**. *Cell Death Dis* 2024, **15**:778.
345. Huang N, Winans T, Wyman B, Oaks Z, Faludi T, Choudhary G, Lai Z-W, Lewis J, Beckford M, Duarte M, et al.: **Rab4A-directed endosome traffic shapes pro-inflammatory mitochondrial metabolism in T cells via mitophagy, CD98 expression, and kynurenine-sensitive mTOR activation**. *Nature Communications* 2024, **15**:2598.
346. van de Leemput J, Boles NC, Kiehl TR, Corneo B, Lederman P, Menon V, Lee C, Martinez RA, Levi BP, Thompson CL, et al.: **CORTECON: a temporal transcriptome analysis of in vitro human cerebral cortex development from human embryonic stem cells**. *Neuron* 2014, **83**:51-68.
347. Burke EE, Chenoweth JG, Shin JH, Collado-Torres L, Kim SK, Micali N, Wang Y, Colantuoni C, Straub RE, Hoeppner DJ, et al.: **Dissecting transcriptomic signatures of neuronal differentiation and maturation using iPSCs**. *Nat Commun* 2020, **11**:462.
348. Nabet B, Roberts JM, Buckley DL, Paulk J, Dastjerdi S, Yang A, Leggett AL, Erb MA, Lawlor MA, Souza A, et al.: **The dTAG system for immediate and target-specific protein degradation**. *Nature Chemical Biology* 2018, **14**:431-441.

349. Damhofer H, Radzisheuskaya A, Helin K: **Generation of locus-specific degradable tag knock-ins in mouse and human cell lines**. *STAR Protoc* 2021, **2**:100575.
350. Abudoukelimu M, Fu ZY, Maimaiti A, Ma YT, Abudu M, Zhu Q, Adi D, Yang YN, Li XM, Xie X, et al.: **The association of cholesterol absorption gene Numb polymorphism with Coronary Artery Disease among Han Chinese and Uighur Chinese in Xinjiang, China**. *Lipids Health Dis* 2015, **14**:120.
351. Zeitlinger J, Stark A: **Developmental gene regulation in the era of genomics**. *Developmental Biology* 2010, **339**:230-239.
352. Park J, Lee K, Kim K, Yi S-J: **The role of histone modifications: from neurodevelopment to neurodiseases**. *Signal Transduction and Targeted Therapy* 2022, **7**:217.
353. Sanulli S, Justin N, Teissandier A, Ancelin K, Portoso M, Caron M, Michaud A, Lombard B, da Rocha ST, Offer J, et al.: **Jarid2 Methylation via the PRC2 Complex Regulates H3K27me3 Deposition during Cell Differentiation**. *Mol Cell* 2015, **57**:769-783.
354. Lavarone E, Barbieri CM, Pasini D: **Dissecting the role of H3K27 acetylation and methylation in PRC2 mediated control of cellular identity**. *Nature Communications* 2019, **10**:1679.
355. Moonen JR, Chappell J, Shi M, Shinohara T, Li D, Mumbach MR, Zhang F, Nair RV, Nasser J, Mai DH, et al.: **KLF4 recruits SWI/SNF to increase chromatin accessibility and reprogram the endothelial enhancer landscape under laminar shear stress**. *Nat Commun* 2022, **13**:4941.
356. Sun X, Yu W, Li L, Sun Y: **ADNP Controls Gene Expression Through Local Chromatin Architecture by Association With BRG1 and CHD4**. *Frontiers in Cell and Developmental Biology* 2020, **Volume 8 - 2020**.
357. Sanyal A, Lajoie BR, Jain G, Dekker J: **The long-range interaction landscape of gene promoters**. *Nature* 2012, **489**:109-113.
358. Oti M, Falck J, Huynen MA, Zhou H: **CTCF-mediated chromatin loops enclose inducible gene regulatory domains**. *BMC Genomics* 2016, **17**:252.
359. Vaute O, Nicolas E, Vandel L, Trouche D: **Functional and physical interaction between the histone methyl transferase Suv39H1 and histone deacetylases**. *Nucleic Acids Res* 2002, **30**:475-481.
360. Gaurav N, O'Hara R, Hyder U, Qin W, Her C, Romero H, Kumar A, Marcaida MJ, Singh RK, Hovius R, et al.: **The HP1 box of KAP1 organizes HP1α for silencing of endogenous retroviral elements in embryonic stem cells**. *Nature Communications* 2025, **16**:5066.
361. Puca F, Tosti N, Federico A, Kuzay Y, Pepe A, Morlando S, Savarese T, D'Alessio F, Colamaio M, Sarnataro D, et al.: **HMGA1 negatively regulates NUMB expression at transcriptional and post transcriptional level in glioblastoma stem cells**. *Cell Cycle* 2019, **18**:1446-1457.
362. Vaira V, Faversani A, Martin NM, Garlick DS, Ferrero S, Nosotti M, Kissil JL, Bosari S, Altieri DC: **Regulation of lung cancer metastasis by Klf4-Numb-like signaling**. *Cancer Res* 2013, **73**:2695-2705.
363. Chastagner P, Israël A, Brou C: **AIP4/Itch Regulates Notch Receptor Degradation in the Absence of Ligand**. *PLOS ONE* 2008, **3**:e2735.

364. Blatnik MC, Gallagher TL, Amacher SL: **Keeping development on time: Insights into post-transcriptional mechanisms driving oscillatory gene expression during vertebrate segmentation**. *Wiley Interdiscip Rev RNA* 2023, **14**:e1751.
365. Martin-Blanco NM, Checquolo S, Del Gaudio F, Palermo R, Franciosa G, Di Marcotullio L, Gulino A, Canelles M, Screpanti I: **Numb-dependent integration of pre-TCR and p53 function in T-cell precursor development**. *Cell Death Dis* 2014, **5**:e1472.
366. Hapak SM, Rothlin CV, Ghosh S: **PAR3-PAR6-atypical PKC polarity complex proteins in neuronal polarization**. *Cell Mol Life Sci* 2018, **75**:2735-2761.
367. Wang Z, Sandiford S, Wu C, Li SS: **Numb regulates cell-cell adhesion and polarity in response to tyrosine kinase signalling**. *Embo j* 2009, **28**:2360-2373.
368. Cheng Y, Luo H, Izzo F, Pickering BF, Nguyen D, Myers R, Schurer A, Gourkanti S, Brüning JC, Vu LP, et al.: **m6A RNA Methylation Maintains Hematopoietic Stem Cell Identity and Symmetric Commitment**. *Cell Reports* 2019, **28**:1703-1716.e1706.
369. Li Q, Zhang W, Qiao XY, Liu C, Dao JJ, Qiao CM, Cui C, Shen YQ, Zhao WJ: **Reducing polypyrimidine tract-binding protein 1 fails to promote neuronal transdifferentiation on HT22 and mouse astrocyte cells under physiological conditions**. *Exp Ther Med* 2024, **27**:72.
370. Wang B, Yang M, Li S: **Numb and Numblike regulate sarcomere assembly and maintenance**. *J Clin Invest* 2022, **132**.
371. Uhlén M et al.: **Tissue-based map of the human proteome.** . *Science (2015)* 2015, **PubMed: 25613900**
372. Hiraoka Y, Komine O, Nagaoka M, Bai N, Hozumi K, Tanaka K: **Delta-like 1 regulates Bergmann glial monolayer formation during cerebellar development**. *Molecular Brain* 2013, **6**:25.
373. Ferent J, Giguère F, Jolicoeur C, Morin S, Michaud J-F, Makihara S, Yam PT, Cayouette M, Charron F: **Boc Acts via Numb as a Shh-Dependent Endocytic Platform for Ptch1 Internalization and Shh-Mediated Axon Guidance**. *Neuron* 2019, **102**:1157-1171.e1155.
374. Lei W, Li W, Ge L, Chen G: **Non-engineered and Engineered Adult Neurogenesis in Mammalian Brains**. *Frontiers in Neuroscience* 2019, **13**.
375. Narsinh KH, Plews J, Wu JC: **Comparison of human induced pluripotent and embryonic stem cells: fraternal or identical twins?** *Mol Ther* 2011, **19**:635-638.
376. Bar S, Seaton LR, Weissbein U, Eldar-Geva T, Benvenisty N: **Global Characterization of X Chromosome Inactivation in Human Pluripotent Stem Cells**. *Cell Reports* 2019, **27**:20-29.e23.
377. Wang Z, Feng, X., & Li, C. S. (**SCDevDB: a database for insights into single-cell gene expression profiles during human developmental processes.** . *Frontiers in Genetics* 2019, **10, 903.**

XII.- APPENDIX

12.1- Antibodies used in this study.

Primary Antibodies			
Functions	**Antibody targeting**	**Catalog number**	**Company**
Location and expression of Numb protein	Numb	ab4147	Abcam
	Numb	ab155415	Abcam
	Numb	PA1-32452	ThermoFisher Scientific
	Numb	AF4338	RyD systems
	Numb	C29G11	Cell signalling technology
Notch markers	Hes5	NBP2-41305	Novus Biotec
	DLL1	ab85346	Abcam
Western Blot Controls	Vinculin	13901S	Cell signaling technology
	GAPDH	5174S	Cell signaling technology
	B-actin	66009-1-Ig	Proteintech
Lentiviral expression	SNAP	P9310S	New England Biolabs
Pluripotency or neural markers	Neun	MAB377	Sigma Millipore
	OCT4	2750S	Cell signaling technology
	SOX2	11064-1-AP	Proteintech
Epigenetic marks	H3K27me3	9733S	Cell signaling technology
	H3K27Ac	8173S	Cell signaling technology
	H3K4me3	9751S	Cell signaling technology
	EZH2	5246S	Cell signaling technology
ChIPseq control	Anti-spike in	61686	Active Motif
Chromatin organization	LMNB2	ab151735	Abcam

Secondary antibodies			
	Antibody	**Catalog Number**	**Company**
Immunofluorescence (IF)	Donkey anti mouse 488	A32766	Invitrogen
	Donkey anti rabbit 647	A31537	Invitrogen
	Donkey anti goat 594	A11058	Invitrogen
	Donkey anti mouse 594	A21203	Invitrogen
	Donkey anti rabbit 594	A21207	Invitrogen
	Donkey anti rabbit 488	A322790	Invitrogen
	Donkey anti goat 647	A21447	Invitrogen
Western Blot (WB)	Goat anti mouse IgG HRP	31430	Invitrogen
	Donkey anti goat IgG HRP	A15999	Invitrogen
	Donkey anti rabbit IgG HRP	A16023	Invitrogen

Table 13: Primary and secondary antibodies used in this study.

12.2- mRNA and protein accession codes.

mRNA		Protein	
Name	**Accession number**	**Name**	**Accession number**
Transcript variant 1	NM_001005743.2	**Numb isoform 1**	AAD54279.1
Transcript variant 2	NM_001005744.2	**Numb isoform 2**	AAD54280.1
Transcript variant 3	NM_003744.6	**Numb isoform 3**	AAD54281.1
Transcript variant 4	NM_001005745.2	**Numb isoform 4**	AAD54282.1

Table 14: Numb mRNA and protein accession numbers.

12.3 - Primer list used in this study.

Name	Sequence	goal
Exon.1_NUMBdTAG1_sgRNA	GATGAAGGCGTTCGCAC	sgRNA
Exon.1_NUMBdTAG2_sgRNA	TCAATTGGAGCATGCCGGCG	
Exon.10-NUMB_SGRNA.1	GAAGGATGTTTATGTTCCAG	
Exon.10-NUMB_SGRNA.1	ACAAATTACGGCAAAGTTTT	
U6 F	GATACAAGGCTGTTAGAGAG	Sequencing of px458 insertion
U6 R	CAGTGCAGGGGAAAGAATAGTAGAC	
NUMB-dTAG-donor-Xho1-F	CGCTCGAGAGAAACTGTTAGCAGTCTATAATTTG	gBlock-Numb-dTAG amplifying
NUMB-dTAG-donor-Sac1-R	CGgagctcGTATTTAAGAGAGCTGACTTCCAC	
NUMB-N-dTAG -F	ATTCATTTTCCCTTTACACTGTGC	Cloning into pBlueScript
NUMB-N-dTAG- R	CAGCTCTTACCTTAACCGGGA	
P1	ACCCAGGCATCATCCCACCACA	Heterozygote and homozygote of dTAG insertion
P2	TTCCGGTGCGAACGCCTTCTTC	
P3	TGTACAAATTTCCATTTTCAGGGGT	
Numb Exon 10 F	CAAAAGGATCCACTGGGCAG	Detection of the 4 Numb isoforms by sequencing
Numb Exon 2 R	AACTTGGCCATGTAGAAGTTG	
pLVx F	TGTCACTCTCTTACCCGTCA	
pLVx TET SNAP V5 R AfeI	ACTTTCCGTACCACTTCCTACCCTCGT	
Flag pLLx F	GGTTTGTCGGATTTGCCCAT	
Flag pLVX TET F	GCAAGACTTTCTGCGGAACA	
pLVx SVB13 R	GAATAGCTCAGAGGCCGAGG	
pLVx PGK R	GGGAGAGAGGTCGGTGATTC	

Table 15: Primers used in this study.

12.4- Examples of detection of Numb canonical and new Numb Isoforms detected by sequencing.

By using primers flanking the exons of interest and comparing our results with well-characterized isoforms, such as the full-length p72 or the variants lacking exons 3 and/or 9 we can determine whether the observed isoforms correspond to known forms or represent previously uncharacterized isoforms expressed during neurodevelopment.

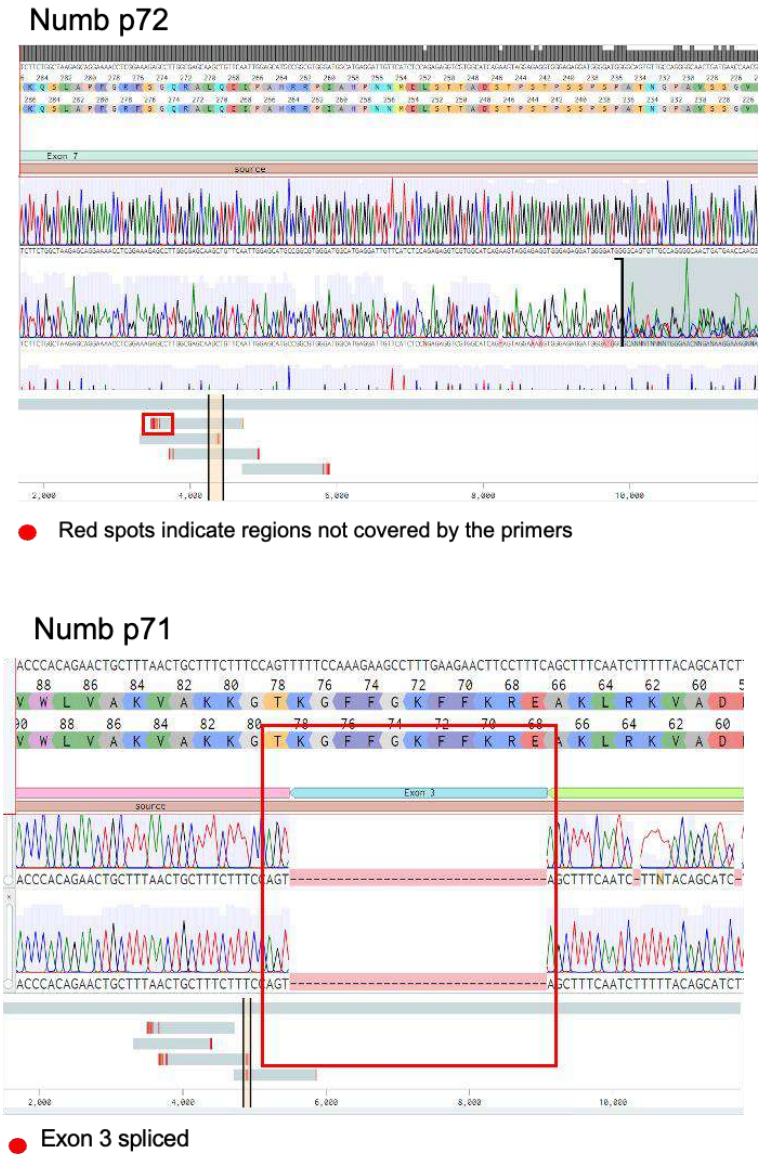

Figure 59: Sequencing tracks illustrating both Numb p72 and Numb p71 isoforms.

The upper panel displays the full-length Numb transcript (p72), while the lower panel highlights the p71 variant, which is distinguished by the absence of exon 3. These representative images provide a clear comparison between canonical and variant Numb isoforms detected through sequencing, aiding in the identification and characterization of alternative splicing events during neurodevelopment.

The following image illustrates examples of how newly identified isoforms can be visualized. In this particular case, the isoform is characterized by the absence of part of exon 10, the complete omission of exon 7, and partial deletions in exons 1 and 2.

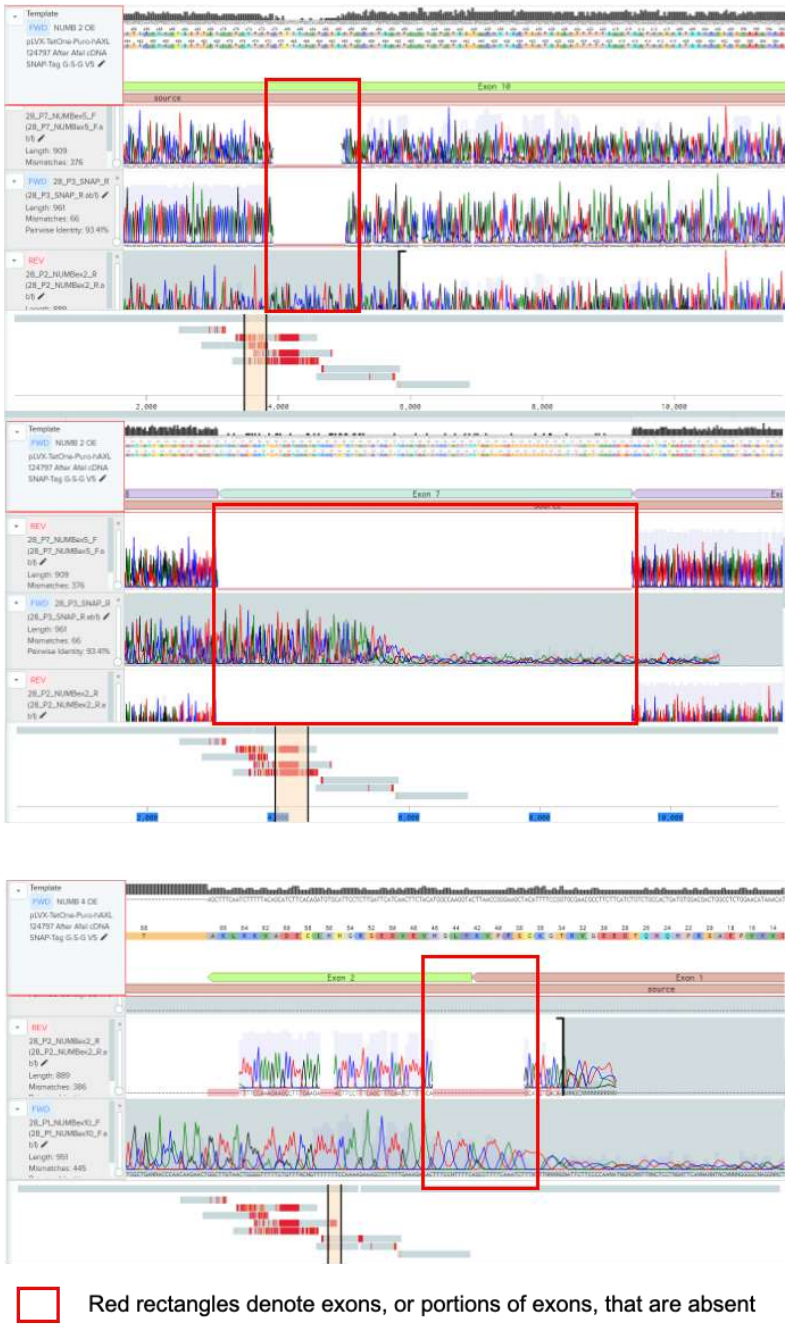

Figure 60: Sequencing tracks depicting newly discovered Numb isoforms.

The first panel demonstrates the partial deletion of exon 10, a complete absence of exon 7, and missing segments in exons 1 and 2. These visualizations highlight the complex alternative splicing events that lead to the generation of novel Numb transcript variants during neurodevelopment.

12.5- Coding for dataset analyses from Leemput et al., 2014.

12.5.1- Expression markers at different stages.

```
# Expression of hESC markers at different stages

NANOG_plots <- plot_gene_expression_timecourse(
  dds_object = dds,
  gene_name = "NANOG",
  output_dir = "results/hESC/expression", # Saves to a subfolder
  plot_log2_scale = TRUE # Generate both plots
)
# Display the linear plot directly in the document
print(NANOG_plots$linear_plot)
# Expression of NSC marker gene SOX1

SOX1_plots <- plot_gene_expression_timecourse(
  dds_object = dds,
  gene_name = "SOX1",
  output_dir = "results/hESC/expression", # Saves to a subfolder
  plot_log2_scale = TRUE # Generate both plots
)
# Display the linear plot directly in the document
print(SOX1_plots$linear_plot)
# Expression of NPC marker gene PAX6

PAX6_plots <- plot_gene_expression_timecourse(
  dds_object = dds,
  gene_name = "PAX6",
  output_dir = "results/hESC/expression", # Saves to a subfolder
  plot_log2_scale = TRUE # Generate both plots
)
# Display the linear plot directly in the document
print(PAX6_plots$linear_plot)
# Expression of NEURON marker gene SYP

SYP_plots <- plot_gene_expression_timecourse(
  dds_object = dds,
  gene_name = "SYP",
  output_dir = "results/hESC/expression", # Saves to a subfolder
  plot_log2_scale = TRUE # Generate both plots
)
# Display the linear plot directly in the document
print(SYP_plots$linear_plot)
# Call the function for your gene of interest
NUMB_plots <- plot_gene_expression_timecourse(
  dds_object = dds,
  gene_name = "NUMB",
  output_dir = "results/hESC/expression", # Saves to a subfolder
  plot_log2_scale = TRUE # Generate both plots
)
# Display the linear plot directly in the document
print(NUMB_plots$linear_plot)
```

```
# You could optionally display the log2 plot as well:
# print(EZH1_plots$log2_plot)


# Call the function for your gene of interest
NUMBL_plots <- plot_gene_expression_timecourse(
  dds_object = dds,
  gene_name = "NUMBL",
  output_dir = "results/hESC/expression", # Saves to a subfolder
  plot_log2_scale = TRUE # Generate both plots
)
# Display the linear plot directly in the document
print(NUMBL_plots$linear_plot)
# You could optionally display the log2 plot as well:
# print(EZH2_plots$log2_plot)


# Call the function for your gene of interest
EZH1_plots <- plot_gene_expression_timecourse(
  dds_object = dds,
  gene_name = "EZH1",
  output_dir = "results/hESC/expression", # Saves to a subfolder
  plot_log2_scale = TRUE # Generate both plots
)
# Display the linear plot directly in the document
print(EZH1_plots$linear_plot)
# You could optionally display the log2 plot as well:
# print(EZH1_plots$log2_plot)


# Call the function for your gene of interest
EZH2_plots <- plot_gene_expression_timecourse(
  dds_object = dds,
  gene_name = "EZH2",
  output_dir = "results/hESC/expression", # Saves to a subfolder
  plot_log2_scale = TRUE # Generate both plots
)
# Display the linear plot directly in the document
print(EZH2_plots$linear_plot)
# You could optionally display the log2 plot as well:
# print(EZH2_plots$log2_plot)
```

12.5.2- Splicing events upon differentiation.

```
# Splicing events
# --- Read Splicing Event Data ---
# *** REPLACE WITH YOUR ACTUAL RMATS FILENAME AND PATH ***
rmats_file <- file.path("data/hESC/rMATS_filter",
"numb_splicing_all_types_filtered.txt")

if (!file.exists(rmats_file)) stop(paste("Error: rMATS input file not
found at:", rmats_file))
rmats_data <- read_tsv(rmats_file, show_col_types = FALSE)
required_cols <- c("name", "position", "inclusion_value")
if (!all(required_cols %in% names(rmats_data))) stop(paste("Error:
Input file must contain:", paste(required_cols, collapse=", ")))

# --- Loop Through Events and Plot ---
if (nrow(rmats_data) > 0) {
  # Use lapply or purrr::map for cleaner iteration than a for loop
  # This applies the function to each row and returns a list of plots
  plot_list <- lapply(1:nrow(rmats_data), function(i) {
    event_row <- rmats_data[i, ]
    # Explicitly print inside lapply/loop for Quarto to capture *each*
plot
    plot_obj <- tryCatch({
        plot_splicing_event_points(
            event_data = event_row,
            coldata_ordered = coldata_plot,
            output_dir = "results/hESC/splicing/individual_plots", #
Specific subdir
            save_plot = TRUE # Ensure plots are saved
        )
      }, error = function(e) {
        # Don't print warnings in the final doc, rely on #| warning:
false
        # warning(paste("Failed for row:", i, ". Error: ", e$message))
        return(NULL)
    })
    # ** CRUCIAL: Explicitly print the plot object for Quarto **
    if (!is.null(plot_obj)) {
        print(plot_obj) # This makes Quarto render the plot
    }
    return(plot_obj) # Return plot object for the list (optional)
  })
  # Remove NULLs if any plots failed
  plot_list <- plot_list[!sapply(plot_list, is.null)]
} else {
  # message("Input rmats_data file is empty or has no rows.") #
Message suppressed
}
```

12.6- Coding for dataset analyses from Burke *et al.*, 2020.

12.6.1- Expression markers at different stages.

```
Expression of hESC marker at different stages

NANOG_plots <- plot_gene_expression_timecourse(
  dds_object = dds,
  gene_name = "NANOG",
  output_dir = "results/hiPSC/expression", # Saves to a subfolder
  plot_log2_scale = TRUE # Generate both plots
)
# Display the linear plot directly in the document
print(NANOG_plots$linear_plot)
# Expression of NSC marker gene SOX1

SOX1_plots <- plot_gene_expression_timecourse(
  dds_object = dds,
  gene_name = "SOX1",
  output_dir = "results/hiPSC/expression", # Saves to a subfolder
  plot_log2_scale = TRUE # Generate both plots
)
# Display the linear plot directly in the document
print(SOX1_plots$linear_plot)
# Expression of NPC marker gene PAX6

PAX6_plots <- plot_gene_expression_timecourse(
  dds_object = dds,
  gene_name = "PAX6",
  output_dir = "results/hiPSC/expression", # Saves to a subfolder
  plot_log2_scale = TRUE # Generate both plots
)
# Display the linear plot directly in the document
print(PAX6_plots$linear_plot)
# Expression of NEURON marker gene SYP

SYP_plots <- plot_gene_expression_timecourse(
  dds_object = dds,
  gene_name = "SYP",
  output_dir = "results/hiPSC/expression", # Saves to a subfolder
  plot_log2_scale = TRUE # Generate both plots
)
# Display the linear plot directly in the document
print(SYP_plots$linear_plot)
# Call the function for your gene of interest
NUMB_plots <- plot_gene_expression_timecourse(
  dds_object = dds,
  gene_name = "NUMB",
  output_dir = "results/hiPSC/expression", # Saves to a subfolder
  plot_log2_scale = TRUE # Generate both plots
)
# Display the linear plot directly in the document
print(NUMB_plots$linear_plot)
```

```
# You could optionally display the log2 plot as well:
# print(EZH1_plots$log2_plot)


# Call the function for your gene of interest
NUMBL_plots <- plot_gene_expression_timecourse(
  dds_object = dds,
  gene_name = "NUMBL",
  output_dir = "results/hiPSC/expression", # Saves to a subfolder
  plot_log2_scale = TRUE # Generate both plots
)
# Display the linear plot directly in the document
print(NUMBL_plots$linear_plot)
# You could optionally display the log2 plot as well:
# print(EZH2_plots$log2_plot)


# Call the function for your gene of interest
EZH1_plots <- plot_gene_expression_timecourse(
  dds_object = dds,
  gene_name = "EZH1",
  output_dir = "results/hiPSC/expression", # Saves to a subfolder
  plot_log2_scale = TRUE # Generate both plots
)
# Display the linear plot directly in the document
print(EZH1_plots$linear_plot)
# You could optionally display the log2 plot as well:
# print(EZH1_plots$log2_plot)


# Call the function for your gene of interest
EZH2_plots <- plot_gene_expression_timecourse(
  dds_object = dds,
  gene_name = "EZH2",
  output_dir = "results/hiPSC/expression", # Saves to a subfolder
  plot_log2_scale = TRUE # Generate both plots
)
# Display the linear plot directly in the document
print(EZH2_plots$linear_plot)
# You could optionally display the log2 plot as well:
# print(EZH2_plots$log2_plot)
```

12.6.2- Splicing events upon differentiation.

```
# Splicing events
# --- Read Splicing Event Data ---
# *** REPLACE WITH YOUR ACTUAL RMATS FILENAME AND PATH ***
rmats_file <- file.path("data/hESC/rMATS_filter",
"numb_splicing_all_types_filtered.txt")

if (!file.exists(rmats_file)) stop(paste("Error: rMATS input file not
found at:", rmats_file))
rmats_data <- read_tsv(rmats_file, show_col_types = FALSE)
required_cols <- c("name", "position", "inclusion_value")
if (!all(required_cols %in% names(rmats_data))) stop(paste("Error:
Input file must contain:", paste(required_cols, collapse=", ")))

# --- Loop Through Events and Plot ---
if (nrow(rmats_data) > 0) {
  # Use lapply or purrr::map for cleaner iteration than a for loop
  # This applies the function to each row and returns a list of plots
  plot_list <- lapply(1:nrow(rmats_data), function(i) {
    event_row <- rmats_data[i, ]
    # Explicitly print inside lapply/loop for Quarto to capture *each*
plot
    plot_obj <- tryCatch({
        plot_splicing_event_points(
            event_data = event_row,
            coldata_ordered = coldata_plot,
            output_dir = "results/hESC/splicing/individual_plots", #
Specific subdir
            save_plot = TRUE # Ensure plots are saved
        )
      }, error = function(e) {
        # Don't print warnings in the final doc, rely on #| warning:
false
        # warning(paste("Failed for row:", i, ". Error: ", e$message))
        return(NULL)
    })
    # ** CRUCIAL: Explicitly print the plot object for Quarto **
    if (!is.null(plot_obj)) {
        print(plot_obj) # This makes Quarto render the plot
    }
    return(plot_obj) # Return plot object for the list (optional)
  })
  # Remove NULLs if any plots failed
  plot_list <- plot_list[!sapply(plot_list, is.null)]
} else {
  # message("Input rmats_data file is empty or has no rows.") #
Message suppressed
}
```